Niche Construction, Sustainability and Evolutionary Ecology of Cancer

by

Irina Kareva

A Dissertation Presented in Partial Fulfillment
of the Requirements for the Degree
Doctor of Philosophy

Approved Decembery 2011 by the
Graduate Supervisory Committee:

Carlos Castillo-Chavez, Chair
James Collins
John Nagy
Hal Smith

ARIZONA STATE UNIVERSITY

May 2012

ABSTRACT

In complex consumer-resource type systems, where diverse individuals are interconnected and interdependent, one can often anticipate what has become known as the tragedy of the commons, i.e., a situation, when overly efficient consumers exhaust the common resource, causing collapse of the entire population. In this dissertation I use mathematical modeling to explore different variations on the consumer-resource type systems, identifying some possible transitional regimes that can precede the tragedy of the commons. I then reformulate it as a game of a multi-player prisoner's dilemma and study two possible approaches for preventing it, namely direct modification of players' payoffs through punishment/reward and modification of the environment in which the interactions occur. I also investigate the questions of whether the strategy of resource allocation for reproduction or competition would yield higher fitness in an evolving consumer-resource type system and demonstrate that the direction in which the system will evolve will depend not only on the state of the environment but largely on the initial composition of the population. I then apply the developed framework to modeling cancer as an evolving ecological system and draw conclusions about some alternative approaches to cancer treatment.

DEDICATION

To my parents

ACKNOWLEDGEMENTS

The author would like to sincerely thank her mentor Carlos Castillo-Chavez for introducing her to mathematical biology through two summers of MTBI, as well as for his unfailing and undiminished support and infinite patience all throughout her graduate studies, her co-adviser John Nagy, who taught her to be able to translate between biology and mathematics without losing credibility to specialists on either side, and also for introducing her to adaptive dynamics, James Collins for giving her as strong an introduction to theoretical ecology as one could wish for, Faina Berezovskaya for teaching her all the bifurcation theory she knows, and Georgy Karev for teaching her how to use the Reduction theorem and most importantly, how to think about and approach mathematical modeling. Also a very big thank you is due to her office mates David Murillo and Benjamin Morin both for teaching her and helping her with most of her Matlab programming skills, and for just being great fun to be around.

The following papers were included in this dissertation:

Chapter 2: Kareva, Irina, Faina S Berezovskaya, and Carlos Castillo-Chavez. "Niche Construction and Sustainability in Resource-Dependent Competition Models." Mathematical Biosciences, *in press.*

Chapter 3: Kareva, Irina, Benjamin Morin, and Georgy P Karev. "Preventing the tragedy of the commons through punishment of over-consumers and encouragement of under-consumers.", *in preparation.*

Chapter 4: Kareva, Irina, Faina S Berezovskaya, and Georgy P Karev. "Mixed Strategies and Natural Selection in Ecological Niche Construction", *in preparation.*

Chapter 5: Kareva, Irina and John Nagy. "Biological stoichiometry in tumor microenvironment", *in preparation.*

Chapter 6: Kareva, Irina. "Prisoner's Dilemma in Cancer Metabolism." PloS One, *in press.*

Chapter 8: Kareva, Irina, Faina Berezovskaya, and Carlos Castillo-Chavez. 2010. "Myeloid

cells in tumour-immune interactions." Journal of Biological Dynamics 4 (4): 315-327.

Chapter 9: Kareva, Irina. 2011. "What can ecology teach us about cancer?" Translational Oncology 4 (5): 266-270.

This project has been partially supported by grants from the National Science Foundation (NSF - Grant DMPS-0838705), the National Security Agency (NSA - Grant H98230-09-1-0104), the Alfred P. Sloan Foundation and the Office of the Provost of Arizona State University.

Contents

CHAPTER Page

Contents v

List of Tables vi

List of Figures vii

PREFACE xix

1 INTRODUCTION 1

2 TRANSITIONAL REGIMES AS EARLY WARNING SIGNALS 6

3 PUNISHMENT/REWARD SYSTEM IN PREVENTING THE TRAGEDY OF THE COMMONS 26

4 MIXED STRATEGIES IN RESOURCE ALLOCATION 53

5 BIOLOGICAL STOICHIOMETRY IN TUMOR MICROENVIRONMENT 70

6 PRISONER'S DILEMMA IN CANCER METABOLISM 89

7 AGENT-BASED MODELING OF COMPLEX SYSTEMS. WARBURG EFFECT. . 106

8 CANCER-IMMUNE SYSTEM INTERACTIONS AS PREDATOR-PREY 116

9 WHAT CAN ECOLOGY TEACH US ABOUT CANCER? 128

10 CONCLUSIONS 138

Bibliography 144

APPENDIX 159

A SELECTION SYSTEMS AND THE REDUCTION THEOREM. 159

B TRANSITIONAL REGIMES AS EARLY WARNING SIGNALS 163

C MIXED STRATEGIES IN RESOURCE ALLOCATION. 168

D BIOLOGICAL STOICHIOMETRY IN TUMOR MICROENVIRONMENT. 182

E PRISONER'S DILEMMA IN CANCER METABOLISM. 185

F MYELOID CELLS IN TUMOR-IMMUNE INTERACTIONS. 192

List of Tables

2.1 Summary of variables and parameters used throughout the Chapter. 10

2.2 Sample parameter values 10

2.3 Summary of possible dynamical regimes of System (2.4); Domain 6 exists only when $\delta > 5+\sqrt{24}$ 16

3.1 Summary of variables and parameters of System (3.1) 28

3.2 Adaptive dynamics and Reduction theorem 50

5.1 Summary, brief description and range of all parameters in System 5.2 75

6.1 Summary of variables and parameters used throughout the Chapter 94

6.2 Sample parameter values 94

7.1 Summary of assumptions necessary for building an agent-based model of Warburg effect. 108

8.1 Meaning and sample values of parameter values. 120

8.2 Values of parameters in α and β in three domains in Figure (8.1) 125

List of Figures

2.1 Null-clines of System (2.4) for $\gamma = \delta = e = 1$, when c is varied. Equilibrium A exists in sections (a-d) and does not exist in e. 12

2.2 Bifurcation diagram of the equilibrium point O, shown through blowing-up transformations. 13

2.3 Behaviors of System (2.4) (a) within parameter space close to the boundary K, corresponding to the separatrix of the "infinite" equilibrium. (b) within parameter space close to boundary S, corresponding to the heteroclinic connection of separatrices of the saddle point B and the saddle-node point O; (c) within parameter space close to the boundary H; C is the boundary, where stable and unstable cycles annihilate. 14

2.4 Bifurcation diagram of System (2.4) in the (γ, c) and (N, z) phase spaces for fixed positive parameters e and δ. The non-trivial equilibrium point A is globally stable in Domain 1; it shares basins of attraction with equilibrium O in Domains 2 and 3. The separatrix of O and the unstable limit cycle that contains point A, serve, correspondingly, as the boundaries of the basins of attraction. Only equilibrium O is globally stable in Domains 4, which also contains an unstable non-trivial A, and 5, which contains the elliptic sector. Domain 6 exists only for $\delta > 5 + \sqrt{24}$, where the stable limit cycle that is in turn contained inside an unstable limit cycle, shares basins of attraction with equilibrium O. Boundaries between Domains $O\gamma, K, S, H, Nul, C$ correspond respectively to appearance of point B, appearance of an attractive sector in a neighborhood of O, appearance of unstable limit cycle containing A, change of stability of equilibrium A via Hopf bifurcations, disappearance of positive A and saddle-node bifurcation of limit cycles. 15

2.5 Comparison of trajectories of Systems (2.3) and (2.7) under different values of c and $[\alpha, \beta]$ respectively. Other parameter values are taken from set 1 of Table 2.2. 19

2.6 System (2.9) with initial truncated exponential distribution on the interval (α, β), with parameter values from set 1 in Table 2.2. This is an example of what transitional regimes the System can go through before the population crashes, with trajectories for the total population size $N(t)$, total amount of renewable resource $z(t)$ and expected value of the parameter c on the left, and the change over time of the distribution of various clone types within the population on the right. 20

2.7 System (2.9) with initial truncated exponential distribution on the interval (α, β), with parameter values taken from set 2 in Table 2.2. An example of what transitional regimes the System can go through before the population crashes, with trajectories for the total population size $N(t)$, total amount of renewable resource $z(t)$ and expected value of the parameter c on the left, and the graph of the change over time in distribution of various clone types within the population on the right. Initial conditions fall within the parameter range of Domain 6 of the phase-parameter portrait of the the non-distributed system. Since the rate of natural resource decay is high, it takes more time even for the most efficient consumer to "get to it", and so the population survives longer, and the transitional regimes are more evident. 21

3.1 Case 1. Punishment-reward function of the form $f(c) = a\frac{1-c}{1+c}$ and its effects on population growth. 31

3.2 Selection gradient and pairwise invasibility plots for function of the type $f(c) = a\frac{1-c}{1+c}$. Blue regions correspond to parameter values where the mutant cannot invade; red regins correspond to parameter values where it can invade. (a) selection gradient, defined in 3.6, where $a \in [3-2\sqrt{2}, 3+2\sqrt{2}]$ (b) PIP for $a = 1$; the singular strategy c^*_{res} is evolutionarily unstable and convergence stable (c) PIP for $a = 4$; the singular strategy c^*_{res} is evolutionarily unstable and convergence stable. Ths punishment/reward function is not effective against agressive overconsumers. 32

3.3 Case 2. Punishment-reward function of the form $f(c) = a(1-c)^3$ and its effects on population growth 33

3.4 Selection gradient and pairwise invasibility plots for function of the type $f(c) = a(1-c)^3$. Blue regions correspond to parameter values where the mutant cannot invade; red regins correspond to parameter values where it can invade. (a) selection gradient, defined in 3.6, where $a < 0.15$ (b) PIP for $a = 0.05$; the singular strategy c^*_{res} is evolutionarily and convergence stable (c) PIP for $a = 0.14$; the singular strategy c^*_{res} is evolutionarily and convergence stable. This punishment/reward function is effective against agressive overconsumers. 33

3.5 Pairwise invasibility plots for function type $f(c) = \rho(1-c^\eta),\ \eta = 0.9$. The effectiveness of this function is the same as was for case 1: punishment is not severe enough to keep over-consumers out of the population. 35

3.6 Pairwise invasibility plots for function type $f(c) = \rho(1-c^\eta),\ \eta = 1.2$. The effectiveness of this function is the same as was for case 2: punishment is sufficiently severe to keep over-consumers out of the population. 35

3.7 Initial distributions (a) truncated exponential with parameter $\mu = 10$ (b) Beta distribution with parameters $[\alpha,\beta] = [2,2]$ and $[\alpha,\beta] = [2,5]$. 38

3.8 (a) Truncated exponential, moderate punishment (case 1), set 1, $a = 0$. (b) Truncated exponential, case 1, set 1, $a = 0.5$. (c) Truncated exponential, case 1, set 1, $a = 1$. (d) Truncated exponential, case 1, set 1, $a = 2$. 39

3.9 Truncated exponential distribution, set 1, case 1, dynamics of the total population size and total resource with respect to different values of a (different levels of severity of imposed punishment). One can see that successful management of overconsumers was possible only when punishment implementation was very high. 39

3.10 (a) Beta distribution with parameters $[\alpha,\beta] = [2,2]$, case 1, set 1, $a = 0$, (b) $a = 1$, (c) $a = 2$, (d) $a = 2.05$. 40

3.11 Beta distribution with parameters $[\alpha,\beta] = [2,2]$, set 1, case 1, dynamics of the total population size and total resource with respect to different values of a (different levels of severity of imposed punishment). The value of a that is necessary to manage the over-consumers and prevent resource over-consumption and the tragedy of the commons is higher than it was, when the clones in the population were initially distributed according to truncated exponential distribution. . . . 40

3.12 Beta distribution with parameters $[\alpha,\beta]=[2,5]$, set 1, case 1 (a) $a=0$, (b) $a=1$, (c) $a=1.5$, (a) $a=2$. 41

3.13 Beta distribution with parameters $[\alpha,\beta]=[2,5]$, set 1, case 1, dynamics of the total population size and total resource with respect to different values of a (different levels of severity of imposed punishment). One can see that successful management of overconsumers was possible only when punishment implementation was very high; also, the value of a that is necessary to manage the over-consumers and prevent resource over-consumption and the tragedy of the commons is higher than it was, when the clones in the population were initially distributed according to truncated exponential distribution. 41

3.14 Case 2, set 1, truncated exponential distribution. (a) $a=0$, (b) $a=0.1$, (c) $a=0.135$, (d)$a=0.2$. One can see that with this punishment function, the intensity of implementation of punishment that is necessary to prevent the tragedy of the commons is much lower; when $a=0.2$, the clones that are able to persist in population under this punishment function are as over-consumerist as the system can tolerate but at the same time, they are not so parasitic as to destroy the common resource. 42

3.15 Case 2, set 1, truncated exponential distribution. Dynamics of resource and the entire population size under severe punishment of over-consumers. 42

3.16 Beta distribution with parameters $[\alpha,\beta]=[2,2]$, $c\in[0,3]$. (a) $a=0$, (b) $a=0.1$, (c) $a=0.17$, (d) $a=0.2$. One can see the population going through transitional regimes before collapse, when the punishment is implemented severely but not quite severely enough (when $a=0.7$). This most probably corresponds to the expected value of parameter c going through region 3 in the phase parameter portrait of the non-distributed system (see Figure 4.1). 43

3.17 Case 2, set 1. Beta distribution with parameters $[2,2]$. Changes in total population size and of the common resource over time. 43

3.18 Beta distribution, parameters $[\alpha,\beta]=[2,5]$, $c\in[0,3]$. (a) $a=0$, (b) $a=0.1$, (c) $a=0.14$, (d) $a=0.2$ 44

3.19 Beta distribution with parameters $[\alpha,\beta]=[2,5]$. Dynamics of resource and population size over time. 44

3.20 $f(c)=\rho(1-c^{\eta})$, initial Beta distribution with parameters $[\alpha,\beta]=[2,2]$, $c\in[0,3]$, $\eta=1.2$. 45

3.21 The importance of evaluating the range of possible values of c_f, illustrated for different initial distribution. Punishment function is of the type $f(c)=\rho(1-c^{\eta})$, where $\rho=0.6$, $\eta=1.2$. Initial distributions are taken to be truncated exponential with parameter $\mu=10$, and Beta with parameters [2,2] and [2.5]; $\rho=0.6$, $\eta=1.2$. The top row corresponds to $c\in[0,3]$; the bottom row corresponds to $c\in[0,4]$. 46

3.22 Tragedy of the commons as prisoner's dilemma. The tragedy can be avoided if the immediate payoffs of all the players are modified through appropriate punishment/reward function. 51

4.1 Bifurcation diagram of the System (1.2), where (a),(b),(c) and(d) represent (α, c_1)-slices of parameter space of the model for $e = \phi = 1$and (e) presents typical (N, z)-phase portraits whose numeration is identity to those in parameter portraits. In Domain 1, we can observe sustainable coexistence with the common resource, which can also be interpreted as a successfully formed niche (non-trivial globally attracting equilibrium point A). In Domain 2, there appears a region of bistability, i.e., a niche will be successfully formed only depending on the initial population size and the amount of resource. In Domain 3, an unstable limit cycle is formed around the point A, further shrinking the range of possible initial conditions that will lead to successful formation of a niche. In Domain 4, point A loses stability, so any perturbation will lead to population collapse. In Domain 5, the trajectory becomes an elliptic sector ("the devil's loop") which implies that a population is bound for extinction after a sufficiently long amount of time. Domain 6 exists only when the level of both natural resource restoration and natural resource decay is very high; in this case, the population can go into a stable oscillatory regime. Finally, Domain 0 corresponds to the case, when only trivial equilibrium $B(0, \gamma/\delta)$ is globally attractive, which is of no biological and dynamical interest. 58

4.2 Mixed niches, different growth curves (a) $c_1 = c_2 = 1, \phi = 0.01$ (b) $c_1 = c_2 = 1, \phi = 0.2$. 61

4.3 Trajectories and distribution of clones throughout the completely "altruistic" population (starting in Domain 1). Even a very slight change in the value of an intrinsic parameter ϕ (natural death rate of individuals that invest primarily in fecundity) causes the system to evolve towards the dominance of one or the other strategy (investment in fecundity in the top case and investment into carrying capacity in the bottom case). The total population size and the total amount of resource are virtually the same in both cases. All parameters held constant at $r = 1$, $e = 1$, $b = 1$, $k = 1$, $N_0 = .1$, $c_2 = .2$, $c_1 = .6$, $d = 1$, $p = 1, \phi = 0.09$. (c-d): all parameters held the same, except $\phi = 0.14$. 63

4.4 Trajectories and distribution of clones throughout the population. In this case, one not only observes stable oscillatory behavior in the amount of resource and total population size but also a shift between the two strategies. That is, the population evolves not towards eventual dominance of just one pure strategy but shifts between two strategies. Initial distribution is uniform. Initial conditions are such as to fall within Domain 6. Parameters are $r = 1$, $e = 1$, $b = .9$, $k = 1$, $\phi = 1.2$, $N_0 = .1$, $c_2 = 8.75$, $c_1 = 9$, $d = 24$, $p = 7.72$. 64

4.5 The effects of difference in the initial composition of the population with respect to different strategies. Different initial distributions were chosen to be (a) uniform initial distribution (b) truncated exponential initial distribution, with parameter $\mu = 1.1$ (note: population crashes after time $t = 32$) and (c) truncated exponential initial distribution, with parameter $\mu = 10.1$. Initial conditions are such as to fall within Domain 1. All parameters held constant at $r = 1$, $e = 1$, $b = 1$, $k = 1$, $N_0 = .1$, $c_2 = .2$, $c_1 = .6$, $d = 1$, $p = 1$, $\phi = 0.14$. One can see that the initial composition of the population can have dramatic effects on the direction in which the population will evolve over time. (Note: the values of μ were chosen arbitrarily for illustrative purposes). 65

4.6 The effects of difference in the initial composition of the population with respect to different strategies. Different initial distributions were chosen to be (a) uniform (b) $\mu = 10.1$ and (c) $\mu = 30.1$. Other parameters held constant at $r = 2$, $e = 2$, $b = 1$, $k = 1$, $N_0 = .1$, $c_2 = .2$, $c_1 = 2$, $d = 1$, $p = 1$, $\phi = 0.05$. 65

5.1 Schematic representation of the interaction between the two growth strategies. Depending on the amount of resource z, either the competitive or the proliferative strategy clones have higher growth rates. At the intersection of the two curves neither strategy gives the clones an advantage, regardless of the distribution of clones in the population (i.e., regardless of the value of α). 73

5.2 Diagram of mechanism described in System 5.2 75

5.3 The higher the rate of external P inflow, the longer it takes for the population to go back to primarily competitive phenotype until finally it just remains composed mostly of proliferative clones, with short-lived "bursts" of competitiveness. . . . 78

5.4 Changes in the mean of α vs time vs external phosphorus inflow. 79

5.5 Changes in the mean of α and the full population size at $P_0 = 20$ with respect to differences in growth rates. As one can see, it is possible for the population composition to be very different without it being reflected in the overall population size. 80

5.6 Changes in the mean of α and the full population size at $P_0 = 50$ with respect to differences in nutrient uptake ratesAs one can see, proliferative clones are either practically unaffected or at a loss regardless of the relative values of parameters m_c and m_p, which suggests that targeting phosphorus transporters might in fact give advantage to proliferative clones regardless of which clone type may have this adaptation. 80

5.7 Evolution of the system under the same set of initial conditions ($P_0 = 40$) but with different initial distributions of clone types within the population. The results suggest that just knowing the state of tumor microenvironment is not enough to be able to predict in which direction the population will evolve – one must also know the composition of the population. 82

5.8 A possible scenario of evolving towards competitive phenotype as a "transitionl regime". 87

6.1 Schematic diagram of the process described in System 6.1 93

6.2 Relative positions of growth rates for aerobic ($x'_\alpha = r_a C^{in} \frac{\beta}{\beta + C^{in}}$, solid blue line) and glycolytic ($x'_\alpha = r_g C^{in}$, dashed lines) cell types for different initial states of the microenvironment (amount of resource $C^{in}$and amount of oxygen β) and different relative intrinsic growth rates $r_a$and r_g of both cell types. One can see that different clone types have higher fitness relative to each other depending on carbon (C^{in}) and oxygen (β) availability and the values of intrinsic parameters r_a and r_g. 94

6.3 Quantifying the effects of differences in growth rates of aerobic and glycolytic cell clones. (a) Changes in the mean number of glycolytic cells $E^t[\alpha]$ over time for $r_a = 0.2,\ r_g = 0.21, 0.22, 0.23, 0.24$ (b) $E^t[\alpha]$ at $t = 4000$ for C_0 varied from 5 to 600, evaluated for $r_a = 0.2, r_g = 0.21, 0.22, 0.23, 0.24$ (c) Changes in $E^t[\alpha]$ over time with respect to differences in C_0 for $r_a = 0.2, r_g = 0.21$ (d) Changes in $E^t[\alpha]$ over time with respect to differences in C_0 for $r_a = 0.2, r_g = 0.24$ 96

6.4 Quantifying the effects of oxygen availability on the growth of aerobic and glycolytic cell clones. (a) Changes in the mean number of glycolytic cells $E^t[\alpha]$ over time for $\beta = 2, 10, 15$ (b) $E^t[\alpha]$ at $t = 4000$ for C_0 varied from 5 to 600, evaluated for $\beta = 2, 10, 15$ (c) Changes in $E^t[\alpha]$ over time with respect to differences in C_0 for $\beta = 2$ (d) Changes in $E^t[\alpha]$ over time with respect to differences in C_0 for $\beta = 15$. 97

6.5 Quantifying the effects of natural death rates on the changes in proportion of glycolytic cell clones in the population. (a) Changes in the mean number of glycolytic cells $E^t[\alpha]$ over time for (b) $E^t[\alpha]$ at $t = 4000$ for C_0 varied from 5 to 600, evaluated for $d = 0.04, 0.03, 0.02, 0.01$ (c) Changes in $E^t[\alpha]$ over time with respect to differences in C_0 for $d = 0.02$ (d) Changes in $E^t[\alpha]$ over time with respect to differences in C_0 for $d = 0.04$. 98

6.6 Quantifying the effects of differences in resource uptake rates on the changes in proportion of glycolytic cell clones in the population. (a) Changes in the mean number of glycolytic cells $E^t[\alpha]$ over time for $p_a = 0.1,\ p_g = 3, 1, 0.5, 0.1$ (note the scale on y-axis) (b) $E^t[\alpha]$ at $t = 4000$ for C_0 varied from 5 to 600, evaluated for $p_a = 0.1, p_g = 3, 1, 0.5, 0.1$(note the scale on y-axis) (c) Changes in $E^t[\alpha]$ over time with respect to differences in C_0 for $p_a = 0.1,\ p_g = 0.2$ (d) Changes in $E^t[\alpha]$ over time with respect to differences in C_0 for $p_a = 0.1, p_g = 3$. 99

6.7 Evolutionary suicide can occur when the proportion of glycolytic cells $E^t[\alpha]$ within the total cell population reaches approximately 10% under given parameter values. Trajectories depict (a) the changes in the mean value of glycolytic cells in the population $E^t[\alpha]$ (b) extracellular carbon C^{ex}, (c) intracellular carbon C^{in}, (d) total population size $N(t)$ over time and (e) the distribution of cell clones $P_t[\alpha]$ changing over time. 100

6.8 Changes in the microenvironment can lead to changes in population composition, which in turn can lead to the population evolving away from the dominant aerobic-aerobic "defecting" strategy, which keeps the system stable, to glycolytic-glycolytic "cooperation", which can eventually lead to evolutionary suicide (cancer killing the patient and thus killing itself). 104

7.1 Initial number of glycolytic cells is 36; glycolytic strategy could not be adopted, and all patches are acid-free or have some acid in low concentrations. 113

7.2 Initial number of glycolytic cells is 76. The initial population of glycolytic cells is large enough to get a collective competitive advantage from increased toxicity. The microenvironment around the blue (glycolytic) cells is very acidic, which is reflected through increased patch brightness. 113

7.3 Initial number of glycolytic cells is 134. In this case, some aerobic cells manage to adapt to the highly acidic environment, as can be seen by a patch of red (aerobic) cells among the blue (glycolytic) cells. 114

7.4 Initial number of glycolytic cells is 242. In this case, too many glycolytic cells exhibit extremely high nutrient demands, so they are not able to secure enough nutrients to survive before producing large amounts of lactic acid, and as a result, they do not survive in the tissue. 114

8.1 Phase-parameter portrait of system 8.4 at $\gamma = \tilde{\gamma} = 0.47$. H^- and H^+correspond to boundaries of subcritical and supercritical Hopf bifurcations of co-dimension 1, respectively. D corresponds to the saddle-node limit cycle bifurcation of co-dimension 1. 124

9.1 Schematic representation of the possible mechanism of tumor initiation and progression from an ecological point of view. Tumor initiation corresponds to the mechanism of species invasion, and is hypothesized to be possible when the environment is permissive, in particular, when there are excess nutrients (new niche) and when competitors (somatic cells) are less fit, compared to the invaders. Tumor promotion corresponds to niche colonization and modification by the invading species through pH alteration, recruitment of growth factors, etc., as well as avoidance of predators (immune suppression). 134

C.1 Phase-parameter portraits of System (4.1) with $\alpha = 0$ under variation of parameter c_2: in Domain 0 (where $0 < c_2 < \phi$), only the trivial equilibrium B is an attractor. In Domain 1, non-trivial equilibrium point A is a global attractor. Domain 2 is a region of bistability: there are two attracting points, A and origin O, whose basins of attraction are divided by separatrix of point O. Point A is a stable focus, attracting only those trajectories that fall within its domain of attraction. In Domain 3, an unstable limit cycle is formed around stable point A, further decreasing its basin of attraction. Finally, in Domain 4, the limit cycle shrinks, "sits" on the point A, making it unstable. Starting from Domain 2 most trajectories in fact travel outside of the first quadrant, predicting negative population size and resource amount, thus rendering the model biologically irrelevant in this region of phase-parameter space. 169

C.2 A schematic bifurcation diagram of the equilibrium point O for System (C.1) in the (γ, c_1) parameter-and (N, z)- phase spaces for positive fixed values of parameters $e \leq 1, c_2 > \phi$, $c_{2>\delta}$. The parameter space is divided into three domains: Domain 1 contains hyperbolic sector only, Domain 2 contains hyperbolic and attractive parabolic sectors, in Domain 3 there exists an elliptic sector (family of homoclinic orbits). The boundary K between domains 1 and 2 corresponds to the non-local heteroclinic bifurcation; the boundary Nul between domains 2 and 3 corresponds to disappearance of hyperbolic sector and non-trivial equilibrium. 175

C.3 (a) Only equilibrium B is attractive, (b) equilibrium O is attractive and repelling simultaneously, no more attracting equilibria, (c) equilibrium O is attractive, other attractive manifolds have to exist, (d) O is repelling (a saddle), other attractive manifolds must exist. 178

C.4 Schematic bifurcation diagrams of heteroclinics- and Hopf bifurcations that are realized in the System (C.1): (a) appearance\disappearance of attractive parabolic sector in a neighborhood of the origin; (b) appearance/disappearance of unstable limit cycle containing A, and (c) generalized Hopf bifurcation $L_1(H) = 0$ in a neighborhood of A. 179

PREFACE

This dissertation is devoted to the study of consumer-resource type ecological systems, characterized by high levels of population heterogeneity, and is aimed to answer questions that deal with sustainable coexistence with common resource, recognizing early signals that may precede resource exhaustion due to over-consumption, and possible mechanisms of intervention that may save the system from collapse. These results are then applied to viewing cancer as a type of an evolving ecological system, suggesting alternative approaches to dealing with the disease.

The dissertation is organized as follows: methodology, and specifically, a way to reduce otherwise infinitely dimensional systems of differential equations to finite dimensionality in order to be able to study parametrically heterogeneous systems of ODEs using the Reduction theorem, is discussed in Chapter 1. A simple case of application of the Reduction theorem to a consumer-resource type model is going to be studied in Chapter 2, focusing particularly on the questions of *identification of transitional regimes* that a system can go through when the resource is consumed at a higher rate than it is replenished, potentially leading to what has become known as a *tragedy of the commons*. The situation is then going to be reformulated as a *game of prisoner's dilemma*, and one way of dealing with the question of prevention of the tragedy of the commons is going to be discussed in Chapter 3. In Chapter 4 a case when *two possible strategies for interacting with the common resource* are possible will be evaluated with the caveat that in a heterogeneous population, there is no optimal strategy for avoiding the tragedy of the commons.

In the second part of this dissertation, the *ecological framework will be applied to cancer*, evaluating *different strategies* for interaction with the resources that are available to cancer cells within the body in Chapter 5, looking at *cancer metabolism as a game of prisoner's dilemma* in Chapter 6, at *interactions with the immune system in a predator-prey framework* in Chapter 8, and concluding with an *overview of how ecological concepts can be used to forward our understanding and potentially improve cancer treatment* in Chapter 9. A brief introduction to agent-based modeling and a sample model dealing with cancer metabolism is given in Chapter 7. Final conclusions are summarized in Chapter 10.

Chapter 1

INTRODUCTION

On the importance of population heterogeneity

Heterogeneity is one of the major driving forces behind the dynamics of evolving complex systems. When it is heritable and when it affects fitness, heterogeneity is what makes evolution possible [27, 42]. This comes from the fact that the environment in which the individuals interact within one community is composed not only of the outside world (such as the resources necessary for survival, or members of other species) but also of individuals themselves; thus, selective pressures that are imposed on them come both from the environment and from each other, and the pressures from each other will be imposed and perceived differently depending in population composition, which in turn may be changing as a result of these selective pressures.

In a vast majority of conceptual, and often even in descriptive mathematical models of population dynamics, whether it is in models of predator-prey interactions, spread of infectious diseases or tumor growth, population homogeneity is the first simplification that is made. It is not treated as homogeneity per se – rather, one assumes that an average rate of growth or death or infectiousness is a reasonable enough assumption if the system has already reached some kind of stabilized state of evolutionary development. However, by ignoring population heterogeneity in such a way, one ends up either ignoring natural selection or assuming that it has already "done its work", while natural selection is in fact what drives the dynamics of most systems that are of interest and importance.

Evolving populations and adaptive environments

In 1932 Sewall Wright introduced a notion of a fitness landscape, which can be represented as a map, on which the highest fitness (largest difference between birth and death rates) corresponds to the highest elevation. Within this construct the individuals are evolving in such a way as to "climb" the nearest peak, of which there can be just one (single-peak, or simple landscape) or many (rugged landscape) [120]. In an evolving complex system, one can think of environmental changes that stem not only from external forces, such as competition for the resources, but also from internal forces, such as intraspecies competition,

or cooperation, or other types of interactions, as making the fitness landscape on which the population evolves dynamic [58]. This has been termed "dancing landscapes" [120] or seascapes [106, 107] and refers to a situation, where fitness peaks, whether single or multiple, can change over time.

Because the environment in such a framework is dynamic, there exists a type of constant co-adaptation between the individuals and their environment, which can have a number of both positive and negative implications [58]. Some general aspects of modeling this phenomenon are briefly addressed in the next three Chapters of this dissertation, during the discussion on niche construction. Possible implications and consequences of such co-adaptation mechanisms are elaborated on extensively in Chapters 6-9, when the modifications to the tissue microenvironment that are done by cancer cells lead to increased challenges in disease management and treatment.

On methodology: modeling parametrically heterogeneous systems using the Reduction theorem for replicator equations

Equation-based models are usually avoided in questions that require modeling high levels of heterogeneity due to inevitable increase of system dimensionality to the point at which obtaining any kind of qualitative understanding of the system studied becomes impossible. Consequently, one of the main assumptions typically made in equation based models is that of population homogeneity, which, while making systems of equations computationally and sometimes even analytically manageable, make them lose many aspects of system dynamics that come from intraspecies interactions and natural selection. However, the Reduction theorem provides a way to overcome this problem of immense system dimensionality in some selection systems of differential equations.

Notation and some definitions

Selection system: a mathematical model of an inhomogeneous population, in which every individual is characterized by a vector-parameter $\alpha = (\alpha_1, ..., \alpha_n)$ that takes on values from set $\mathbb{A}$.

Clone x_α : set of all individuals that are characterized by a fixed value of parameter α.

Total population size: $N(t) = \sum_{\mathbb{A}} x_\alpha$ if the number of possible values of α is finite and $N(t) = \int_{\mathbb{A}} x_\alpha d\alpha$ if it is infinite.

Growth rate of a clone: $\frac{dx_\alpha}{dt}$

Fitness of an individual within the population: $\frac{dx_\alpha}{dt}/x_\alpha$

Distribution of clones within the population: $P_\alpha(t) = \frac{x_\alpha(t)}{N(t)}$

For all expressions of the type $\frac{\sum_{\mathbb{A}} f(\alpha) x_\alpha d\alpha}{N(t)}$, standard notation $E^t[f]$ of the expected value is used.

General approach

Assume that each individual clone x_α in a population studied is characterized by some parameter value α, which corresponds to a measure of some intrinsic heritable trait, such as birth rate, death rate, resource consumption rate, etc. Then, since different clones can grow and die at different rates, the distribution of clones within the population $P_\alpha(t) = \frac{x_\alpha(t)}{N(t)}$ can change over time due to system dynamics. Consequently, the mean value of the parameter $E^t[\alpha]$, which now becomes a function of time, changes over time as well.

The approach itself requires the following sequence of steps:

1. Analyze autonomous parametrically homogeneous system.
2. Replace parameter α with its mean value $E^t[\alpha]$, which is a function of time.
3. Introduce an "escort" system of differential equations, which define "keystone" variables that actually determine the dynamics of the system. (Note: the term "keystone" is chosen here in parallel to the notion of keystone species in ecology. Just like keystone species have disproportionately large effect on their environment relative to their abundance, keystone variables determine the direction in which the system will evolve, without being explicitly present in the original system).
4. Express the mean of the distributed parameter, which now changes over time due to system dynamics, through keystone variables. The mean of the parameter can now

"travel" through the different domains of the phase-parameter portrait of the original parametrically homogeneous system.

5. Calculate numerical solutions.

Exact rormulation of the Reduction theorem can be found in Appendix. The complete theory underlying the method can be found in Karev [69, 70].

Advantages and drawbacks of the Reduction theorem

One of the most most important properties of the method is that it *allows reducing an otherwise infinitely dimensional system to low dimensionality*.

Like with any method, there are drawbacks to the the Reduction theorem. Most importantly, the transformation can be done (with some generalizations) only to Lotka-Volterra type equations of the form $x(t)' = x(t)F(t, f(E^t[\alpha])$, where $x(t)$ is a vector, α is a parameter or a vector of parameters that characterize individual heterogeneity within the population, and where the form of $f(E^t[\alpha])$ is system-specific. It can also increase the dimensionality of the original parametrically homogeneous system at a possible cost of keystone equations. Finally, the resulting system is typically non-autonomous, so one cannot do standard bifurcation analysis and has to resort to calculating numerical solutions.

When studying numerical solutions of such parametrically heterogeneous systems, one can observe trajectories that one could not previously have seen in parametrically homogeneous systems. This phenomenon results from the expected value of the parameter "traveling" through the phase parameter portrait, undergoing qualitative phase transitions as it crosses the bifurcation boundaries. Moreover, now, if there exists a complete bifurcation diagram for the specific parametrically homogeneous model, one can identify what boundaries have been crossed during the transition.

One can also not only track the distribution of different clones within the population as the system evolves but also observe that different initial distribution can lead to different

trajectories. One can therefore capture this effect of sensitivity to initial population composition both to changes in intrinsic properties of the individuals (such as birth or death rates) or to changes in the external factors (environment) without observing chaotic behavior. This results from the fact that different clones have different fitness depending on initial population composition, since the selective pressures that are imposed on them result not only from the external environment but from surrounding clones as well.

Therefore, the Reduction theorem allows for equation-based models to generate complex behaviors by incorporating all the properties of a complex system (heterogeneity, interdependence, interconnectedness and adaptability) without significantly increasing system dimensionality. Unlike agent-based models, which are the standard computation tool for studying complex systems, the Reduction theorem does not allow incorporating spatial heterogeneity. However, it does have the advantage of formalizing theory through equations and thus at times being able to get analytical conditions to define bifurcation boundaries.

Chapter 2

TRANSITIONAL REGIMES AS EARLY WARNING SIGNALS

Abstract

In this Chapter a question of "how much overconsumption a renewable resource can tolerate" is addressed using a mathematical model, where individuals in a parametrically heterogeneous population not only compete for the common resource but can also contribute to its restoration. Through bifurcation analysis a threshold of system resistance to over-consumers (individuals that take more than they restore) was identified, as well as a series of transitional regimes that the population goes through before it exhausts the common resource and thus goes extinct itself, a phenomenon known as "the tragedy of the commons". It was also observed that 1) for some parameter domains a population can survive or go extinct depending on its initial conditions, 2) under the same set of initial conditions, a heterogeneous population survives longer than a homogeneous population and 3) when the natural decay rate of the common resource is high enough, the population can endure the presence of more aggressive over-consumers without going extinct.

Keywords: resource overconsumption, transitional regimes, tipping points, tragedy of the commons

Introduction

The identification of mechanisms responsible for the observed patterns of coexistence in populations whose survival is intimately connected to their ability to share a common resource is central to the study of ecological sustainability. The notion of niche construction provides but one way to organize and understand how populations can sustainably coexist with their resources. It is the goal of this Chapter to study this question using a simple resource-consumer framework.

The term "niche" was first introduced by Grinnell in 1917 [56] in his efforts to describe how an organism or a population responds to and competes for a common resource. The

interactions of organisms or populations with available resources within their niche are not limited to consumption. Odling-Smee [116] referred to the notion of "niche construction" in situations where organisms not only adapt in response to environmental pressures (for example, consuming the resource in the most efficient manner) but in the process also modify the environment. These adaptive interactions of consumers with their environment re-shape the niche to the needs of the communities that share the resource.

The focus of the discussion throughout this dissertation are consumer-producer systems (C-Ps), where the individuals that compete for resources also contribute differentially to "increases in the size of the pie". The carrying capacity of C-P systems turns out to be a function of the adaptive interactions between resources and the C-Ps. For example, through efficient handling of nutrients some plant species create and support positive feedback loops in their ecosystems and consequently, we observe that while in nutrient-poor environments plants produce slowly-decomposing litter, they grow rapidly and produce easily decomposable substances in nutrient-rich surroundings [60].

Processes of co-adaptation are observed in social environments as well. Individuals learn to respond to or get their clues from the "state" of the environment. Understanding the ramifications of these co-evolving interactions is particularly relevant to the study of how systems respond in times of crisis. Adaptive governance systems, for instance, self organize, drawing on individual characteristics and experiences of the people for the development of shared policies and principles [43, 83, 89, 145].

The impact of co-evolutionary interactions is often a defining force. For example, earthworm burrows carry organic material into the soil, mixing it with inorganic material, creating in the process a basis for microbial activity, causing changes in the inner chemistry of the soil [115, 122, 139]. The environment (soil) has thus been altered over many generations, changing the evolutionary landscape and modifying the selective pressures faced by current generations [115]. *Niche is therefore not a static concept but is an adaptive system in itself.*

Recently, the question, "How can the 'sustainability' of alternative trajectories of human-environment interactions be usefully and rigorously evaluated?" was posed [21]. The need for the development of mathematical frameworks was explicitly addressed: "The central

goal of such frameworks is to help us understand which uses of the natural environment (seen as natural capital) generate sufficiently large, wide-spread and long term benefits to human well-being that they can be valued as supporting sustainable development. (Having an answer to this challenge is what keeps 'sustainability' from being a euphemism for 'environmental protection.')".

The ability to understand and predict possible directions in which the consumer-resource may evolve is crucial in order to successfully achieve sustainable coexistence with common resources. It has been suggested that bifurcations in dynamical systems can correspond to "tipping points" in complex adaptive systems, which in turn may signal upcoming crises. The work presented in this Chapter will elaborate on this notion and present a framework within which one could in fact use transitional regimes in a dynamical system as early warning signs that may signal the need for increased efforts for resource preservation.

For these purposes a generalized model introduced by Krakauer et al. [75] is used, in which individuals within a population compete with each other for common renewable resources. First we investigate the question of the effects of the increases of resource (over)consumption on the entire population, identifying all possible dynamical regimes that the population can go through as it increasingly depletes its resources. Next, we evaluate what transitional regimes the population can go through when it is composed of both individuals that invest into the common resource, and those who over-consume. We conclude this paper with a discussion of the relationship between bifurcations and tipping points, and how one can use understanding of the system's dynamical regimes and bifurcation boundaries to forecast approaching collapse.

Model description

Consider the following generalization of the model introduced in [75], where a population of individual consumers x_c (from here on referred to as clones) compete for the common renewable resource $\widehat{z}$ in such a way as to not only consume the resource but to also be able to contribute to its restoration:

$$\begin{cases} \frac{dx_c}{dt} = rcx_c(1 - \frac{b\sum_{\mathbb{A}} x_c}{kc\widehat{z}}), \\ \frac{d\widehat{z}}{dt} = \gamma + \frac{e}{\widehat{z}+\sum_c x_c}(\sum_{\mathbb{A}} x_c(1-c)) - d\widehat{z}. \end{cases} \tag{2.1}$$

Each clone x_c is characterized by a value of the parameter c, with constant per capita birth rate rc. The per capita death rate is proportional to $\frac{b\sum_{\mathbb{A}} x_c}{kc\widehat{z}}$, where b is the rate of resource consumption, and k is the efficiency of resource consumption by each individual x_c and $\mathbb{A}$ is the range of possible values of c. In this formulation, $\frac{b}{kc}$ denotes "competition efficiency" in obtaining the renewable resource $\widehat{z}$. Resources $\widehat{z}$ are restored naturally at constant rate γ, deteriorate at the rate $d\widehat{z}$ and can be replenished by the activity of x_c; note that the units for x_c and $\widehat{z}$ are the same (biomass).

The rate of consumption/restoration of the common resource in response to the activity of x_c is modeled by the function $\frac{e}{\widehat{z}+\sum_{\mathbb{A}} x_c}\sum_c x_c(1-c)$, where $\frac{\sum_{\mathbb{A}} x_c(1-c)}{\widehat{z}+\sum_{\mathbb{A}} x_c}$ denotes the total resource consumption/restoration rate by all the clones x_c, given both the competition with other clones $\sum_{\mathbb{A}} x_c$ and limitations on total resource accessibility; parameter e denotes the proportion of total resource that is consumed or restored, which can also be seen as per resource rate of restoration. One other way to think about this fractional relationship is in terms of mass action law, or ratio-dependence, i.e. as $e(1-c)\frac{(\sum_{\mathbb{A}} x_c)/\widehat{z}}{1+(\sum_{\mathbb{A}} x_c)/\widehat{z}}$. As the number of consumers x_c increases, the amount of resource $\widehat{z}$ will increase or decrease depending on the value of the parameter $c \geq 0$.

The resource consumption/restoration parameter c is restricted to the interval $c \in [0, \beta]$, since within the frameworks of this model, the rate of niche-construction can neither be negative nor infinite. Letting $\beta = 1$ implies that the individuals in the population never consume more than they produce, making the population completely "altruistic". Letting $\beta > 1$ allows for the presence of over-consumers in the system, so $(1-c)$ can take on negative values, which accounts for strictly consumerist behavior.

The solutions to the equation for population growth (for x_c' and for $N(t)'$) always remain positive. Solutions for the equation for dz/dt can become negative when $c > 1 + \frac{\gamma}{e}$, since $\frac{dz}{dt}|_{z=0} = \gamma + e(1-c)$, which is positive only when $c \in (0, 1+\frac{\gamma}{e})$. For the parametrically heterogeneous system, this condition is modified to be $E^t[c] \in (0, 1+\frac{\gamma}{e})$, which allows some

	Meaning	Range	Units
$\widehat{z}$	amount of renewable resource	$\widehat{z} \geq 0$	$biomass$
x_c	population of clones competing for the resource	$x_c \geq 0$	$biomass$
γ	intrinsic rate of resource growth independent of x_c	$p \geq 0$	$resource/time$
d	per capita rate of natural resource decay	$d \geq 0$	$resource/time$
e	efficiency of niche construction/destruction	$e \geq 0$	$1/time$
r	Malthusian growth rate of x_c	$r \geq 0$	$1/time/resource$
b	rate of resource consumption	$b \geq 0$	$resource$
c	rate of resource consumption\restoration	$c \in [\alpha, \beta]$	$resource$
k	efficiency of resource conversion to population biomass	$k \geq 0$	$clone/resource$
$\widehat{N}$	total population size	$\widehat{N} \geq 0$	$biomass$
N_0	initial population size	$N_0 \geq 0$	$biomass$
μ	parameter of exponential distribution	$\mu \neq 0$	n/a
α	lower boundary value of parameter c	$\alpha \geq 0$	n/a
β	upper boundary value of parameter c	$\beta \geq 0$	n/a

Table 2.1: Summary of variables and parameters used throughout the Chapter.

	γ	d	e	r	b	k	N_0	z_0	μ	α	β
set 1	1	1	1	1	1	1	0.6	0.1	10	0	2.5
set 2	7.72	22	1	1	1	1	0.6	0.1	10	0	9.12

Table 2.2: Sample parameter values

individuals to have higher value of c, as long as the mean of c remains within the specified boundary. This condition becomes important when the system is approaching collapse.

All the variables and parameters are summarized in Table 2.1; sample parameter values used for calculations are given in Table 2.2.

We first revisit the analysis of the case involving a population consisting of a single "average" clone type x_c interacting with a renewable resource in order to identify all the possible dynamical regimes for this system.

Letting $\widehat{N(t)}$ denote the total population size of the population leads to the following simplified version of System (2.1)

$$\begin{cases} \frac{d\widehat{N}}{dt} = r\widehat{N}(c - \frac{b\widehat{N}}{k\widehat{z}}), \\ \frac{d\widehat{z}}{dt} = \gamma + e\frac{(1-c)\widehat{N}}{\widehat{N}+\widehat{z}} - d\widehat{z}. \end{cases} \tag{2.2}$$

Analysis of the parametrically homogeneous system

To simplify the analysis of System (2.2), we first re-scale it by setting $\widehat{N} = A \cdot N$, $\widehat{z} = B \cdot z$, $t = D \cdot \tau$. Taking $A = B = D = r^{-1}$, $\psi = \frac{k}{b}$, $\delta = \frac{d}{r}$, we end up with the following system of differential equations:

$$\begin{cases} \frac{dN}{d\tau} = N(c - \frac{N}{\psi z}), \\ \frac{dz}{d\tau} = \gamma + e(1-c)\frac{N}{N+z} - \delta z. \end{cases} \tag{2.3}$$

The qualitative behavior of System (2.3) depends on the positive parameters c, γ, δ, e and ψ. Taking $\psi = 1$ and fixing e, we divide the parameter space into domains corresponding to topologically different phase portraits of System (2.3) in such way that the boundaries between the parameter domains correspond to bifurcations of the system.

System (2.3) has a singular point at the origin $O(N = 0, z = 0)$. To handle this singularity, we consider the following topologically equivalent system of equations, obtained from System (2.3) via transformation $d\tau = (N+z)z d\widetilde{\tau}$:

$$\begin{cases} N' = N(cz - N)(N + z), \\ z' = ((\gamma - \delta z)(N + z) + eN(1-c))z, \end{cases} \tag{2.4}$$

The trajectories inside the first quadrant Systems (2.3) and (2.4) are topologically orbitally equivalent everywhere except for the point O, which is an equilibrium point of System (2.4) for all parameter values but not for System (2.3).

In the next section we show that System (2.4) can have two more non-negative equilibria, and study structures of all the equilibria.

Null-clines and general structures of non-trivial equilibria.

Five typical cases of null-cline disposition for different values of parameter c (with all other parameters set to 1 for now) are shown in Figure 2.1. Analysis of System (2.4) leads to the following statement concerning the existence and characteristics of non-trivial equilibrium points.

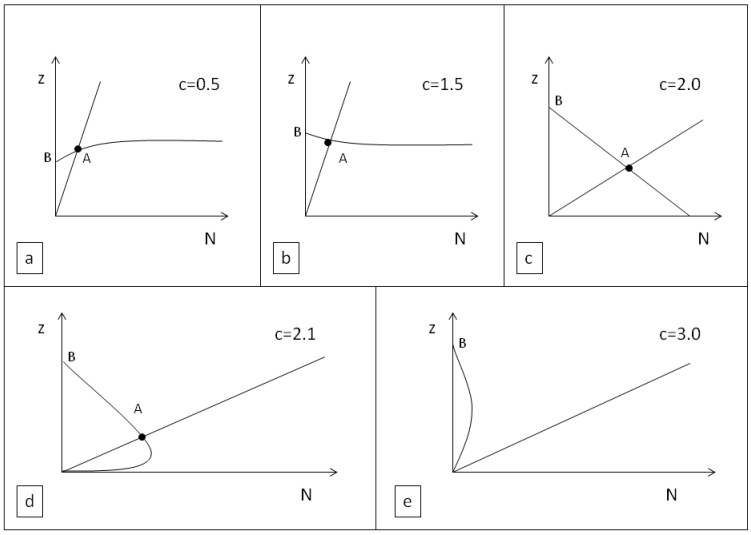

Figure 2.1: Null-clines of System (2.4) for $\gamma = \delta = e = 1$, when c is varied. Equilibrium A exists in sections (a-d) and does not exist in e.

Proposition 1. *Assume $\delta > 0$. Then in the first quadrant, System (2.4) has*

(1) equilibrium point $B(N = 0, z = \frac{\gamma}{\delta})$, which is a saddle.

(2) equilibrium point $A(N = \frac{c}{\delta}(\frac{c(1-c)e}{1+c} + \gamma), z = \frac{1}{\delta}(\frac{c(1-c)e}{1+c} + \gamma))$ for $\frac{\gamma}{e} > \frac{c(c-1)}{c+1}$.

The point A is a topological node, which is stable when $\frac{\gamma}{e} > \frac{c(c-1)(c+c^2+2\delta+c\delta)}{(1+c)^2(c+\delta)} > 0$ and is unstable when $\frac{c(c-1)}{(1+c)} < \frac{\gamma}{e} < \frac{c(c-1)(c+c^2+2\delta+c\delta)}{(1+c)^2(c+\delta)}$.

The proof of the Proposition is given in Appendix.

We use Proposition 1 to identify three parameter boundaries (see Figures 2.1 and 2.4) that correspond to qualitatively different phase portraits of System (2.4):

$$O\gamma : \gamma = 0; Nul : \frac{\gamma}{e} = \frac{c(c-1)}{c+1}; H : \frac{\gamma}{e} = \frac{c(c-1)(c+c^2+2\delta+c\delta)}{(1+c)^2(c+\delta)}.$$

Crossing the boundary Nul from bottom to top is accompanied by the appearance of a positive node A; crossing the boundary $O\gamma$ leads to the appearance of a saddle B in the first quadrant; the boundary H corresponds to changing of stability of equilibrium A, which is accompanied by appearance or disappearance of a limit cycle in the phase plane (Andronov-Hopf bifurcation). Analysis of the model behavior in a neighborhood of equilibrium point A

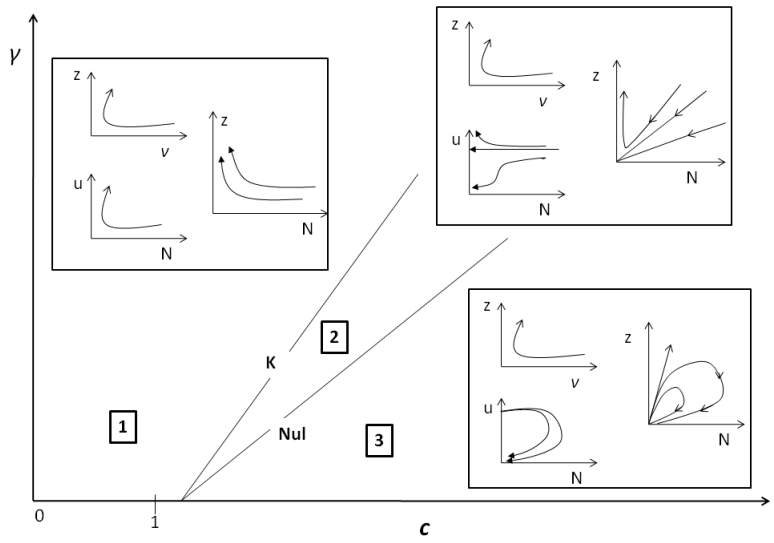

Figure 2.2: Bifurcation diagram of the equilibrium point O, shown through blowing-up transformations.

with parameters close to the boundary H is performed in Section .

Structure of the singular point at the origin

The point O is the non-hyperbolic equilibrium of System (2.4), since both eigenvalues of the Jacobian matrix at the point O are equal to zero. We will apply the "blowing-up transformation" to analyze this point (for general aspects of this method see [12] and references within). We show that the orbit structures in a neighborhood of the point O depend on the parameters in the following way:

Proposition 2. *For any positive fixed values of parameters e and δ, parameter half-plane ($\gamma \geq 0, c \geq 0$) of System (2.4) in a neighborhood of point O is divided into three domains of topologically different phase portraits (see Figure 2.2). Boundaries between the domains are $O\gamma : \gamma = 0$ and $K : \frac{\gamma}{e} = c - 1$.*

The non-trivial asymptote of orbits tending to O is

$$N = -\frac{\gamma}{(1-c)e+\gamma} z(1+o(1)),$$

where $0 < \frac{\gamma}{e} < c - 1$.

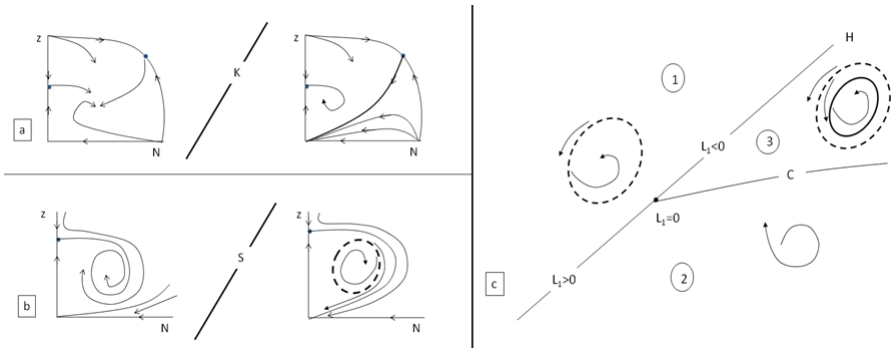

Figure 2.3: Behaviors of System (2.4) (a) within parameter space close to the boundary K, corresponding to the separatrix of the "infinite" equilibrium. (b) within parameter space close to boundary S, corresponding to the heteroclinic connection of separatrices of the saddle point B and the saddle-node point O; (c) within parameter space close to the boundary H; C is the boundary, where stable and unstable cycles annihilate.

The proof of the Proposition is given in the Appendix.

Hopf bifurcation and separatrix bifurcations in the model

Proposition 3

(1) For fixed value of parameter e, System (2.4) has the co-dimension 1 subcritical Hopf bifurcation in the equilibrium A (see Figure 2.3c, Domains 1 and 2) when parameters cross the boundary H : $(\frac{\gamma}{e} = \frac{c(c-1)(c+c^2+2\delta+c\delta)}{(1+c)^2(c+\delta)})$ and parameter $\delta \in (0, 5+\sqrt{24})$, and the co-dimension-1 supercritical Hopf bifurcation when the parameters cross the boundary H and $\delta > 5+\sqrt{24}$ (see Figure 2.3c, Domains 1 and 3).

(2) For $c = c^* = \frac{\delta-1+\sqrt{1-10\delta+\delta^2}}{2}$, the co-dimension 2 generalized Hopf (Bautin) bifurcation is realized in the equilibrium A of the System (2.4) (see Figure 2.3c, Domains 1,2,3).

The proof of the Proposition is given in Appendix.

Unstable limit cycle that surrounds the stable equilibrium point A (see Figure 2.3, Domain 1) appears from heteroclinics composed from the separatrices of the saddle point B and the saddle-node O (see Figure 2.3b), where S is the corresponding parameter boundary. In our analysis we were able to numerically identify this cycle.

Existence of another heteroclinic bifurcation, corresponding to the appearance of attracting parabolic sector in a positive neighborhood of equilibrium O of System (2.4) was

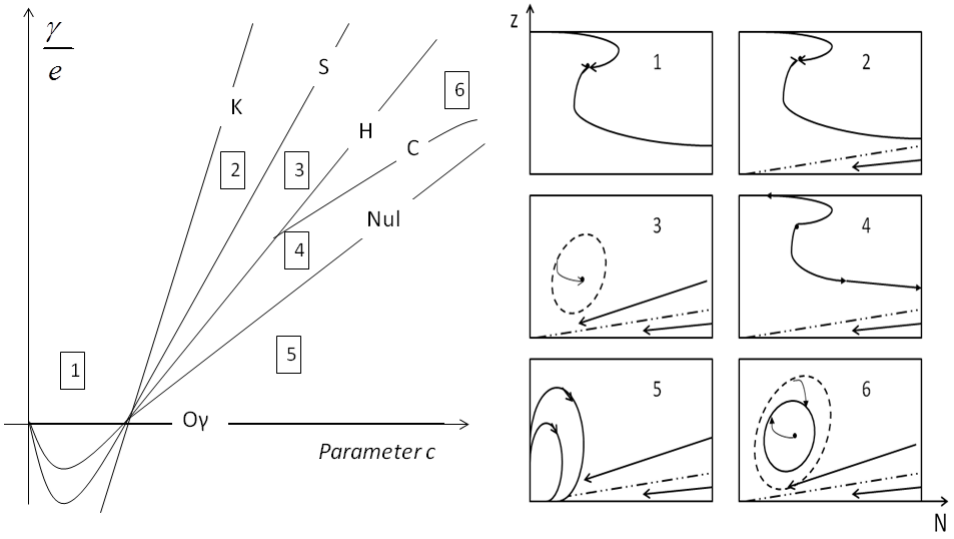

Figure 2.4: Bifurcation diagram of System (2.4) in the (γ, c) and (N, z) phase spaces for fixed positive parameters e and δ. The non-trivial equilibrium point A is globally stable in Domain 1; it shares basins of attraction with equilibrium O in Domains 2 and 3. The separatrix of O and the unstable limit cycle that contains point A, serve, correspondingly, as the boundaries of the basins of attraction. Only equilibrium O is globally stable in Domains 4, which also contains an unstable non-trivial A, and 5, which contains the elliptic sector. Domain 6 exists only for $\delta > 5 + \sqrt{24}$, where the stable limit cycle that is in turn contained inside an unstable limit cycle, shares basins of attraction with equilibrium O. Boundaries between Domains $O\gamma, K, S, H, Nul, C$ correspond respectively to appearance of point B, appearance of an attractive sector in a neighborhood of O, appearance of unstable limit cycle containing A, change of stability of equilibrium A via Hopf bifurcations, disappearance of positive A and saddle-node bifurcation of limit cycles.

shown analytically. This sector appears within parameter values belonging to the boundary K, for which the separatrix of the "infinite" equilibrium in the Poincaré coordinates $(y = \frac{1}{N}, u = \frac{z}{N})$ reaches O (see Figure 2.3a).

The results are summarized in Table 2.3. *For any fixed value of parameter e, (γ, c, δ)-parameter space of the model is divided into 5 domains of different phase behaviors if parameter $0 < \delta < 5 + \sqrt{24}$, and into 6 domains of different phase behaviors if parameter $\delta > 5 + \sqrt{24}$.* Schematic bifurcation diagram is presented in Figure 2.4.

Modeling parametric heterogeneity

In the previous section we studied in detail the effects of resource overconsumption on a parametrically homogeneous population, i.e., the population that is composed of a single "average" consumer type. The system's qualitative behavior in this case will depend solely

Domain	Stability	Attracting sets	Boundary of basin
1	monostability	equilibrium A	global stability
2	bistability	equilibrium A, origin	serapartix $z = \frac{N}{c+\delta}, N \gg 1$
3	bistability	equilibrium A, origin	unstable limit cycle
4	monostability	origin	global stability
5	monostability	origin	elliptic sector
6	bistability	stable limit cycle, origin	unstable limit cycle, A

Table 2.3: Summary of possible dynamical regimes of System (2.4); Domain 6 exists only when $\delta > 5 + \sqrt{24}$

on the the initial conditions and parameter values, and especially on the initial value of c.

Now, consider a situation, where the population is parametrically heterogeneous with respect to the value of c, namely, when there are distinct classes of individuals within the population that consume and restore the common resource at different rates. Mathematically, this is described by assigning a different value of parameter c to each clone x_c.

Let $\mathbb{A}$ denote the range of possible values of parameter c. Denote the total population size to be $N(t) = \sum_A x_c$ if the number of possible values of c is finite and $N(t) = \int_{\mathbb{A}} x_c dc$ if it is infinite. Define $P_c(t) = \frac{x_c(t)}{N(t)}$ and $E^t[c] = \int cP_c(t)dt$. Then, applying re-parametrization, given in Subsection , to System (2.1), we obtain that $\int_{\mathbb{A}} x_c(1-c) = N - N\int_{\mathbb{A}} cP_c(t)dc = N(1-E^t[c])$, which yields the following system of equations:

$$\begin{cases} \frac{dx_c}{dt} = x_c(c - \frac{N}{\psi z}), \\ \frac{dz}{dt} = \gamma + e(1-E^t[c])\frac{N}{N+z} - \delta z. \end{cases} \tag{2.5}$$

Let us also introduce a keystone variable $q(t)$, such that $\frac{dq}{dt} = \frac{N(t)}{\psi z}$. Then $x_c' = rx_c(c - q')$. Consequently

$$x_c(t) = x_c(0)e^{ct - q(t)},$$

and thus

$$N(t) = \int_{\mathbb{A}} x_c(t)dc = N_0 e^{-q(t)} \int_{\mathbb{A}} e^{ct} P_c(0)dc = N_0 e^{-q(t)} M_0(t),$$

where $P_c(0) = \frac{x_c(0)}{N(0)}$ and $M_0(t) = \int_0^\infty e^{ct} P_c(0) dc$ is the moment generating function (mgf) of the initial distribution of clones $P_c(0)$ within the population. The frequency of each individual x_c in the population is given by $P_c(t) = \frac{x_c(t)}{N(t)} = P_c(0)\frac{e^{ct}}{M_0(t)}$, which, as one can see, in this case does not depend on the keystone variable $q(t)$.

From the equations for the moment generating function of the initial distribution and the frequency of clones x_c in the population one can easily calculate the expected value of c at each time point t:

$$E^t[c] = \int_{\mathbb{A}} cP_c(t)dc = \int_{\mathbb{A}} cP_c(0)\frac{e^{ct}}{M_0(t)}dc = \frac{M_0(t)'}{M_0(t)}. \tag{2.6}$$

We can now rewrite System (2.1) in the following form:

$$\begin{cases} \frac{dN}{dt} = N(E^t[c] - \frac{N}{\psi z}), \\ \frac{dz}{dt} = \gamma - \delta z + \frac{eN}{N+z}(1 - E^t[c]), \end{cases} \tag{2.7}$$

where $E^t[c]$ is defined above.

The dynamics of System (2.7) will thereby be fully determined by the mgf of the initial distribution of individuals x_c within the population.

Note that in comparison to the parametrically homogeneous System (2.4), in the parametrically heterogeneous System (2.7) the fixed value of the parameter c has been replaced by the expected value of c at each time instant t. It is easy to verify that the rate of change of $E^t[c]$ is equal to the variance of c at each time moment t in accordance to Fisher's fundamental theorem, so as the system evolves with time, the expected value of c will also change with each time step, causing it to "travel" through the phase-parametric portrait [69].

Exponential initial distribution

Complete data about initial distribution of clones within the population is not always available. If this is the case, then, according to [64] and [68], if the mean value of a non-negative random variable is the only quantity that can be estimated from observations, then exponential distribution with the estimated mean is the most likely distribution of the

variable. Moreover, when the values of the random variable are bounded and belong to an interval, and the mean value of the reproduction rate is again prescribed, then according to the maximum entropy principle, the initial distribution is a truncated exponential on that interval (for more details see [68]).

So, let us first assume that the value of the parameter c is exponentially distributed within the population; it can take on values in the range $(0,\infty)$. Its mgf is $M_0(t) = \frac{\mu}{\mu - t}$, where μ is the parameter of the exponential distribution. The mean of c is $E^t[c] = \frac{1}{\mu - t}$, and so System (2.7) can be rewritten as:

$$\begin{cases} \frac{dN}{dt} = N(\frac{1}{\mu - t} - \frac{N}{\psi z}), \\ \frac{dz}{dt} = \gamma - \delta z + \frac{eN}{N+z}(1 - \frac{1}{\mu - t}) \end{cases} \tag{2.8}$$

In this case the mean value of $E^t[c] \to \infty$ when $\mu = t$, and so the population becomes extinct in finite time.

Truncated exponential initial distribution

Of course, the assumption that parameter c can take on arbitrarily large values is not realistic, although it does simplify asymptotic analysis. Hence, we proceed to consider the situation when the value of the parameter c is exponentially distributed within the population but is bounded on an interval $c \in [0, \beta]$.

The mgf of truncated exponential distribution is $M_0(t) = (\frac{\mu}{e^{\beta\mu} - 1})(\frac{e^{\beta\mu} - e^{\beta t}}{\mu - t})$, where μ is the parameter of truncated exponential distribution, and β is the boundary value of the parameter c. System (2.7) in this case becomes

$$\begin{cases} \frac{dN}{dt} = N(t)(\frac{\beta e^{\beta t}}{e^{\beta t} - e^{\beta\mu}} + \frac{1}{\mu - t} - \frac{N(t)}{\psi z(t)}), \\ \frac{dz}{dt} = \gamma - \delta z(t) + \frac{eN(t)}{N(t) + z(t)}(1 - \frac{\beta e^{\beta t}}{e^{\beta t} - e^{\beta\mu}} - \frac{1}{\mu - t}) \end{cases} \tag{2.9}$$

In case of the truncated exponential distribution, the question of finding the threshold of system resistance to overconsumption becomes of particularly interesting. Intuitively, we would expect that if the parameter c does not surpass the threshold of resistance to over-consumption, i.e., stays outside of Domains 4 and 5 outlined in Figure 2.4, then the

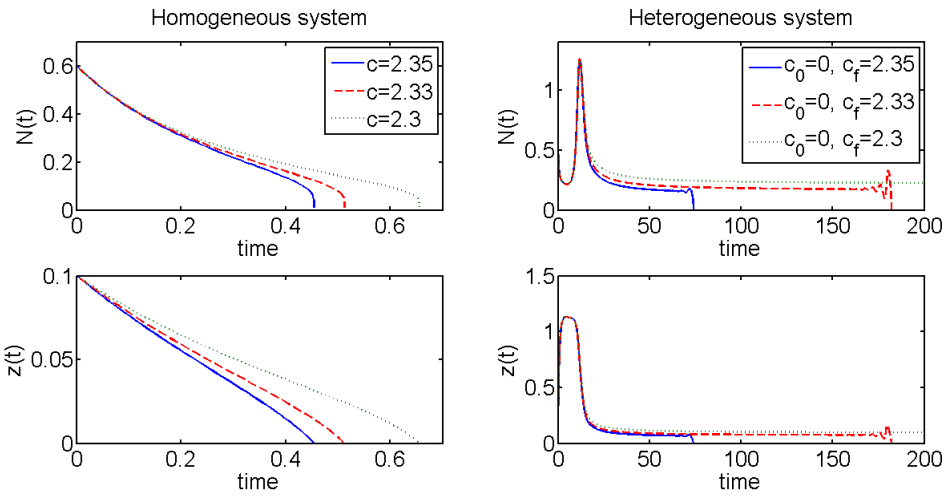

Figure 2.5: Comparison of trajectories of Systems (2.3) and (2.7) under different values of c and $[\alpha, \beta]$ respectively. Other parameter values are taken from set 1 of Table 2.2.

population, while evolving towards the highest value of c and favoring the most efficient consumers, would nevertheless fail to exhaust its resources. However, if the maximum value of the parameter c falls beyond the threshold of system resistance to over-consumers, which was analytically identified in the previous section, then c will eventually reach its maximum possible value, slipping into one of the trajectories that lead to resource exhaustion and eventual population extinction (see Figure 2.5b).

A particularly curious and unexpected effect can be observed when one varies the value of the parameter δ, which represents the rate of natural resource decay (in terms of original parameters, $\delta = \frac{d}{r}$, where d is the per capita rate of resource degradation and r is the Malthusian growth rate of each clone x_c). Parameter δ accounts for the appearance of a domain of coexistence of two limit cycles (generalized Hopf, or Bautin bifurcation), which can be observed when $\delta > 5 + \sqrt{24}$ (a condition that was obtained analytically through calculation of the first Lyapunov value). In this region, a stable limit cycle is trapped between an unstable limit cycle on the outside and a stable equilibrium point inside. This effect can be observed either when the rate of natural resource decay is very high or when the number of competing individuals left within a population is very small.

Another question of interest would be to compare the tolerance thresholds of the parametrically homogeneous and heterogeneous systems. Intuitively we would expect the

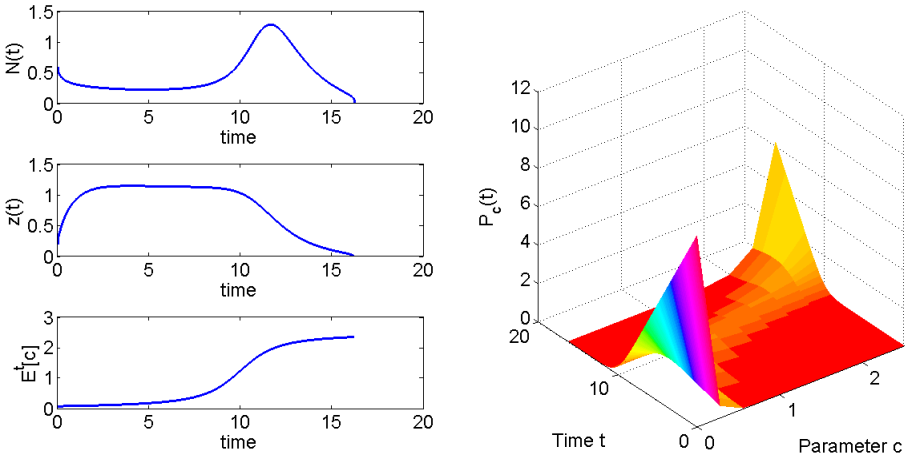

Figure 2.6: System (2.9) with initial truncated exponential distribution on the interval (α, β), with parameter values from set 1 in Table 2.2. This is an example of what transitional regimes the System can go through before the population crashes, with trajectories for the total population size $N(t)$, total amount of renewable resource $z(t)$ and expected value of the parameter c on the left, and the change over time of the distribution of various clone types within the population on the right.

tolerance threshold of the parametrically heterogeneous system to be higher. Even though in the parametrically heterogeneous system there are more over-consumers present in the population, there are also more "altruists", or under-consumers (unlike the parametrically homogeneous system, where all individuals are characterized by a single average value of c).

Indeed, in the parametrically homogeneous System (2.3), as c increases, the total population size grows until the number of over-consumers becomes so large that they consume more than the system can support. However, a parametrically heterogeneous population can survive much longer, since the depletion of resources caused by over-consumers is at least temporarily compensated for by the activity of under-consumers, as can be seen on Figure 2.5.

Discussion

In this Chapter we modify a generalized consumer-producer type model with renewable resource that was introduced by [75] in order to investigate two questions: 1) whether a largely consumerist homogeneous population can nevertheless sustainably coexist with common renewable resources and 2) whether a heterogeneous population that consists of both “altruistic” under-consumers and “selfish” over-consumers can successfully establish a niche,

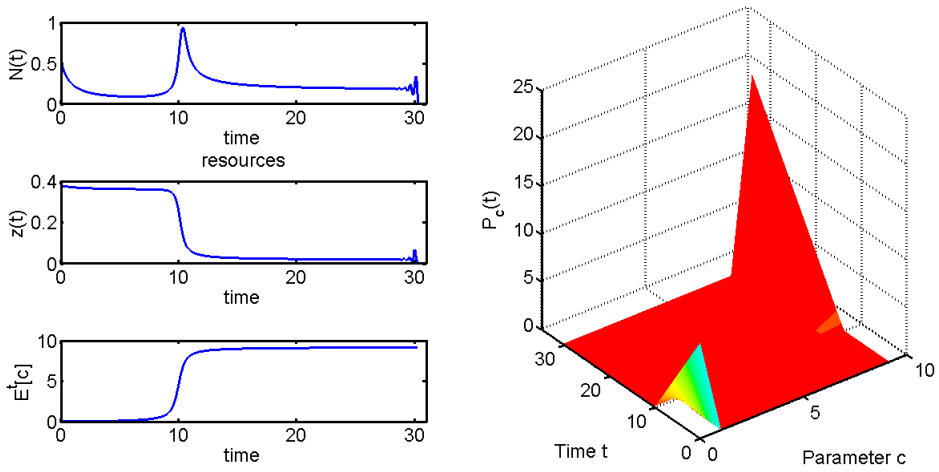

Figure 2.7: System (2.9) with initial truncated exponential distribution on the interval (α, β), with parameter values taken from set 2 in Table 2.2. An example of what transitional regimes the System can go through before the population crashes, with trajectories for the total population size $N(t)$, total amount of renewable resource $z(t)$ and expected value of the parameter c on the left, and the graph of the change over time in distribution of various clone types within the population on the right. Initial conditions fall within the parameter range of Domain 6 of the phase-parameter portrait of the the non-distributed system. Since the rate of natural resource decay is high, it takes more time even for the most efficient consumer to "get to it", and so the population survives longer, and the transitional regimes are more evident.

which in our framework is defined as the population maintaining non-zero size without exhausting the commons resource over time, and if it cannot, what dynamical regimes it goes through before it collapses.

First, we investigated the possible dynamical regimes that can be observed in the system, when the population is parametrically homogeneous, i.e., when each individual in the population has the same value of the resource consumption/restoration parameter c. Our analysis indicates that even when the population consists of a large number of over-consumers, there is a threshold for system resistance to over-consumers, which is directly proportional to the average natural growth rate of the resource γ and inversely proportional to individuals' average efficiency of niche construction, modeled by the parameter e. Hence, the system can tolerate more over-consumers if it can restore itself quickly enough or if the individuals are not overly efficient in resource consumption.

As the number of over-consumers increases (modeled via increases in the value of

parameter c), the population goes through a series of transitional regimes (see Figure 2.4) before it collapses. When the value of c is small, consumers-producers and the resource can coexist peacefully (stable non-trivial equilibrium point). As c increases, an unstable limit cycle appears around the stable equilibrium point. Further increases in c drive the dynamics into the domain, where the non-trivial equilibrium point still exists but is unstable. Interestingly, if the value of the parameter $\delta = \frac{d}{r}$ in the region of oscillatory behavior is above a certain threshold, specifically when the natural resource decay rate d is very high or the rate of growth r of each individual within the population is small, the system realizes a supercritical Hopf bifurcation, resulting in coexistence of a stable limit cycle trapped between an unstable equilibrium point and an unstable limit cycle; both cycles disappear only after passing this region, leaving an unstable non-trivial equilibrium point. Further increases in c lead to disappearance of the non-trivial equilibrium from the first quadrant, changing the point $O(0,0)$ from a saddle-node to an elliptic sector, which corresponds to eventual extinction of both the resource and the population, although in infinite time.

The system has a non-hyperbolic singular point at the origin that, as the parameters are varied, changes its structure from a saddle to a stable saddle-node with a sector of trajectories tending to the origin, to an elliptic sector. As parameters are varied, the non-trivial equilibrium in the model changes its stability as a result of a "catastrophic" Andronov-Hopf bifurcation, yielding a parameter region, where an unstable limit cycle divides the basins of attraction of the non-trivial equilibrium and the origin. No stable oscillations can be observed, and the system eventually "dies out" because as c increases, an increasing number of trajectories tend towards the origin. It is the mutual placement of separatrices that determines the structure of the phase portrait (or in other words, it is the ratio of the consumer to the resource that determines the existence of the attractive sector at the origin). Notably, the unstable limit cycle appears from heteroclinic orbits of the origin and the saddle point B. These are new type of dynamics compared to other models that have a complex equilibrium point at the origin [10–12, 61, 76].

Next, a heterogeneous population involving both individuals that contribute to the growth of common resource and those that consume more than they restore, was considered.

We reformulated the original system of equations by replacing the fixed parameter c by its current mean value, which was computed with the help of moment generating function of the initial distribution of the individuals throughout the population [69].

Within the framework of this problem, the value of c is restricted to the positive half plane, thus limiting the possible choices of the initial distribution. If the only information available about c within the population is its mean, then the exponential distribution is a good choice for an initial distribution since it does not require any additional assumptions. In particular, according to the principle of maximum entropy or MaxEnt [64, 68], if the mean value of a non-negative random variable is the only quantity that can be estimated from observations or other data, then the most likely (the maximum entropy) distribution of the variable is the exponential with the estimated mean. Moreover, when the values of the random variable are bounded and belong to an interval, and the mean value of the reproduction rate is again prescribed, then according to the MaxEnt principle, the initial distribution is the truncated exponential in that interval [68].

Therefore, we first assumed that the parameter c is distributed exponentially within the population. In this case the parameter c can take on values that by far surpass the threshold of system resistance to over-consumers. As a result, the clones with an arbitrarily large parameter value is favored by natural selection at each time point, ensuring extinction of the population due to resource exhaustion regardless of the initial state of the population or the resources. Arbitrarily large rates of consumption allowed by the exponential distribution are clearly unrealistic, since the population goes extinct in finite time.

Next, we restricted the values of c to a finite interval, thus assuming truncated exponential distribution. Intuitively, we would once again expect the population to evolve in such a way as to favor the most efficient consumer, i.e. until c reaches its largest possible value.

Numerical solutions computed for the parametrically heterogeneous model with truncated exponential distribution show that some regimes of the original model are just transitional (see Figures 2.6, 2.7). We observed that even though the boundary for the threshold of system tolerance to over-consumers is the same for both parametrically homogeneous

and heterogeneous systems, the time to extinction is longer for the parametrically heterogeneous model (Figure 2.5). So, population heterogeneity ensures longer period of survival both for the population and the resource than would have been observed in a homogeneous population.

Conclusions

The situation, when overly efficient consumers over-exploit the common resource in such a way as to eventually make it useless for everyone, playing out the tragedy of the commons [57], occurs quite frequently, such as when overly efficient parasites, bacteria and cancer cells commit evolutionary suicide by ruining their resource (the host); instances of the tragedy of the commons have also been observed in microbes [128], slime molds [44], plants [173], as well as in human populations. These examples are representative of so-called "tight co-evolution", where the survival of the population is intimately tied to a particular resource, as opposed to "diffuse co-evolution", when the population's survival is determined by interactions with other species and multiple resources [85, 87].

It's not always clear that system collapse is approaching, and so one has to learn to recognize early warning signals, such as increased flickering and data auto-correlation [137], in order to try and and prevent the tragedy of the commons. Scheffer [136, 137] suggested that tipping points in complex systems correspond to bifurcational boundaries in dynamical systems. Application of Reduction theorem for replicator equations [69] to relevant systems of ODEs allows to visualize exactly how the system passes through these dynamical regimes as it evolves. One can see that while changes in population size and the resource over time may seem to give no cause for alarm, the mean value of the parameter of over-consumption may signal trouble: the system will be recalibrating towards maximizing c, and as soon as the buffer capacity of the resource (in this case it is proportional to natural resource restoration and decay rates) is exhausted, both the population and the resource collapse (see Figure 2.7).

This can be important for a number of reasons. Firstly, given sufficient understanding of the system that one may wish to study, one may be able to write a sufficiently conceptually simple model, where it is possible to analytically find bifurcation boundaries. In this case, one

would know exactly what parameters would need to be manipulated in what combinations in order to try and avoid the tragedy, if it is still possible.

Secondly, this gives an opportunity to identify another early warning signal of approaching system collapse in addition to flickering and increased auto-correlation [137]. One can try to see what the expected value of the characteristic in question is and match that up with the corresponding predicted possible dynamical regimes. A challenge here is of course that even if one can identify the bifurcation boundaries, even if only numerically, it may not always obvious in which direction the system will evolve, and which clone type will be favored. The answer to this question is going to be system specific and needs to be taken carefully into account if one is to use these methods in order to make qualitative predictions about population evolution within any dynamical system.

Chapter 3

PUNISHMENT/REWARD SYSTEM IN PREVENTING THE TRAGEDY OF THE COMMONS

Abstract

The conditions that can lead to the exploitative depletion of a shared resource, i.e., tragedy of the commons, can be reformulated as a game of prisoner's dilemma: while preserving the common resource is in the best interest of the group as a whole, over-consumption is in the interest of each particular individual at any given point in time. One way to try and prevent the tragedy of the commons is through infliction of punishment for over-consumption and rewarding under-consumption, thus selecting against over-consumers. The effectiveness of various punishment functions in an evolving consumer-resource system is evaluated within a framework of an infinitely-dimensional system of ODEs. Conditions leading to the possibility of sustainable coexistence with the common resource for a subset of cases are identified analytically using adaptive dynamics; the effects of punishment on heterogeneous populations with different initial composition are evaluated using the Reduction theorem for replicator equations. Obtained results suggest that one cannot prevent the tragedy of the commons through rewarding of under-consumers alone - one also needs to implement some degree of punishment, which may vary depending on the initial distribution of clones in the population.

Keywords: tragedy of the commons, prisoner's dilemma, payoff modification through punishment, adaptive dynamics, population heterogeneity

Introduction

Complex adaptive systems from ecology and the social sciences are composed of diverse agents that are interconnected and interdependent [102, 119, 120]. Heterogeneity within these systems often drives the evolution and adaptability of the system components enabling them to withstand and recover from environmental perturbations. However, it is also heterogeneity that makes the appearance and prosperity of over-consumers possible, which

in turn can lead to exhaustion of the common resources (tragedy of the commons [57]) and consequent collapse of the entire population, leading to what has become known as evolutionary suicide [129].

Elinor Ostrom [117] has focused on the question of avoiding the tragedy of the commons from the point of view of collective decision making in small fisheries. She observed that the mutually satisfactory and functioning institution of collective action could be developed in small communities where the possible overconsumption of each individual made a significant enough difference to be immediately noticeable and punishable. This illustrates a first path to prevent the tragedy of the commons: *infliction of punishment/ tax for over-consumption* effectively selecting against over-consumers.

Another situation, when the tragedy was successfully avoided, is when the community introduces some kind of "social currency", where one is rewarded for cooperation with social status [101, 162]. This can be an example of a second approach to preventing the tragedy of the commons: *bestowing reward/ subsidy to under-consumers.*

The dynamics of trade-offs between personal and population good have been studied through classical game theory [114, 161, 165]. However, many of the potentially relevant results have been obtained for either two-player or infinite-player games, while intermediate situations are still poorly understood. We study such models using two recently developed methods for studying evolving heterogeneous populations through ordinary differential equations: adaptive dynamics [52] and the Reduction theorem for replicator equations [69, 70].

This Chapter is organized as follows: first we will describe different approaches for studying the effects of punishment and reward on population composition, namely, adaptive dynamics and the Reduction theorem for replicator equations. Then we apply the two techniques to a variety of punishment/ reward structures, obtaining both analytical and numerical results for populations that differ in their initial composition with respect to over- and under-consumers. The Chapter ends with a reformulation of the obtained results in the context of the prisoner's dilemma, as well as witha comparison of the two modeling methods.

Model description

Consider the previously studied model of ecological niche construction, where a pop-

Variable/ Parameter	Meaning	Range
$x_c(t)$	Individual consumers, characterized by the value of c	$x_c > 0$
$z(t)$	Renewable resource	$z(t) > 0$
$N(t)$	Total population size $N(t) = \sum_c x_c(t)$	$N(t) \geq 0$
a	Severity of enforcement of punishment/reward	$a \geq 0$
c	Parameter of resource overconsumption	$c \geq 0$
r	Intrinsic growth rate of consumers	$r \geq 0$
b	Rate of resource consumption	$b \geq 0$
k	Efficiency of resource consumption	$k > 0$
p	Natural resource renewal rate	$p \geq 0$
d	Natural resource decay rate	$d \geq 0$
e	Proportion of resource consumed by competing clones	$e \geq 0$
μ	Parameter of truncated exponential distribution	$\mu \in \mathbb{R}$
$[\alpha, \beta]$	Parameters of Beta distribution	$\alpha > 0, \beta > 0$

Table 3.1: Summary of variables and parameters of System (3.1)

ulation of consumers-producers $x(t)$ interact with the common dynamic resource $z(t)$ in such a way as to be able to not only consume the resource but also contribute to its restoration (see System 2.1 on page 9). Each consumer-producer is characterized by his or her own intrinsic value of resource consumption/restoration, denoted by parameter c. Now assume that each over-consumer is punished for over-consumption, or rewarded for restoring the resource, according to some general function $f(c) \in C^1(\mathbb{R}^+)$, which directly affects fitness of each consumer-producer, depending on the value of c. The system thus becomes:

$$\begin{cases} \underbrace{x_c}_{\text{clones}}(t)' = \underbrace{rx_c(t)\Big(\underbrace{c}_{\text{consumption}} - \frac{b\sum_{\mathbb{A}} x_c(t)}{kz(t)}\Big)}_{\text{carrying capacity is dynamic resource}} + \underbrace{x_c(t)f(c)}_{\text{punishment/reward}} \\ \underbrace{z(t)'}_{\text{resource}} = \underbrace{p}_{\text{natural restoration}} + \underbrace{e\frac{\sum_{\mathbb{A}} x_c(t)(1-c)}{z(t)+\sum_{\mathbb{A}} x_c(t)}}_{\text{total resource consumption}} - \underbrace{dz(t)}_{\text{natural decay}} \end{cases} \tag{3.1}$$

Meaning of all the variables and parameters is summarized in Table 3.1.

No punishment

The case, where $f(c) = 0$ was previously completely studied in Chapter 2. The results are summarized in Figure 2.4 on page 15 and can be interpreted as follows: in Domain 1, when the parameter of overconsumption is small, the population can stably and sustainably coexist

with the common renewable resource, since no individual is taking more resource than they restore. In Domain 2, a parabolic sector appears near the origin, decreasing the domain of attraction of the non-trivial equilibrium point A. The population can still sustainably coexist with the resource even with moderate levels of over-consumption but the range of initial conditions, where it is possible, decreases. As the value of c is further increased, the range of possible initial conditions that allow sustainable coexistence with the common resource decreases and is now bounded by the unstable limit cycle, which appears around point A from a loop of separatrices that connect points B and Oin Domain 3, and via generalized Hopf bifurcation in Domain 6, where the outer unstable limit cycle appears from the separatrix loop and inner stable cycle arises due to a Hopf bifurcation of point A. Finally, in Domain 4 and 5, population extinction is inevitable due to extremely high overconsumption rates that the resource can no longer support.

In this Chapter the question of whether punishment for overconsumption can prevent the tragedy of the commons by selecting against over-consumers using different punishment functions that directly affect individuals' fitness will be investigated. We will also investigate the degree of effectiveness of punishment depending on initial composition of the population with respect to parameter c. Finally, we will try to investigate the question of whether punishing those who over-consumer or rewarding those who do not, will yield better results. These questions will be addressed using two recently developed methods for modeling parametrically heterogeneous populations, namely, adaptive dynamics [52] and Reduction theorem for replicator equations [69, 70].

Adaptive dynamics

Adaptive dynamics is a series of techniques that have been developed in the past twenty years to address questions of system invasibility by rare "mutant" clones. The main focus of this method is in evaluating whether a mutant will or will not be able to proliferate in an environment, set up the resident population, using ideas of frequency dependence from game theory and standard bifurcation analysis [52]. We will use this method to answer analytically the questions of the intensity of punishment that may need to be imposed on over-consumers in order to prevent the tragedy of the commons.

Assume that the population has reached some kind of an equilibrium state, and the invading over-consumer is very rare. Consider the equation for the dynamics of the rare mutant x_m in an environment set by the resident x_{res}:

$$\frac{x'_m}{x_m} = r(c_m - \frac{b(x_{res}+x_m)}{kz}) + f(c_m). \tag{3.2}$$

The total population is $x_m + x_{res} \approx x_{res}$ since x_m is assumed to be present at such low frequency that its contribution to the size of the entire population is negligible; $f(c)$ is the punishment/reward function.

Let x^*_{res} satisfy $\frac{dx_{res}}{dt} = 0$, which implies that $x^*_{res} = \frac{kz}{br}(f(c_{res}) + rc_{res})$. Now introduce a mutant, such that

$$\frac{dx_m}{dt} = rx_m(c_m - b\frac{x_m + x_{res}}{kz(t)}) + x_m f(c_m). \tag{3.3}$$

When the two subpopulations interact, the outcome of their interaction is determined by the sign of the dominant eigenvalue of System

$$\begin{cases} \frac{dx_{res}}{dt} = rx_{res}(c_r - b\frac{x_m+x_{res}}{kz(t)}) + x_{res}f(c_{res}), \\ \frac{dx_m}{dt} = rx_m(c_m - b\frac{x_m+x_{res}}{kz(t)}) + x_m f(c_m), \\ \frac{dz}{dt} = p + e^{\frac{x_{res}(1-c_{res})+x_m(1-c_m)}{z+x_{res}+x_m}} - dz. \end{cases} \tag{3.4}$$

The largest eigenvalue that governs the dynamics of this system at the point $x_{res} = x^*_{res}$, $x_m = 0$ is given by $\lambda_2 = r(c_m - c_{res}) - f(c_{res}) + f(c_m)$. The two eother eignevalues λ_1 and λ_3 govern the dynamics on the monomorphic subspace $(x_{res}, 0, z)$ and by assumption have negative real part. Otherwise, the non-trivial resident equilibrium would by definition be unstable, rendering the question of system invasibility irrelevant.

These conditions allow answering the question of "short term" invasibility, i.e., whether a mutant with arbitrarily different value of $c_m$will be able to invade the population.

Invasion fitness of the mutant, i.e., the expected growth rate of a mutant in an environment set by the resident, is given by

$$\lim_{T\to\infty} \frac{1}{T}\int_0^T r(c_m - \frac{bx_{res}(t)}{kz(t)}) + f(c_m)dt = r(c_m - \frac{b}{k}\overline{(\frac{x_{res}}{z})}) + f(c_m) = r(c_m, E_{res}) \tag{3.5}$$

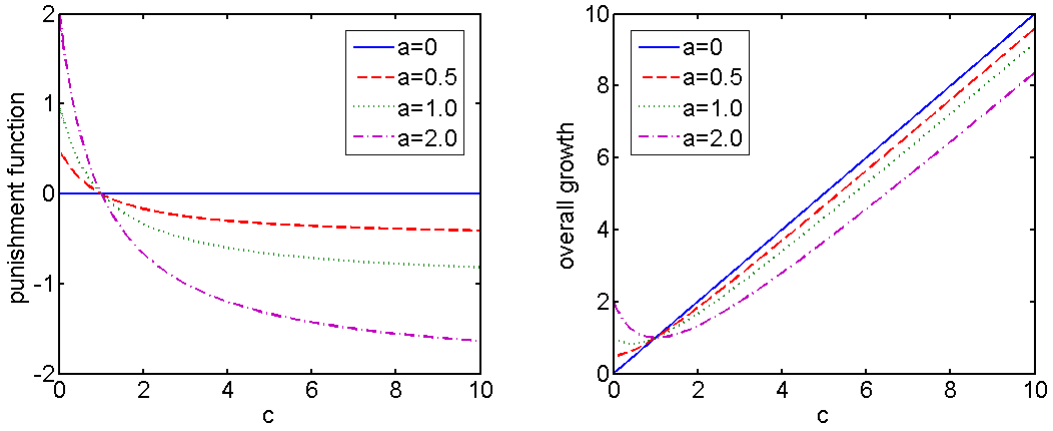

Figure 3.1: Case 1. Punishment-reward function of the form $f(c) = a\frac{1-c}{1+c}$ and its effects on population growth.

and the selection gradient, which is defined as the slope of invasion fitness and which determines whether the invasion will be successful (positive sign of the selection gradient predicts successful invasion), is then given by

$$D(c_m) = \frac{\partial}{\partial c_m} r(c_m, E_r)|_{[c_m = c_{res}]} = r + f'(c_m). \tag{3.6}$$

These conditions allow answering a question of "long-term" invasibility, i.e., whether a mutant with a slightly difference value of $c_m$will be able to permanently invade the population of individuals, characterized by parameter c_{res}.

Another way to derive the same condition is by looking directly at the expression for λ_2, which can be rewritten as $r(c_m - c_{res}) - f(c_{res}) + f(c_m) = r + \frac{f(c_m)-f(c_{res})}{c_m - c_{res}} \approx r + f'(c_m)$. The points where selection gradient is zero are known as evolutionarily singular strategies and are denoted here as c^*_{res}. Stability of c^*_{res} for different types of punishment/reward functions is discussed below; summary of some of the possible types of c^*_{res} is summarized in Table 3.2.

Different types of punishment/reward functions

Case 1. Moderate punishment\reward.

Consider the case when the punishment function is of the form $f(c) = a\frac{1-c}{1+c}$ (see Figure 3.1).

In this case, the PIP can be seen on Figure 3.4a,c, for $a = 1$ and $a = 4$. Blue regions correspond to the case when $\lambda_2(c_{res}, c_m) < 0$, and consequently the mutant cannot invade; red

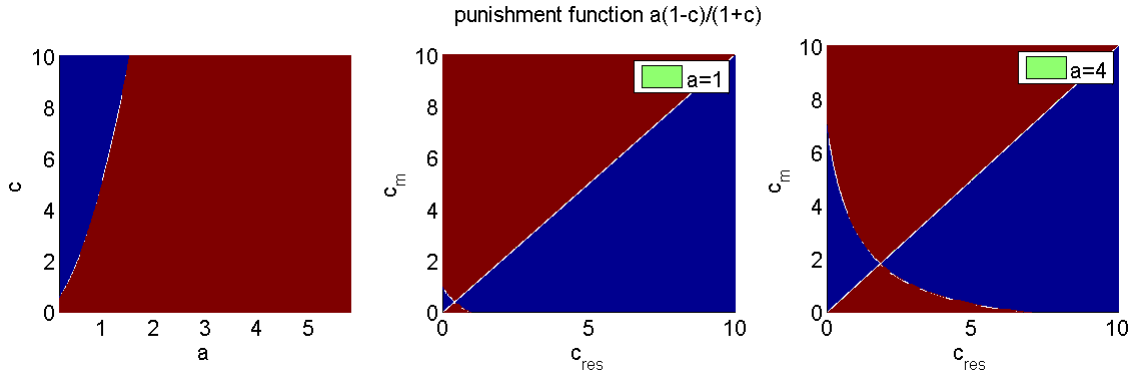

Figure 3.2: Selection gradient and pairwise invasibility plots for function of the type $f(c) = a\frac{1-c}{1+c}$. Blue regions correspond to parameter values where the mutant cannot invade; red regins correspond to parameter values where it can invade. (a) selection gradient, defined in 3.6, where $a \in [3-2\sqrt{2}, 3+2\sqrt{2}]$ (b) PIP for $a = 1$; the singular strategy c^*_{res} is evolutionarily unstable and convergence stable (c) PIP for $a = 4$; the singular strategy c^*_{res} is evolutionarily unstable and convergence stable. Ths punishment/reward function is not effective against agressive overconsumers.

regions correspond to the case when $\lambda_2(c_{res}, c_m) > 0$, and the mutant can invade. The point of intersection of the two curves corresponds to a convergence stable (CSS) evolutionarily unstable strategy, which can be invaded by "mutants" with large enough values of c_m.

Modest punishment can therefore protect only from modest over-consumers. However, severe over-consumers cannot be kept of out the population, as the punishment is not severe enough.

The selection gradient for this punishment function is $D(c_m) = r - \frac{2a}{(1+c_m)^2}$, which is equal to zero when $c_m = \sqrt{2a/r} - 1$, so the mutant can invade, when $a > \frac{r}{2}$.

Case 2. Severe punishment\generous reward.

Now consider a case, when the punishment function is of the form $f(c) = a(1-c)^3$ (see Figure 3.3).

The PIP for this functional form can be seen on Figure 3.4 for $a = 0.05$ and $a = 0.14$. Once again, blue regions correspond to the case when $\lambda(c_{res}, c_m) < 0$, and consequently the mutant cannot invade; red regions correspond to the case when $\lambda(c_{res}, c_m) > 0$, and the mutant can invade.

For this type of punishment/reward function, there is a region where invader can

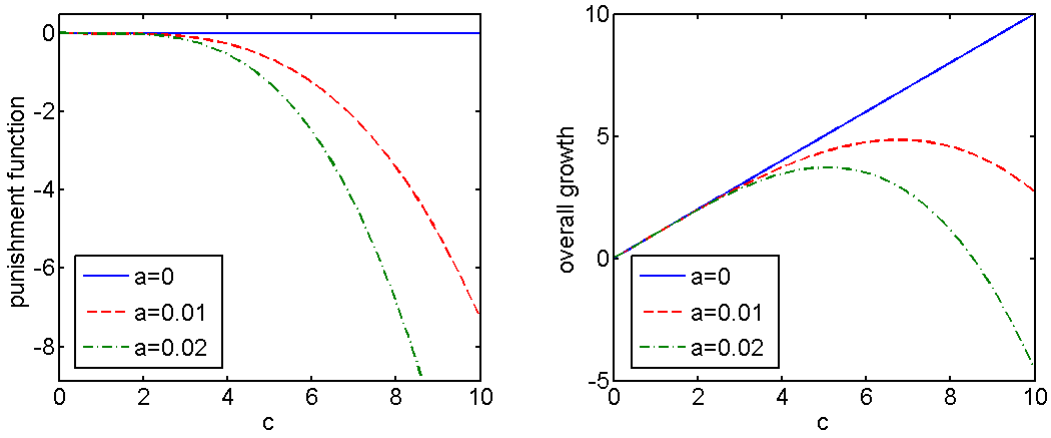

Figure 3.3: Case 2. Punishment-reward function of the form $f(c) = a(1-c)^3$ and its effects on population growth

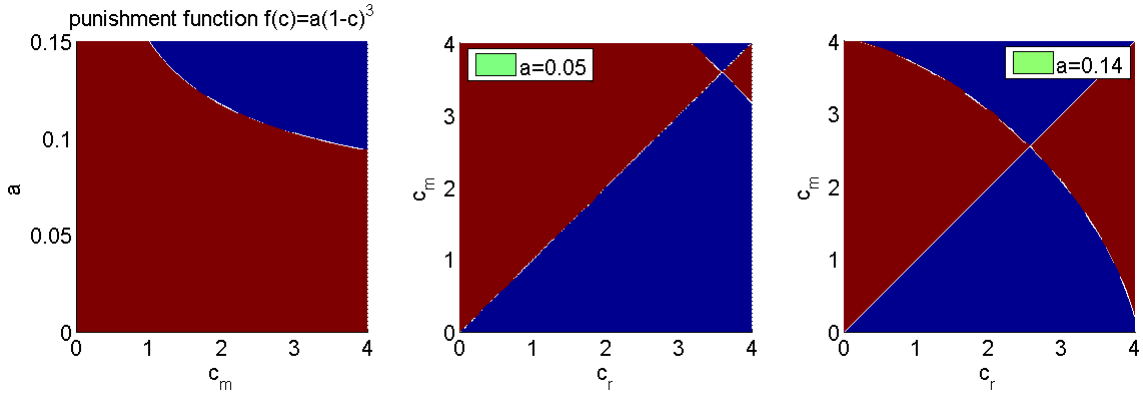

Figure 3.4: Selection gradient and pairwise invasibility plots for function of the type $f(c) = a(1-c)^3$. Blue regions correspond to parameter values where the mutant cannot invade; red regins correspond to parameter values where it can invade. (a) selection gradient, defined in 3.6, where $a < 0.15$ (b) PIP for $a = 0.05$; the singular strategy c^*_{res} is evolutionarily and convergence stable (c) PIP for $a = 0.14$; the singular strategy c^*_{res} is evolutionarily and convergence stable. This punishment/reward function is effective against agressive overconsumers.

invade but unlike the previous case, there is an upper boundary for the possible values of c_m for the invader to be successful. Unlike in the previous case, singlular strategy is stable, which predictably implies that punishment needs to be severe enough in order to be able to prevent invasion by overconsumers.

For this type of punishment function, the selection gradient is $D(c_m) = r - 3a(1-c)^2$, which is zero when $c_m = 1 \pm \sqrt{\frac{r}{3a}}$. One critical threshold is $a = r/3$. One can see that there exists a region, where the mutant cannot invade even when the force of the punishment a is quite small. Perhaps this can be interpreted as the rewards of overconsumption being too small below the red invasibility zone, and the costs of punishment being too great above the red invasibility zone.

Moreover, suppose there exists a maximum consumption value C_{max}. Then it may be reasonable to invoke the notion of a relative "size" of the invasibility region,

$$V = \frac{2\sqrt{\frac{r}{3a}}}{C_{max}}.$$

From this we can infer that invasion is *likely* to occur, given random mutations, if $V > 0.5$, or in other words when

$$a < \frac{16}{3}\frac{r}{C_{max}^2}.$$

Interestingly, from this condition one can infer that invasion becomes *more likely* as r increases but *less likely* with increasing C_{max}.

Case 3. Separating punishment and reward.

Finally, consider the following punishment/reward function: $f(c) = \rho(1-c^\eta)$. This functional form allows separating the influence of punishment for overconsumption, which is increased or decreased depending on the value of parameter η, and reward for underconsumption, which is influenced primarily by the value of parameter ρ.

As one can see on Figures 3.5 and 3.6, this type of function behaves like case 1 for $\eta < 1$ and like case 2 for $\eta > 1$. These results reiterate the claim that was made in the previous two cases: punishment needs to be severe enough in order to successfully prevent invasion by over-consumers.

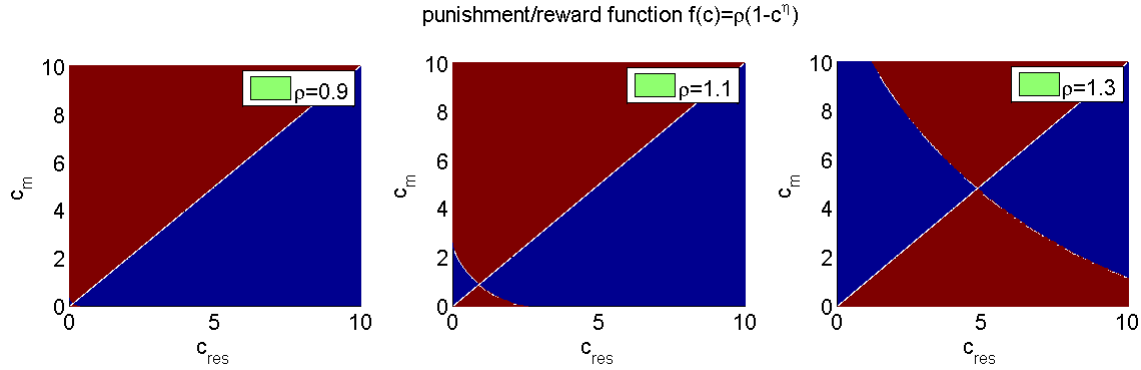

Figure 3.5: Pairwise invasibility plots for function type $f(c) = \rho(1 - c^{\eta})$, $\eta = 0.9$. The effectiveness of this function is the same as was for case 1: punishment is not severe enough to keep over-consumers out of the population.

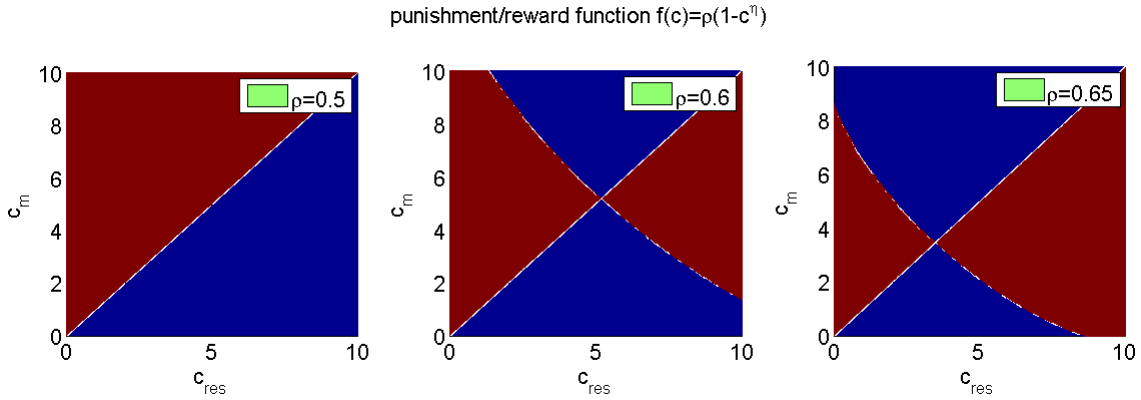

Figure 3.6: Pairwise invasibility plots for function type $f(c) = \rho(1 - c^{\eta})$, $\eta = 1.2$. The effectiveness of this function is the same as was for case 2: punishment is sufficiently severe to keep over-consumers out of the population.

The main advantage of adaptive dynamics is that one can get very clear analytical conditions for the cases when invading mutants are rare. However, what if the initial mutant is not rare (invasion by a group)? What if there is more than one type of mutant (the system did not have time to recalibrate before the new mutant came along)? We'll try to address these questions through application of Reduction theorem for replicator equations.

Modeling parametrically heterogeneous populations using the Reduction theorem

Even though without incorporating heterogeneity one cannot study the effects of natural selection on the system, until recently any attempts to write such models resulted in systems of immense dimensionality t. However, the proposed approach allows one to overcome this problem.

Once again, denote total population size $N(t) = \sum_{\mathbb{A}} x_c$. Let us introduce a keystone variable $q(t)$, which satisfies equation $q(t)' = \frac{bN(t)}{kz(t)}$, so that we can rewrite the first equation in System (3.1) in the following form:

$$\begin{cases} \frac{x_c(t)'}{x_c(t)} = r(c - q(t)') + f(c) \\ z(t)' = p - dz(t) + e\frac{N(t)(1-E^t[c])}{N(t)+z(t)} \end{cases} \tag{3.7}$$

The dynamics of x_c can be explicitly calculated through

$$x_c(t) = x_c(0)e^{-q(t)+t(rc+f(c))} \tag{3.8}$$

Total population size is then

$$N(t) = N(0)\int_c e^{-q(t)+t(rc+f(c))}P_0(c)dc = N(0)e^{-q(t)}\int_c e^{t(rc+f(c))}P_0(c)dc \tag{3.9}$$

where $P_c(0) = \frac{x_c(0)}{N(0)}$, and the current pdf is given by

$$P_c(t) = \frac{x_c(t)}{N(t)} = \frac{e^{rc+f(c)}P_c(0)}{\int e^{t(rc+f(c))}P_c(0)} \tag{3.10}$$

Now, the expected value of c can be calculated from the definition:

$$E^t[c] = \int_c cP_t(c) = N(0)\int_c c\frac{e^{-q(t)+t(rc+f(c))}}{N(t)} = \frac{\int_c ce^{t(rc+f(c))}P_0(c)dc}{\int_c e^{t(rc+f(c))}P_0(c)dc} \tag{3.11}$$

where $N(t)$ is defined above.

So, the final system of equations becomes:

$$\begin{cases} z'(t) = p - dz + e\frac{N(t)(1-E^t[c]}{N(t)+z(t)} \\ q'(t) = \frac{bN(t)}{kz(t)} \end{cases} \tag{3.12}$$

where$N(t)$, $E^t[c]$ and $P_c(0)$ are defined above.

The case when $f(c) = 0$ was investigated in Chapter 2. We observed that although it takes longer for a heterogeneous population to go extinct, tragedy of the commons eventually

happens if the maximum value of is high enough. Moreover, one could observe transitional regimes as was increasing, which can be used to forecast upcoming crisis and start implementing punishment functions.

In the proposed form of the punishment function, in the parametrically homogeneous system, i.e., when $E^t[c]$ is constant, $f(c)$ can be factored into equation $\frac{x'}{x} = r(c + f(c) - \frac{bx}{kz})$, and consequently, the spectrum of possible dynamical behaviors for this modified but still parametrically homogeneous system should be qualitatively the same compared to the phase parameter portrait given in Figure 2.4 and previously studied in Chapter 2. However, while in the model, considered in Chapter 2, nothing prevented increase of $E^t[c]$ up to the maximum possible value, here we want to investigate possible punishment functions that will prevent the increase of $E^t[c]$ in such a way as to move the system outside of the regions of sustainable coexistence with the common resource.

Results

We evaluated the effectiveness of the moderate (Figure 3.1 on page 31) and severe (Figure 3.3 on page 33) punishment functions on the dynamics of growth and interaction with the common resource of a population of over-consumers, whose parameter of overconsumption lies in the range $c \in [0,3]$. We evaluated the effects of the same type of punishment on populations with two different types of initial distributions of clones, namely truncated exponential with parameter $\mu = 10$, and Beta distribution with parameters $[\alpha,\beta] = [2,2]$ and $[\alpha,\beta] = [2,5]$ (see Figure 3.7). Parameter values were chosen in such a way as to give different shapes of the initial distribution of clones within the population. We hypothesize that the effectiveness of punishment will vary depending on the initial composition of the population, and particularly, that higher levels of punishment/reward will be necessary for initial distributions, where population composition is spread out further away from small values of c, such as Beta diustributions with parameters [2,5] and even more so Beta distribution with parameters [2,2] (see Figure 3.7b) compared to truncaed exponential distribution, where fewer overconsumers are initially present in the population, and lower frequencies (see Figure 3.7a).. Other parameter values were taken from Table 2.2 on page 10.

First we evaluated the effectiveness of the moderate punishment function of type

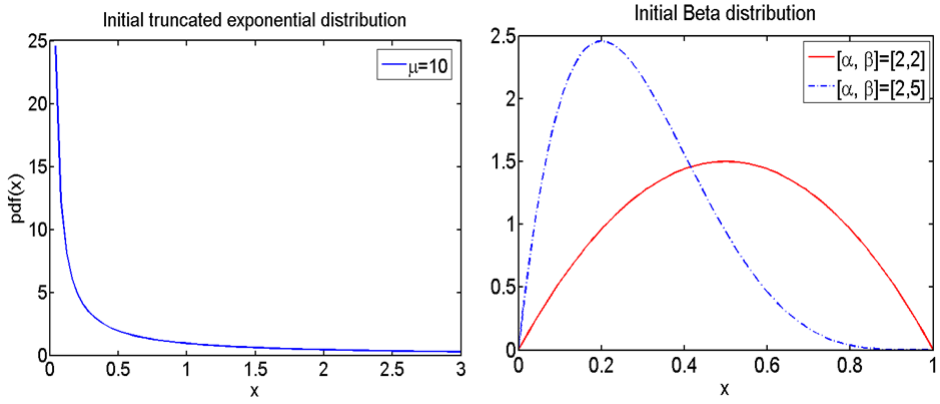

Figure 3.7: Initial distributions (a) truncated exponential with parameter $\mu = 10$ (b) Beta distribution with parameters $[\alpha,\beta] = [2,2]$ and $[\alpha,\beta] = [2,5]$.

$f(c) = a\frac{1-c}{1+c}$; the severity of punishment is captured through varying parameter a. The initial distribution was taken to be truncated exponential with parameter $\mu = 10$. We took parameter $a = 0; 0.5; 1; 2$ and plotted the changes in $x_c(t)$ for various c over time (Figure 3.8), as well as the changes in the total population size and the amount of resource (Figure 3.9). We observed that when the punishment imposed is moderate, overconsumption could be avoided only when the value of a was very high, i.e., when it is imposed very severely.

Similar results were observed for the cases of Beta distribution with parameters $[\alpha,\beta] = [2,2]$ (see Figures 3.10, 3.11) and $[\alpha,\beta] = [2,5]$ (see Figures 3.12, 3.13). However, the value of a that is necessary to successfully manage over-consumers varied depending on different initial distributions, indicating that in order to prevent the tragedy of the commons, one needs to evaluate not only the type of punishment and the severity of its enforcement but also match it to the initial composition of the population, since one level of punishment can be effective for one initial distribution and not another. (Noticeably, this kind of insight would be impossible to obtain using just analytical methods of adaptive dynamics).

Next, we conducted the same set of numerical experiments for the more severe punishment function $f(c) = a(1-c)^3$. We observed that the intensity of implementation of the more severe punishment function required to prevent the system from committing evolutionary suicide was much lower than in the previous case for all initial distributions considered here (see Figures 3.14, 3.15, 3.17, 3.17, 3.18, 3.19). The system was able to

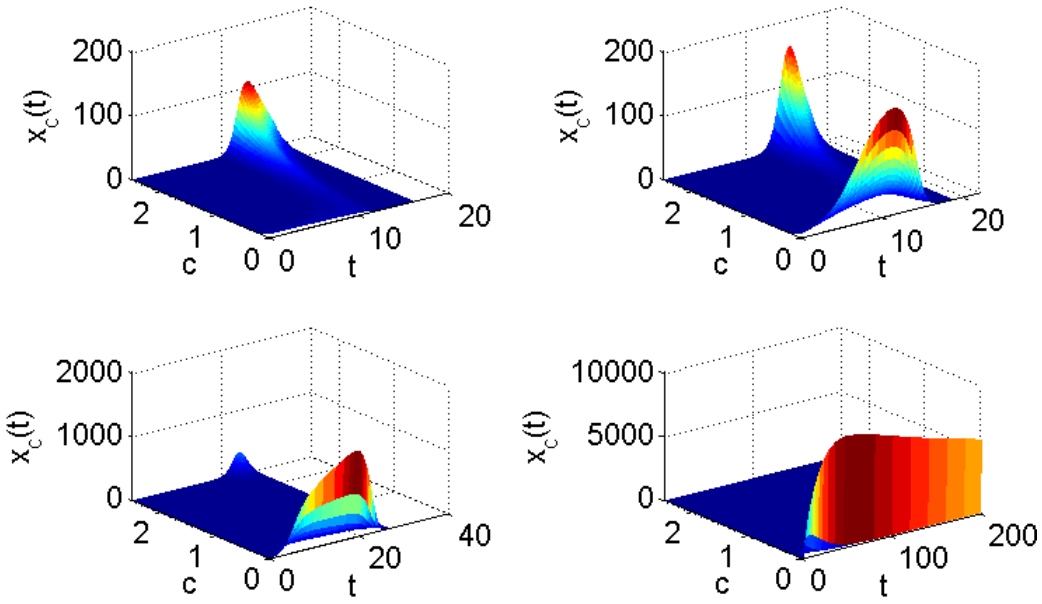

Figure 3.8: (a) Truncated exponential, moderate punishment (case 1), set 1, $a = 0$. (b) Truncated exponential, case 1, set 1, $a = 0.5$. (c) Truncated exponential, case 1, set 1, $a = 1$. (d) Truncated exponential, case 1, set 1, $a = 2$.

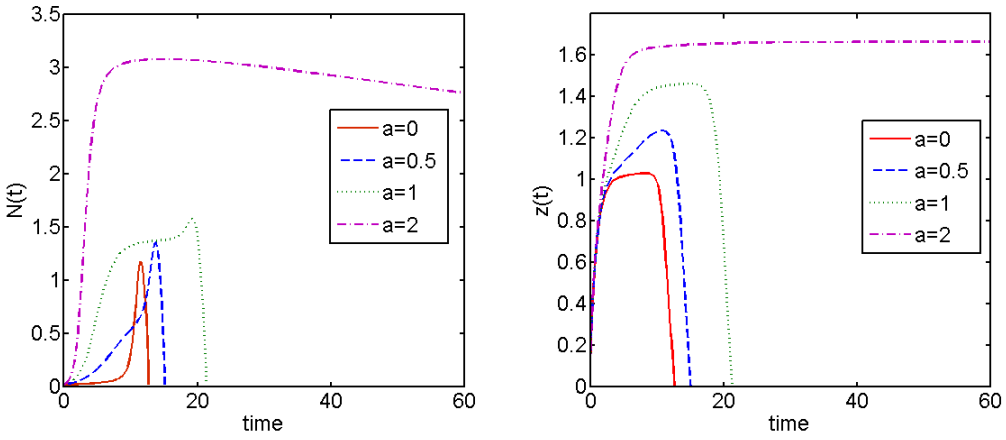

Figure 3.9: Truncated exponential distribution, set 1, case 1, dynamics of the total population size and total resource with respect to different values of a (different levels of severity of imposed punishment). One can see that successful management of overconsumers was possible only when punishment implementation was very high.

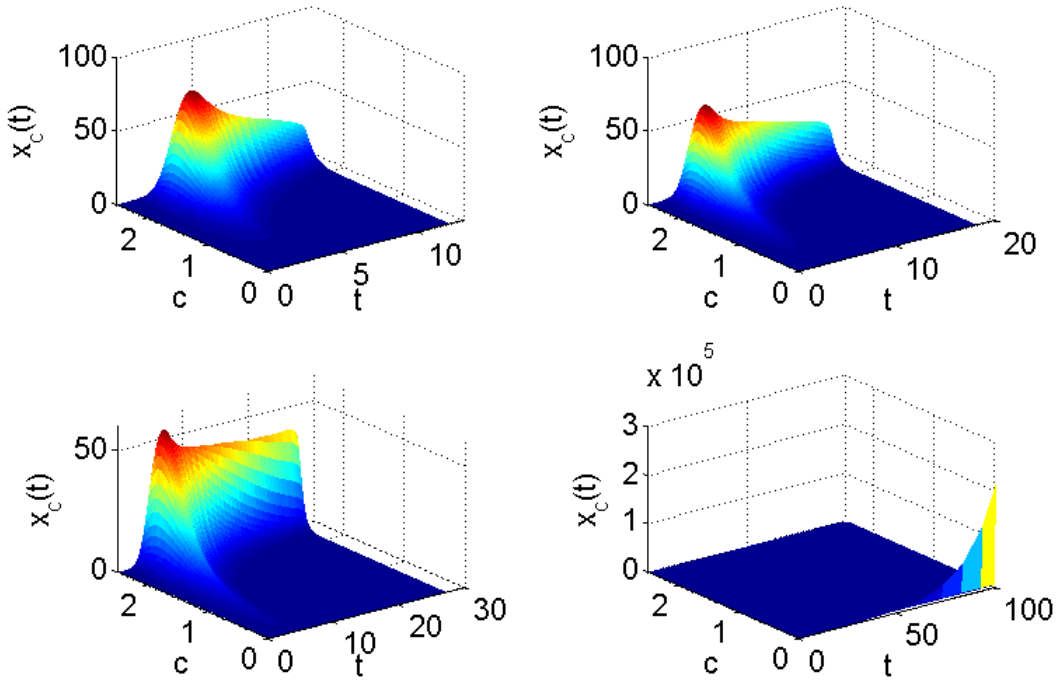

Figure 3.10: (a) Beta distribution with parameters $[\alpha,\beta]=[2,2]$, case 1, set 1, $a=0$, (b) $a=1$, (c) $a=2$, (d) $a=2.05$.

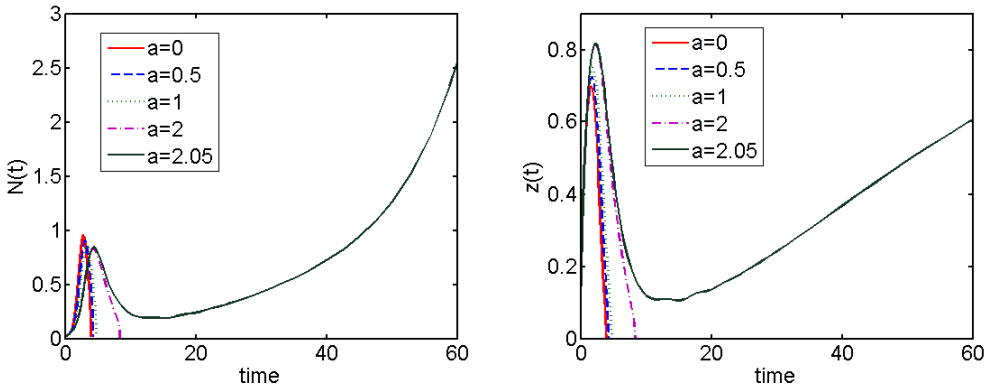

Figure 3.11: Beta distribution with parameters $[\alpha,\beta]=[2,2]$, set 1, case 1, dynamics of the total population size and total resource with respect to different values of a (different levels of severity of imposed punishment). The value of a that is necessary to manage the over-consumers and prevent resource over-consumption and the tragedy of the commons is higher than it was, when the clones in the population were initially distributed according to truncated exponential distribution.

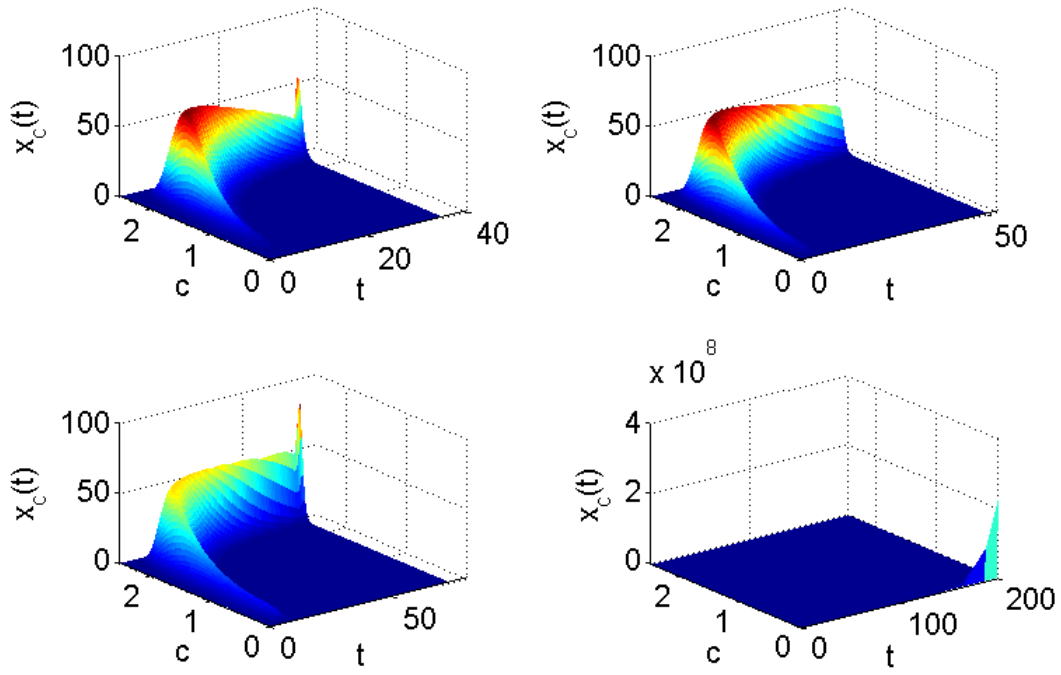

Figure 3.12: Beta distribution with parameters $[\alpha,\beta]=[2,5]$, set 1, case 1 (a) $a=0$, (b) $a=1$, (c) $a=1.5$, (a) $a=2$.

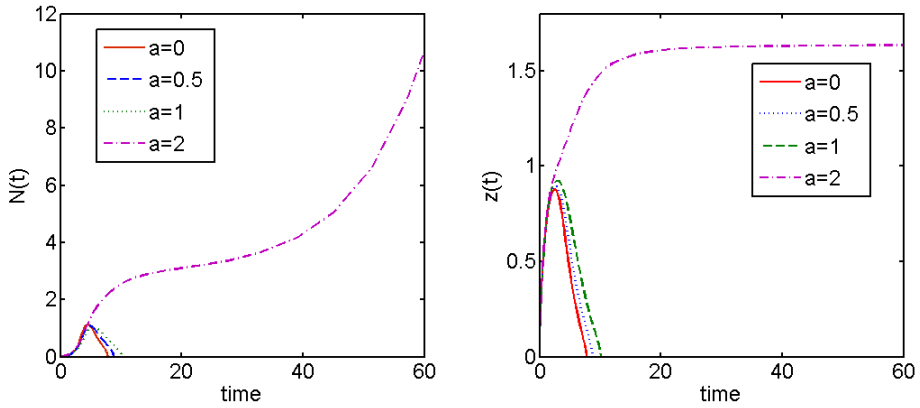

Figure 3.13: Beta distribution with parameters $[\alpha,\beta]=[2,5]$, set 1, case 1, dynamics of the total population size and total resource with respect to different values of a (different levels of severity of imposed punishment). One can see that successful management of overconsumers was possible only when punishment implementation was very high; also, the value of a that is necessary to manage the over-consumers and prevent resource over-consumption and the tragedy of the commons is higher than it was, when the clones in the population were initially distributed according to truncated exponential distribution.

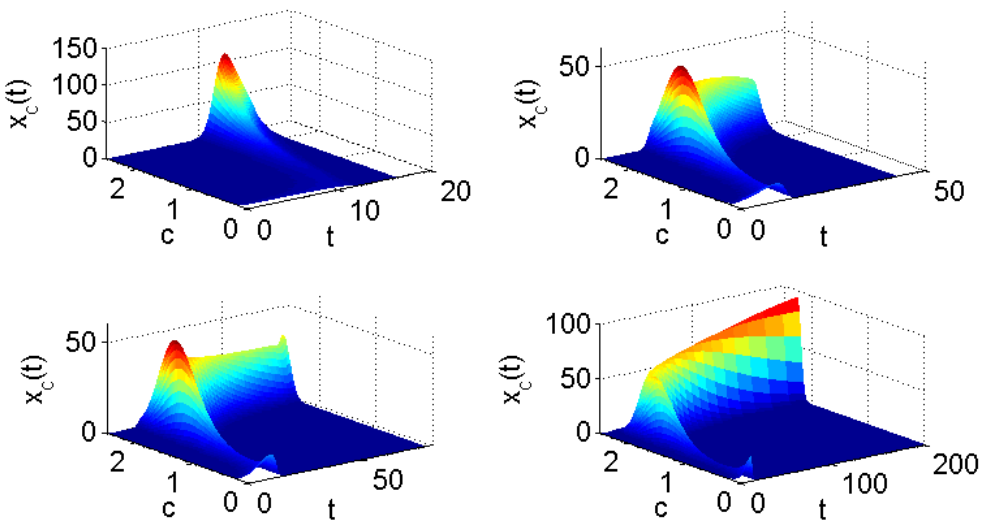

Figure 3.14: Case 2, set 1, truncated exponential distribution. (a) $a = 0$, (b) $a = 0.1$, (c) $a = 0.135$, (d)$a = 0.2$. One can see that with this punishment function, the intensity of implementation of punishment that is necessary to prevent the tragedy of the commons is much lower; when $a = 0.2$, the clones that are able to persist in population under this punishment function are as over-consumerist as the system can tolerate but at the same time, they are not so parasitic as to destroy the common resource.

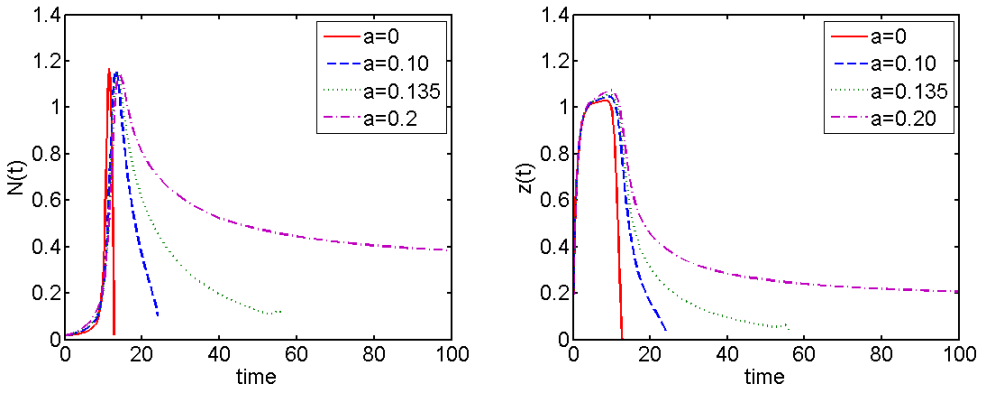

Figure 3.15: Case 2, set 1, truncated exponential distribution. Dynamics of resource and the entire population size under severe punishment of over-consumers.

support individuals with higher values of over-consumption parameter than in the previous case but still sustainably coexist with the common resource. In some cases we were also able to observe brief periods of oscillatory transitional regimes before the system collapsed (Figure 3.16). This was seen when the punishment was enforced quite strongly but still not

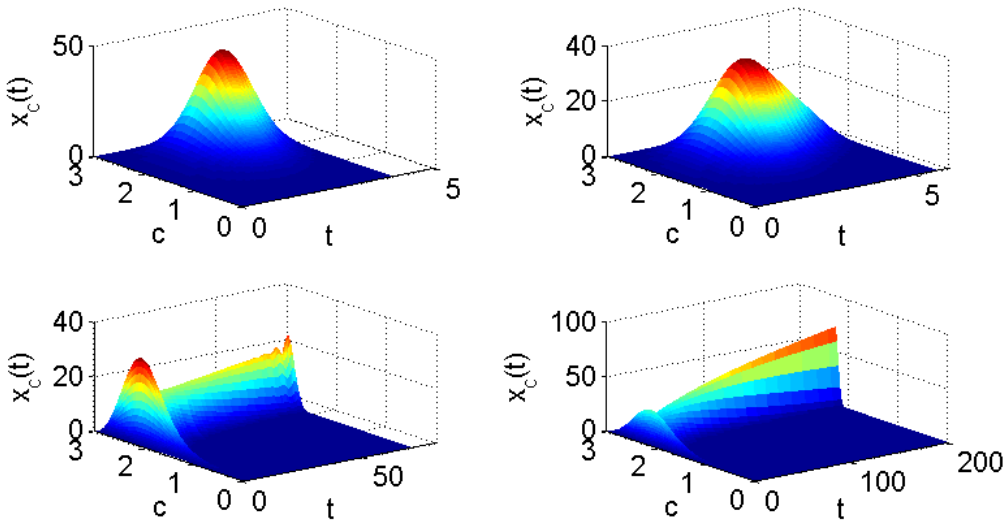

Figure 3.16: Beta distribution with parameters $[\alpha,\beta]=[2,2]$, $c\in[0,3]$. (a) $a=0$, (b) $a=0.1$, (c) $a=0.17$, (d) $a=0.2$. One can see the population going through transitional regimes before collapse, when the punishment is implemented severely but not quite severely enough (when $a=0.7$). This most probably corresponds to the expected value of parameter c going through region 3 in the phase parameter portrait of the non-distributed system (see Figure 4.1).

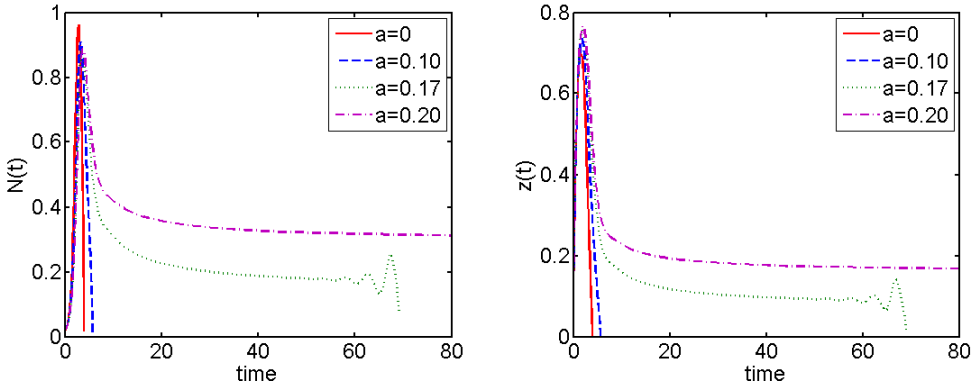

Figure 3.17: Case 2, set 1. Beta distribution with parameters $[2,2]$. Changes in total population size and of the common resource over time.

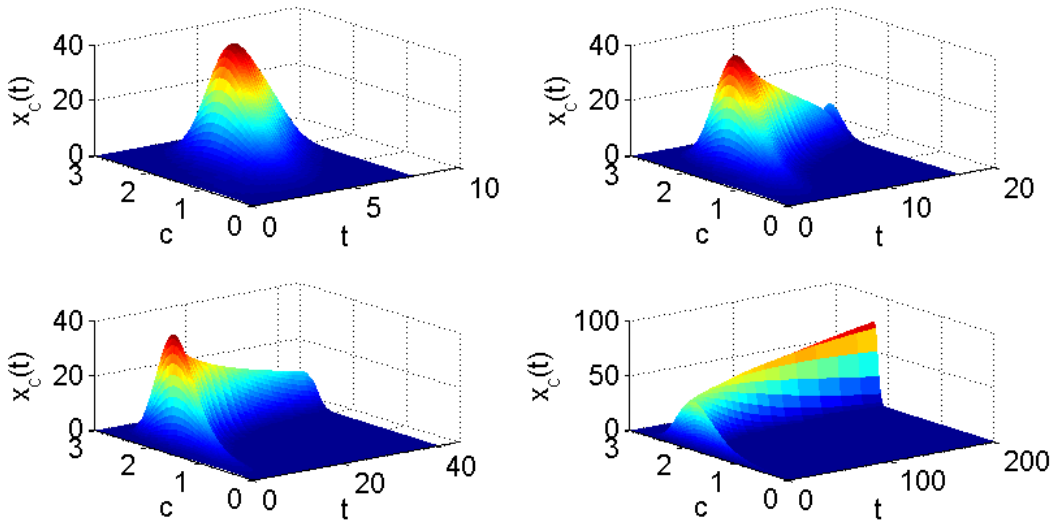

Figure 3.18: Beta distribution, parameters $[\alpha,\beta]=[2,5]$, $c\in[0,3]$. (a) $a=0$, (b) $a=0.1$, (c) $a=0.14$, (d) $a=0.2$

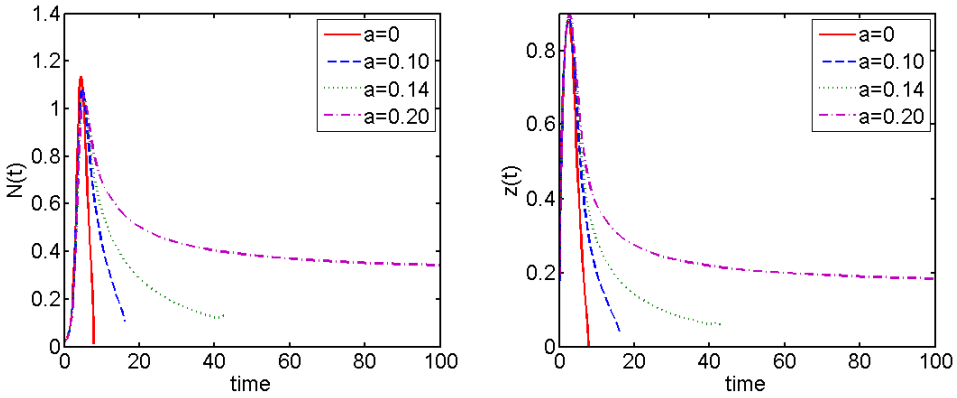

Figure 3.19: Beta distribution with parameters $[\alpha,\beta]=[2,5]$. Dynamics of resource and population size over time.

strongly enough (Figure 3.17).

Finally, we evaluated punishment function of the type $f(c)=\rho(1-c^{\eta})$, where the intensity of punishment and reward are accounted for by parameters η and ρ respectively. We observed that in order to evaluate the expected effectiveness of the punishment/reward system one needs to not only adjust parameters ρ and η (see Figure 3.20) but also be able to evaluate the expected range of parameter c (see Figure 3.21), since one level of punishment may be appropriate for one set of initial conditions but not another. r. For instance, as one can see on Figure 3.21, the time to collapse under fixed values of parameter ρ and η is

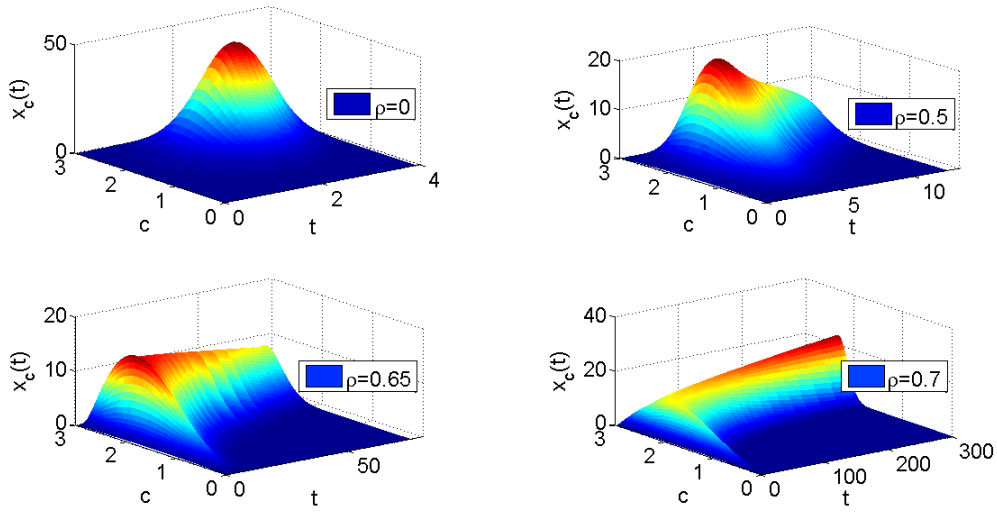

Figure 3.20: $f(c) = \rho(1-c^{\eta})$, initial Beta distribution with parameters $[\alpha,\beta] = [2,2]$, $c \in [0,3]$, $\eta = 1.2$.

different for different initial distributions depending on the maximum value of c present in the initial population. Moreover, in accordance with our hypothesis, indeed the time to collapse varies depending on the initial distribution of the clones within the population, and the higher the frequency of overconsumers is in the initial population, the worse the prognosis. For the examples considered, truncated exponential distribution is more less prone to collapse due to overconsumption than Beta distribution with parameters [2,5], which in turn is slightly less prone to collapse than Beta distribution with parameters [2,2].

Discussion

In this Chapter a parametrically heterogeneous mathematical model of consumer-resource interactions was studied in order to answer the question of whether infliction of punishment for over-consumption can successfully prevent, or at least delay, the tragedy of the commons, i.e., the situation when a shared resource is depleted due to overexploitation. We evaluated the effectiveness of two types of punishment functions, as well as the effects of punishment on heterogeneous populations with different initial composition of individuals with respect to the levels of resource (over)consumption.

The proposed model was studied analytically in Chapter 2 without incorporating any punishment/reward for over-/under- consumption. It describes the interactions of a popu-

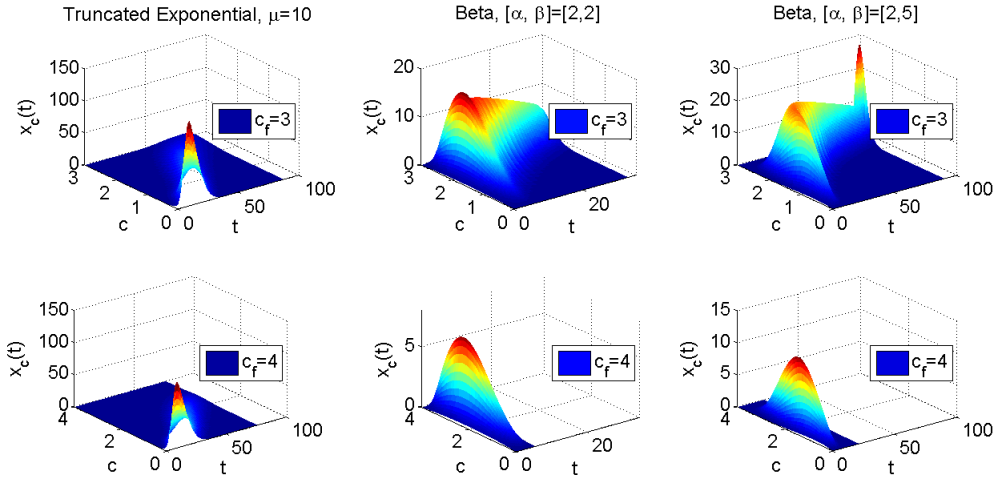

Figure 3.21: The importance of evaluating the range of possible values of c_f, illustrated for different initial distribution. Punishment function is of the type $f(c) = \rho(1-c^\eta)$, where $\rho = 0.6$, $\eta = 1.2$. Initial distributions are taken to be truncated exponential with parameter $\mu = 10$, and Beta with parameters [2,2] and [2.5]; $\rho = 0.6$, $\eta = 1.2$. The top row corresponds to $c \in [0,3]$; the bottom row corresponds to $c \in [0,4]$.

lation of consumers, characterized by the value of an intrinsic parameter c with a common renewable resource in such a way that each individual can either contribute to the common resource ($c < 1$) or take more than they restore ($c > 1$). As the value of c increases, the population goes through a series of transitional regimes from sustainable coexistence with the resource to oscillatory regime to collapse, eventually committing evolutionary suicide through exhausting its resources.

First, we identified analytically the conditions leading to the possibility of sustainable coexistence with the common resource for a subset of cases using adaptive dynamics. This method allows to address a question of whether a mutant (in our case, an individual with a higher value of c) can invade a parametrically homogeneous resident population of consumers-producers. We evaluated the effectiveness of four types of punishment functions: linear punishment of the form $f(c) = a(1-c)$; moderate punishment of the form $f(c) = a\frac{1-c}{1+c}$; severe punishment $a(1-c)^3$, where parameter a denotes the severity of implementation of punishment on individuals with the corresponding value of parameter c, and function of the type $\rho(1-c^\eta)$, which allows to separate the influence of reward for underconsumption, primarily accounted for with parameter ρ, and punishment for overconsumption, primarily

accounted for with parameter η.

We demonstrated that linear punishment is effective only until the severity of punishment\reward matches exactly the per resource growth rate of the population, i.e., when $a \leq r$. The severe punishment/generous reward approach is uniformly effective, almost irrespective of the value of a, and allows invasion of moderate overconsumers only in the small region of $c \approx 1$, when the punishment is not yet severe enough to outweigh the benefits of moderate overconsumption (see Figures 3.16 and 3.19), and the reward does not yet provide sufficient payoffs in terms of higher growth rates.

Finally, we investigated a functional form of the type $f(c) = \rho(1 - c^{\eta})$ that allowed separating the influence of punishment overconsumption (parameter η) from that of rewarding underconsumption (parameter ρ). Our analysis suggests that just rewarding underconsumers is not enough to prevent invasion by overconsumers and hence *one should not expect to be able to prevent the tragedy of the commons through reward alone* (see Figure 3.5 and 3.6). However, an "intervention" can be much more successful if sufficient punishment of overconsumers is coupled with rewarding of underconsumers (see Figure 3.20).

Adaptive dynamics techniques do not yet allow answering the question of system invasibility when the mutant is not rare, such as in cases of migration and consequent invasion by a group. We will address these questions using the Reduction theorem for replicator equations [69, 70].

If each individual consumer is characterized by their own value of the intrinsic parameter c, and if this trait value affects fitness, then the distribution of clones (a set of individuals characterized by the same value of c) will change over time due to system dynamics. Consequently, the mean of the parameter will also change over time, affecting system dynamics, since the clones will experience selective pressures not only from the external environment, competing for the limited resource, but also from each other. The mean of the parameter can be computed at each time point from the moment generating function of the initial distribution of clones, which allows to evaluate the effectiveness of different types of punishment\reward functions on population composition by tracking how the distribution of clones changed over time with respect to the mean value of c.

We once again evaluated the effectiveness of the four types of punishment/reward functions on the evolution of the system depending on the initial distribution of clones within the population, which were taken to be truncated exponential with parameter $\mu = 10$, and Beta distribution with parameters $[\alpha, \beta] = [2,2]$ and $[2,5]$. The initial distributions were chosen in such a way as to give significantly different shapes of the initial probability density function and should be matched to real data, when it is available. We observed that depending on the initial distribution, the intensity of implementation of punishment\reward has to differ if one is to successfully stop overconsumption, and so in order to be able to make any reasonable predictions one needs to understand what the initial composition of the affected population is. We hypothesized that the higher the frequency of overconsumers in the initial population, the more severe the punishment for overconsumption would have to be, and the more generous the reward; specifically, for our examples, we anticipated the prognosis to be the most favorable for initial truncated exponential distribution, followed by Beta distribution with parameters [2,5] and then finally [2,2]. While intuitively obivious, this effect would imply that results obtained analytically from adaptive dynamics can only be relevant for a subset of cases, i.e. when the invader is rare (such as highly skewed truncated exponential distribution) but not for the cases of other types of initial distributions.

As anticipated, we observed that severe punishment/generous reward approach was much more effective in preventing the tragedy of the commons than the moderate punishment/reward function, which was particularly important for the cases, when over-consumers were present at higher frequencies (such as both Beta initial distributions). Specifically, we observed that the level of implementation, a, could be nearly ten times lower for severe punishment/generous reward system as compared to the moderate punishment function ($a \approx 0.2$ vs $a \approx 2$) in order to obtain the same effect of selecting against the over-consumers, which can become a very important factor when there are large costs associated with implementation of such intervention syustems. This comes not only from the severity of punishment but also from the fact that moderate punishment allows more time for the over-consumers to replicate, and thus by the time the punishment has an appreciable effect, the population composition had changed, and the moderate punishment will no longer be effective. So, in punishment implementation one needs to take into account not only the severity of punish-

ment but also the time window that moderate punishment may allow for the over-consumers to proliferate. Within the frameworks of the proposed model, moderate implementation of more severe punishment\reward system is more effective than severe implementation of moderate punishment\reward.

Adaptive dynamics and the Reduction theorem: comparative analysis

In order to address our questions we have used two recently developed methods for modeling parametrically heterogeneous populations: adaptive dynamics [52] and the Reduction theorem for replicator equations [69, 70]. Adaptive dynamics allows addressing the questions of whether a rare "mutant" clone that invade the population using standard bifurcation theory. The method allows identification of analytical conditions, which can be conveniently visualized using pairwise invasibility plots (PIPs). However, the method does not allow addressing questions of system invasibility by clones that are not rare, such as in cases of invasion by a group.

This question in turn can be addressed using the Reduction theorem for replicator equations. The method requires the assumption that all "invaders" must be present initially in the population and fall within some known distribution, and then allows to see which clone type(s) will be favored over time due to natural selection. The outcome may be different depending on the initial distribution of the clones within the population, as well as on the initial state of the system, i.e., fixed parameter values. This cannot be taken into account using adaptive dynamics; however, the system of ODEs that results from the transformation done using the Reduction theorem is typically non-autonomous; hence no analytical conditions can typically be obtained using standard bifurcation theory. The two methods therefore can complement each other; a more detailed comparison of the two methods is given in Table 3.2.

Tragedy of the commons as prisoner's dilemma

The conditions that can lead to the tragedy of the commons can be reformulated as a game of prisoner's dilemma - while preserving the common resource is in the best interest of the group as a whole, over-consumption is in the interest of each particular individual. In the cases, when the decision about the resource is made one individual at a time, tragedy

	Adaptive dynamics	Reduction theorem
Goal	Model evolution of parametrically heterogeneous populations	
Assumptions	Clonal reproduction	
	Separation of evolutionary and ecological time scales	
Environment	Can be variable and affected by changes in population composition (also known as seascape, or a dancing landscape)	
Population	Two types: invader and resident	Any number of types
	Small initial frequency of the invader	Initial population composition can be arbitrary
	Can introduce new "mutants"	All types must initially be present in the population, even if at a near-zero frequency
	Requires a special form of differential equations ($x' = xF(t)$)	
Purpose/ question	Invasion: can a mutant invade the resident population?	Evolution of a parametrically heterogeneous system over time due to natural selection
	Uses both theoretical analysis (bifurcation theory) and numerical solutions	
Visual representation	Pairwise invasibility plot (PIP)	Bifurcation diagram of the corresponding parametrically homogeneous system
Concepts	Evolutionarily singular strategy: selection gradient is zero	Evolutionarily singular distribution: dominance of one type or possible oscillation between several types tracked through changes in mean values
	Evolutionarily stable strategy - singular strategy that cannot be locally invaded by neighboring mutants	Distributed evolutionarily stable state (DESS) - a distribution of strategies that is resistant to invasion [15]
	Convergence stability - a small perturbation of the population away from ESS (DESS) will result in those clones having the advantage that can get the population back to ESS (DESS)	
	Continuously stable strategy (distribution) - a strategy (distribution) that is both evolutionarily and continuously stable	

Table 3.2: Adaptive dynamics and Reduction theorem

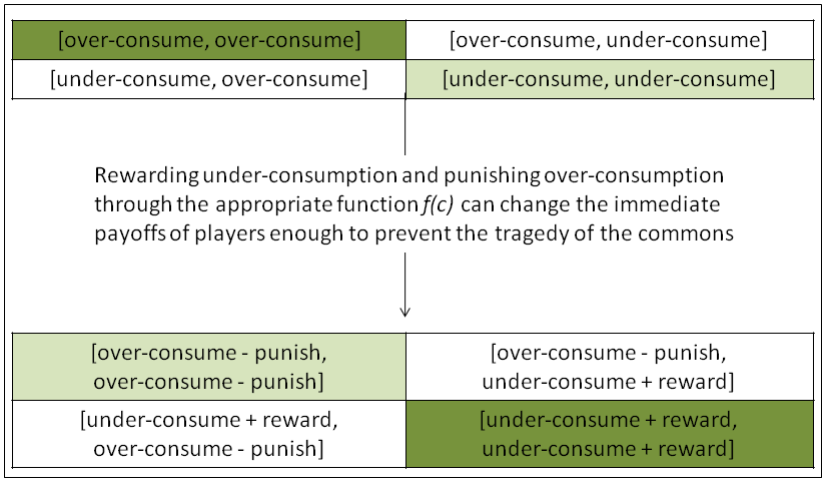

Figure 3.22: Tragedy of the commons as prisoner's dilemma. The tragedy can be avoided if the immediate payoffs of all the players are modified through appropriate punishment/reward function.

of the commons seems to be inevitable. However, Elinor Ostrom [117] observed a number of cases, when the tragedy could be avoided, if the individuals within the population were able to communicate with each other. The common thread that runs through many of her examples is that 1) in small groups the effects of overconsumption were immediately noticeable, since within a small population each individual's actions are more visible than in larger populations, and 2) punishment was enforced without delay.

From the point of view of game theory, we are dealing with a game of prisoner's dilemma, and with punishment functions $f(c)$ affecting payoffs in such a way as to outweigh the benefits of overconsumption (see Figure 3.22). In this Chapter we were able to demonstrate that preventing the tragedy of the commons through solely rewarding underconsumers is unlikely and one also needs to enforce punishment; however, the effectiveness of such an "intervention" is increased when both rewarding and punishment systems are enforced.

In a two-player game of prisoner's dilemma the outcome is easily predicted: the strategy that gives the individual the higher payoff is going to be favored. However, this is not necessarily the case when more than two players are involved, since the choices of individuals may be affected not only by their immediate payoffs but also by the actions of those surrounding them. Therefore, if one is to try and avert the tragedy of the commons

through punishing over-consumption and rewarding under-consumption, one needs to not only find an appropriate punishment/reward function but also calibrate it to be appropriate to each individual population.

Alternative punishment/reward systems

Proposed here is just one way to try and modify individuals' payoffs in order to prevent resource overconsumption - through inflicting punishment or reward that affects their growth rates directly. This approach can be modified depending on different situations to punish or reward based not just on the intrinsic value of c but on total resource that was consumed by clone c, i.e., make punishment function of the form $f(c,z)$.

Another approach would be to limit/expand access to the common resource based on the value of c and impose punishment through making parameter e in the equation for dz/dt a function of c, i.e., $e_1 = f(c)$ or $f(c,z)$. Such a scheme would correspond to making c a measure of reliability, such as a credit score in financial systems.

One can also introduce a policing system, i.e., split the population of consumers into regular consumers and police. The latter could get rewarded for successfully enforcing punishment through either faciliated access to the resource, or through direct increase in growth rates, such as was done in this chapter.

Finally, one can also introduce complementrary cheaper or more easily renewable resource, i.e., split the resource into two components, and reward consumers for using it, such as encouraging the use of solar energy or hybrid cars.

The applicability of each approach will of course depend on the particular circumstances of each particular situation.

Chapter 4

MIXED STRATEGIES IN RESOURCE ALLOCATION

Abstract

In the previous chapters we have been focusing on the cases when the direction in which the system will evolve was intuitively obvious, since from the point of view of maximizing fitness at each time point, it is the most successful over-consumer (i.e., an individual with the highest possible value of c) that would be selected. Proposed here is an alternative model, where the individuals competing for the common resources have the choice of allocating those resources towards their own reproduction or towards competition. We demonstrate the importance of individual variation within the system, emphasizing the claim that there is no one "optimal" strategy that the individuals can adopt in order to maximize its fitness. We classify the possible dynamic regimes of the system and demonstrate that if one wants to predict where a system will evolve, just knowing the rules that govern its dynamics is not enough to make an accurate prediction. One will also need to know the composition of the population that is playing by these rules.

Keywords: mixed strategies, resource allocation, individual variation

Introduction

Interactions with resources often determine much of the dynamics of any population, since there are no unlimited resources available to any population, and since it is successful competition for the resource that will determine, whether individuals will be able to survive and reproduce. This consideration in turn raises a question of optimizing resource allocation strategies for fitness maximization under the constraint of differenct selective pressures that the population may be experiencing at each point in time. The two strategies that that can be adopted by different species in response to different selective pressures that come from their environment are either to invest the resources into reproduction, which has been suggested to be the preferable strategy in unstable environments, or into competition, which would allow maximizing fitness in more stable conditions [35, 92, 124]. The main criticism

of this theory came from empirical studies: however intuitive the heuristic may seem, the adaptations that were predicted by either selective strategy were simply not observed in nature [150–152, 168].

The models that were used to make predictions about what environmental conditions could lead to the dominance of either type of resource allocation strategy assumed population homogeneity, or at least a level of heterogeneity that would not affect the dynamics of the overall system, since the choice of the dominant strategy was assumed to be determined solely by the environment. This assumption may be valid if there is sufficient evidence to believe that the process that is being observed and described takes place on a sufficiently slow time scale, so that natural selection will simply have had no time to have any serious effect on population dynamics. In this case the assumption of homogeneity is a reasonable enough simplification. Otherwise, it is reasonable to believe that competition between individuals within the population poses as much, if not more selective pressures on the entire population than do interactions with the resources. That is, other members of the population are just as big a part of the environment as the resource. And if the population composition is changing, so can the overall dynamics of the population. However, this important aspect of population dynamics becomes buried under the assumption of homogeneity.

In this paper we construct and study a consumer-producer type model based on two models previously proposed by [75], where the individuals within a population differ in their choice of what proportion of the common renewable resource is allocated towards reproduction or competition. Examples of such situations can for instance be clearly observed in microbial populations, as the bacteria aggregate into biofilms or disperse depending on environmental conditions [23, 125]. In this paper we want to investigate the question of whether either strategy can become intrinsically dominant if a heterogeneous population, where individuals can choose to invest limited resources primarily into reproduction or competition, is allowed to evolve over time. Becuase of the importance of both limited resources and intraspecies competition, we hypothesize that one cannot predict which strategy will come to dominate over time without understanding both the rules that govern the dynamics of the system and knowing the initial composition of the population.

It is important to note that the purpose of this work is not to test what birth, death, competition or any other rates would render either strategy more or less optimal for maximizing the population's fitness when consuming a dynamic resource, or to provide a case study for a specific biological system. Instead, we want to construct a conceptual theoretical framework, where we investigate how the distribution of individuals that can adopt different strategies evolves over time depending on the initial state of the system. The asymptotic distribution will show what strategy (if any) will be selected in the process of natural evolution of the system. The resulting insights can then be fine-tuned and applied to more specific biological, social or economical systems.

This Chapter is organized as follows: first the formulation of the mathematical model is given. Then, a parametrically homogeneous system is analyzed in order to identify the possible dynamical regimes of the model. Next, parametric heterogeneity with respect to strategy choice is introduced. The resulting infinitely-dimensional system is then reduced to low dimensionality using the Reduction theorem [69, 70]. The changes in population composition over time are investigated numerically under the assumption of different initial distributions of individuals within the population with respect to strategy choices. The Chapter concludes with a discussion of results and conclusions.

Model description

Consider a heterogeneous population of consumers x_α, competing for the common renewable resource z using two different strategies with different probabilities: the individuals can either use the resource to invest in high fecundity or to increase environmental carrying capacity. Each consumer is characterized by its own value of parameter $\alpha \in [0, 1]$, which represents the proportion of each strategy that the consumer uses in their interaction with the resource. That is, the closer α is to zero, the more resource the corresponding individual uses to invest in fecundity, and the higher the value of α, the more resource in the individual's disposal goes to increasing the environmental carrying capacity. Since in this model formulation, the only difference between the individuals is the value of parameter α, we find it appropriate to refer to them as α-clones.

When $\alpha = 0$, each individual of this clone type invests into increasing their fecundity;

the per capita growth rate is of the form $r(c_2\frac{z}{N+z}-\phi)$, where ϕ is the individuals' average death rate and $N(t)=\sum_\alpha x_\alpha$ is the total population size. This growth function can also be seen as a version of "mass action law", where population growth is proportional both the current population size and the amount of total available resource.

When $\alpha=1$, each individual of this clone type invests in increasing environmental carrying capacity. In this case, the per capita growth rate is the logistic-like form $r(c_1-\frac{bN}{kz})$, where the carrying capacity is not constant but is rather determined by the amount of the common dynamic resource $z(t)$. If the individual uses both strategies with the probabilities α and $1-\alpha$ accordingly, then the per capita growth rate of each α-clone is $\alpha(c_1-\frac{N(t)}{kz(t)})+(1-\alpha)(\frac{c_2z(t)}{N(t)+z(t)}-\phi)$.

Derivation of the equation for z' is given in Chapter 2 on page on page 9.

For the purposes of initial analysis, let us first consider the case, when the parameter is fixed, so that the entire population consists of a single α-clone. (It can be interpreted as follows: if natural selection has had the time to "pick its winner", the final outcome can be seen as there being some kind of an "optimal proportion" of each strategy within the population, if such a proportion exists). This assumption will be relaxed later in the chapter.

In this case, $N(t)=x_\alpha$, i.e., the population is homogeneous with respect to α. The resulting system becomes:

$$\begin{cases} \frac{dN}{dt}=\underbrace{N(t)\alpha(c_1-\frac{N(t)}{kz(t)})}_{\text{invest in competition}}+\underbrace{N(t)(1-\alpha)(\frac{c_2z(t)}{N(t)+z(t)}-\phi)}_{\text{invest in proliferation}}, \\ \frac{dz}{dt}=\underbrace{\gamma-\delta z}_{\text{resource restoration and decay}}+\underbrace{eN(t)(\underbrace{\frac{\alpha(1-c_1)}{N(t)+z(t)}}_{\text{competitive clones}}+\underbrace{\frac{(1-\alpha)(1-c_2)}{N(t)+z(t)}}_{\text{proliferative clones}})}_{\text{total resource consumed/restored}}. \end{cases} \tag{4.1}$$

The case, where $\alpha=1$, $c_1\geq 1$ was analyzed completely in Chapter 2. The case, where $\alpha=0$, $c_2>0$ is briefly discussed in the Appendix (the model loses biological relevance for $c_2>1$ because trajectories fall outside the positive quadrant for a wide range of initial values). The values of z are guaranteed to remain in the positive quadrant for $e>\frac{\gamma}{c_2-1+\alpha(c_1-c_2)}$. Identification and investigation of dynamical regimes that result from a mixture of these two

strategies with the possibility of having over-consumers in the population is focus of this chapter.

Analysis

Bifurcation analysis performed on System (4.1) revealed seven possible topologically non-equivalent types of phase-parameter portraits in the positive half-plane (N,z) andc_1, c_2, e,δ, γ-parameter space. Results are also summarized in Figure 4.1, which depicts schematic slices of complete bifurcation portraits, projected to the planes (α,c_1) and (N,z). The boundary lines correspond to bifurcations of co-dimension 1, and points of intersections of the lines correspond to bifurcations of higher co-dimensions.

First, we fix α and study the dynamics of the model with respect to variations of parameter c_1, holding all other parameters in the system constant. In Domain 1 of the phase parameter portrait (when no over-consumption of the resource is allowed, i.e., when $c_1 < 1$, $c_2 \in (\phi,1)$), point A is a global attractor, and the general set of trajectories tend to this point with time. That is, a niche, which is defined here as a state of sustainable coexistence with a common renewable resource, will successfully be formed regardless of the initial population size or initial amount of resource available.

Increasing c_1 moves us to Domain 2, where there appears a region of bistability. This implies that successful formation of the niche is going to be possible depending on the appropriate initial conditions: if the initial population is too large or the initial amount of the resource is too small, the population will go extinct (see Figure 4.1, e2).

Further increases in c_1 move us to Domain 3, where an unstable limit cycle appears around the stable equilibrium point A_α, thus further shrinking its domain of attraction and consequently decreasing the range of initial conditions that permit sustainable coexistence of the population and the resource. So, a niche can be formed successfully but only as long as the initial conditions fall within the limits delineated by the limit cycle.

In Domain 4, the limit cycle merges with the equilibrium point A, making it unstable. This implies that any small perturbation from the state of equilibrium will make the population go extinct.

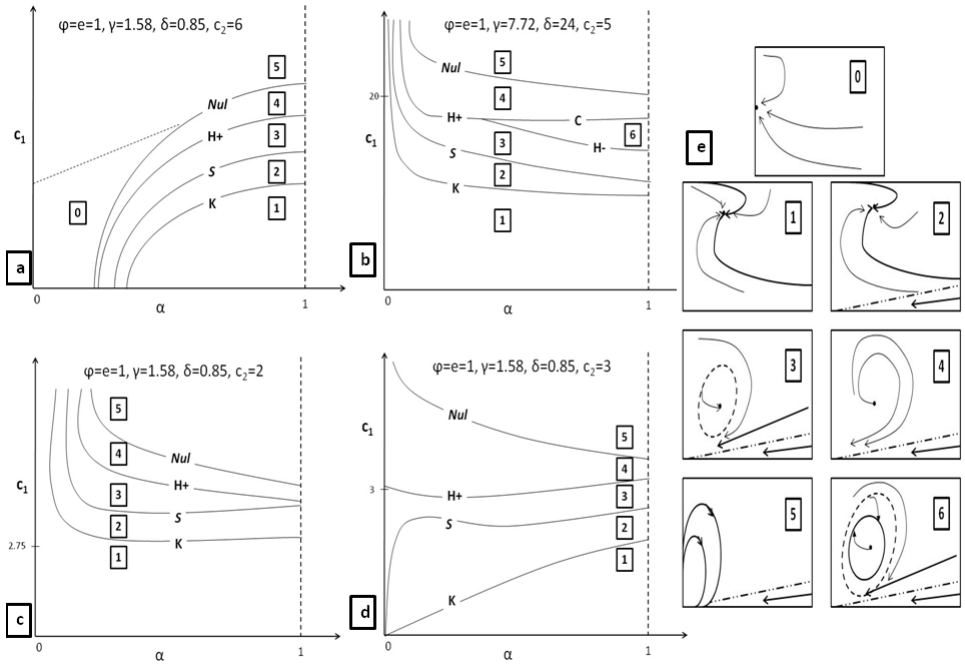

Figure 4.1: Bifurcation diagram of the System (1.2), where (a),(b),(c) and(d) represent (α, c_1)-slices of parameter space of the model for $e = \phi = 1$and (e) presents typical (N, z)-phase portraits whose numeration is identity to those in parameter portraits. In Domain 1, we can observe sustainable coexistence with the common resource, which can also be interpreted as a successfully formed niche (non-trivial globally attracting equilibrium point A). In Domain 2, there appears a region of bistability, i.e., a niche will be successfully formed only depending on the initial population size and the amount of resource. In Domain 3, an unstable limit cycle is formed around the point A, further shrinking the range of possible initial conditions that will lead to successful formation of a niche. In Domain 4, point A loses stability, so any perturbation will lead to population collapse. In Domain 5, the trajectory becomes an elliptic sector ("the devil's loop") which implies that a population is bound for extinction after a sufficiently long amount of time. Domain 6 exists only when the level of both natural resource restoration and natural resource decay is very high; in this case, the population can go into a stable oscillatory regime. Finally, Domain 0 corresponds to the case, when only trivial equilibrium $B(0, \gamma/\delta)$ is globally attractive, which is of no biological and dynamical interest.

Further increasing c_1 causes point A to move closer and closer to the origin, finally merging with it in Domain 5, which results in the appearance of an elliptic sector (see Figure 4.1, e5) and thus inevitable, albeit delayed, population extinction. Moving into Domains 5 could be interpreted as "the tragedy of the commons'', when overly efficient consumers exhaust the common resource and thus cause extinction of the entire population.

Finally, Domain 6 exists for a very narrow range of parameters δ and γ (natural rates of resource decay and restoration), and only when α is closer 1 than to 0. Within this region, a regime of stable oscillatory behavior is possible. An interesting effect of high natural resource decay rate is realized here: even though the average level of over-consumption is high, the resource "slips away" from all individuals alike, regardless of their intrinsic properties, which allows for the possibility of the sustained oscillatory behavior.

Domain 0 is biologically irrelevant, since it corresponds to the case, when the resource grows and decays independently of consumers, which within the frameworks of this model can only happen if the population size is 0.

Also, it is important to note that while the location of the boundaries changes for different α, the order in which the described dynamical regimes appear remains unchanged. Bifurcation diagram can be used conceptually to not only understand the possible dynamical regimes but also to make predictions about possible implications of changes in population composition, as well as changes in intrinsic properties of individuals within the population.

An important conclusion from the full bifurcation analysis performed on the system is as follows: while sustainable coexistence with the common resource is possible regardless of the strategy, the domain of phase parameter space where it can happen decreases as $\alpha \to 0$. Thus, in a stabilized population, investment into increasing environmental carrying capacity would seem to generally be a more successful strategy for sustainable coexistence with the common resource.

Modeling parametric heterogeneity

Until now we have been assuming that the proportion of clones that adopt either strategy is fixed, i.e., that α is a constant. It can happen if the system has already had time to evolve and reach some kind of a steady state, concentrating near the "average" parameter

value. However, what if the selection process is still ongoing? What if there is no a proper optimal proportion of each strategy within the population, but rather the population tends to a distribution of strategies? How will this affect system dynamics?

Assume that the initial state of the population can be described by a given distribution of the parameter $\alpha \in [0,1]$, given by $P_\alpha(0) = \frac{x_\alpha(0)}{N(0)}$. In this case, instead of the 2-dimensional parametrically homogeneous System (4.1), we consider the infinitely dimensional parametrically heterogeneous system:

$$\begin{cases} \frac{dx_\alpha}{dt} = rx_\alpha(t)(\alpha(c_1 - \frac{bN(t)}{kz(t)}) + (1-\alpha)(\frac{c_2 z(t)}{N(t)+z(t)} - \phi)), \\ \frac{dz}{dt} = p - dz(t) + re(E^t[\alpha](1-c_1) + (1-E^t[\alpha])(1-c_2))\frac{N(t)}{z(t)+N(t)}. \end{cases} \tag{4.2}$$

If the selective forces of the system dynamics are strong enough, we should expect to see the distribution of clones, $P_\alpha(t) = \frac{x_\alpha(t)}{N(t)}$ to change over time, and the question of what the final distribution will be, or what the transitional regimes will be observed, does not have an intuitive and predictable answer. This is due to the fact that now the state of the environment in which the population evolves is determined not only on the amount of resources that the individuals have to compete for but also by the population composition and individuals themselves; consequently, different types of clones can impose different selective pressures on each other, further affecting the dynamics. These selective pressures that are imposed on the population cannot be captured without taking into account population heterogeneity.

The proportion of each type of clone within the population can be tracked through the expected value of the parameter α, which in the homogeneous system was of course just a constant but in a parametrically heterogeneous system becomes a function of time. It can be calculated depending on the initial distribution of α within the population.

Each individual tries to maximize his or her own fitness through allocating the resource in such a way as to maximize their fitness, which in the framework of ODEs is measured as the growth rate per individual, i.e., $\frac{dx_\alpha}{dt}/x_\alpha$. If only two clones adhering to 2 pure strategies were interacting, the predominant strategy would be determined only by the relative value of $\frac{dx_\alpha}{dt}$ of each clone at each time point(see Figure 4.2). However, if many clones are interacting, it is not immediately clear, which strategy will come to dominate

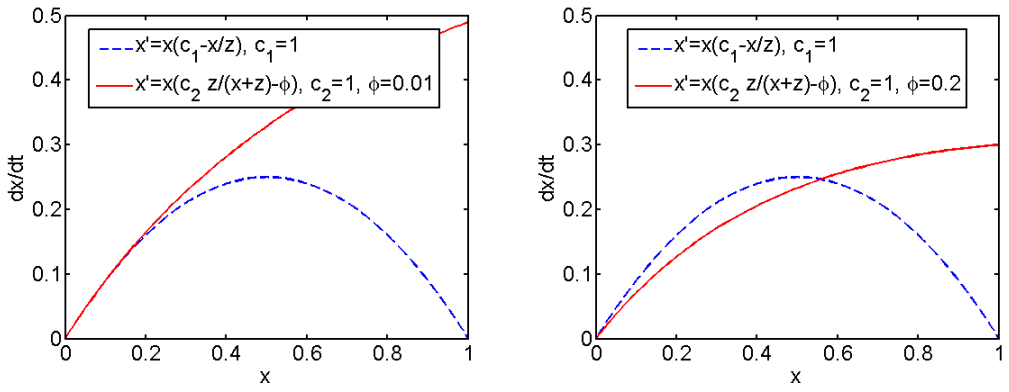

Figure 4.2: Mixed niches, different growth curves (a) $c_1 = c_2 = 1, \phi = 0.01$ (b) $c_1 = c_2 = 1, \phi = 0.2$.

through natural selection, since both population composition and the amount of resources available would be changing.

In order to investigate this question, let us introduce keystone variables $q(t)$ and $g(t)$ such that

$$\begin{cases} \frac{dq}{dt} = \frac{z(t)}{z(t)+N(t)}, \\ \frac{dg}{dt} = \frac{bN(t)}{kz(t)}. \end{cases} \tag{4.3}$$

Then the equation for the rate of change of the frequency of each clone x_α can be rewritten as

$$x_\alpha(t)' = r x_\alpha(t)(\alpha(c_1 - g(t)') + (1-\alpha)(c_2 q(t)' - \phi)). \tag{4.4}$$

Integrating both sides of the equation, we get that

$$x_\alpha(t) = x_\alpha(0) e^{[r((\alpha c_1 - (1-\alpha)\phi)t + (1-\alpha)c_2 q(t) - \alpha g(t))]} \tag{4.5}$$

Then the total population size $N(t)$ becomes:

$$\begin{aligned} N(t) = \int_\alpha x_\alpha(t) d\alpha = N(0) \int_\alpha e^{r(c_2 q(t) - \phi t)} \cdot e^{r\alpha((c_1+\phi)t - c_2 q(t) - g(t))} P_0(\alpha) d\alpha \\ = N(0) e^{r(c_2 q(t) - \phi t)} \cdot M_0[r((c_1+\phi)t - c_2 q(t) - g(t))] \end{aligned} \tag{4.6}$$

where $N(0)$ is initial population size, and M_0 is the moment generating function (mgf) of the initial distribution of α in the population, which is a known function if P_0 is given. The

distribution of clones over time is given by

$$P_\alpha(t) = \frac{x_\alpha(t)}{N(t)} = \frac{e^{\alpha\Omega(t)}}{M_0[\Omega(t)]}, \tag{4.7}$$

where $\Omega = r((c_1+\phi)t - c_2 q(t) - g(t))$. The mean value of α at time t is

$$E^t[\alpha] = \int \alpha P_t(\alpha) d\alpha = \int P_0(\alpha) \frac{\alpha e^{\alpha\Omega}}{M_0(\Omega)} d\alpha = \frac{M_0'(\Omega)}{M_0(\Omega)}. \tag{4.8}$$

Putting together all the expressions that have been obtained as a result of these transformations, we can now reduce inhomogeneous System (4.2) to the following system:

$$\begin{cases} \frac{dz}{dt} = p - dz(t) + re(E^t[\alpha](1-c_1) + (1-E^t[\alpha])(1-c_2))\frac{N(t)}{z(t)+N(t)}, \\ \frac{dq}{dt} = \frac{z(t)}{z(t)+N(t)}, \\ \frac{dg}{dt} = \frac{bN(t)}{kz(t)}, \end{cases} \tag{4.9}$$

where $N(t)$ is defined in 4.6 and $E^t[\alpha]$ is the mean value of the parameter α, which can be calculated from Equation (4.8). Hence, we have reduced the infinitely-dimensional System 4.2 to a system of only three equations. The keystone variables $q(t)$ and $g(t)$, which were not present in the original model, are actually the "keystone" quantities that govern the system dynamics and determine the model solution and all of its the statistical characteristics. The details on this approach to studying replicator equations can be found in [69, 70].

Differences in intrinsic properties of the population

In order to investigate, how such a heterogeneous system can evolve over time depending on different initial parameter values, we will consider two different initial distributions of clones within a population: uniform and truncated exponential (of which uniform distribution can be considered a special case). The choice of truncated exponential distribution can be justified through the principle of maximum entropy (MaxEnt): if the mean value of the random variable is the only quantity that can be estimated from observations or other data, then the most likely distribution of the variable is exponential with the estimated mean [68]. Given that α is bounded on the interval $[0,1]$, then, according to MaxEnt principle, we should choose the truncated exponential in this interval as the initial distribution.

Parameter values for the trajectories, illustrated in Figure 4.3a and 4.3c were chosen explicitly to fall into Domain 1. The two figures differ only in the value of parameter ϕ, which

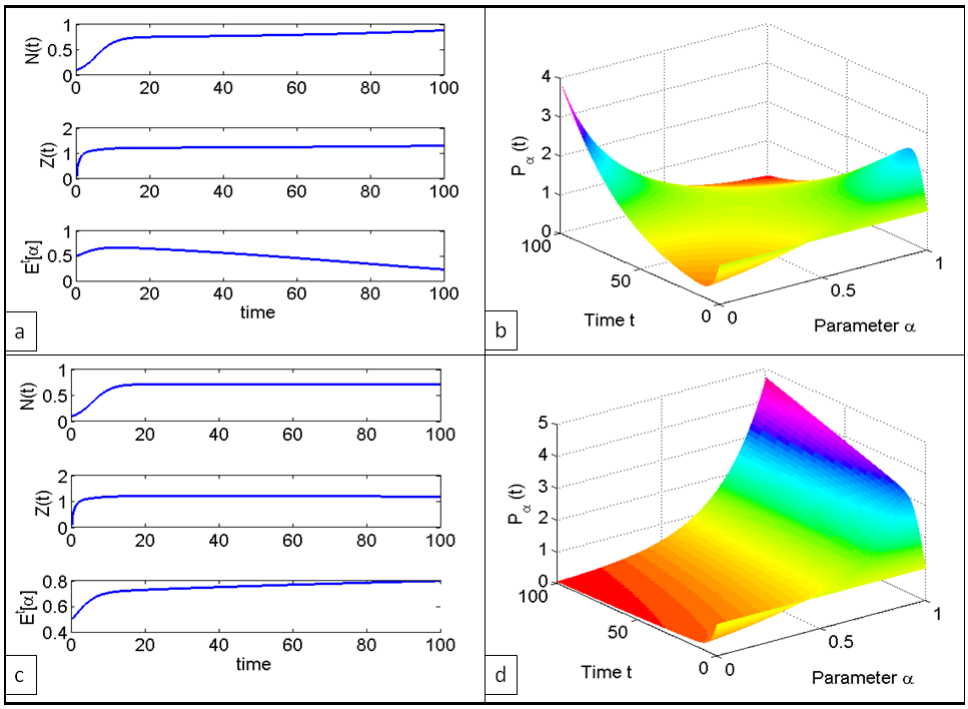

Figure 4.3: Trajectories and distribution of clones throughout the completely "altruistic" population (starting in Domain 1). Even a very slight change in the value of an intrinsic parameter ϕ (natural death rate of individuals that invest primarily in fecundity) causes the system to evolve towards the dominance of one or the other strategy (investment in fecundity in the top case and investment into carrying capacity in the bottom case). The total population size and the total amount of resource are virtually the same in both cases. All parameters held constant at $r = 1$, $e = 1$, $b = 1$, $k = 1$, $N_0 = .1$, $c_2 = .2$, $c_1 = .6$, $d = 1$, $p = 1$,$\phi = 0.09$. (c-d): all parameters held the same, except $\phi = 0.14$.

is taken to be $\phi = 0.09$ in Figure 4.3a and $\phi = 0.14$ in Figure 4.3c, and nevertheless one can already observe that the population evolves towards different expected values of α, This is most evidently reflected in the graph for how the distribution of clones changes over time in Figs. 4.3b and 4.3d. This suggests that even a small change in the intrinsic properties of individuals within the population can have critical effect on which way a heterogeneous population will evolve.

However, the mean value of α does not always reach an equilibrium value, i.e., the population does not always tend towards some fixed strategy, whether pure or mixed. Starting in Domain 6, we can observe that not only do the population size and amount of resource start oscillating (which corresponds to the system "entering'' inside the domain of attraction of the stable limit cycle) but so does the $E^t[\alpha]$. So, as the system evolves, no

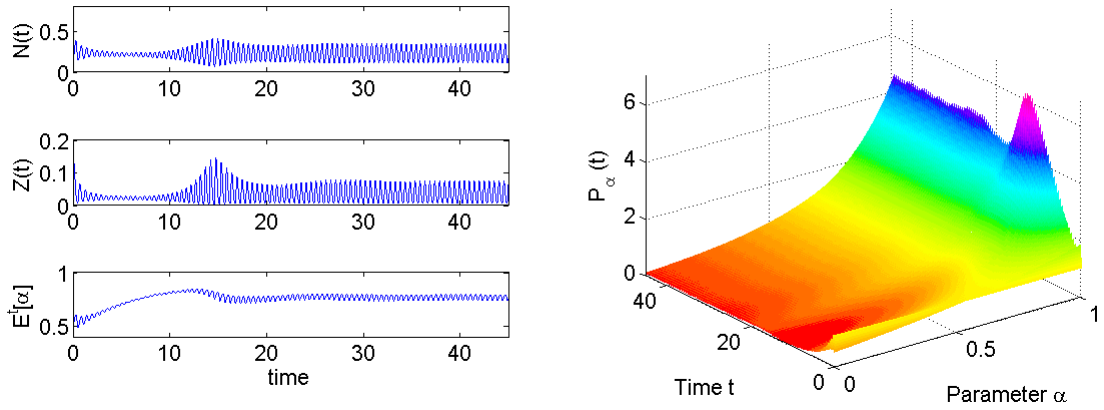

Figure 4.4: Trajectories and distribution of clones throughout the population. In this case, one not only observes stable oscillatory behavior in the amount of resource and total population size but also a shift between the two strategies. That is, the population evolves not towards eventual dominance of just one pure strategy but shifts between two strategies. Initial distribution is uniform. Initial conditions are such as to fall within Domain 6. Parameters are $r = 1$, $e = 1$, $b = .9$, $k = 1$, $\phi = 1.2$, $N_0 = .1$, $c_2 = 8.75$, $c_1 = 9$, $d = 24$, $p = 7.72$.

final distribution of clones gets fixed over time (Figure 4.4). This suggests that the standard approach using a fixed value of the parameter α (or its mean value) can yield incorrect predictions within this domain of the model parameters and, hence, is not justified in general case.

Differences in initial composition of the population

Now we would like to investigate how the changes in initial distribution of clones will affect the direction in which the population will evolve. That is, even if the intrinsic properties of the individuals within the system are stabilized (that is, birth and death and resource consumption rates are fixed), what are going to be the effects of selective pressures that are imposed by other individuals in the population? Or in other terms, how will the evolution of the system be affected by the strategic choices made by others?

In Figures 4.5 and 4.6, one can observe the changes in the population size $N(t)$, resource amount $z(t)$ and the mean value $E^t[\alpha]$ over time under different initial distributions, given that all other initial conditions were the same for both cases.

In Figure 4.5, part (a) corresponds to initial uniform distribution, part (b) to initial truncated exponential distribution with parameter $\mu = 1.1$, and part (c) to initial truncated

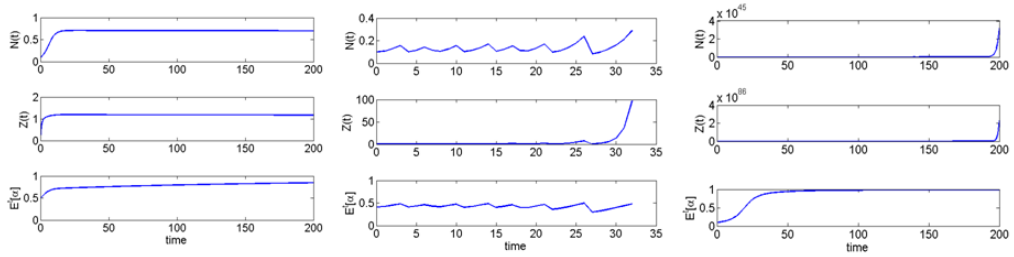

Figure 4.5: The effects of difference in the initial composition of the population with respect to different strategies. Different initial distributions were chosen to be (a) uniform initial distribution (b) truncated exponential initial distribution, with parameter $\mu = 1.1$ (note: population crashes after time $t = 32$) and (c) truncated exponential initial distribution, with parameter $\mu = 10.1$. Initial conditions are such as to fall within Domain 1. All parameters held constant at $r = 1$, $e = 1$, $b = 1$, $k = 1$, $N_0 = .1$, $c_2 = .2$, $c_1 = .6$, $d = 1$, $p = 1$, $\phi = 0.14$. One can see that the initial composition of the population can have dramatic effects on the direction in which the population will evolve over time. (Note: the values of μ were chosen arbitrarily for illustrative purposes).

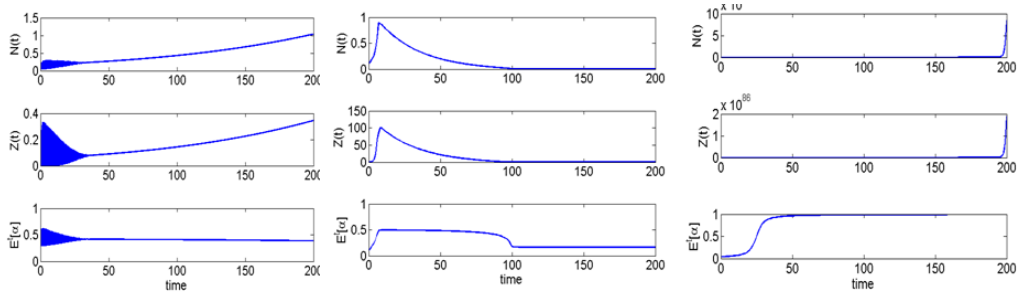

Figure 4.6: The effects of difference in the initial composition of the population with respect to different strategies. Different initial distributions were chosen to be (a) uniform (b) $\mu = 10.1$ and (c) $\mu = 30.1$. Other parameters held constant at $r = 2$, $e = 2$, $b = 1$, $k = 1$, $N_0 = .1$, $c_2 = .2$, $c_1 = 2$, $d = 1$, $p = 1$, $\phi = 0.05$.

distribution with parameter $\mu = 10.1$. One can see that the trajectories look strikingly different as the population evolves, passing through different regions of the phase-parameter space. Noticeably, in Figure 4.5b, the population size crashed at $t = 32$, while in parts a and c one could observe stable coexistence with the resource. This effect is due to the trajectory moving outside of domain of attraction of the non-trivial equilibrium point A in Figure 4.5b.

Discussion

Ecological systems consist of interdependent diverse entities that can adapt to changes in their environment. This ability to adapt is rooted in their diversity, as individuals within the system can affect each other and thus also the direction in which the system evolves.

The ability of individuals to "co-evolve" with their resource has been termed "niche construction" [116], and it is possible if the resource is also dynamic. The study of complex interactions between a heterogeneous population of individuals that can not only consume their resource but also contribute to its restoration, and identification of the different regimes that the system can go through as the population evolves, is the focus of this Chapter. Sustainable coexistence with the common resource (successful formation of a niche) is accounted for by existence of the non-trivial equilibrium point A. Its coordinates (the population size and the corresponding amount of common resource available for everyone) change as the parameters α (proportion of individuals that choose to invest into increasing environmental capacity) and c_1 (niche-construction abilities of the carrying-capacity oriented individuals) are varied.

At first, full bifurcation analysis was performed on the model, where the population was assumed to be homogeneous. This was done to identify all possible dynamical regimes in the system to then evaluate the effects of natural selection on population heterogeneity within the same model, i.e., to see how these dynamic regimes will change in a parametrically heterogeneous system. The obtained bifurcation diagram describes the possible dynamical regimes of a population that is homogeneous with respect to α.

In order to investigate how a heterogeneous population will behave, we applied the Reduction theorem, which allows reducing an otherwise infinitely dimensional System (4.2) to a 3-dimensional system of non-autonomous ODEs.

The approach can be summarized as follows: assume each individual within the heterogeneous population is characterized by their own intrinsic value of the parameter α. Assume also that the individuals can be grouped in such a way as to fall into some distribution that is known at the initial time moment. Replacing the constant average value of α of a homogeneous population with an expected value of α at each time moment, which can be tracked through the moment generating function of the initial distribution, allows observing the mean ofα moving across (traveling) through the phase parameter portrait as the population evolves. This approach to studying the dynamics of the parametrically inhomogeneous system was justified by the Reduction theorem.

Several interesting effects were observed that allow answering, at least in part, the questions posed in the beginning of this work. We were able to observe that the direction in which the population will evolve is largely determined by what domain in the phase parameter space one starts in. We also showed that the strategy towards which the population eventually evolves is not always a pure strategy. Moreover, we have been able to observe regimes when the mean value of α oscillates sustainably, as do population size and amount of resource (this occurs when the system enters Domain 6). Also, one frequently can observe oscillatory behavior before a strategy stabilizes and the mean of α reaches an equilibrium. However, sustained oscillations can in fact signal that population collapse is approaching, since this most often occurs when the trajectory passes through Domain 2 (unstable limit cycle) to Domain 4 (unstable node), and from there either to directly to the origin (immediate extinction), or to Domain 5 (elliptic sector).

Full bifurcation analysis of System (4.2) reveals analytically that the population can sustainably coexist with the resource for all $0 < \alpha \leq 1$. The parametric space of sustainable coexistence with the resource decreases if α decreases from $\alpha = 1$ to $\alpha = 0$, which can be interpreted as suggestive of the fact that investment into environmental carrying capacity would generally be a more successful strategy for sustainable coexistence with the common resource. However, this observation does not necessarily hold for heterogeneous systems: starting with different initial distributions, even within the same domain on the phase-parameter portrait, can lead to different system behaviors and different strategies being favored by natural selection in the long run. We could observe it by calculating numerical solutions of the system, with uniform initial distribution of strategies within the population, and truncated exponential initial distribution (parameter α bounded on the interval $[0, 1]$) with different parameters of the distribution (Matlab code used is available upon request). As one can see in Figures 4.4 and 4.5, even when everything else is equal, the direction in which the system will evolve depends greatly on the initial distribution.

Some empirical examples

Examples of population heterogeneity and intraspecies interactions driving the population towards one or the other strategy can be observed in many systems and on many levels of selection.

On the molecular level, Voytek and Joyce [163] reported that continuous in vitro evolution can be observed as 2 different "species" of RNA enzymes are made to compete against each other for common limited resources (in this case substrates). In the described experiment, the substrates were necessary for amplification of RNA. The authors observed that as the system evolved, so did the enzymes, whose biochemical characterization revealed distinct differences in their strategies: enzymes that invested in being efficient rather than proliferative, reacted with the substrate nearly hundredfold faster than the other; highly proliferative selected enzymes, while not as reactive, produced 2-3 times more progeny.

Elser et al. [39] investigated the question of resource management at the cellular level, looking particularly at competition for the common resource among different types of tumors. The authors found that in some tissues, such as in colon and lung, the environment is such as to promote selection of most rapidly proliferating clones, while conditions in other organs may favor the clones with lower mortality rate. This suggests that even within the same tumor, different conditions might favor evolution towards different strategies, an idea, which will be investigated in detail in Chapter 5. This, of course, is only possible because of tumor heterogeneity, i.e., the fact that tumors are genetically heterogeneous, composed of populations of genetically diverse cells [63, 100, 153] that in addition to competing for the common resources also impose selective pressures on each other.

Another example of selection on the cellular level has been shown by Chikatsu et al. [19]. The authors studied two types of rat embryo fibroblasts and were able to observe that not only did conditions in the culture affect selection in cell clones with respect to growth strategy but also that presence of one type of clones affected fitness of another type of clones under the same environmental conditions.

On the organismal level, distinct ecological strategies emerge and evolve in unicellular organisms like bacteria. Denef et al. [33] observed that in natural acidophilic biofilm communities two genotypic groups of *Leptospirillum* bacteria are unequally represented in the bacterial population during different stages of colonization. At the early stages of colonization, the environmental resources (compatible solutes) are directed towards osmoprotection (increasing environmental carrying capacity), while in the successive stages more resources

are redirected towards metabolism and investing in fecundity.The importance of intraspecies variation and its effects on biodiversity has also been documented in multicellular organisms, such as forest trees [20], malaria mosquitoes [134], hylid frogs [1], Eurasian badgers [93], as well as in human social "ecological systems" [53].

These empirical observations, coupled with the theoretical predictions of the conceptual model that was proposed here, lead us to make the following important conclusion: when predicting where the system will evolve, just knowing the rules that govern its dynamics might not be enough to make a more or less accurate prediction. One needs to also know the composition of the population that is playing by these rules. This is true even in the case of perfect information, i.e., when every individual in the population knows the rules and plays to maximize his or her own fitness.

Conclusions

Variability that is heritable and that affects fitness is what makes natural selection possible. In any ecological system, the environment is composed not only of the resource but also of other individuals in the same population, which may often impose no less of a selective pressure than the pressures of resource limitations or interactions with the members of other populations and even of other species. Therefore, if one wants to make predictions about any evolving system, one has to take into account population heterogeneity – assumption of homogeneity is an oversimplification.

Chapter 5

BIOLOGICAL STOICHIOMETRY IN TUMOR MICROENVIRONMENT

Abstract

In this chapter the conceptual framework, developed in Chapter 4, is applied to cancer. Whatever the intrinsic properties each individual cell within the tumor may possess, it first needs to survive before it can turn to proliferation. Depending on nutrient availability, tumor as a whole may evolve towards primarily competitive or proliferative phenotype. According to the growth rate hypothesis (GRH), increased phosphorus availability in the ecosystem, such as tumor microenvironment, may shift evolution within the tumor towards a more proliferative and thus potentially more malignant phenotype. Here we show that limiting phosphorus availability thus might promote intracellular competition within the tumor, delaying disease progression, using an infinitely dimensional system of ordinary differential equations that are reduced to low dimensionality using the Reduction theorem. We also show that tumors respond differently to changes in their microenvironment depending on initial distribution of clones within the tumor, regardless of its initial size, which suggests that composition of the tumor as a while needs to be evaluated in order to maximize therapy efficacy.

Keywords: tumor heterogeneity, growth rate hypothesis, resource allocation, microenvironment manipulation

Introduction

One can think about cancer as an ecological system: a tumor is a heterogeneous population of cells that compete for space and nutrients with each other and with somatic cells in the environment of the human body [25, 71, 100, 109]. Whatever the cells' intrinsic properties may be, whether it is increased proliferation or low mortality, they need nutrients to survive before they can proliferate and further invade the body.

Carbon is the main energy source for all cells and is required for cell survival before proliferation. Phosphorus is the source of cell building materials for the cells, going into

creating DNA, RNA, ribosomes, etc. And even more importantly, unlike other microelements, it is not replaceable. Experimental evidence suggests that indeed, when the amount of phosphorus in the tumor microenvironment goes up, so does tumor growth [65]. However, it seems like it is not just the absolute amounts of carbon and phosphorus that are important for cell growth; instead, it is a stoichiometric ratio of carbon to phosphorus that the cell is sensitive to. In fact, it has been proposed that increased availability of phosphorus relative to carbon favors expansion of fast growing organisms, a conjecture that has become known as the growth rate hypothesis (GRH) [38] and which has been partially experimentally validated for cancer cells [39].

Tumors are complex adaptive systems, composed of interconnected and interdependent genetically diverse cells. Adaptive ecosystems are too complex to be controlled but changing the environment in which its inhabitants interact may give a way to harness the system, directing its evolution in the more desired direction. In order to maximize their fitness, i.e., the overall growth rates reflected through the difference between birth and death rates, and depending on selective pressures from the environment, individuals within one population can invest either in increasing their fecundity (proliferative clones) or in competition. Proliferative clones would be investing primarily in maximizing their growth rates, while competitive clones would be investing in minimizing their death rates. Now assume that a tumor is a population of cells, where each individual cell is characterized by its own strategy choice (competitive or proliferative). Since the entire population in itself is heterogeneous, different strategies may be represented in different proportions at different times, depending on the selective pressures that the population experiences as a whole. The clones that invest primarily in reproduction may be favored under one set of micro-environmental conditions, making the tumor more proliferative, and clones that invest primarily in competition and not proliferation could be favored under another set of micro-environmental conditions. In this Chapter we would like to investigate what these micro-environmental conditions may be from an ecological perspective, and how/whether this understanding can be used to design better cancer therapies.

In this Chapter a mathematical model is used to evaluate the effects of stoichiomet-

ric ratio of carbon to phosphorus on tumor growth and in particular, we will try to evaluate whether manipulation of this ratio can direct evolution of the tumor towards primarily competitive or proliferative phenotype.

Model description

Let us assume that the tumor cell population is composed of cell clones that use the common resources z, which will be defined and discussed in detail in subsection , to invest either primarily in reproduction or in competition. The subpopulation of more proliferative clones is assumed to grow at rate $r_p\frac{z}{N+z^2}$ and die at some constant rate d_1. The functional form for the growth term is chosen in such a way as to incorporate the assumptions that 1) all the available resource is directly invested into increasing the number of cells and 2) that there exists some optimal relationship between carbon and phosphorus, such that excess P would in fact slow down cell growth, as was observed in other ecosystems [13]. This is accounted for in the model with z^2. The growth rate of more competitive clones is accounted by the functional form $r_c(1-\frac{N}{z})$, where the amount of resource, which in itself is a dynamic variable, determines the carrying capacity for this subpopulation.

Now let us introduce parameter$\alpha \in [0,1]$, which represents the proportion of total resources z that are used to invest in competition, thus effectively leaving $(1-\alpha)$ proportion of total resources for proliferation. Total population size is then given by $N(t) = \sum_{\mathbb{A}} x_\alpha$, and the equation to describe the dynamics of the entire cell population becomes

$$\frac{dx_\alpha}{dt} = x_\alpha(t)\underbrace{(\underbrace{\alpha r_c(1-\frac{N(t)}{z(t)})}_{\text{competitive}} + \underbrace{(1-\alpha)r_p(\frac{z(t)}{N(t)+z(t)^2}-d)}_{\text{proliferative}})}_{\text{total cell growth}} \tag{5.1}$$

where $N(t) = \sum_\alpha x_\alpha$.

Each clone $x_\alpha(t)$ within the population tries to maximize its fitness by investing the available resources $z(t)$ either in increasing reproduction or decreasing mortality. As the population grows and/or as environmental conditions change (i.e., $z(t)$ changes), the clones are selected depending on the strategy that maximizes their overall growth rate, reflected through the value of $dx_\alpha(t)/dt$. The transitional regime in terms of population composition with respect to the strategies occurs at the intersection point of the two growth functions,

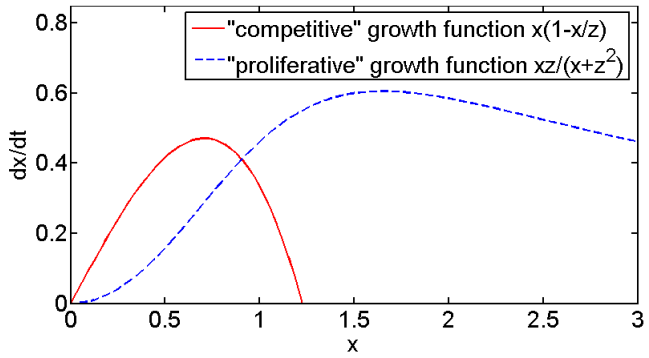

Figure 5.1: Schematic representation of the interaction between the two growth strategies. Depending on the amount of resource z, either the competitive or the proliferative strategy clones have higher growth rates. At the intersection of the two curves neither strategy gives the clones an advantage, regardless of the distribution of clones in the population (i.e., regardless of the value of α).

i.e., when $\frac{z(t)}{N(t)+z(t)^2} - d = 1 - \frac{N(t)}{z(t)}$, which occurs when

$$N(t) = \frac{z(t)}{2r_c}(r_c + d - r_c z(t) + \sqrt{d^2 + 2dr_c(1+z(t)) + r_c(-4r_p + r_c(1+z(t)^{2)})}$$

At this point neither growth strategy gives a competitive advantage to either clone type.

Composite resource and biological stoichiometry

In order to evaluate the effects of difference in elemental composition of the environment on growth and proliferation of its inhabitants, a simple ratio of carbon to phosphorus has been previously used [13, 38, 103]. However, while this functional form may be valid for the cases when the amounts of C and P are comparable, it becomes invalid at the extremes, i.e., when either of the elements is orders of magnitude more abundant than the other. Moreover, it predicts the same impact on growth rates regardless of whether there is very little of either element, or when there is a lot, which is not plausible. In order to address these two issues we propose using not the simple ratio of $C:P$ but a saturation function of the form $z = \frac{CP}{C+P}$. When the amounts of carbon and phosphorus are comparable, this function can be approximated by the traditionally used $C:P$; however, this particular functional form also allows to make more plausible predictions and eliminate inconsistencies that would have otherwise been observed when the amounts of C and P are very different.

The full model

The equations for the changes in extracellular and intracellular phosphorus concentrations are derived from chemostat equations (see, for instance, [81]). The extracellular

phosphorus is replenished from the blood stream at a rate $g_2(P_0 - P^{ex})$, is consumed by the cells based on concentration differences between extracellular and intracellular P at a rate $mN(\frac{P^{ex}-P^{in}}{k_2+P^{ex}-P^{in}})$ and is replenished also through cell death at a rate dNP^{in}. Extracellular phosphorus is consumed at a rate $mN(\frac{P^{ex}-P^{in}}{k_2+P^{ex}-P^{in}})$, and the differences in resource uptake rates by different clones are captured through the term $m = m_p(1-\alpha) + m_c\alpha$. The absolute amounts of nutrients are then recalculated into concentrations, yielding the following system of equations:

$$\begin{cases} \frac{dx_\alpha}{dt} = x_\alpha F_\alpha(t) \\ \frac{dP^{ex}}{dt} = \underbrace{g_2(\frac{P_0 - P^{ex}(t)}{N(t)})}_{\text{external inflow}} - \underbrace{m\frac{P^{ex}(t) - P^{in}(t)}{k_2 + (P^{ex}(t) - P^{in}(t))} - \underbrace{P^{ex}(t)E^t[F]}_{\text{chain rule}}}_{\text{phosphorus uptake by the cells}} + \underbrace{dP^{in}(t)}_{\text{P recycled from dead cells}} \\ \frac{dP^{in}}{dt} = \underbrace{m\frac{P^{ex}(t) - P^{in}(t)}{k_2 + (P^{ex}(t) - P^{in}(t))} - \underbrace{P^{ex}(t)E^t[F]}_{\text{term derived from chain rule}}}_{\text{phosphorus uptake by the cells}} \end{cases} \tag{5.2}$$

where

$z = \frac{C^{in}P^{in}}{C^{in}+P^{in}}$

$F_\alpha(t) = \underbrace{\underbrace{\alpha r_c(1-\frac{N}{z})}_{\text{competitive}} + \underbrace{(1-\alpha)r_p(\frac{z}{N+z^2} - d)}_{\text{proliferative}},}_{\text{total cell growth}}$

$m = \underbrace{\underbrace{m_p(1-\alpha)}_{\text{proliferative}} + \underbrace{m_c\alpha}_{\text{competitive}}}_{\text{rate of phosphorus uptake by all cells}},$

$E^t[F] = E^t[\alpha]r_c(1-\frac{N}{z}) + (1-E^t[\alpha])r_p(\frac{z}{N+z^2} - d),$

$E^t[\alpha] = \frac{\sum \alpha x_\alpha}{N(t)}.$

Detailed derivation of the model is given in Appendix. The conceptual structure of the model is captured in Figure 5.2 and the meanings of all variables and parameters are

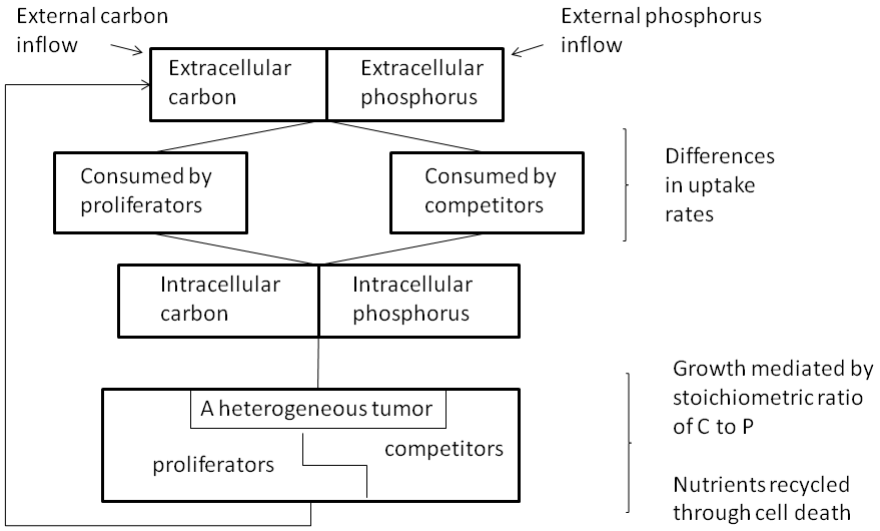

Figure 5.2: Diagram of mechanism described in System 5.2

Parameter	Meaning	Range
α	Proportion of competitive cells in the population	$\alpha \in [0,1]$
r_c	Growth rate of competitive cells	$r_c > 0$
r_p	Growth rate of proliferative cells	$r_p > 0$
d	Natural cell death rate	$d > 0$
g_2	Scaling constant for P inflow	$g_2 > 0$
P_0	Gradient constant for amount of external P inflow	$P_0 > 0$
k_2	Saturation constant for P uptake by the cells	$k_2 > 0$
h	Scaling constant for optimal C:P ratio	$h > 0$
m_c	Phosphorus uptake rate of competitive cells	$m_c > 0$
m_p	Phosphorus uptake rate of proliferative cells	$m_p > 0$
$m = m_c(\alpha) + m_p(1-\alpha)$	Total carbon uptake rate	$m > 0$
C^{in}	Concentration of intracellular carbon	$C^{in} > 0$

Table 5.1: Summary, brief description and range of all parameters in System 5.2

summarized in Table 5.1.

Modeling parametric heterogeneity

Since the goal of the proposed model is to evaluate the changes in external nutrient supply, and particularly variations of parameter P_0 on the changes in the distribution of cell phenotypes within the tumor, we need a way to measure how the composition of the cell population changes over time. Assume that different clones within the tumor are represented in different proportions depending on the value of parameter α, falling within some initial known distribution. If the choice of strategy with respect to interactions with the resource (investing in competition or proliferation) affects fitness, then each subpopulation of clones, characterized by α, is going to be growing at different rates. Consequently, the distribution of clones within the entire cell population will be changing over time, and so will the expected value of α. In its current form, System 5.2 is infinitely dimensional. However, let us introduce keystone variables $q(t)$ and $g(t)$ such that

$$\begin{cases} q(t)' = r_c(1 - \frac{N(t)}{z(t)}) \\ g(t)' = r_p(\frac{z(t)}{N(t)+z^2(t)}) \end{cases} \tag{5.3}$$

Then the equation for the total population of cells $x_\alpha(t)$ can be rewritten as

$$\frac{dx_\alpha(t)}{x_\alpha(t)} = \alpha q'(t) + (1-\alpha)(g'(t) - d) \tag{5.4}$$

Integrating equation 5.4 yields the following explicit expression for x_α in terms of keystone variables $g(t)$ and $q(t)$:

$$x_\alpha(t) = x_\alpha(0)e^{\alpha q(t)+(1-\alpha)(g(t)-dt)} \tag{5.5}$$

Then the full population size becomes

$$N(t) = \int_\alpha x_\alpha(t)d\alpha = N(0)\int_\alpha e^{g(t)-dt}e^{\alpha(q(t)-g(t)+dt)}P_\alpha(0)d\alpha = N(0)e^{g(t)-dt}M_0[q(t)-g(t)+dt] \tag{5.6}$$

where $P_\alpha(0) = \frac{x_\alpha(0)}{N(0)}$ and M_0 is the mgf of P_0, so that the final distribution of clones over time becomes

$$P_\alpha(t) = \frac{x_\alpha(t)}{N(t)} = \frac{e^{\alpha(q(t)-g(t)+dt)}}{M_0[g(t)-q(t)+dt]} \tag{5.7}$$

With these transformations, the otherwise infinitely-dimensional System 5.2 can now be rewritten as a system of four non-autonomous ODEs:

$$\begin{cases} \frac{P^{ex}(t)}{dt} = g_2(\frac{P_0 - P^{ex}(t)}{N(t)}) - m\frac{P^{ex}(t) - P^{in}(t)}{k_2 + (P^{ex}(t) - P^{in}(t))} - P^{ex}(t)E^t[F] + dP^{in}(t) \\ \frac{P^{in}(t)}{dt} = m\frac{P^{ex}(t) - P^{in}(t)}{k_2 + (P^{ex}(t) - P^{in}(t))} - P^{ex}(t)E^t[F] \\ \frac{dq(t)}{dt} = r_c(1 - \frac{N(t)}{z(t)}) \\ \frac{dg(t)}{dt} = r_p(\frac{z(t)}{N(t) + z^2(t)}) \end{cases} \tag{5.8}$$

where the mean value of parameter α is given by

$$E^t[\alpha] = \int \alpha P_\alpha(t) d\alpha = \int \alpha \frac{e^{\alpha(q(t) - g(t) + dt)}}{M_0[g(t) - q(t) + dt]} = \frac{M_0'[g(t) - q(t) + dt]}{M_0[g(t) - q(t) + dt]}, \tag{5.9}$$

and total population size is defined above. Population composition with respect to strategy choice can now be tracked through changes in the mean of α such that the higher the value of $E^t[\alpha]$, the more competitive clones there are in the population, and therefore the fewer cells remain that will invest primarily into proliferation.

Results

First we evaluated the hypothesis that increased phosphorus inflow could shift population composition towards more proliferative phenotype. This is measured through the expected value of parameter α as P_0 is increased. The higher the value of α, the larger the proportion of cells that invest primarily in competition. The initial conditions are taken to be $N_0 = 2$, $P^{ex}(0) = 10$, $P^{in}(0) = 9$, $E^t[\alpha] = 0.05$, $q(0) = g(0) = 0$ and all the parameter values are taken to be $d = .03$, $r_p = .2$, $r_c = .2$, $m_p = .2$, $m_c = .2$, $P_0 = 10$, $h = 1$, $k_2 = 1.1$, $g_2 = 1$, unless indicated otherwise. Numerical solutions were calculated until $t_{max} = 6000$. The initial distribution was taken to be truncated exponential on the interval $\alpha \in [0, 1]$. Matlab2010a code used is available upon request.

Numerical solutions to System (5.8) support our hypothesis that increasing availability of extracellular phosphorus indeed creates an environment that favors expansion of more proliferative clones, which is reflected in the changes in the expected values of α, and which can also be observed in the changes in the density $P_\alpha(t)$ (see Figure 5.3). When the value of P_0 is increased beyond 30, one can observe unexpected transitional regimes. The population size first decreases briefly and then increases again, now composed of a different

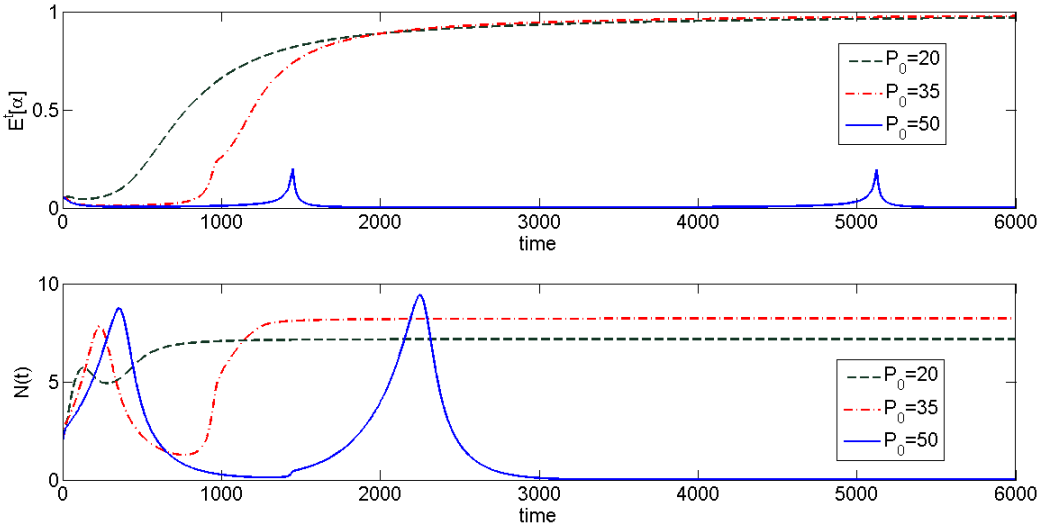

Figure 5.3: The higher the rate of external P inflow, the longer it takes for the population to go back to primarily competitive phenotype until finally it just remains composed mostly of proliferative clones, with short-lived "bursts" of competitiveness.

type of cell clones, as can be evaluated through the changes in the mean of α. Finally, the most unexpected effect is observed when $P_0 > 40$. In this case one starts to see oscillations in population composition and size over time in such a way that the population composition never returns to primarily competitive phenotype. Interestingly, this effect is only observed then proliferative clones grow according to Holling type III function (exhibit the property of futile metabolism at very high ratio of C to P); assumption of Holling type II functional form (regular saturation function), i.e., when $N_1' = r_p N_1(\frac{z}{N+z} - d)$, did not predict saltatory tumor growth regardless of the concentration of extracellular phosphorus.

This effect can be seen also in Figure 5.4, where the changes in the mean value of α are recorded over time with respect to varying P_0; one can clearly see that while at low P_0 the population always eventually returns to predominantly competitive phenotype ($E^t[\alpha] \to 1$), at very high P_0 it remains composed primarily of proliferative clones ($E^t[\alpha] \to 0$).

Differences in growth rates and nutrient uptake rates

We evaluated changes in population dynamics in response to differences in nutrient uptake rates for both clone types. When more competitive clones have higher nutrient uptake rates, it does not affect their growth rate significantly, since growth limitations are imposed by carbon availability, which in our model is kept constant (Figure 5.6). However, interestingly

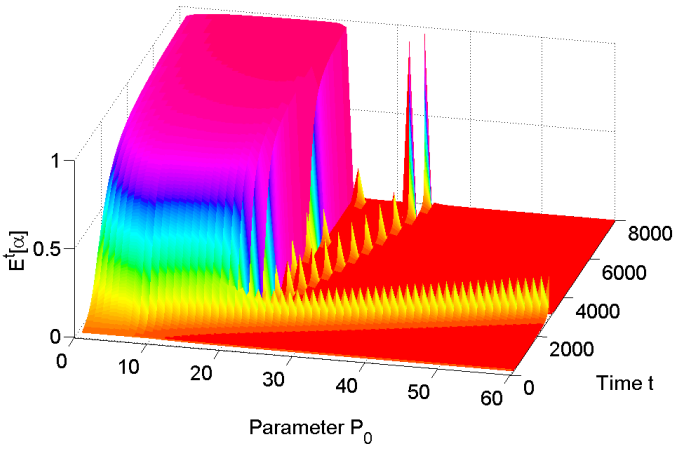

Figure 5.4: Changes in the mean of α vs time vs external phosphorus inflow.

and counter-intuitively, when proliferative clones have higher nutrient uptake rates, it does not give them a competitive advantage. This effect can be explained in the following way: even though more proliferative clones take up more phosphorus, unless they have enough carbon to meet the energy demands for proliferation, they cannot use it, thus engaging in what can be termed "futile metabolism". The model suggests that proliferative clones seem to be most successful when their uptake rates match those of competitive clones, and so targeting phosphorus transporters would in fact promote proliferative phenotype rather than hinder it.

Next, we evaluated the effects of changes in intrinsic growth rates of either clone type on the overall population composition (Figure 5.6). Even though predictably, increasing growth rates of more competitive clones shifted the population composition towards being dominated by competitive phenotype, the overall final population size remained the same regardless of population composition. This suggests that the size of the tumor is not a good predictor of population composition, and the distribution of clones within the tumor needs to be evaluated, since depending on the initial distribution of clones the tumor may respond differently to any micro-environmental changes, whether it is nutrient availability or the presence of therapeutic agents.

Different initial distributions

Since tumors are evolving heterogeneous systems, the overall composition of cell population may vary over time, and hence the population as a whole may respond differently

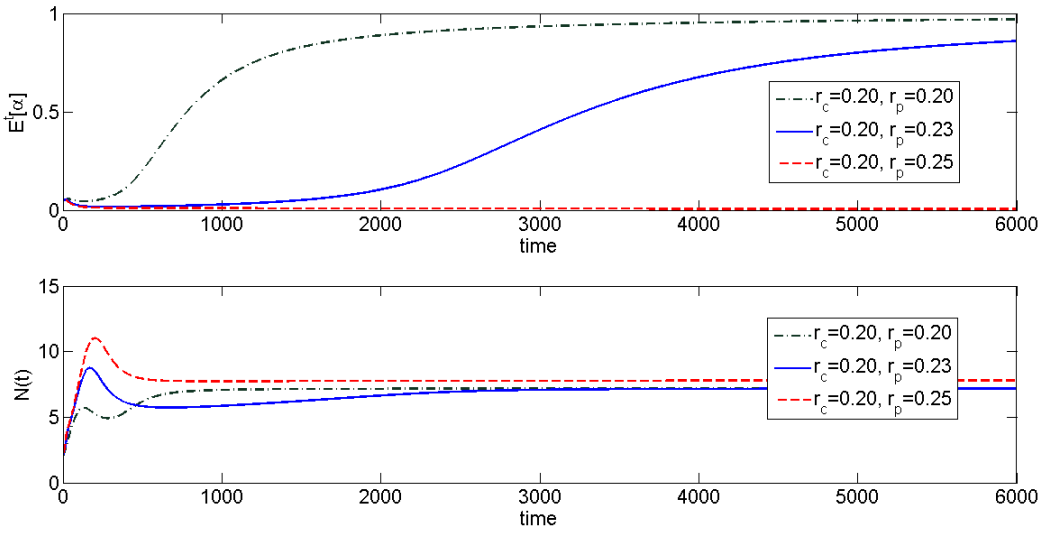

Figure 5.5: Changes in the mean of α and the full population size at $P_0 = 20$ with respect to differences in growth rates. As one can see, it is possible for the population composition to be very different without it being reflected in the overall population size.

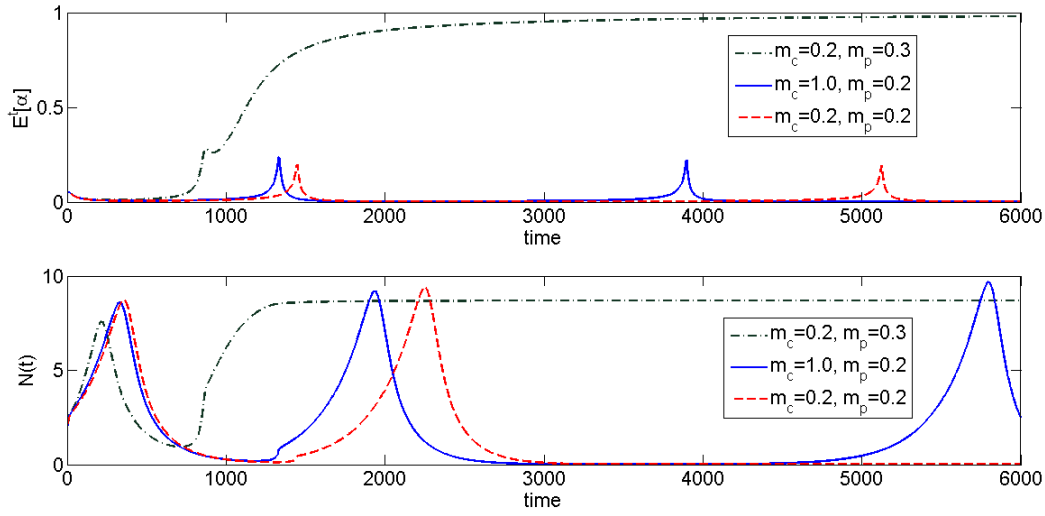

Figure 5.6: Changes in the mean of α and the full population size at $P_0 = 50$ with respect to differences in nutrient uptake ratesAs one can see, proliferative clones are either practically unaffected or at a loss regardless of the relative values of parameters m_c and m_p, which suggests that targeting phosphorus transporters might in fact give advantage to proliferative clones regardless of which clone type may have this adaptation.

to the same set of micro-environmental conditions. We evaluated this effect through varying the initial distribution of clones within the population. We observed that under exactly the same set of initial conditions and under high fixed rate of phosphorus inflow, the population as a whole may or may not evolve towards to more proliferative phenotype, depending on the initial distribution of cell clones in the population with respect to α (Figure 5.7). Specifically, we observed that the higher the proportion of more proliferative clones in the population, the more phosphorus is required to shift population composition towards being dominated by a more proliferative phenotype. This is due to the fact that the direction in which the system evolves depends not only on the external factors but also on population composition, since cells within the population impose as much of a selective pressure on each other as is imposed on them by their extrinsic environment.

This result suggests the following therapeutic approach: one can first try to quantify level of heterogeneity within the tumor with respect to competitive vs. proliferative phenotype and based on this information evaluate the extent of micro-environmental manipulation that would be necessary to shift the composition of the tumor away from the proliferative phenotype.

Discussion

Tumors are adaptive ecological systems. They consist of heterogeneous populations of cells that compete with each other and with somatic cells for space and nutrients, both of which can be limited. Whatever properties the cells may have acquired through mutations, they first need nutrients to survive, and may adapt different strategies to achieve this goal. Specifically, they can choose to invest the available resources primarily in proliferation or in competing with each other. Competitive cells might be getting too distracted with competition thus investing less energy and resources in proliferation, which could delay disease progression. Depending on the environment, in which these interactions occur, one might be able to shift the overall population composition towards one or the other phenotype.

We propose focusing on phosphorus as one of the key elements of the cell microenvironment, and specifically, on stoichiometric ratios between phosphorus and carbon, which, according to the growth rate hypothesis (GRH), may determine which clone type will be

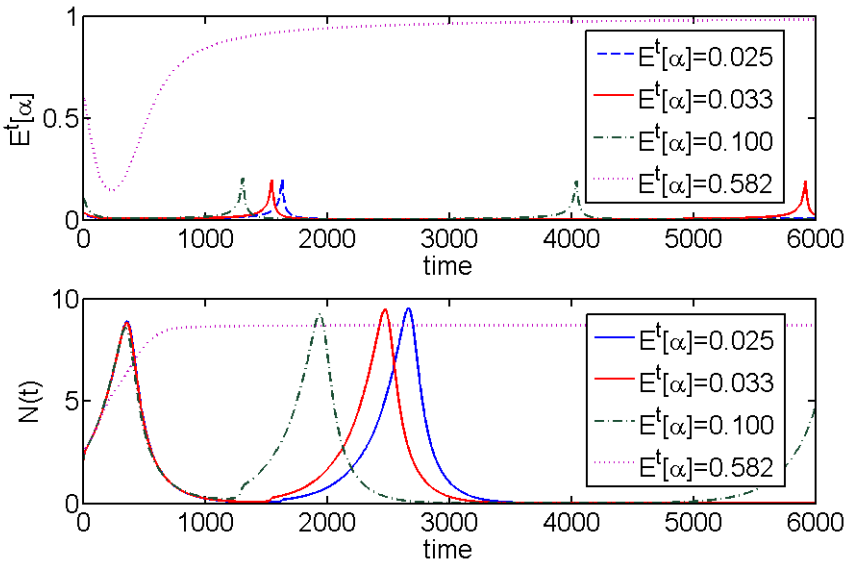

Figure 5.7: Evolution of the system under the same set of initial conditions ($P_0 = 40$) but with different initial distributions of clone types within the population. The results suggest that just knowing the state of tumor microenvironment is not enough to be able to predict in which direction the population will evolve – one must also know the composition of the population.

favored by natural selection as the system evolves over time [38]. We hypothesize that increased availability of phosphorus in the cell microenvironment might shift cell population composition within the tumor towards a more proliferative and thus potentially malignant phenotype. The hypothesis is tested using an infinitely dimensional system of ODEs, which is reduced to low dimensionality using the Reduction theorem for replicator equations [69].

We assume that each cell within the population is characterized by a value of parameter $\alpha \in [0, 1]$, where $\alpha = 1$ corresponds to using the resource to invest solely in competition, i.e., maximizing their fitness through decreasing death rates, and $\alpha = 0$ corresponds to using the resource to invest solely in proliferation, i.e., maximizing their fitness through upregulating growth rates, with the possibility of the full spectrum of mixed strategies. Changes in population composition are tracked through the changes in the mean value of α as the system evolves over time.

We were able to demonstrate that indeed, increased inflow of extracellular phosphorus promotes a shift towards more proliferative phenotype largely in accordance to GRH, which

was also experimentally suggested by [39], where the authors found that in some tumors the intracellular concentration of phosphorus was indeed significantly higher than both in other tumors and in somatic cells. It is possible that different tumors that were sampled by the authors having been evolving towards the more competitive or more proliferative phenotype depending on micro-environmental conditions in each particular organ of tumor origin. Evolutionary and ecological perspective on tumor development also suggests that sampling a tumor at just one time point might not give accurate information about the stage of development of the tumor since it is an evolving system that changes both genotypically and phenotypically over time.

We were also able to observe an interesting effect at very high concentrations of extracellular phosphorus: both tumor size and composition fluctuated but not in a steady oscillatory manner. Instead, the population composition evolved primarily towards proliferative phenotype but with occasional temporary appearance of more competitive cells (Figure 5.4); in terms of tumor size, these bursts correspond to temporary decreases in the total population size (see Figure 5.3). A possible clinical manifestation of this effect could be salutatory tumor growth, which can be observed in several tumor types, such as breast cancer [130, 169] and hemangioblastomas [3, 5, 148]. In our model, the concentration of metabolically available carbon is assumed to be constant, simulating the conditions in the brain. Our model thus proposes an explanatory mechanism in terms of changing composition of cells within the tumor, which can manifest itself as fluctuations in tumor size. Even though within the frameworks of our model this effect comes from increased nutrient availability, it is possible that these fluctuations that come from changes in cell composition can be caused by other micro-environmental changes that are not yet understood. Also, interestingly, this effect of salutatory tumor growth could be observed only if the assumption of futile metabolism was incorporated, i.e., when growth rate of proliferative clones started to decrease if the amount of phosphorus available per carbon was too high. It was not observed under the assumption of stabilized growth rate (Holling type II growth function vs Holling type III).

We also evaluated the effects of upregulation of nutrient transporters on the direction in which the cell population evolved. We observed that increasing nutrient uptake rates of the

competitive clones did not give them much of a competitive advantage, since their growth is limited also by carbon concentration, which was held constant. However, unexpectedly, increasing nutrient uptake rates of proliferative cells achieved the effect of actually putting proliferative clones at a disadvantage (Figure 5.6). This could be explained by the fact that after taking up more phosphorus than they can use, which could also be restricted by availability of carbon in the cell microenvironment, the cells might be starting to engage in what can be seen as "futile metabolism", i.e., wasting energy on pumping out excess phosphorus instead of proliferating. Proliferative clones were demonstrated to have the highest advantage when their rates of nutrient uptakes were matched by those of competitive clones, suggesting that targeting phosphorus transporters therapeutically would be counter-productive. Instead, one should attempt to encourage even more competition between tumor cells so that the resources that are available to the cells are spent on competing and not on proliferating or developing therapeutic resistance.

Next, we evaluated the effects of changing growth rates of different cell types. We observed that while population composition with respect to each strategy may be vastly different, depending on which clone type has a higher growth rate, the final population size that was reached was the same regardless of population composition (Figure 5.6). The significance of this observation lies in the fact that the entire cell population may respond very differently to changes in microenvironment depending not on its size but on its initial composition.

We evaluated the effect of changes in the microenvironment on population composition when different clones are present in different proportions at the initial time moment. We observed that under the same set of micro-environmental conditions, the cell population did or did not evolve towards the more proliferative phenotype, depending on how many of the proliferative clones there were initially present in the population (Figure 5.7). More specifically, the more skewed the initial distribution of clones was to $\alpha = 1$, the more extracellular phosphorus was required to shift population composition towards a more proliferative phenotype. This effect is due to population heterogeneity: if the cell population were homogeneous, a micro-environmental perturbation would have a clear-cut bifurcation point,

i.e., one would be able to predict exactly when the population will or will not start evolving towards either strategy. However, since the population is heterogeneous, the fitness of each cell is affected not only by the availability of resource and by its intrinsic properties but also by what properties other cells have and how many of them there are, and so the population as a whole may respond differently to the same micro-environmental perturbation. Therefore, any predictions about system dynamics that are made without taking into account population heterogeneity are likely to be incorrect. Consequently, in order to be able to direct evolution of the system through micro-environmental manipulations, one needs to understand not only the properties of the individual cells but the composition of the cell population as a whole.

This effect could also account for why the same treatment for the same cancer type may be effective for one patient and not the other: it is not only the type of tumor that matters and not only the microenvironment within the person but also cell composition within the tumor itself. It should be taken into account when devising and revising therapies, since the tumors evolve during therapeutic intervention much faster than before them due to increased selective pressures imposed by the therapy on all cancer cells.

Tumor dormancy

One possible manifestation of what has been termed here "the competitive phenotype" is tumor dormancy. Crocker et al. [26] make the following distinction between the two types of cancer cells that may be classified as dormant: solitary dormant cells that are believed to be quiescent, defined by lack of both proliferation and apoptosis, and micrometastastatic dormant cells characterized not by the absence of proliferation and apoptosis but by their balance. It is these latter cells that we believe could be interpreted within the frameworks of the proposed model as exhibiting competitive phenotype.

Several mechanisms have been proposed to explain what could disturb the cells out of their dormant state, since it seems like a very large proportion of them can remain dormant throughout a person's lifetime [2, 26, 159]. It's been proposed that they can be kept in the dormant state by immune system [132, 155], lack of angiogenesis [2, 111, 112], surgery that disturbed the microenvironment [32], trauma [112], or through remaining in prolonged G phase [159]. Our model suggests that another, perhaps complimentary, mechanism of

disturbance of tumor cells out of the dormant state could come from nutrition and specifically, the relative amounts of carbon and phosphorus in the diet.

Cancer metabolism and the lesser of the two evils

One other possible more competitive phenotype in cancer cells could be directly related to how cells metabolize not phosphorus but glucose. Ordinarily, for glucose metabolism any cell in the body can use either the slower more efficient oxygen-dependent aerobic metabolism, which yields approximately 30 ATPs per glucose molecule, or faster less efficient oxygen-independent glycolysis, which yields 2 ATPs per glucose molecule and lactic acid as a byproduct, depending on oxygen availability. However, many cancer cells persist in using glycolysis even in the areas of ample oxygen supply (a phenomenon known as Warburg effect), presumably because lactic acid in sufficient quantities creates a microenvironment that is toxic to somatic cells, making cancer cells better competitors [50]. (This question is explored in more detail in Chapter 6)

Increased glycolysis has its drawbacks in possibly promoting metastatic progression by allowing cancer cells to spread through space freed up by the somatic cells that were killed by increased micro-environmental toxicity; however, it is possible that this competitive phenotype is still the lesser of the two evils. One can think of it as a "transitional regime" – either cells evolve directly towards proliferative phenotype or they can first go through the competitive phase until the conditions are more favorable for high proliferation (see Figure 5.8). So, creating an environment in which cancer cells are encouraged to compete with each other might result in a slower growing tumor, which would give more time for therapeutic intervention and thus increase the patients' chances for longer survival.

Conclusions

Tumors are evolving systems. It is their strength as they manage to adapt and survive cytotoxic therapies. Acquired therapeutic resistance and disease recurrence is a natural consequence of tumor heterogeneity as cytotoxic therapies wipe out the numerous more susceptible cancer cells, leaving small subpopulations of resistant cells to grow and expand. Decades of clinical evidence support the notion that shrinking the tumor does not necessarily result in the patient living longer and better nearly often enough to not start looking for

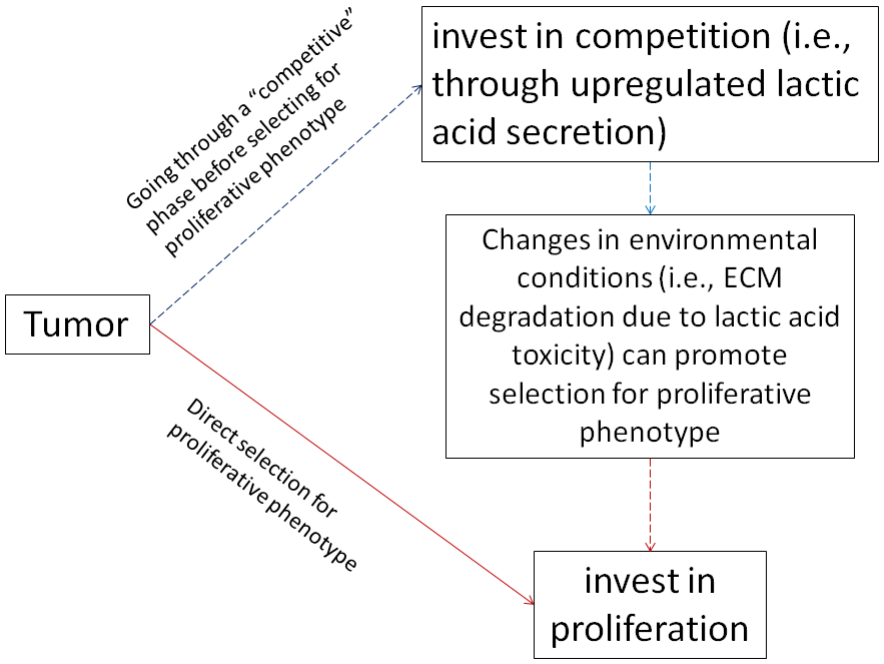

Figure 5.8: A possible scenario of evolving towards competitive phenotype as a "transitionl regime".

alternatives to cytotoxic therapies. One such alternative is to try to make cancer a chronic disease much like what happened with AIDS: the virus cannot be eradicated but AIDS is no longer a death sentence. Similarly, the goal of cancer therapy should be extending patient life and improving its quality and not solely trying to kill as many tumor cells as possible, as the two are not equivalent. Gatenby [48] proposed an analogy from our experience with dealing with pests: even though pests can often not be eliminated even with the most aggressive pesticides, sometimes keeping the pest population at a manageable level yields better crop protection than looking for more toxic poisons.

One can try to use tumor heterogeneity for therapeutic purposes instead of attempting to fight and eliminate it, making it also the tumor's weakness. It is conceivable that creating an environment which favors more competitive rather than more proliferative cell clones, might allow delaying disease progression. For instance, it has been demonstrated in mice that keeping the tumor at a constant size using adaptive (rather than constant) chemotherapy allowed keeping mice alive with tumors indefinitely [51]. So perhaps a com-

bination of moderate therapy (not maximum tolerable but minimum necessary), reversing adaptations that tumors created for themselves [71], such as neutralizing glycolysis induced acidic microenvironment [131] to prevent metastatic progression, as much as possible, and controlling nutrition (such as limiting phosphorus and carbon intake) might give cancer patients a better chance for a longer and better life than intensive cytotoxic therapies.

Chapter 6

PRISONER'S DILEMMA IN CANCER METABOLISM

Abstract

One possible manifestation of the "competitive" phenotype, discussed in Chapter **??**, deals with the way some tumor cells metabolize glucose. As tumors outgrow their blood supply and become oxygen deprived, they switch to less energetically efficient but oxygen-independent anaerobic glucose metabolism. However, cancer cells maintain glycolytic phenotype even in the areas of ample oxygen supply (Warburg effect). It has been hypothesized that the competitive advantage that glycolytic cells get over aerobic cells is achieved through secretion of lactic acid, which is a by-product of glycolysis. It creates acidic microenvironment around the tumor that can be toxic to normal somatic cells. This interaction can be seen as a prisoner's dilemma: from the point of view of metabolic payoffs, it is better for cells to cooperate and become better competitors but neither cell has an incentive to unilaterally change its metabolic strategy. In this Chapter a novel mathematical technique, which allows reducing an otherwise infinitely dimensional system to low dimensionality, is used to demonstrate that changing the environment can take the cells out of this equilibrium and that it is cooperation that can in fact lead to the cell population committing evolutionary suicide.

Keywords: Warburg effect, prisoner's dilemma, microenvironment manipulation

Introduction

Cancer can be viewed as a long evolutionary process within one person. Even in the cases of most severe DNA damage, such as was experienced by the survivors of atomic bombing in Hiroshima and Nagasaki, it is not until the 50s that one could observe dramatically increased cancer incidence [126]. Damaged cells, whatever properties they may have acquired, need to survive and proliferate in the tissue, competing with somatic cells for space and nutrients.

As the primary tumor increases in size, the cells outgrow their blood supply, thus also losing access to oxygen. This leads to cells in hypoxic areas switching from aerobic

metabolism to glycolysis, a mode of glucose metabolism that is less energetically efficient, yielding 2 ATPs instead of approximately 30, but that is faster and, most importantly, unrestricted by oxygen. However, tumor cells often continue metabolizing carbon glycolytically even in the areas of ample oxygen supply [67, 72, 160]. This has become known as Warburg effect, named after a German biochemist Otto Warburg, who was the first to observe it over fifty years ago [164]. This choice of metabolic strategy does not come from loss of function of mitochondria – it has been verified that a vast majority of tumor cells have completely functional mitochondria [166], and the damage that might be occurring is reversible [14].

From the point of view of natural selection, it has been hypothesized that, although glycolysis is energetically inefficient, lactic acid that is secreted as its by-product becomes toxic to healthy tissues, thus making glycolytic cells better competitors at a cost of being efficient consumers [49, 50]. However, a single cell is not likely to secrete enough lactic acid to cause significant changes in its microenvironment, i.e., it cannot provide enough "public goods" to benefit everyone [123]. The core population of glycolytic cells needs to be large enough to gain this competitive advantage. Proposed here is a game-theoretical approach for addressing the question of how such a population could arise.

Game theory in cell metabolism

As advantageous as glycolysis may be to cancer cells as a group, one glycolytic cell is not enough to generate enough lactic acid to become a successful competitor. Enough cells need to choose this metabolic strategy in order for the group as a whole to receive the competitive advantage. However, it is not in the interest of each individual cell to metabolize carbon glycolytically if all other cells metabolize it aerobically. It would not secrete enough lactic acid to successfully compete with them and at the same time, it would get nearly 15 times less energy.

In this framework, the problem becomes a version of multi-player prisoner's dilemma. There are two metabolic strategies: aerobic, which yields 30 ATPs per glucose and no lactic acid, and glycolytic, which yields 2 ATPs per glucose but yields some lactic acid. The amount of lactic acid generated by just one glycolytic cell is insignificant to cause any damage to somatic cells. Lactic acid secreted by several cells is enough to shift energetic payoffs, which

could in part be due to not only decrease in competition but also to the fact that intracellular stores of nutrients of the cells can be recycled and thus used up by neighboring cells [39, 40]. For illustration we currently assume 2 players but in fact many more would need to cooperate to get this "public goods" effect [123]. This becomes a game of prisoner's dilemma if the payoff for both cells is greater when they both choose the glycolytic strategy, i.e., if [30 ATP $<$ 2+toxicity+reduced competition]. In this case, the aerobic-aerobic equilibrium is in fact a stable equilibrium of this game, i.e., no cell has an incentive to unilaterally change its metabolic strategy [110, 138]. So, from the point of view of metabolic activity, one can argue that aerobic cells are in fact at an evolutionarily steady state [146], and so the tissue cannot be "invaded" by glycolytic clones.

Nevertheless, "glycolytic invasions" do happen as the Warburg cells migrate out of the primary tumor into the new environment composed primarily of aerobic cells, where they theoretically should have no advantage in persisting to metabolize glucose glycolytically. One explanation for this effect could be that they in fact migrate out in groups large enough to generate enough lactic acid for everyone to receive sufficient "public goods" benefit.

Another (perhaps complementary) explanation comes from invasion ecology, and particularly from the work of David Tilman, who argued that invasions of exotic species are largely facilitated when there are excess resources available in the target habitat for the invaders to utilize [157, 158]. In the case of aerobic and glycolytic cells, if there are enough resources in the environment into which the cell migrates out to, then a glycolytic cell will no longer have to care about its metabolic inefficiency ("who cares about fuel demands if gas is cheap?"). That is, from the point of view of payoffs of each metabolic strategy, if the environment, in which the players interact, changes sufficiently, glycolytic invasion becomes possible.

To test this hypothesis, a mathematical model is proposed. The change in the composition of the population of cells that differ by their choice of metabolic strategy (glycolysis vs oxidative phosphorylation) in response to increased carbon inflow is tracked using a system of ordinary differential equations. In the model, the growth of aerobic cells is restricted both by carbon and oxygen, while glycolytic cells are restrained only by carbon. The effects

of changes in oxygen availability, glucose uptake rates, natural cell death rates, cell growth rates, as well as the initial composition of the cell population are evaluated.

Model description

Suppose that each cell is characterized by a value of parameter α, which represents the proportion of total carbon that is used aerobically, thus effectively leaving $(1-\alpha)$ proportion of total carbon for consumption through glycolysis; x_α then denotes a set of all cells that are characterized by a fixed heritable value of parameter α. The total population size is then taken to be $N(t) = \sum_A x_\alpha$ if the number of possible values of α is finite and $N(t) = \int_{\mathbb{A}} x_\alpha d\alpha$ if it is infinite.

Glycolysis is less metabolically efficient and is limited only by glucose supply, denoted by C^{in}; aerobic metabolism is more efficient but is limited both by carbon availability C^{in} and by oxygen supply, which is accounted for with parameter β. Each cell x_α is thus characterized by its own intrinsic value of α, allowing to model population heterogeneity with respect to metabolic strategy.

There are two types of carbon that are taken into account in the model: extracellular carbon and intracellular carbon. Extracellular carbon C^{ex} is replenished in the tissue microenvironment through blood inflow and also is recycled from intracellular stores of cells that have died [39, 40]. It is consumed by the cells, becoming intracellular carbon, based on differences in concentration between C^{in} and C^{ex}. Different cells can consume carbon at different rates: glycolytic cells get less energy per one molecule of glucose, but their rate of carbon uptake is much greater due to upregulation of glucose transporters in the cell membrane [47]. This is accounted for by the parameter $p = p_a(1 - E^t[\alpha]) + p_g E^t[\alpha]$. The consumed extracellular carbon is then metabolized by the cells; the higher efficiency of metabolism by aerobic cells is accounted for by the parameter ξ.

Taking into account all of these assumptions, the model becomes System

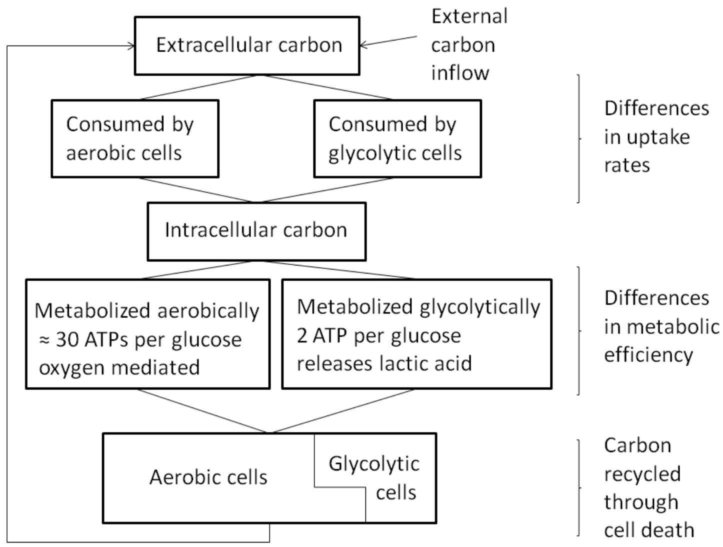

Figure 6.1: Schematic diagram of the process described in System 6.1

$$\begin{cases} \frac{dx_\alpha}{dt} = x_\alpha\Big(\underbrace{r_a(1-\alpha)\frac{\beta C^{in}}{\beta + C^{in}}}_{C^{\text{in}}\text{ and } O_2 \text{ lmited aerobic growth}} + \underbrace{r_g \alpha C^{in}}_{C^{\text{in}}\text{ limited glycolytic growth}} - \underbrace{d}_{\text{death rate}} \Big), \\ \frac{dC^{ex}}{dt} = \underbrace{g_1\big(\frac{C_0 - C^{ex}}{N}\big)}_{C^{\text{ex}}\text{ inflow from blood}} - \underbrace{\big(\underbrace{p_g E^t[\alpha]}_{\text{glycolytic cells}} + \underbrace{p_a(1-E^t[\alpha])}_{\text{aerobic cells}}\big)\frac{C^{ex} - C^{in}}{k_1 + (C^{ex} - C^{in})}}_{\text{total } C^{\text{ex}}\text{uptake based on concentration differences}} + \underbrace{\underbrace{C^{in} d}_{\text{natural cell death}}}_{C\text{recycled via cell death}} \\ \frac{dC^{in}}{dt} = \underbrace{(p_g E^t[\alpha] + p_a(1-E^t[\alpha]))\frac{C^{ex} - C^{in}}{k_1 + (C^{ex} - C^{in})}}_{\text{total } C^{\text{in}}\text{ inflow based on concentration differences}} - sC^{in}\big(\underbrace{r_a \xi (1-E^t[\alpha])}_{C\text{used aerobically}} + \underbrace{r_g E^t[\alpha]}_{C\text{used glycolitically}}\big). \end{cases} \tag{6.1}$$

A detailed model derivation is given in Appendix. The summary and description of all parameters is given in Table 6.1, and the general overview of the proposed mechanism is given in Figure 6.1.

Each cell clone x_α tries to maximize its fitness by metabolizing glucose either aerobically or glycolytically. Depending on initial population composition, on intrinsic growth and death rates, and the amount of carbon available, the clones are selected depending on which metabolic strategy maximizes their overall growth rate per cell, reflected through the value of $\frac{dx_\alpha}{x_\alpha}/x_\alpha$. Relative positions of the two growth curves with respect to resource availability

Variable/Parameter	Meaning	Range
α	proportion of glycolytic cells	$\alpha \in [0,1]$
r_a	growth rate of aerobic cells	$r_a \geq 0$
r_g	growth rate of glycolytic cells	$r_g \geq 0$
ξ	scaling constant to account for higher efficiency of aerobic metabolism (2 ATP vs ≈30 ATP)	$\xi \gg 0$
β	oxygen availability (normal blood oxygen is 20%, hypoxia occurs around 2-5%)	$\beta > 10$
d	natural cell death rate	$d \geq 0$
g_1	rate of resource consumption	$g_1 \geq 0$
C_0	rate of external carbon inflow (normal carbon concentration in the blood is $\approx 100mg/100ml$)	$C_0 > 0$
k_1	saturation constant for carbon uptake by the cells	$k_1 \geq 0$
s	scaling constant for how much carbon is metabolized by cells	$s \in (0,1]$
p_a	rate of carbon uptake by aerobic cells	$p_a \geq 0$
p_g	rate of carbon uptake by glycolytic cells	$p_g \geq 0$
$p = p_g(\alpha) + p_a(1-\alpha)$	lower boundary value of parameter c	$p \geq 0$
$b_\alpha = B - b_1\alpha$	toxicity induced cell mortality	$b_\alpha > 0, b_1 < \frac{B}{\alpha}$

Table 6.1: Summary of variables and parameters used throughout the Chapter

$N(0)$	$C^{ex}(0)$	$C^{in}(0)$	d	r_a	r_g	p_a	p_g	β	$E^{t=0}[\alpha]$	s	k_1	g_1
10.0	10.6	1.3	0.03	0.2	0.22	0.1	0.2	15	0.056	0.2	1.1	1.0

Table 6.2: Sample parameter values

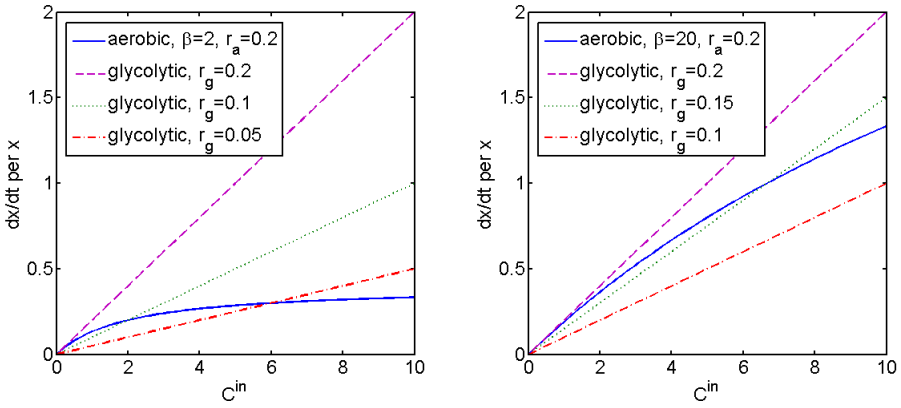

Figure 6.2: Relative positions of growth rates for aerobic ($x'_\alpha = r_a C^{in} \frac{\beta}{\beta + C^{in}}$, solid blue line) and glycolytic ($x'_\alpha = r_g C^{in}$, dashed lines) cell types for different initial states of the microenvironment (amount of resource $C^{in}$and amount of oxygen β) and different relative intrinsic growth rates $r_a$and r_g of both cell types. One can see that different clone types have higher fitness relative to each other depending on carbon (C^{in}) and oxygen (β) availability and the values of intrinsic parameters r_a and r_g.

are shown in Figure 6.2.

Modeling population heterogeneity

In a heterogeneous population, where each cell is characterized by its own value of parameter α, the mean number of glycolytic clones $E^t[\alpha]$ is a dynamic variable that can change over time. Therefore, the composition of a heterogeneous population of cells will also change as a result of the dynamics of other variables and will be different depending on initial conditions, parameter values, as well as the initial distribution of the clones within the population. (Note: in the current formulation, System 6.1 is an infinitely-dimensional system of ODEs. However, it can be reduced to a finitely-dimensional system of equations through addition of two keystone equations. The details of the transformation are described in Appendix.)

System (6.1) was solved numerically using Matlab R2010a in such a way as to evaluate, how the composition of the population, tracked through $E^t[\alpha]$, changes over time in response to increasing inflow of extracellular carbon, achieved through systematic increase of parameter C_0 (external carbon inflow). The changes in $E^t[\alpha]$ in carbon-rich environments were also evaluated with respect to changes in oxygen levels (parameter β), glucose uptake rates (changing relationship between parameters p_a and p_g), growth rates (r_a and r_g) and natural death rates (parameter d).

Results

The initial distribution of clones within the population was taken to be truncated exponential with parameter α restricted to the interval $\alpha \in [0, 1]$, and skewed towards $\alpha = 0$, i.e., such that the vast majority of cells in the initial population are aerobic. This is to account for the differences in access to the oxygen and nutrients as a result of slight variations in distance from the blood vessels. Initial conditions and parameter values used for calculating numerical solutions are summarized in Table 6.2, unless indicated otherwise.

The results of all the calculations are presented using four types of graphs. The first type of graph depicts the changes in the proportion of glycolytic cells in the population $E^t[\alpha]$ over time under variation of parameters that represent intrinsic properties of cells (proliferation, death, resource uptake rates, etc). On the second type of graph, external

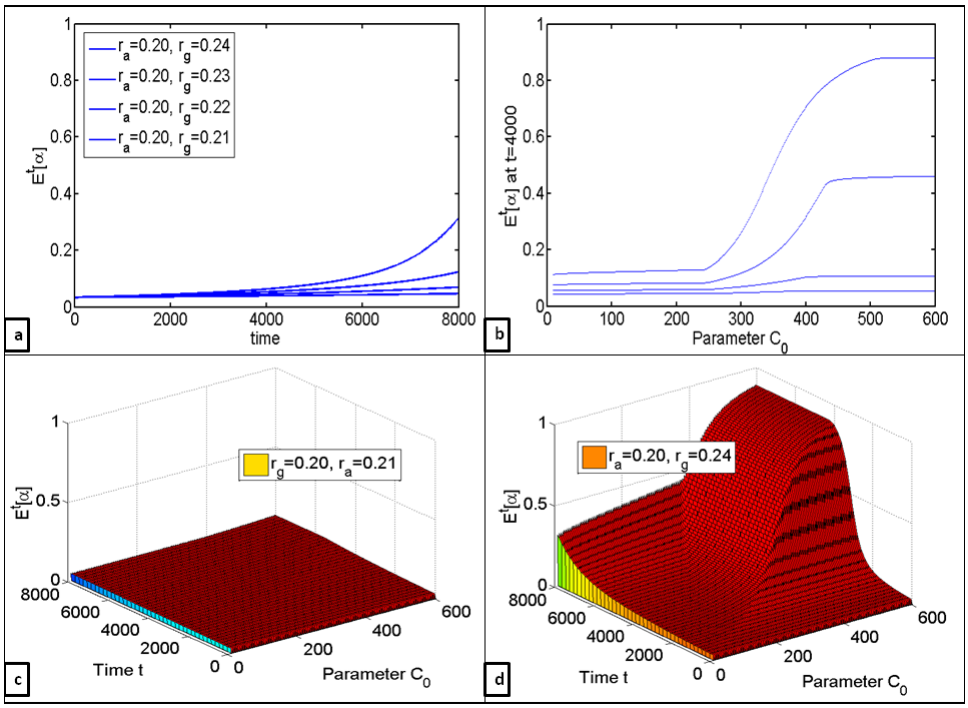

Figure 6.3: Quantifying the effects of differences in growth rates of aerobic and glycolytic cell clones. (a) Changes in the mean number of glycolytic cells $E^t[\alpha]$ over time for $r_a = 0.2$, $r_g = 0.21, 0.22, 0.23, 0.24$ (b) $E^t[\alpha]$ at $t = 4000$ for C_0 varied from 5 to 600, evaluated for $r_a = 0.2, r_g = 0.21, 0.22, 0.23, 0.24$ (c) Changes in $E^t[\alpha]$ over time with respect to differences in C_0 for $r_a = 0.2, r_g = 0.21$ (d) Changes in $E^t[\alpha]$ over time with respect to differences in C_0 for $r_a = 0.2, r_g = 0.24$

carbon inflow C_0 is varied and the value of $E^t[\alpha]$ is recorded at $t = 4000$ as the values of intrinsic parameters are varied. This is done to uniformly measure the effects of changes in external factors (nutrient availability) on glycolytic expansion; time point $t = 4000$ is chosen arbitrarily. The third type of graph is a 3-dimensional representation of how $E^t[\alpha]$ changes over time under different values of C_0. Finally, the fourth type of graph depicts the change in the distribution of clones with respect to strategy choice, over time.

Growth rates

At first the effects of changes in intrinsic growth rates were evaluated (see Figure 6.3). It can be observed that while, naturally, higher growth rates of anaerobic cells will always lead to increased proportion of glycolytic cells in the population (Figure 6.3a), increases in

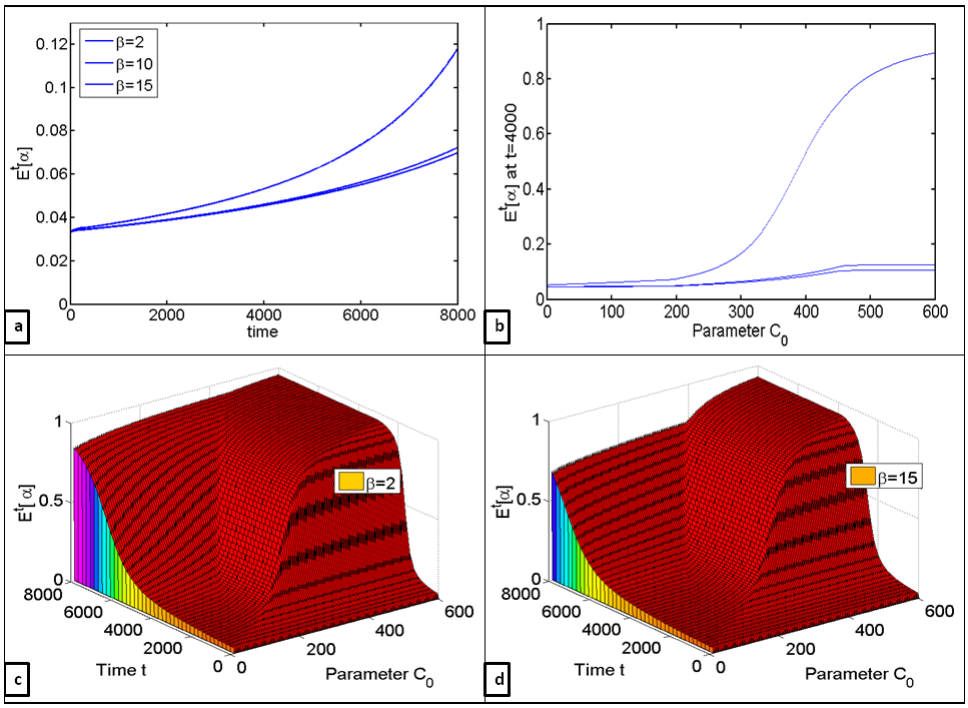

Figure 6.4: Quantifying the effects of oxygen availability on the growth of aerobic and glycolytic cell clones. (a) Changes in the mean number of glycolytic cells $E^t[\alpha]$ over time for $\beta = 2, 10, 15$ (b) $E^t[\alpha]$ at $t = 4000$ for C_0 varied from 5 to 600, evaluated for $\beta = 2, 10, 15$ (c) Changes in $E^t[\alpha]$ over time with respect to differences in C_0 for $\beta = 2$ (d) Changes in $E^t[\alpha]$ over time with respect to differences in C_0 for $\beta = 15$.

the rates of external carbon inflow C_0 accelerate this process dramatically (Figure 6.3b-d).

Oxygen availability

The effects of oxygen availability, accounted for with parameter β, were evaluated in Figure 6.4, and in particular, the question of whether oxygen deprivation will have more or less effect on glycolytic expansion than increased carbon inflow. As anticipated, lower β resulted in faster growth of glycolytic cells (Figure 6.4a). However, increases in carbon inflow resulted in nearly as much of glycolytic expansion as was caused by oxygen deprivation (Figure 6.4b-d), which suggests that under nutritionally favorable conditions benefits of glycolysis do indeed outweigh its drawbacks.

Death rates

Next, the effects in changes of natural cell death rates were evaluated. Interestingly, decreasing the value of parameter d actually slowed down glycolytic expansion (Figure 6.5). That is, lower death rates are in fact less advantageous for glycolytic cells at this stage of

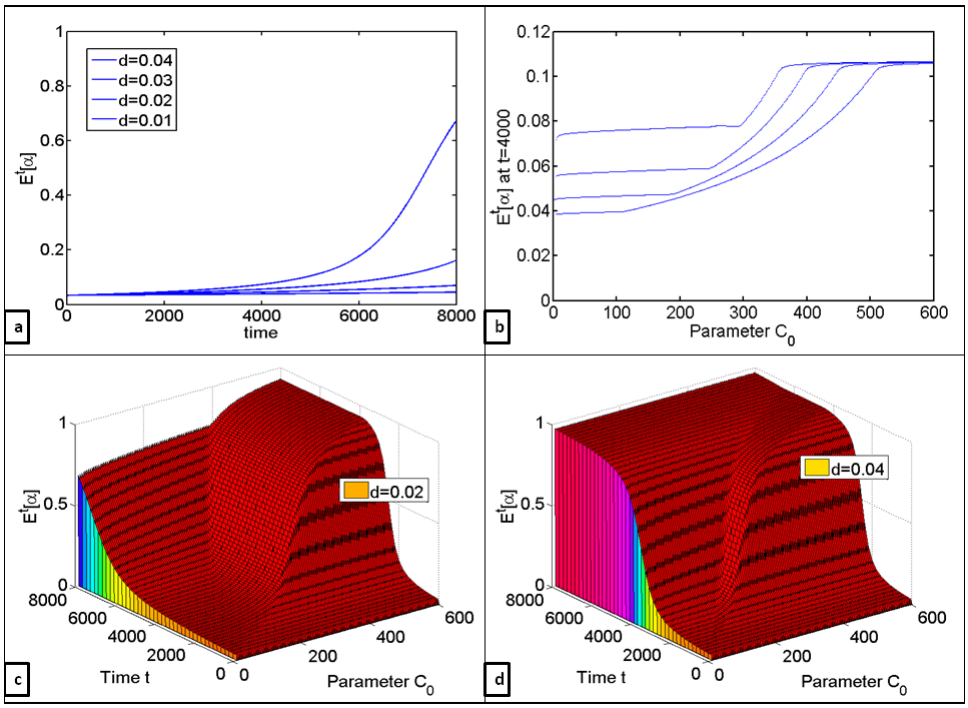

Figure 6.5: Quantifying the effects of natural death rates on the changes in proportion of glycolytic cell clones in the population. (a) Changes in the mean number of glycolytic cells $E^t[\alpha]$ over time for (b) $E^t[\alpha]$ at $t = 4000$ for C_0 varied from 5 to 600, evaluated for $d = 0.04, 0.03, 0.02, 0.01$ (c) Changes in $E^t[\alpha]$ over time with respect to differences in C_0 for $d = 0.02$ (d) Changes in $E^t[\alpha]$ over time with respect to differences in C_0 for $d = 0.04$.

tumor development. This effect could be due to the fact that higher cell death rates imply higher cell turnover within the population, thus actually speeding up the selective process. Lower death rates on the contrary cause a delay in the progression of the evolutionary process.

Nutrient uptake rates

The effects of differences in nutrient uptake rates were evaluated, since cancer cells have been observed to consume extracellular carbon much quicker than aerobic cells, with uptake rates between the two types differing as much as 10-20 times [47]. The question here was whether upregulation of glucose transporters would be enough to give cancer cells significantly greater selective advantage, everything else being equal. It can be observed in Figure 6.6 that even thirty-fold increase in the rates of glucose uptake by the glycolytic cells does not make much of a difference in terms of when exactly the rapid increase in the mean of α will occur. However, it does raise the maximum value that is reached at higher glucose concentrations. This suggests that upregulation of glucose transporters in glycolytic cells is

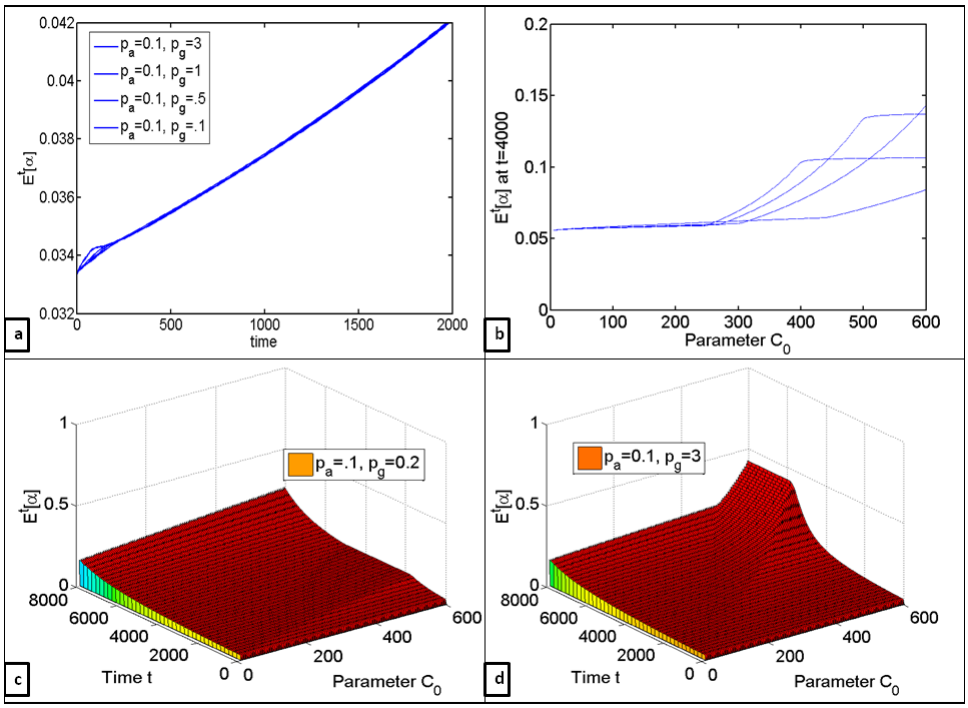

Figure 6.6: Quantifying the effects of differences in resource uptake rates on the changes in proportion of glycolytic cell clones in the population. (a) Changes in the mean number of glycolytic cells $E^t[\alpha]$ over time for $p_a = 0.1,\ p_g = 3,1,0.5,0.1$ (note the scale on y-axis) (b) $E^t[\alpha]$ at $t = 4000$ for C_0 varied from 5 to 600, evaluated for $p_a = 0.1, p_g = 3,1,0.5,0.1$(note the scale on y-axis) (c) Changes in $E^t[\alpha]$ over time with respect to differences in C_0 for $p_a = 0.1,\ p_g = 0.2$ (d) Changes in $E^t[\alpha]$ over time with respect to differences in C_0 for $p_a = 0.1, p_g = 3$.

an adaptation rather than the driving force behind Warburg effect, and therefore therapies targeting glucose transporters would probably not be very effective.

Modeling evolutionary suicide

Until now we have been focusing only on the question of whether the increased availability of nutrients can in fact allow the population of glycolytic cells to expand despite the metabolic inefficiency of glycolysis. Now, we would like to consider a case when the increased number of glycolytic cells in the population yields enough lactic acid to be toxic to aerobic cells. This is accounted for through adding an extra death term to the equation that describes the dynamics of the cell population, as well as an additional inflow term in the equation for the changes in the concentration of extracellular carbon, accounting for carbon that is recycled through cell death. On Figure 6.7 one can see that under given parameter values, the population initially increases in size, but as the proportion of glycolytic

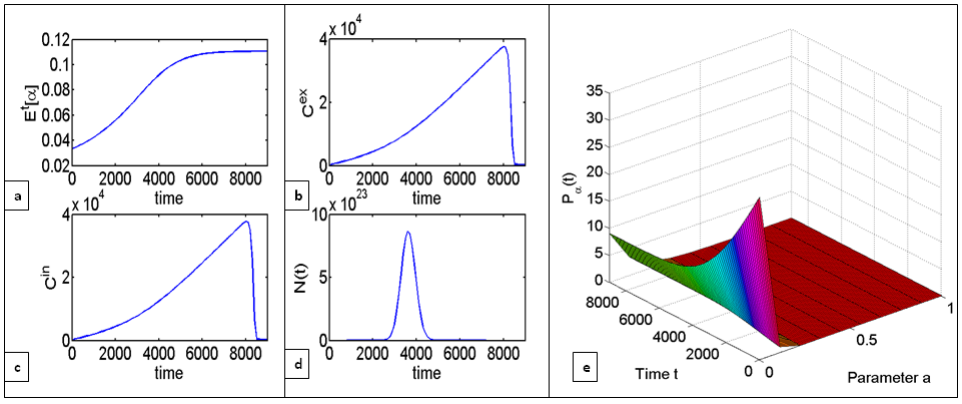

Figure 6.7: Evolutionary suicide can occur when the proportion of glycolytic cells $E^t[\alpha]$ within the total cell population reaches approximately 10% under given parameter values. Trajectories depict (a) the changes in the mean value of glycolytic cells in the population $E^t[\alpha]$ (b) extracellular carbon C^{ex}, (c) intracellular carbon C^{in}, (d) total population size $N(t)$ over time and (e) the distribution of cell clones $P_t[\alpha]$ changing over time.

cells reaches $E^t[\alpha] \approx 0.1$, the toxicity from lactic acid becomes higher than cell growth rates. This can be interpreted as the cells committing evolutionary suicide through being overly good competitors.

Discussion

From the point of view of game theory, tumor cells are playing a game of prisoner's dilemma both with somatic cells and with each other. If there are no limitations on oxygen availability, i.e., no severe pressure to choose one metabolic strategy over the other, then the payoffs for aerobic and glycolytic cells are measured in terms of efficiency of metabolism (getting more energy per same amount of glucose) and competitive ability (creating a microenvironment that will be toxic to competitors). It two cells are playing the game of prisoner's dilemma, then one can see using aerobic metabolism as "defecting" and glycolytic as "cooperating" – the cells will get the competitive advantage only if enough of them cooperate. However, the stable equilibrium for the game of prisoner's dilemma is for both players to defect, i.e., for all cells to use aerobic metabolism.

In this particular case one cannot change intrinsic payoffs for the players, i.e., the amount of ATP that each cell receives when it metabolizes glucose aerobically or glycolytically. However, one can change the environment in which they interact in such a way as to minimize the drawbacks of using the "cooperative" strategy. One such way is to supply

enough resources for the anaerobic cells to not be held back by the inefficiency of glycolysis.

In order to investigate whether increasing the amount of available nutrients can in fact push the cells out of the stable equilibrium, a mathematical model is proposed to track the change in composition of a parametrically heterogeneous population with respect to the choice of metabolic strategy, i.e., aerobic or glycolytic metabolism. The model is a three dimensional system of ordinary differential equations based on a mathematical model of a chemostat system [81]. There are three state variables that are being kept track of: concentration of extracellular carbon, which is constantly replenished from some external source and is consumed based on difference of concentrations between extra and intracellular concentrations; concentration of intracellular carbon, which is metabolized more efficiently by aerobic cells; and a heterogeneous cell population composed of aerobic and glycolytic cells. The growth of aerobic cells is modeled in such a way as to be constrained both by carbon and oxygen availability. The growth of glycolytic cells is restrained solely by carbon. Parametric heterogeneity within the system is captured by assuming that each cell clone is characterized by an intrinsic value of parameter α, which can range from 0 to 1. The initial distribution of cell clones is assumed to be truncated exponential on the interval $[0, 1]$, skewed towards $\alpha \to 0$ such that a vast majority of clones in the initial cell population are aerobic. The change in population composition is tracked through the change in the mean value of the parameter α, which in this formulation becomes a function of time and thus changes as the system evolves.

Through computation of numerical solutions one could observe that increased inflow of extracellular carbon did indeed cause dramatic changes in the composition of cell population over time (Matlab code is available upon request). However, in order to see any changes in the composition of cell population, glycolytic cells had to have higher growth rates, even if only slightly. This suggests that while increased nutrient availability cannot induce glycolytic switch, it can accelerate disease progression. Decreases in oxygen availability in nutrient-limited environment caused as much of a glycolytic expansion as did dramatic increases in external carbon inflow in normoxic conditions (Figure 6.4). It was also demonstrated that lower death rates actually slowed down tumor progression at this stage of tumorogenesis be-

cause of slower cell turnover rates; increases in death rates caused dramatic increases in the rate of glycolytic expansion because of increased cell turnover (Figure 6.5), which suggests that cytotoxic therapies would in fact speed up cancer progression. Finally, the effects of differences in resource uptake rates were evaluated, revealing that even 30-fold increases in carbon uptake rates by glycolytic clones do not have nearly as much effect on the rate of glycolytic expansion as do increases in external nutrient inflow.

The two games

Staying within the aerobic-aerobic equilibrium of the metabolic prisoner's dilemma keeps the tumor (at least temporarily) from switching preferentially to glycolysis, which would lead to creating toxic microenvironment and facilitating metastatic invasion [49, 131]. However, if the environment is changed enough, cells can push away towards glycolytic-glycolytic strategy (everything else being equal), eventually entering the domain of attraction of the stable equilibrium of another, larger game, which can lead to evolutionary suicide [129]. Now glycolytic cells that have become numerous enough are cooperating, jointly increasing the toxicity of the surrounding microenvironment, and becoming more efficient competitors as a group, eventually killing the host and consequently killing themselves.

In the model, this is captured through introduction of the additional toxicity term that captures increased mortality of aerobic cells proportional to the amount of lactic acid secreted by glycolytic cells. Indeed, one can observe that the cell population initially grows, peaks and then eventually collapses, going to extinction (see Figure 6.7). So, the either equilibrium within the same game of prisoner's dilemma can become attracting not because of the changes in payoffs for each cell but due to different initial composition of the population of players, which happens solely through natural selection.

Tumors as complex adaptive systems

One way to look at tumors is through the lens of complexity science. Complex systems are diverse and adaptive, and all parts within them are interconnected and interdependent [102]. Tumors fit this definition: they are composed of genetically heterogeneous cells; they are interconnected and interdependent, competing for resources and space with each other and with somatic cells; and they are very adaptable to changes in their microen-

vironment.

Complex systems are not nearly as predictable as just complicated systems (the ones that have all the characteristics of complex systems except adaptability). They are robust, and they can generate such phenomena as tipping points, which are thresholds of rapid phase transitions [102]. For instance, in the proposed system, changes in the cell microenvironment induced selection for the "cooperative" glycolytic metabolic strategy, which can be viewed as an example of such a tipping point. This can lead to a rapid increase in the amount of lactic acid produced, which in turn can lead to a sudden increase in metastatic spread of the disease due to increased degradation of the extracellular membrane [49]. On a larger scale, one can think of cachexia, nutritionally irreversible loss of body mass, which is often observed in terminal cancer patients, as an example of such a tipping point.

Complex systems cannot be controlled but they can be harnessed, that is, even if one cannot change the intrinsic properties (or in case of game theory, payoffs) of the individual clones, or agents, in the complex systems, one can sometimes change the microenvironment in such a way as to direct system evolution in the desired direction (create an environment, where the players will "want" to choose the strategy that we want them to choose rather than try to force them to do so). For instance, in the metabolism experiment described here, it is the changes in the nutrient availability that enabled the shift within the system towards an otherwise unstable equilibrium (persistence of glycolytic metabolism) by decreasing the negative effect of glycolysis, i.e. low ATP yield, but keeping all of its benefits, i.e., better competitive ability (Figure 6.8).

Reversing the changes that occurred as a result of surpassing a tipping point in complex systems is usually not possible because of the changes that will have already occurred to the population composition. That is, it is no longer the same "set of players" that is interacting, and therefore their threshold is most probably different. However, tipping points can be anticipated and sometimes even delayed. For instance, several prospective studies have shown that mortality from cancer was much lower in those individuals that had higher muscle mass, regardless of their body mass index (BMI), even though the incidence of cancer was the same (see, for instance, [62, 170]). From the point of view of cell metabolism, this

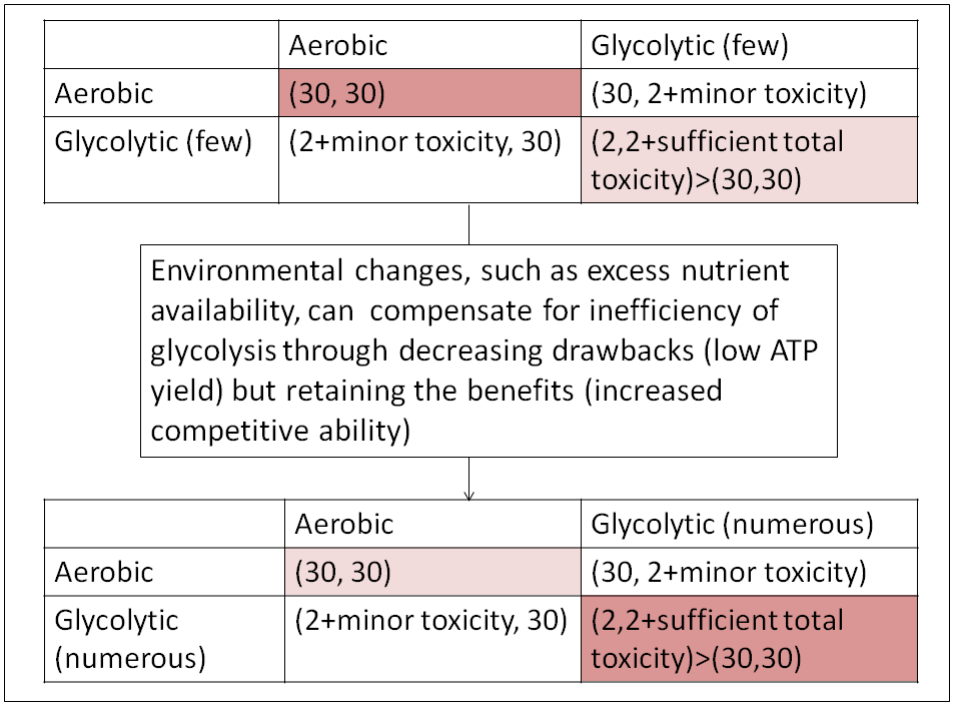

Figure 6.8: Changes in the microenvironment can lead to changes in population composition, which in turn can lead to the population evolving away from the dominant aerobic-aerobic "defecting" strategy, which keeps the system stable, to glycolytic-glycolytic "cooperation", which can eventually lead to evolutionary suicide (cancer killing the patient and thus killing itself).

could be due to the fact that muscle cells have higher energy demands than other somatic cells, thus "beating" the glycolytic cells to the nutrients, delaying progression of the disease. So, while exercising will not affect the probability of the person getting cancer in the first place, it may reduce the risk of dying from it by pushing off the metabolic tipping point, surpassing which leads to cancer progression.

Conclusions

Tumors are complex adaptive systems that consist of a large number of diverse, interconnected and interdependent cells that compete for space and nutrients both with the somatic cells and with each other. One of the measures of tumor diversity could be the type of metabolic strategy that the cell uses for converting glucose to energy: aerobic metabolism has a higher ATP yield and can be seen as an evolutionarily stable metabolic strategy, while glycolysis has a lower ATP yield but it increases the cells' competitive abilities through creating a toxic microenvironment. Tumor cells upregulate glycolysis even in the areas of

ample oxygen supply (Warburg effect). It is hypothesized that the benefits of increased acidity of the microenvironment give a large enough payoff to glycolytic cancer cells to overcome the inefficiency of glycolysis. However, glycolytic cells can get this advantage only if enough of them simultaneously use this strategy.

While it is not possible to change the intrinsic energetic payoffs for these cells, changing the microenvironment through providing increased amounts of nutrients can achieve this by decreasing the negative effects of glycolysis (compensating for low ATP yield by providing more carbon) without affecting the benefits (increased competitive ability through elevated lactic acid production). Here we demonstrate that while availability of excess nutrients cannot induce the glycolytic switch, it facilitates disease progression when some glycolytic cancer cells are already present in the population.

It is a common viewpoint that somatic cells always cooperate and cancer cells are the ones that defect, rebelling against cell cooperation within the tissue. However, from the point of view of game theory, choosing aerobic metabolism is in fact a stable "defect-defect" equilibrium in the multi-player game of prisoner's dilemma. And it is the dominance of the defecting strategy that stabilizes the tissue, preventing (as long as possible) occasional glycolytic cooperators from committing evolutionary suicide.

Chapter 7

AGENT-BASED MODELING OF COMPLEX SYSTEMS. WARBURG EFFECT.

Abstract

The purpose of this small chapter is to introduce briefly the method of agent-based modeling, demonstrate some of the results that can be obtained through this type of imitative models, and to provide a connecting link that has motivated research done in Chapter 6.

Keywords: agent-based modeling, Warburg effect, growth rate hypothesis

Brief introduction to agent-based modeling

Agent-based models (ABMs) are a computational tool that allows running in silico simulations of complex systems. Unlike equation-based models, the output of ABMs is not exact numerical solutions but simulations.

ABMs consist of entities (agents) of various types that display interdependent behaviors and are embedded in a network. Each agent is assigned a set of rules that will determine the nature of the agent's interactions with other agents and with the environment. The rules may be fixed, or may change in response to changes in the agents' changing environment.

In many ABMs, the agents take discrete actions, such as moving to different locations, cooperating or defecting, joining or exiting a particular activity, etc. The actions of the agents are typically "threshold based", i.e., the agent's behavior remains the same until some threshold is met; once the threshold is surpassed, the agent changes its behavior.

The nature and intrinsic properties of agents, as well as the rules that determine their behavior, is conventionally summarized in an ODD (Overview, Design concepts and Details) protocol [54].

While agent-based modeling is not used in this dissertation, a sample model that could potentially be used to address some of the similar questions is formulated in this

section.

An agent-based model of cancer metabolism

Consider a situation, when there exists a core population of cells in the population that maintain glycolytic phenotype in normoxic conditions. To survive and reproduce, both aerobic and glycolytic cells require energy sources. The two resources that we will focus on are carbon and phosphorus. Carbon is metabolized much more efficiently by the aerobic cells (30 ATPs vs 2 ATPs for same amount of carbon) [143]. Phosphorus, although not a direct requirement for metabolism, is necessary for reproduction of both types of cells, as it goes into ribosomes and making of RNA and DNA, which was discussed in detail in Chapter 5.

A byproduct of carbon metabolism by glycolytic cells is lactic acid, which can be toxic to aerobic cells. Once a cell dies, it releases its inner stores of carbon and phosphorus into the surrounding microenvironment, where they can be taken up by the nearby cells. The rate of uptake is determined by differences in intra and extracellular concentrations of carbon and phosphorus (concentration gradient).

Moreover, as was discussed in detail in Chapter 5, according to the growth rate hypothesis (GRH), there exists a ratio of carbon to phosphorus that is optimal for cell reproduction. When C:P is below this threshold, the cell reproduces most efficiently. When it is above this optimality threshold, the cell is forced to spend metabolic energy to pump out excess phosphorus rather than to spend it on reproduction and metabolism.

All of these considerations are summarized in Table 7.1

Questions that could be of interest are:

1. Is the competitive advantage obtained through eliminating competition through lactic acid secretion sufficient for glycolytic cells to out-compete aerobic cells? If so, under which conditions?
2. Is there a minimum population size of glycolytic cells that needs to be present for them to be able to remain in the population?
3. Is there a maximum population size of glycolytic cells, after which competition does

		Aerobic	Glycolytic
Metabolism	advantage	efficiency (≈30 ATP per glucose molecule)	increased competitive ability (lower sensitivity to lactic acid)
	disadvantage	decreased competitive ability (increased sensitivity to lactic acid)	inefficiency (2ATP per glucose molecule)
	mechanism of nutrient uptake	based on differences in intracellular and extracellular concentrations of C and P	
Survival	limitations	need sufficient O_2 and C; sensitive to lactic acid	need sufficient C
Reproduction	limitations	appropriate $C:P$	
	specifics	excessive P leads to futile metabolism (waste of C without increase in reproduction)	
	crowding (optional)	will not reproduce if there are too many neighbors in the environment, regardless of $C:P$	oblivious to crowding; reproduction limited only by $C:P$

Table 7.1: Summary of assumptions necessary for building an agent-based model of Warburg effect.

not yield enough of a competitive advantage to outweigh the benefits of metabolic efficiency?

4. Under what conditions do resource limitations promote selection either for reproduction or for survival?

To address these questions, we propose an agent-based model that will track the evolution of glycolytic cells within a population of aerobic cells as the cells compete for carbon and phosphorus to be used for survival, metabolism and reproduction.

Overview, Design concepts and Details (ODD) protocol

The process takes place on a lattice grid. Each microenvironment is characterized by carbon, phosphorus and lactic acid concentrations. Each cell is characterized by intracellular carbon and phosphorus concentrations. As of right now we assume normoxic conditions (as

we want to investigate the effect of persistence of the glycolytic phenotype even when plenty of oxygen is present) and so we will not keep track of oxygen concentrations.

Once the cell is on the microenvironment, it first needs to survive (check minimum carbon and lactic acid concentrations). If the survival criteria are not met, the cell dies, releasing its inner stores of carbon and phosphorus into the microenvironment. If it has survived, it needs to eat (uptake extracellular carbon and phosphorus to balance out with intracellular C and P concentrations).

After eating, the cell evaluates if it can reproduce by checking the intracellular C:P threshold. If the appropriate conditions are met, an aerobic cell will use some carbon and phosphorus and will divide. A glycolytic cell, in addition to this, will consume 2-3 times more of its inner stores of the resource and will secrete some lactic acid into its microenvironment, which will then diffuse to neighboring microenvironments. If the C:P criterion was not passed, the cell will use inner carbon to pump out inner phosphorus without reproducing.

At each time point the following sequence of steps is performed:

A. Survival

a. Check inner carbon threshold

i. If inner carbon is too low, die and release inner carbon and phosphorus into microenvironment; otherwise, proceed to metabolism

b. Check lactic acid threshold

i. If inner lactic acid concentration on the microenvironment about the threshold, die and release inner carbon

and phosphorus into microenvironment; otherwise, proceed to metabolism

c. Cells can also die naturally at some intrinsic rate

B. Metabolism

a. When a cell eats, it takes up carbon and phosphorus from the patch

i. Takes up half of extracellular carbon and phosphorus

ii. A glycolytic cell takes up much more carbon and phosphorus than an aerobic cell

iii. When a glycolytic cell eats, it secretes some lactic acid, which is then diffused into neighboring patches

C. Reproduction

a. Aerobic cell will not reproduce if the number of cells on the patch is greater than some number

b. To reproduce, the cell needs to check the C:P ratio

i. If it is below a threshold, divide inner carbon and phosphorus in half and hatch 1, letting the new cell occupy a neighboring patch at random; mutate the threshold of resistance to lactic acid

ii. If it is above the threshold, set half inner carbon and phosphorus, add the pumped out phosphorus to the microenvironment but do not divide

D. Microenvironment

a. Lactic acid, as well as extracellular carbon and phosphorus diffuse to neighboring patches

b. The shade of the color of the patch is determined by lactic acid presence: the lighter the patch, the more lactic acid there is there. This allows to track the toxicity of the microenvironment

c. The resources (carbon and phosphorus) in the microenvironment are renewed completely every once in a while to simulate blood inflow

Design concepts

Adaptation. There is one adaptive trait in this experiment: the threshold of tolerance to lactic acid. It is cell-type specific and change each time the cell divides.

Fitness. Cell fitness in the model is determined by their birth and death rates. It can evolve over time as the threshold for lactic acid resistance evolves, thus reducing the death rate of the corresponding cells.

Prediction. Cells do not have the ability to predict the availability of resources in the microenvironments.

Sensing. Normal (aerobic) cells sense being crowded and thus do not divide even when there are ample resources for it available in the microenvironment. Glycolytic cells are oblivious to space constraints and divide regardless of the number of neighbors present in the microenvironment, limited only by the resources

Interactions. There are not direct interactions among the cells. All interactions are indirect via competition for the resources.

Initialization. Some parameter values that gave interesting behaviors are summarized in Table 2.

Input Data. No external sources are used for input.

Preliminary observations

1. Naturally, within the frameworks of this model, the crucial parameters are initial carbon and phosphorus and the threshold for reproduction (C:P)

2. Glycolytic cells are more likely to "gain ground" if there are not too many of them initially. There seems to exist a threshold for "optimal size" of initial glycolytic population. That is, having initially a larger glycolytic population size does not necessarily guarantee successful tumor growth (does it mean that having a larger glycolytic tumor is not necessarily scarier?)

3. Some aerobic cells can survive in the regions of hypoxia; they just don't reproduce. Probably, this is because they can't get to the reproduction-necessary resources like phosphorus quite as quickly as glycolytic cells but when it comes to survival-necessary carbon, they are efficient enough to survive. They developed a strong enough resistance to lactic acid not to die in this acidic environment.

4. A fully glycolytic population will always eventually die as the cells cannot support themselves too long on such high energetic demands. This could be one of the reasons why migration and metastasis have to be selected for.

In the following figures, red arrows denote aerobic cells, blue arrows denote glycolytic cells. The lighter the environment, the more toxic it is (the more lactic acid there is on the microenvironment). For this set of simulations, the reproduction threshold (C:P ratio) was taken to be 0.4, initial carbon available was 31, initial phosphorus was 96, initial number of aerobic cells was taken to be 847, and the initial number of glycolytic cells was varied (parameter values were chosen arbitrarily for illustration purposes).

This simple experiment suggests that there exists an intermediate value of how many glycolytic cells would need to be present initially in order for the "glycolytic invasion" of the tissue to be successful. These experiments also suggest that a minimum number of glycolytic

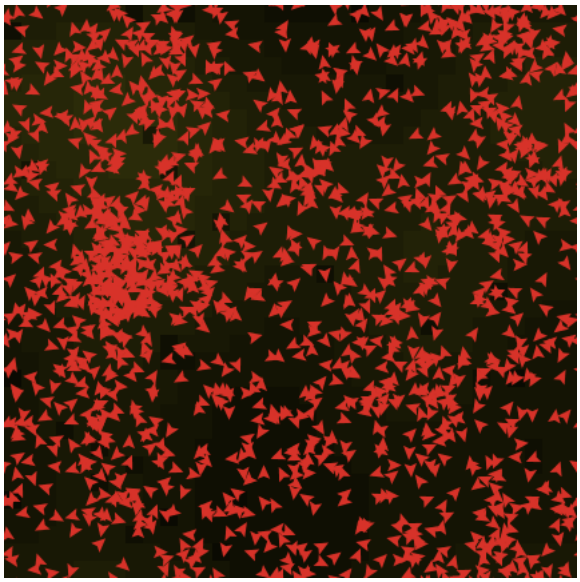

Figure 7.1: Initial number of glycolytic cells is 36; glycolytic strategy could not be adopted, and all patches are acid-free or have some acid in low concentrations.

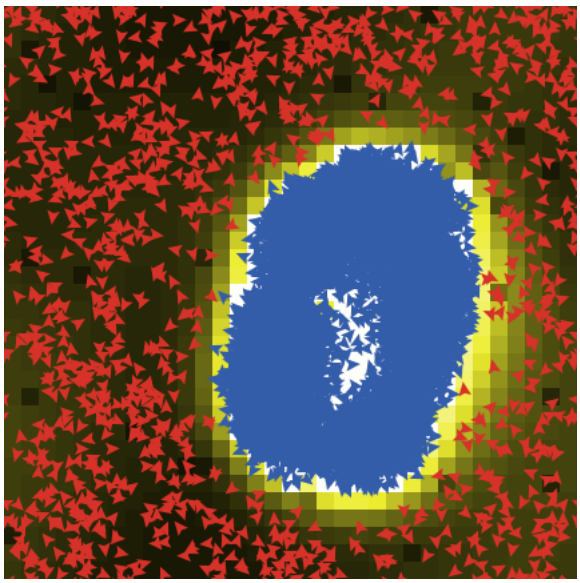

Figure 7.2: Initial number of glycolytic cells is 76. The initial population of glycolytic cells is large enough to get a collective competitive advantage from increased toxicity. The microenvironment around the blue (glycolytic) cells is very acidic, which is reflected through increased patch brightness.

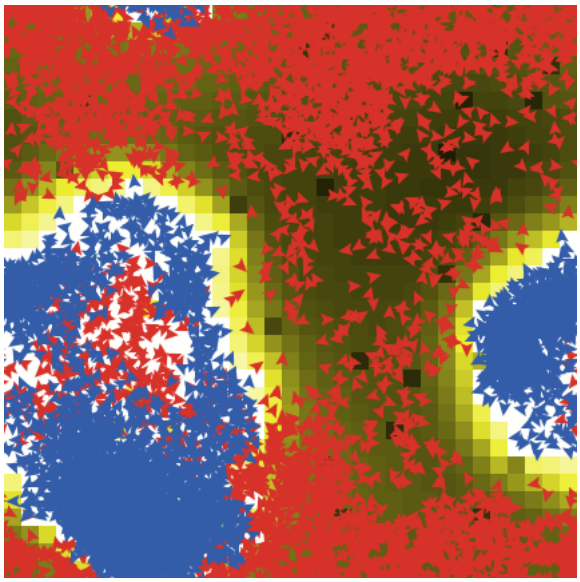

Figure 7.3: Initial number of glycolytic cells is 134. In this case, some aerobic cells manage to adapt to the highly acidic environment, as can be seen by a patch of red (aerobic) cells among the blue (glycolytic) cells.

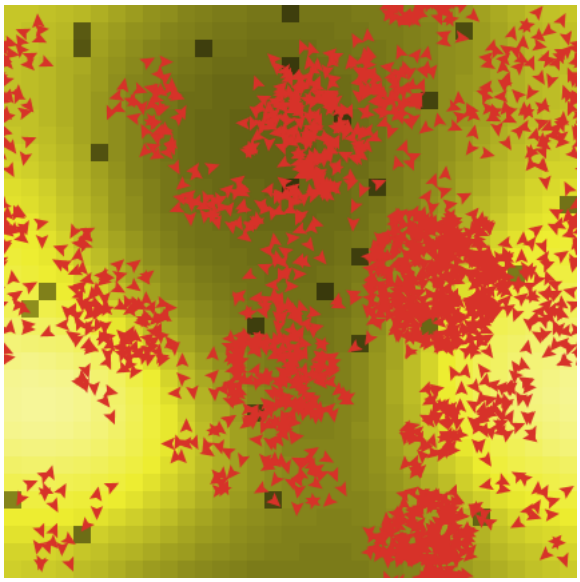

Figure 7.4: Initial number of glycolytic cells is 242. In this case, too many glycolytic cells exhibit extremely high nutrient demands, so they are not able to secure enough nutrients to survive before producing large amounts of lactic acid, and as a result, they do not survive in the tissue.

cells must be present in the cell population in order to be able to observe Warburg effect.

The question of how such a core population could have arisen was studied in detail in Chapter 6.

Chapter 8

CANCER-IMMUNE SYSTEM INTERACTIONS AS PREDATOR-PREY

Abstract

In this chapter we turn to yet another aspect of tumor ecology, which deals with the immune system in the framework of predator-prey type interactions. Despite highly developed specific immune responses, tumor cells often manage to escape recognition by the immune system, continuing to grow uncontrollably. Experimental work suggests that mature myeloid cells may be central to the activation of the specific immune response. Recognition and subsequent control of tumor growth by the cells of the specific immune response has been suggested to depend on the balance between immature (ImC) and mature (MmC) myeloid cells in the body. However, tumor cells produce cytokines that inhibit ImC maturation, altering the balance between ImC and MmC. The focus of the model discussed in this chapter is to study of the potential role of this inhibiting mechanism on tumor growth dynamics. A conceptual predator-prey type model that incorporates the dynamics and interactions of tumor cells, $CD8^+$ T cells, ImC and MmC is proposed in order to address the role of this mechanism. The prey (tumor) has a defense mechanism (blocking the maturation of ImC) that prevents the predator (immune system) from recognizing it. The model, a four-dimensional non-linear system of ordinary differential equations, is reduced to a two-dimensional system using time-scale arguments that are tied to the maturation rate of ImC. Analysis shows that the model is capable of supporting biologically reasonable patterns of behavior depending on the initial conditions. A range of parameters, where healing without external influences can occur, is identified both qualitatively and quantitatively, which could be interpreted as the immune system suppressing dormant cancer cells.

Keywords: cancer, myeloid cells, immune system, time scales, predator-prey

Introduction

Cancer is a general term that encompasses a number of diseases, characterized by uncontrollable division of cells. Many types of cancer are characterized by the development of solid tumors - tightly packed conglomerations of rapidly dividing cells; rapidly dividing

and spreading tumors are considered malignant. Cells of malignant tumors eventually invade surrounding tissues, causing malfunction of internal organs and eventually the patient's death [105].

The uncontrollable growth and the spread of the cancerous cells, regardless of the mechanism, is usually deterred by a battery of immune system responses. Cancerous cells activate the body's innate immune response, which is then followed by activation of the adaptive (specific) immune response [105]. Innate and adaptive immune responses involve populations of white blood cells, including tumor-specific cytotoxic T lymphocytes ($CD8^+$ T cells) and immature and mature myeloid cells [46]. The specific immune response then becomes the dominant force in charge of controlling the growth of a malignant tumor. The $CD8^+$ T cells, which are part of the adaptive immune response, bind to receptors on the surface of the tumor cell and release membrane-damaging chemicals, e.g. perforin. This creates osmotic imbalance inside the cell, forcing it to either swell or shrink. A fraction of the cells of the adaptive immune response remains in the body for extended periods of time after tumor growth is halted, accelerating the activation of the immune system, should the tumor reappear [105].

Each $CD8^+$ T cell is capable of killing numerous tumor cells. Repeated encounters between the tumor and the $CD8^+$ T cells stimulate further $CD8^+$ T cell production. The efficiency of the specific immune response is directly tied to the ability of $CD8^+$ T cells to recognize tumor cells. This process is partially regulated by myeloid cells that produced in the bone marrow. After a period of maturation, immature myeloid cells (ImC) differentiate into macrophages and dendritic cells, becoming mature myeloid cells (MmC). Both macrophages and dendritic cells are antigen-presenting cells (APC), that is, they help the immune system recognize the presence of the tumor cells in the body [82, 105].

Experimental studies suggest that maturation of myeloid cells can be partially blocked by the production of certain cytokines, such as the vascular endothelial growth factor (VEGF), generated by the tumor cells [78]. The presence of the tumor cells thus slows down the ImC maturation process, causing ImC to accumulate at the site of the tumor. As a result, the number of functional APCs in the presence of the tumor gets reduced, and the activation of

the specific immune response decreases dramatically.

A number of mathematical models have been introduced in order to capture the dynamics between tumor and immune system (see, for instance, [28, 29, 73]); a number of them have also modeled cancer-immune system interactions in the context of predator-prey. However, the focus of existing models has mostly been on identification and evaluation of optimal treatment options. No model to our knowledge has incorporated the maturation dynamics of ImC on the effectiveness of the immune response. So, a predator-prey type model is introduced where the prey (tumor) has a defense mechanism that allows it to escape recognition by the predator.

Model description

It is assumed that the tumor grows exponentially in the absence of an immune response. Consequently, the role of the immune system response is directly tied to the immune system's ability to deal effectively with uncontrolled tumor growth. The activation of the adaptive immune response arises from the activity of the innate immune response, such as natural killer (NK) cells [**?**, 105], a step that is not included in our model, since the focus is on the dynamics of the activated $CD8^+$ T cells.

It is also assumed that the production of tumor-specific $CD8^+$ T cells can only take place in the presence of tumor cellsincluding tumor cells that were previously killed both by NK cells and $CD8^+$ T cells. The effectiveness of the immune response is limited by the fact that tumor cells are not always recognized as foreign and therefore can escape destruction [28, 29].

Myeloid cells are constantly being produced in the body. Work by Gabrilovich et al. [18, 46, 78, 79, 108] suggests that a large number of ImC are able to inhibit T cell responses in cancer patients, while the presence of a large number of MmC stimulates the immune response, and that impaired balance between ImC and MmC can in fact be viewed as another one the hallmarks of cancer [78]. In the context of our model, we suggest representation of this mechanism as a ratio term between MmC and ImC as they come in contact with the $CD8^+$ T cells.

In their immature state, dendritic cells are phagocytic and reside in peripheral tissues

to take up pathogens. Upon maturation, triggered by various stimuli such as presence of the tumor cells, DCs undergo a series of phenotypic changes, which are characterized by displaying tumor-specific antigens on the surface of the dendritic cell. Then they migrate to lymph nodes. Upon presentation of processed antigens to T cells, the different stimuli that induce maturation of DCs also determine the production of cytokines that facilitate the polarization of T cell responses [97].

Mature myeloid cells are central to the ability of $CD8^+$ T cells to recognize tumor cells as foreign [78, 82]. However, their maturation is inhibited by cytokines, such as VEGF, IL-6 or IL-10, produced by tumor cells. Consequently, immature myeloid cells accumulate in the body in the presence of the tumor and inhibit the activity of the $CD8^+$ T cells [78].

If we let $L(t)$ denote the population of $CD8^+$ T cells; $T(t)$ - the population of tumor cells, $M_1(t)$ - the population of immature and $M_2(t)$ the population of mature myeloid cells at time t, then some of the relevant dynamics of the immune system response to tumor growth are captured by the following nonlinear system of differential equations:

$$\begin{cases} \dot{T} &= aT - \mu_T T - eLT\frac{M_2}{M_1+M_2}, \\ \dot{L} &= -\mu_L L + cL^2T\frac{M_2}{M_1+M_2}, \\ \dot{M_1} &= \Omega - \mu_1 M_1 - (\theta - g\frac{T}{p+T})M_1, \\ \dot{M_2} &= (\theta - g\frac{T}{p+T})M_1 - \mu_2 M_2, \end{cases} \tag{8.1}$$

In this model it is assumed that the tumor growth is exponential in the absence of an immune response. Tumor cells die at the per-capita rate $\mu_T T$ or are removed from the system by the $CD8^+$ T cells. The removal rate is a function of the ratio of mature to the total number of immature and mature myeloid cells in the blood stream. The production of L cells is stimulated by coming in contact with the tumor cells at the rate $cLT(\frac{M_2}{M_1+M_2})L$. More specifically, coming in contact with tumor cells also stimulates cell division of the L cells, which is accounted for by the appearance of the term L^2 in this equation. The natural death rate of the L cells is denoted by $\mu_L L$. The rate of recognition of the tumor cells by L cells increases with the presence of M_2 but decreases with the presence of M_1 cells. The M_2 to M_1+M_2 ratio is used to model the impact of both cell populations on the activity of the

L cells. Clearly, alternative functional relations could and should be explored.

Immature myeloid cells are released in the blood stream from the thymus at the rate Ω, a parameter that is larger by several orders of magnitude when compared to other parameters. It is the largest parameter in the system, a crucial fact that is used in model reduction in the next section. M_1 cells die at a rate $\mu_1 M_1$. θ is the maturation rate of M_1 under a normal pathway of cell differentiation and $g\frac{M_1 T}{p+T}$ is the rate at which tumor cells inhibit M_1 maturation by producing growth factors and cytokines, such as VEGF.

The parameter g in fact combines two opposing forces that are directly tied to the presence of tumor in the body. It could be written as $g = g_1 - g_2$ where g_1 is the suppression of ImC activation caused by the production of VEGF and other maturation-suppressing cytokines by the tumor; g_2 is the increased stimulation of ImC maturation, which is a natural immune response to the presence of the tumor in the body. Depending on which force dominates, the overall sign of the parameter g can be positive or negative. Finally, $\mu_2 M_2$ denotes the per capita natural death rate of MmC.

Full summary of parameter values used in System (8.1) is summarized in Table 8.1.

Table 8.1: Meaning and sample values of parameter values.

Parameter	Units	Description	Value	Source
[0.5ex] a	day^{-1}	Tumor growth rate	0.432	[29]
μ_T	day^{-1}	Tumor natural death rate	0.02	[29, 105]
e	$cell^{-1}day^{-1}$	Rate at which L cells kill tumor cells	2.02 x 10^{-8}	[29, 105]
μ_L	day^{-1}	L cell natural death rate	0.02	[29]
c	$cell^{-2}day^{-1}$	Growth rate of L due to T	1.8 x 10^{-8}	[29]
Ω	day^{-1}	Production rate of M_1	10^7	[105]
μ_1	day^{-1}	M_1 natural death rate	0.02	[29, 105]
θ	day^{-1}	Activation of M_1	0.2	[105]
g	day^{-1}	Activation of M_1 in response to T	0.0125	no data
μ_2	day^{-1}	M_2 natural death rate	0.02	[29, 105]
p		saturation coefficient of T cells	10	no data

Analysis

Dimensionality reduction using time scale arguments

Antigen-presenting cells, MmC in particular, play a crucial role in ensuring the proper recognition of the tumor cells by the immune system [46, 78, 79]. MmC activate tumor-

specific T-lymphocytes, such as $CD8^+$ T cells, partially by coming in contact with the tumor cells and presenting this information to the $CD8^+$ T cells. It has previously been observed that the number and function of MmC cells are significantly reduced in cancer patients. This reduction is closely linked to the accumulation of ImC cells in the patient's blood stream while the presence of MmC cells in tumor tissue may only imply a good clinical prognosis [46].

The process of maturation of ImC cells occurs on a scale of minutes and hours while the growth and establishment of both tumor and $CD8^+$ T cells can take several days, months or even years [105]. Normally, the number of MmC cells is greater than the number of ImC cells, since ImC do not accumulate. However, tumor-induced suppression of ImC maturation causes ImC to accumulate, skewing the ratio of MmC to ImC in the body. In fact, a 1:1 ratio or lower has been observed in almost all patients with advanced stages of cancer [78, 79].

Taking into consideration the difference in rates of maturation and establishment by ImC and MmC when compared to those of the rates associated with tumor and $CD8^+$ T cell response, it is assumed that a balance between immature and mature myeloid cells has been reached before a measurable impact of the interactions between tumor cells and the $CD8^+$ T cells is documented.

Letting $x = AT$, $y = BL$, $\tau = Ct$, $u_1 = E_1M_1$, $u_2 = E_2M_2$ and $\varepsilon = \frac{1}{\Omega}$, where Ω is the largest parameter in the system, we can rewrite system (8.1) as follows:

$$\begin{cases} \frac{dx}{d\tau} &= \frac{(a-\mu_T)x}{C} - xy\frac{E_1eu_2}{CB(E_2u_1+E_1u_2)}, \\ \frac{dy}{d\tau} &= -y\frac{\mu_L}{C} + xy^2\frac{E_1cu_2}{ACB(E_2u_1+E_1u_2)}, \\ \varepsilon\frac{du_1}{d\tau} &= \frac{\Omega}{C}(E_1 - u_1\frac{\mu_1}{\Omega} - \frac{u_1}{\Omega}(\theta - x\frac{g}{Ap+x})), \\ \varepsilon\frac{u_2}{d\tau} &= \frac{1}{C}((\theta - x\frac{g}{Ap+x})u_1\frac{E_2}{E_1} - \mu_2u_2), \end{cases} \tag{8.2}$$

where the small parameter $\varepsilon \leq \frac{1}{24} \approx 0.01$.

The "fast" (u_1, u_2)-subsystem of (8.2) reaches quasi-steady state at:

$$\begin{aligned} u_1^* &= \frac{E_1\Omega}{\mu_1+V} \\ u_2^* &= \frac{E_2\Omega V}{\mu_2(\mu_1+V)} \end{aligned} \tag{8.3}$$

where $V = \theta - x\frac{g}{Ap+x}$ The equilibrium point (u_1^*, u_2^*) is always globally asymptotically stable

(see Appendix ?? for proof), which allows us to use Tikhonov theorem [156] (see also Hoppenstead's theorem [147]) to make the following substitution and reduce our system to two equations:

Letting

$$C = a - \mu_T, A = \frac{-g+\theta}{p\theta}, B = \frac{cp\theta}{(a-\mu_T)(-g+\mu_2+\theta)}$$

we get

$$\frac{M_2}{M_1+M_2} = \frac{E_1 u_2}{E_2 u_1 + E_1 u_2} = \frac{(-g+\theta)(1+x)}{(-g+\mu_2+\theta)(\beta+x)}$$

where $\beta = \frac{(-g+\theta)(\mu_2+\theta)}{\theta(-g+\mu_2+\theta)}$.

Making this substitution into System (8.1) we obtain the following system of equations:

$$\begin{cases} \dot{x} &= x - \alpha x y \frac{1+x}{\beta+x}, \\ \dot{y} &= -\gamma y + x y^2 \frac{1+x}{\beta+x} \end{cases} \tag{8.4}$$

where $\alpha = \frac{e(-g+\theta)}{\theta pc}, \gamma = \frac{\mu_L}{a-\mu_T}, \beta = \frac{(-g+\theta)(\mu_2+\theta)}{\theta(-g+\mu_2+\theta)}, x = \frac{T}{A}, y = \frac{L}{B}$

Equilibrium stability analysis

System (8.4) has two equilibrium points: $O(0,0)$ and $A(\gamma\alpha, \frac{\beta+\alpha\gamma}{\alpha(1+\alpha\gamma)})$. The Jacobian matrix $J(x,y)$ for this system is :

$$\begin{pmatrix} \frac{\beta^2+x^2(1-\alpha y)-\beta(\alpha y+2x(-1+\alpha y))}{(\beta+x)^2} & -\frac{\alpha x(1+x)}{\beta+x} \\ \frac{y^2(\beta+2\beta x+x^2)}{(\beta+x)^2} & -\gamma+\frac{2xy(1+x)}{\beta+x} \end{pmatrix}$$

The determinant of the Jacobian matrix at the trivial equilibrium is $det = -\gamma$, which is less than zero. Therefore, the trivial equilibrium is a saddle point.

At the nontrivial equilibrium point A, the determinant of the system is $det = \gamma$, which is always greater than zero; therefore, point A is either a node or a spiral. The trace of the Jacobian matrix at the non-trivial equilibrium is given by

$$Tr(J(A)) = \frac{\gamma(\beta(1+\alpha(-1+\gamma))+\alpha(1+\gamma+\alpha\gamma^2))}{(1+\alpha\gamma)(\beta+\alpha\gamma)}$$

Hence, the point A becomes unstable, giving rise to periodic solutions via Hopf bifurcation. The condition $Tr(J(A)) = 0$ is satisfied if

$$\beta = \frac{\alpha(1+\gamma+\alpha\gamma^2)}{\alpha(1-\gamma)-1} \tag{8.5}$$

System (8.4) has properties, summarized in Theorem 1.

Theorem 1

In the parameter domain Δ, where $\alpha > 0, \beta > 0, \gamma \in (0,1)$, there exists a subdomain Δ^*, such that for all α, β, $\gamma \in \Delta^*$,

1) System (8.4) exhibits three generic types of quantitatively different dynamical behaviors for $x, y \geq 0$ (see Figure 8.1) which lie within three different domains.

(i) If the point (α, β, γ) belongs to Domain 1, then System (8.4) has a unique stable equilibrium point whose basin of attraction is bounded by an unstable limit cycle. (ii) If the point (α, β, γ) belongs to Domain 2, then System (8.4) has no stable steady states for finite $x, y \geq 0$.

(iii) If the point (α, β, γ) belongs to Domain 3, then System (8.4) has an unstable non-trivial equilibrium point within a unique stable limit cycle whose basin of attraction is bounded by an unstable limit cycle.

2) *(i) The boundary H^- between Domains 1 and 2 is determined by (8.5)*, where

$$\alpha < \frac{2+\gamma-2\gamma^2+\sqrt{4-3\gamma^2}}{2\gamma(1-\gamma)}$$

which corresponds to a co-dimension 1 subcritical Hopf bifurcation of equilibrium point A.

(ii) The boundary H^+ between Domains 1 and 3 is determined by (8.5), where

$$\alpha > \frac{2+\gamma-2\gamma^2+\sqrt{4-3\gamma^2}}{2\gamma(1-\gamma)}$$

which corresponds to the co-dimension 1 supercritical Hopf bifurcation of equilibrium point A.

(iii) The boundary D between Domains 2 and 3 corresponds to the co-dimension 1 saddle-node limit cycle bifurcation.

(3) *Bifurcation boundaries H^-, H^+ and D have a common line HD (not shown), where*

$$\alpha(\gamma) = \frac{2+\gamma-2\gamma^2+\sqrt{4-3\gamma^2}}{2\gamma(1-\gamma)}$$

$$\beta(\gamma) = \frac{\alpha(\gamma)(1+\gamma+\gamma^2\alpha(\gamma))}{\alpha(\gamma)(1-\gamma)-1}$$

For any $(\alpha,\beta,\gamma) \in$ HD, System (8.4) exhibits a co-dimension 2 "zero Lyapunov value" bifurcation.

The proof of Statement 3 is given in the Appendix. Statements 1 and 2 follow from Statement 3 and from the statement below, which describes the structure of trajectories of the system in Poincaré coordinates (at infinity).

Proposition 4 *For all values of parameters $(\alpha > 0, \beta > 0, \gamma \in (0,1))$ and $x, y > 0$, System (8.4) has an equilibrium point E_x $(z \equiv \frac{1}{x} = 0, u \equiv \frac{y}{x} = 0)$ with a unique hyperbolic sector, at the "end" of x-axis and an equilibrium point E_y $(z \equiv \frac{1}{y} = 0, v \equiv \frac{x}{y} = 0)$ with a hyperbolic sector adjacent to the y-axis and an attractive parabolic sector, at the "end" of y-axis.*

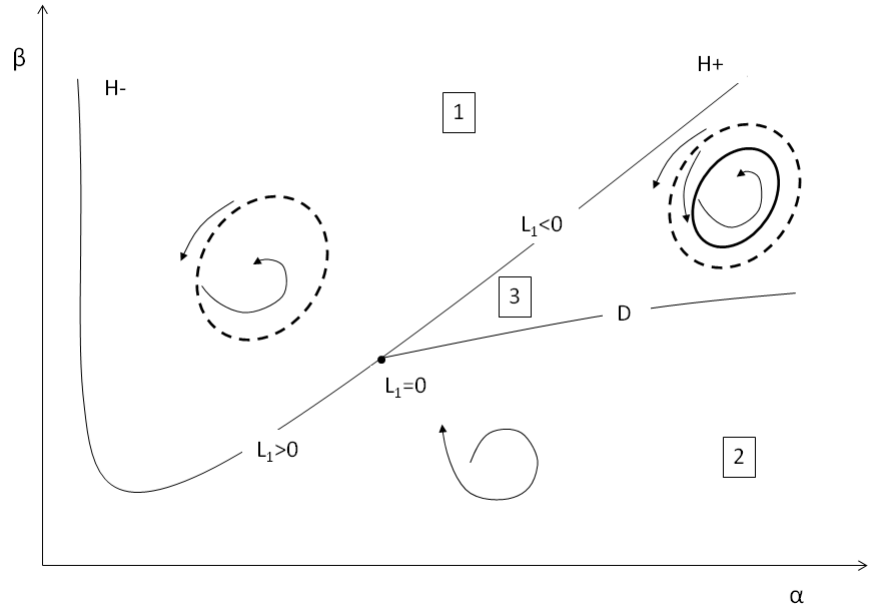

Figure 8.1: Phase-parameter portrait of system 8.4 at $\gamma = \tilde{\gamma} = 0.47$. H^- and H^+ correspond to boundaries of subcritical and supercritical Hopf bifurcations of co-dimension 1, respectively. D corresponds to the saddle-node limit cycle bifurcation of co-dimension 1.

Table 8.2: Values of parameters in α and β in three domains in Figure (8.1)

Parameter	Value in Domain 1	Value in Domain 2	Value in Domain 3
[0.5ex] α	7.0	4.0	16.0
β	9.0	6.0	11.0
θ	0.0186	0.028	0.0173
g	-0.6314	-0.532	-1.3628
c	1.0 x 10^{-8}	1.0 x 10^{-8}	1.0 x 10^{-8}
μ_2	0.02	0.02	0.02
μ_L	0.2	0.2	0.2

Noticeably, the values of the parameter g are negative because g is a combination of two opposing forces, written as $g = g1 - g2$. $g1$ is the rate at with which the tumor blocks maturation of M_1. $g2$ is the rate at which the presence of tumor cells stimulates the body's own immune responses. If $g1 > g2$, then $g > 0$ and the only behavior that exists in the system is uncontrollable tumor growth. If $g1 < g2$ (i.e, immune system surpasses the attempts of tumor cells to block it), then $g < 0$, and the possibility for regimes when the immune system will can over cancer exists.

The proof of Proposition 4 is omitted. For the method (Newton diagram) used in the proof, see [9, 12].

Discussion

In this work we incorporate the dynamics of immature and mature myeloid cells in the model of cancer-immune system interactions in an attempt to explore how the ratio between ImC and MmC cells could influence the effectiveness of the immune response.

The parameters used in numerical simulations come from a number of sources. The values of the parameters for the equations for T and L come from [28, 29]. The values for birth and death rates of M_1 cells were estimated from [105]. Finally, the value of the parameter g was guessed since to our knowledge there is no exact experimental information that would allow us to measure the rate at which tumor cells inhibit M_1 maturation.

The system can be reduced from four equations to two equations using Tikhonov theorem [156] and time scale arguments. The "equivalent" system has only one non-trivial equilibrium. The value of parameter β can be expressed as $\beta = \frac{(\theta - g)(\mu_2 + \theta)}{\theta(\mu_2 + \theta - g)}$. Recall that the ImC maturation parameter g is a combination of two opposing forces and can be written as $g = g_1 - g_2$, where g_1 is the suppression of ImC activation that is caused by the production of VEGF and other maturation-suppressing cytokines by the tumor cells, and g_2 represents

stimulation of ImC maturation, which is a natural response of the immune system to the presence of the tumor in the body. If the overall value of $g > 0$, then the suppression of ImC maturation overpowers, and so the value of $\beta < 1$. In this case the non-trivial equilibrium point is unstable regardless of the values of other parameters, which corresponds to uncontrollable tumor growth (see Domain 2 in Figure 8.1).

However, when $g < 0$, it is the stimulation of the immune system by the tumor that overpowers. In this case the value of the parameter $\beta > 1$. In this case, it is the parameter $\alpha = \frac{e(-g+\theta)}{\theta pc}$, which corresponds to the effectiveness of interactions between the activated $CD8^+$ T cells that determines the behavior of the system. Notice, that its value is also directly tied to the value of the parameter g. In particular, one can identify a region on the parametric space (see Domain 1 in Figure 8.1) where the equilibrium point gains stability. Moreover, there is a small region around the stable equilibrium point, defined by an unstable limit cycle, where the solutions of the system will in fact go to a steady state. The appearance of an unstable limit cycle corresponds to a subcritical Hopf bifurcation. However, if the initial conditions are outside of the limit cycle, the tumor will start growing uncontrollably. The full phase-parametric portrait of the system is given in Figure 8.1. Some of the analytical conditions, necessary for a subcritical Hopf bifurcation to occur are given in Appendix.

The observed dynamics suggest that recovery without treatment is only possible in a very small region which depends directly on the initial state of the patient's immune system and the stage of disease progression.

Conclusions

In this Chapter we introduce a system of four nonlinear ordinary differential equations to model the interactions between tumor and immune system cells. The prey (cancer) has a defense mechanism that allows it to escape recognition by the predator (immune system). In the context of our model it is the maturation of myeloid cells, which are crucial for activation of the immune system that is targeted by cancer cells in their effort to avoid recognition.

In the absence of treatment, if the immune system is weak, the growth of cancer cells is unrestrained. However, if the number of cancer cells in the body is low enough, and the immune system is sufficiently stimulated, then there exists a small region of initial

conditions, where a patient's recovery without treatment can occur. Moreover, we have been able to analytically define a boundary of this region through a combination of parameters that govern the dynamics of myeloid cell maturation. In fact, we found, both numerically and analytically, a small region around a fixed point (low number of cancer cells) that is defined by an unstable limit cycle. If the initial conditions are inside the limit cycle, the solution converges to a stable fixed point, which indicates controlled tumor growth. Initial conditions outside this limit cycle lead to uncontrollable tumor growth. In other words, if the immune system is weak, cancer cells may grow unrestrained and stochastic effects may move us outside the limit cycle, into the region of uncontrollable growth. On the other hand if the number of cancer cells is sufficiently small and the immune reaction is strong enough, then the existence of this small region of parameter space guarantees the possibility of recovery (no uncontrollable growth) without treatment.

One other possible interpretation of observed dynamical regimes deals with tumor dormancy: it has been hypothesized that there exist a number of non-proliferating tumor cells that are repressed by the activity of the immune system [132, 155], which within the frameworks of the proposed model corresponds to remaining within Domains 1 or 3 of the phase parameter space (Figure 8.1). Falling out of the domain of attraction of non-trivial equilibrium A results in uncontrollable tumor growth.

Since the maturation of myeloid cells and its effects on tumor growth are the key point in the proposed model, and since the observed behavior corresponds to the expected general dynamics of the disease, the next question to address becomes: "What factors influence maturation of myeloid cells and what can be done in order to prevent the tumor cells from blocking the activity of the immune system?". There are several possibilities for future investigations. It seems that blocking VEGF (one of the cytokines that is produced by tumor cells that seems to block maturation of ImC) does not help restore the maturation rate of ImCs [45]. However, production of VEGF seems to be stimulated by the presence of a particular molecule called Stat3, and blocking Stat3 has been shown to restore the maturation rate of ImCs ([74, 113, 172]). This is only one of many questions that can be investigated further and incorporated into future models.

Chapter 9

WHAT CAN ECOLOGY TEACH US ABOUT CANCER?

Abstract

In 2008, Pienta et al introduced the term "ecological therapy" for cancer treatment, and in particular, emphasized that destruction of the microenvironment would be more effective than just killing the species inhabiting it. Proposed here is an expansion on the idea of ecological therapy of cancer, incorporating 1) literature on species invasion, i.e., that a right cancerous clone needs to be at the right place at the right time to actually invade its environment and 2) the literature on niche construction, i.e. the idea that once a tumor is formed, tumor cells they modify their microenvironment (niche construction) by changing pH through glycolysis, secreting growth factors and recruiting tumor-associated macrophages (TAMs) to promote their growth, activating fibroblasts, evading predation from immune system, making the cancer that much more difficult to eradicate. Paleontological literature suggests that the largest mass extinctions occurred when environmental stress that would weaken the population was coupled with some pulse destructive event that caused extensive mortality. So, rather than, or at least in addition to killing the cells, one would also need to target the niche that they created for themselves.

Keywords: cancer ecology, niche construction, ecological therapy

Cancer as an ecological system

Over the past decade it has been increasingly recognized that a tumor is not genetically homogeneous but is rather composed of many genetically diverse cancer cells [63, 149, 153]. If variability in the population is heritable and if it affects fitness, then the system is going to evolve, leading to competition for space and common resources and resulting in different clones being selected for or weeded out of the population due to natural selection. Genomic heterogeneity is one of the major reasons why we see acquired therapeutic resistance, since cytotoxic therapy inevitably selects for resistant cells by applying a severe selective pressure on the entire heterogeneous cell population. Moreover, heterogene-

ity within even premalignant lesions has been shown to be indicative of a worse prognosis for the patient [100]. At the same time, prognosis for young cancer patients is typically more favorable, which can be attributed in part to the fact that younger tumors are less heterogeneous and hence are less likely to become resistant to therapy.

Another consequence of tumor heterogeneity is the possibility of so-called "evolutionary suicide" [129] – in their quest for higher growth rates, lower death rates, increased competitiveness and with their ability to migrate out and colonize distant organs, cancer cells defy "cooperation" with somatic tissue, eventually killing the host and thus killing themselves. This evolutionary experiment is run within each cancer patient, sometimes leading to cancer cells committing evolutionary suicide at the expense of the host.

From an ecological perspective, one can look at this process as an attempt of new species (cancer cells), which have different metabolic and reproductive strategies compared to the "resident" population (somatic cells) to invade a new habitat (tissue). Successful invasion will result in the formation of a primary solid tumor. Such perspective might be able to provide a different viewpoint, allowing us to draw parallels with other ecological systems to find answers to such questions as "under what conditions can invasions occur?", "how do invading species adapt to and modify their environment?", and most importantly, "what can be done to eradicate them?"

Mechanisms of species extinction

The mechanisms by which species in nature go extinct can generally be subdivided into two distinct categories – extrinsic factors, such as habitat modification, change in nutrient supply and interactions with predators, and intrinsic factors, such as any change in the genotype, which eventually results in changes in the phenotype.

Intrinsic factors typically reflect how the species have been adapting to their environment over long evolutionary time scale. From an evolutionary game theory point of view, the individuals within the population have been moving towards an evolutionarily stable strategy (ESS), i.e., a state when no individual within the population has an incentive to change their "strategy" in their interactions with the environment. As a result, theoretically, once the ESS is adopted in the population, natural selection alone becomes insufficient to allow invasion

by a new mutant. (It is important to note that being at an ESS does not imply highest fitness in the sense of the largest difference between birth and death rates. It only implies resistance to invasion.)

However, invasions do happen. One of the frequent ways by which species can go extinct is when a more efficient or more proliferative competitor invades their habitat much like cancerous cells can invade and start outcompeting healthy cells in the tissues. Research in the area of invasion ecology has been focused particularly on this question.

Habitat invasion and cancer

A number of mechanisms have been proposed to explain why some habitats are more or less susceptible to invasion, of which habitat modification is most often the common denominator [34, 135, 158]. Invasion can be facilitated when the "native" populations are more specialized towards their niche, while the invaders are "generalists" – perhaps less efficient in some aspects when compared to the natives but capable of taking on multiple roles and exploiting multiple resources [16, 121]. Another, perhaps complementary, theory comes from David Tilman, whose research focus has primarily been on the questions of ecosystem stability and the effects on it of biodiversity. He suggests that more diverse ecosystems are less susceptible to invasion because greater biodiversity ensures more complete resource utilization [157, 158]. Incomplete resource utilization allows for the formation of a new niche, which can be occupied by invaders. And, if the new niche has been available for an extended period of time, invaders will not only have time to find and occupy it but will also be able to "co-evolve with it". This phenomenon is known as niche construction [116], and it refers to a situation when the niche gets modified due to the metabolic activity of its occupants. The adaptations could also be different: an invader can modify the niche to be better suited for them than for any other species, or they can exploit the niche in such a way as to make it uninhabitable by anyone, inducing increased migration (which could be an ecological explanation for the formation of metastases).

When it comes to cells within a tissue, one can argue that they are at an evolutionarily stable state, and thus should not be prone to invasion by a cell that adapts a different metabolic or reproductive strategy. Another way of thinking about the "normal" state of

cells in the tissue is that they are at an adaptive peak [96]. Therefore, in order for a cancerous clone to invade the population of healthy cells, something must take the healthy cells "off of the adaptive peak".

DeGregori suggests that aging is one such mechanism by which the somatic cells gradually slide off of the adaptive peak, allowing for the invasion of cancerous clones [31, 59, 96]. It is possible that aging-associated decline in functionality of cells, tissues, organs, caused by both intrinsic cell mechanisms, such as accumulated mutations, as well as damage caused by extrinsic factors, such as exposure to carcinogens, could be reducing fitness of the resident cell population over time. Some studies also suggest that mitochondrial function declines with age, possibly due to the accumulated damage from exposure to reactive oxygen species (ROS) over individual's life span [6,8,36,77,88,144]. Since most of aerobic metabolism occurs in mitochondria, decline in mitochondrial function would cause loss of fitness advantage for somatic cells. If for cancer initiation, one needs to not only have the right cancer clone (identification of what makes the right clone is the focus of molecular study of cancer genetics) but also have it in the right place at the right time, aging could provide the ever increasing window of that "right time".

Niches in the human body

It is of course not completely clear what defines a niche for a cell population in a human body. If one were to continue with the ecological analogy, one would have to include in the definition nutrients (glucose, phosphorus, iron, lipids and other materials necessary for cell growth and reproduction), space (including extracellular matrix, which is often destroyed by tumors) and predators (cells of the immune system), as well as other microorganisms, such as gut or skin bacteria. The niche would also be characterized by such factors as pH, blood flow and rates at which cell metabolic products, dead cells, as well as external chemicals, such as certain carcinogens, are being washed out from the tissue. Other inhabitants of the niche, in this case the somatic cells, are of course also part of the environment. So, a significant modification in either of these components could hypothetically allow for the creation of a new niche that a budding primary tumor can occupy.

Interactions with the predator: the immune system

Many tumors are characterized by increased inflammation [24, 30, 55, 95]. It is possible that while the immune system is fighting an infection, immune cells secrete growth factors that premalignant cells also partake in, thus creating new growth factor rich microenvironment [66, 133] If the inflammation, and thus inflow of growth factors, continues long enough, it can give the few cancerous clones the boost they need to start growing. A subsequent decrease in the inflammatory response may not be enough to stop the tumor from growing once the process has been initiated, since some tumors either learn to secrete their own growth factors (the so-called hormone-secreting tumors like pituitary adenoma), or learn to manipulate other cells to secrete growth factors for them. A striking example of the latter is the existence of tumor-associated macrophages (TAMs) that accumulate preferentially in the poorly vascularized regions of tumors [55, 84, 94] and secrete cytokines that actually promote tumor growth [30, 66, 94, 167]. Moreover, not only can these cytokines promote tumor growth but they have also been known to suppress activation of $CD8^+$T cells that are most efficient in tumor elimination [46, 78, 79, 104, 127].

Cancer-induced niche modification

Thus, tumor cells, after invading a newly formed niche, have ample ways to modify it as to make it suit their particular needs. A possible unifying mechanism could be as follows: a right cell (exhibiting one or more hallmarks of cancer) has been in the right place (having access to enough nutrients, such as carbon and phosphorus and other building materials) at the right time (during cell division or inflammation, getting access to growth factors, or simply in an older tissue, where the surrounding cells are not as fit). As the primary tumor outgrows its blood supply, an increasing number of cells switch to glycolytic metabolism. Glycolytic cells secrete lactic acid as a by-product of glucose metabolism, creating acidic microenvironment, which can become toxic to surrounding somatic cells [41, 49], thus giving glycolytic cancer cells competitive advantage even in the presence of oxygen.

Normally, glycolysis is up-regulated only in a hypoxic microenvironment, where production of protein HIF-1 is upregulated; under normoxic conditions, its oxygen-sensitive part HIF-1α is degraded via ubiquitin-proteasome pathway [142]. However, in hypoxia, the pres-

ence of HIF-1α stimulates production of VEGF and other angiogenesis promoting factors to stimulate blood flow and bring in more oxygen to the supposedly hypoxic areas [141].

In the presence of a large enough number of glycolytic cells, an acidic microenvironment is created, in which HIF-1 production is up-regulated, and, what is more important, HIF-1α, the oxygen sensitive part of HIF-1, is not degraded. Lu et al. [91] provide evidence that lactate and pyruvate regulate hypoxia-inducible gene expression independently of hypoxia by stimulating the accumulation of HIF-1α at the site. It seems like the function of von Hippel Landau (VHL) protein, a site of HIF-1α recognition by the proteosomes, is neutralized both in hypoxic conditions and in the areas of normoxic acidosis, thus allowing tumors to simulate hypoxia in normoxic conditions [98].

What does this lead to? Corzo et al. [22] showed that when HIF-1 is up-regulated, activation of $CD8^+$T cells is suppressed, and expression of tumor-associated macrophages (TAM) goes up. Also, HIF-1, since its primary purpose is to attract oxygen to hypoxic areas, stimulates production of VEGF, which has a number of different effects. For one, VEGF not only promotes angiogenesis but also down-regulates activation of $CD8^+$T cells, allowing the tumor to grow unrestrained by the immune system [46].

The process can be summarized as follows (see also Figure 9.1):

1. A mutated cell survives and starts proliferating in the tissue. Faced with decreasing oxygen availability, cells within the tumor start switching to glycolytic metabolism, which results in the creation of acidic microenvironment around the tumor.

2. HIF-1 is up-regulated even in normoxic conditions, because VHL protein, a binding cite for cite for HIF-1α degrading proteosomes, becomes neutralized in areas of hypoxia and normoxic acidosis, thus allowing the tumor to simulate hypoxia in normoxic conditions. It has been shown that by-products of glycolysis, lactate and pyruvate, allow up-regulation of HIF-1 even in normoxia.

3. As the production of HIF-1 increases, activation of $CD8^+$T cells decreases (immune system evasion), and recruitment of TAMs increases, thus providing more growth

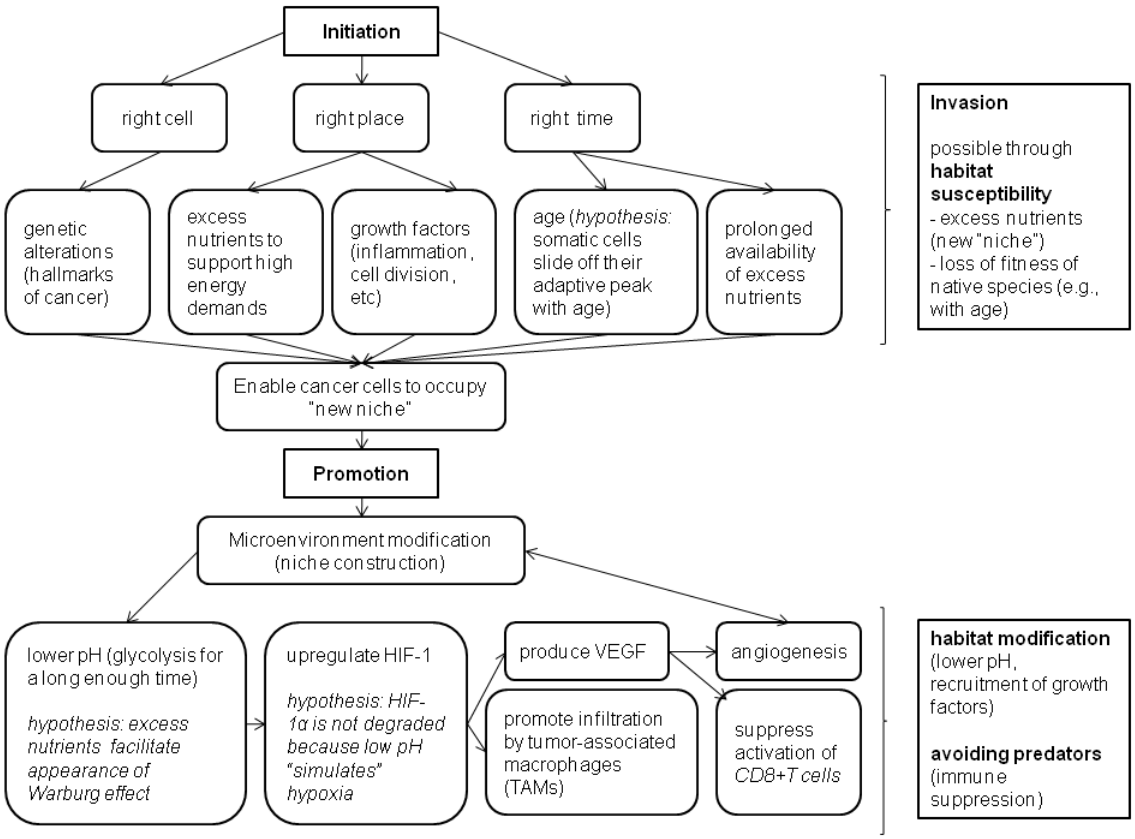

Figure 9.1: Schematic representation of the possible mechanism of tumor initiation and progression from an ecological point of view. Tumor initiation corresponds to the mechanism of species invasion, and is hypothesized to be possible when the environment is permissive, in particular, when there are excess nutrients (new niche) and when competitors (somatic cells) are less fit, compared to the invaders. Tumor promotion corresponds to niche colonization and modification by the invading species through pH alteration, recruitment of growth factors, etc., as well as avoidance of predators (immune suppression).

factors for tumor cells.

4. As HIF-1 concentration increases, so does the production of VEGF, since the main purpose of HIF-1 is to attract more blood vessels to restore oxygen supply, thus promoting angiogenesis. VEGF has also been shown to down regulate $CD8^{+}$T cell activation through suppression of maturation of antigen presenting cells, such as dendritic cells, thus also suppressing the anti-tumor immune response.

Reverse conservation biology and mass extinctions. Lessons from paleontology.

A naturally arising question is then: "If a niche has been created, and if the tumor cells had had the chance to occupy it and settle in it, how can one get rid of them?" Just reversing the initial conditions that had led to the formation of the niche might not be sufficient, since, as it was pointed out above, tumor cells have themselves had the chance to modify their microenvironment. Just targeting the population of tumor cells would also simply free up the space and nutrients to be used by the resistant clones, which could have previously been held back because of space and nutrient limitations, imposed on them by the less aggressive but more abundant cell clones.

A possible answer to this question comes from paleontology, and in particular, from the studies performed to analyze the conditions that precede mass species extinctions that have occurred over the past several million years. Arens and West [4] have suggested based on their analysis of geologic record of impact factors and continental flood basalts that mass extinctions occurred more frequently and were more destructive, when pulse disturbances (such as marine anoxic incursions) that cause extensive mortality, were accompanied by press disturbances (such as climate or sea level change) that weakened and destabilized populations over many generations preceding the pulse disturbance.

In cancer treatment, chemotherapy and radiation therapy act like pulse disturbances for a population, causing extensive cell mortality, and as a result not only selecting for the resistant clones but also freeing up the "niche" that can now be easily (or at least much easier than before) colonized by them. Perhaps, weakening the population through continuous environmental stress before applying the pulse would be more likely to cause mass extinction of cancer cells. That is, rather than just kill the tumor cells, one also needs to eliminate their niche, or at least make it less habitable for those cells that might survive after therapy.

One way to do this could be to reverse the adaptations that the tumor cells made for themselves. For instance, Robey et al. [131] demonstrated in mouse models of metastatic breast cancer that neutralizing acidic tumor microenvironment with sodium bicarbonate reduced formation of spontaneous metastases, an approach similar to what J. Pepper termed

"targeting the public goods" [123]. Counteracting the cells' attempts at modifying their microenvironment poses less of a selective pressure on the cell population and is thus much less likely to propagate evolution of resistant clones.

Blocking growth factors that facilitate tumor growth would be another approach, whether tumors secrete them themselves or "steal" them from tricked macrophages [66]. For instance, vascular endothelial growth factor (VEGF) has been identified to be a key mediator of angiogenesis in cancer: when tumors start outgrowing their blood supply, they upregulate VEGF production, which in turns promotes the formation of new blood vessels [17]. Blocking VEGF receptors in tumors, accompanied by blocking of c-met pathway, has been shown to halt tumor growth in mouse models [171]. This could be due not only to vasculature normalization, which has been suggested to actually keep tumors from spreading because their environment is acceptable enough for them to not need to migrate out, but also due to the fact that it is through growth factors like VEGF that tumors suppress the activation of cytotoxic lymphocytes by blocking the maturation of myeloid derived suppressor cells [46, 127]. Thus as a side effect, there could be an additional activation of the tumor-specific immune response coming from neutralizing tumor-induced changes in the microenvironment.

It is also important to remember that different processes take place on different time scales, and so they may be influencing each other in less obvious ways than anticipated [86, 99]. Biochemical and metabolic reactions take place on the scale of seconds and minutes, while cell growth and expansion occurs on the scale of days. So, modification of the environment that changes on one scale might have delayed effects on the processes that take place on a different time scale.

Also, some nutrients can be functionally replaced (different carbon sources), while some cannot – for instance, nothing but phosphorus can be used for building of DNA, RNA and ribosomes. Jin et al. [65] conducted an experiment where increased amount of phosphorus lead to increased tumor growth in mouse models (everything else being equal), supporting the hypothesis that phosphorus could be a limiting reagent for cell proliferation [40]. Changing the amount of phosphorus present (through phosphorus enriched diet, for instance) would change the composition of the cell microenvironment, creating a new niche

for phosphorus-greedy tumor cells to invade. Glucose transporters are also highly up-regulated in cancer cells to accommodate the high demand for glucose [47], so a sustained diet that is high in carbohydrates would also allow cancer cells to not worry about the drawbacks of glycolysis. Caloric restriction has also been implied to improve mitochondrial function [90, 140], so limiting carbohydrate intake could hypothetically give somatic tissue back their selective advantage.

While changing what constitutes the "right cell" and the "right time" may not be possible, the composition of the "right place", the microenvironment, could potentially be manipulated. Lessons from ecology suggest that it could be of vital importance both for disease prevention and for more successful treatment.

Chapter 10

CONCLUSIONS

Complex systems and ODEs

Complexity science has been gaining ground over the last several decades as a possible mechanism of unifying our understanding of how different parts of the world interact and influence each other, and what effects can be expected to come out as a result of these interactions.

Complex systems involve diverse interactive adaptive agents, whose individual micro-level behavior can cause macro-level changes, to which they in turn adapt [102, 119, 120]. This notion is very similar to that of ecosystem engineering, also known as niche construction, where in ecological systems, individuals within populations modify their environment in such a way as to make it suit them, often eventually co-evolving with it [115, 116]. One of the frameworks, within which one can evaluate such interactions, is in the context of consumer-resource interactions, which are the focus of this dissertation.

Until recently in silico modeling of complex systems was only possible with the help of agent-based models, which involve running simulations of interactions of diverse adapting individual agents on a lattice grid under the restrictions set by the rules that define the nature of the agents' interactions with each other and with their environment [102]. Such experiments allow observing a number of interesting phenomena, such as tipping points, which are the points of critical transitions in complex systems. Another way to view tipping points is through the lens of bifurcation theory. In ordinary differential equations (ODEs), tipping points can be seen as corresponding to bifurcation boundaries, which, unlike in agent-based models, can sometimes even be identified analytically. Normally, incorporating the level of heterogeneity in ODEs comparable to that of ABMs would result in increasing system dimensionality to infinity, thus making qualitative analysis of such systems impossible. This challenge is overcome in this dissertation through application of the Reduction theorem for replicator equations [69, 70].

Major premise in the Reduction theorem comes from the assumption that each indi-

vidual agent, or clone, within the population studied, is characterized by an individual value of some intrinsic parameter, such as birth rates, death rates, rates of resource consumption, etc. Then as the system evolves, different clones are going to impose different selective pressures both on each other and on their environment, and so the distribution of clones with respect to the parameter values studied will also change over time. The changes in the distribution and in the mean value of the individual characteristic studied can be tracked through the moment generating function of the initial distribution of clones in the population and keystone variables. This allows reducing an otherwise infinitely dimensional system to low dimensionality, thus enabling one to calculate numerical solutions of the resulting parametrically heterogeneous system of ODEs, making deterministic predictions about the direction in which this system will evolve. This methodology was used throughout this dissertation in order to answer the questions about evolution of different types of ecological systems.

Summary of results

Part I. Transitional regimes, prisoner's dilemma and tragedy of the commons in consumer-resource models.

Evaluation of the notion of correspondence between bifurcation boundaries in ODEs and tipping points in complex systems was done in Chapter 2. Specifically, its focus was on the question of the effects of resource overconsumption on sustainable coexistence with the common renewable resource of a population of consumers that can not only consume the resource but are also capable of contributing to its restoration. A series of transitional regimes were identified analytically, going from sustainable coexistence with the resource to oscillatory regime to system collapse with the increase of the rate of resource overconsumption. The system was then allowed to evolve, revealing that while the amount of resource available and the population size may appear to be stable, evaluation of the distribution of clones with respect to the rates of resource overconsumption, and specifically the values of the mean value of the corresponding parameter and its position on the bifurcation diagram of the original system, may reveal a warning signal for an approaching collapse, which would not be noticeable otherwise.

Next, a naturally arising question of the possible ways of dealing with the problem of resource overconsumption was investigated in Chapter 3. The problem can be reformulated

as a game of prisoner's dilemma: while the common resource would be better preserved if everyone cooperated, it is in the interest of each individual consumer at each time point to defect and over-consume. This kind of behavior can result in what has become known as the tragedy of the commons [57], i.e., a situation, when over-exploitation of the resource on the level of each individual results in eventual collapse of the resource for all of its consumers.

Elinor Ostrom [117, 118, 162] observed that the tragedy could successfully be avoided in situations, where the act of overconsumption was immediately noticeable because of small community size, such as in small fisheries, and immediately punishable, thus altering the payoffs of all the players in the prisoner's dilemma game in such a way as to make preservation of the resource a more successful strategy for each individual at each time point (see Figure 3.22).

A series of numerical experiments were then conducted in Chapter 3 to evaluate different types of punishment functions and different intensities of execution of such punishment. It was observed that 1) low levels of implementation of severe punishment yield better results that high levels of implementation of moderate punishment and 2) there exists no panacea, no optimal punishment function for preventing the tragedy of the commons, and the level of punishment implementation needs to be adjusted depending on the initial distribution of over-consumers in the population.

A brief comparative analysis of two methods for modeling parametrically heterogeneous populations was also performed in Chapter 3, namely, adaptive dynamics and the Reduction theorem. Adaptive dynamics [52]is a series of techniques that was developed in 1990s to evaluate the question of whether a "mutant", in this case an individual with larger parameter of resource over-consumption, can invade the "resident" population, in this case under-consumers. This technique allows finding analytical conditions for the intensity of punishment implementation for each punishment function, which cannot be achieved with the use of the Reduction theorem. However, adaptive dynamics does not allow to make predictions about the situation when the "mutant" is not rare, i.e., in case of such an "invasion" by a group. This problem can in turn be addressed with the help of Reduction theorem, thus suggesting that the two methods complement each other (a comparison of both methods is

summarized in Table 3.2). Unfortunately, neither method allows incorporating spatial structure of the environment in the modeling process, which for the future could potentially be addressed with the addition of agent-based models (see Section).

Next, a situation, where the individuals in the population can choose whether to allocate their resources to invest in reproduction or in competition was evaluated. This case is of particular interest, since, unlike in the model, studied in Chapter 2, it is not intuitively clear, which strategy would give the individuals a higher competitive advantage. The results of the computations conducted in this Chapter suggest that while in a parametrically homogeneous population, i.e., a population composed of some "average" consumers, investing into competition seems to be a more beneficial strategy, reflected in the fact that in this case, a larger domain of the phase-parameter space corresponds to sustainable coexistence with common resources, in a heterogeneous system one cannot make such conclusions. This stems from the fact that in such a system, the individuals experience not only the pressures from the environment in the form of limited resource, but also impose different selective pressures on each other, which vary depending on the initial distribution of clones in the population. Therefore, in order to be able to try and predict, which way a system will evolve, one would need to not only evaluate the rules by which the interactions occur but also who exactly is playing by these rules.

Part II. Mixed strategies, metabolism and predator-prey interactions in cancer ecology.

In the second part of the dissertation, the notions of niche construction, mixed strategies and tragedy of the commons as prisoner's dilemma are applied to cancer, which can be viewed as a complex ecological system, where a population of heterogeneous cells compete with each other and with somatic cells for common renewable resources, such as carbon and phosphorus. In Chapter 5, tumor growth was evaluated from the point of view of resource allocation, used for competition or for proliferation, similarly to the general model evaluated in Chapter 4. It was hypothesized that manipulation the ratios of carbon (energy source, necessary for survival) and phosphorus (source of building materials, necessary for proliferation) may allow shifting the overall composition of the tumor away from the more dangerous proliferative phenotype and towards a less aggressive competitive phenotype. The hypothesis was evaluated using a system of ODEs, suggesting that indeed, reduction in

phosphorus availability may allow shifting tumor composition towards a more competitive phenotype, emphasizing importance of nutrition for cancer patients.

One possible manifestation of the competitive phenotype can be related to the way cancer cells metabolize glucose. Any cell can metabolize glucose both aerobically, yielding approximately 30 ATP per molecule of glucose, and glycolytically, yielding only 2 ATPs. As the tumor grows, cells become oxygen deprived, switching to glycolysis for survival. However, it has been observed that cancer cells tend to persist in metabolizing glucose glycolytically even in the areas of ample oxygen supply, a phenomenon that has become known as Warburg effect. Although it has been hypothesized that lactic acid, which is a by-product of glycolysis, gives cancer cells the competitive advantage that they lose in ATP yield by creating a microenvironment that is toxic to somatic cells, one cancer cell cannot generate enough lactic acid to become an efficient enough competitor. The question of how a core subpopulation of Warburg cells could have formed was addressed in Chapter 6, where the situation was reformulated as a game of multi-player prisoner's dilemma: from the point of view of metabolic payoffs, it is better for cells to cooperate and become better competitors but neither cell has an incentive to unilaterally change its metabolic strategy. However, changing cell microenvironment by increasing glucose availability, through nutrition for instance, allows shifting population composition towards the "cooperative" glycolytic metabolic strategy by minimizing the drawbacks of glycolysis (low ATP yield per molecule of glucose), while keeping all of its benefits (increased competitive ability). This incidentally provides another approach to dealing with the problem of prisoner's dilemma through modifying the environment in which the interactions occur (see Figure 6.8 on page 104) rather than changing the payoffs of the players directly, as was done in Chapter 3. Interestingly, from the point of view of metabolic payoffs, it is the defecting strategy adopted by somatic cells that stabilizes the tissue, and it is the cooperative strategy adopted by the cancer cells that kills the host.

Another measure of heterogeneity that could be of interest deals with dormant vs. actively proliferating cancer cells and micrometastases. Clinical and experimental evidence suggest that human tumors can persist for long periods of time as microscopic lesions that are in a state of dormancy (non-expanding tumor mass). Several mechanisms have been

proposed to explain what could stimulate the cells to become proliferative again, including surgery and trauma induced angiogenic switch and immune suppression. Some details of the interactions of the latter with cancer cells can in fact be reformulated as predator-prey type systems, which was investigated in Chapter 8.

Finally, all of these components were put together into one possible approach to understanding cancer as a complex evolving ecological system, summarized in Figure 9.1 on page 134 in Chapter 9. A number of ways by which cancer cells modify their microenvironment was discussed (such as altering pH through increased glycolysis), which in turn can be viewed as one possible manifestation of niche construction. These results emphasize the importance of paying attention to tumor microenvironment in order to increase chances of successful treatment.

[1] A. Algar, J. Kerr, and D. Currie. Quantifying the importance of regional and local filters for community trait structure in tropical and temperate zones. *Ecology*, 92(4):903–914, 2011.

[2] Nava Almog. Molecular mechanisms underlying tumor dormancy. *Cancer letters*, 294(2):139–46, August 2010.

[3] Joshua M Ammerman, Russel R Lonser, James Dambrosia, John A Butman, and Edward H Oldfield. Long-term natural history of hemangioblastomas in patients with von Hippel Lindau disease, implications for treatment. *Journal of Neurosurgery*, 105, 2006.

[4] Nan Crystal Arens and Ian D. West. Press-pulse: a general theory of mass extinction? *Paleobiology*, 34(4):456–471, December 2008.

[5] A.R. Ashok R Asthagiri, Gautam U Mehta, Leor Zach, Xiaobai Li, J.A. John A Butman, Kevin A K.A. Camphausen, and Russell R.R. Lonser. Prospective evaluation of radiosurgery for hemangioblastomas in von Hippel Lindau disease. *Neuro-oncology*, 12(1):80–6, January 2010.

[6] Robert S Balaban, Shino Nemoto, and Toren Finkel. Mitochondria, oxidants, and aging. *Cell*, 120(4):483–95, February 2005.

[7] NN Bautin and EA Leontovich. *Methods and Techniques for Qualitative Analysis of Dynamical Systems on the Plane*. Nauka, Moscow, 1976.

[8] Christopher C Benz and Christina Yau. Ageing, oxidative stress and cancer: paradigms in parallax. *Nature reviews. Cancer*, 8:875–879, 2008.

[9] Faina Berezovskaya. The main topological part of plane vector fields with fixed Newton diagram. *Proceedings on Singularity Theory*, pages 55–73, 1995.

[10] Faina S Berezovskaya, Georgy P Karev, and Roger Arditi. Parametric analysis of the ratio-dependent predator-prey model. *Journal of mathematical biology*, 43(4):221–246, 2001.

[11] Faina S Berezovskaya, Georgy P Karev, Baojun Song, and Carlos Castillo-Chavez. A simple epidemic model with surprising dynamics. *Mathematical Biosciences and Engineering*, 1:1–20, 2004.

[12] Faina S Berezovskaya, Artem S Novozhilov, and Georgy P Karev. Population models with singular equilibrium. *Mathematical biosciences*, 208(1):270–299, 2007.

[13] Maarten Boersma and James J. Elser. Too Much of a Good Thing: on Stoichiometrically Balanced Diets and Maximal Growth. *Ecology*, 87(5):1325–1330, May 2006.

[14] Sébastien Bonnet, Stephen L Archer, Joan Allalunis-Turner, Alois Haromy, Christian Beaulieu, Richard Thompson, Christopher T Lee, Gary D Lopaschuk, Lakshmi Puttagunta, Sandra Bonnet, Gwyneth Harry, Kyoko Hashimoto, Christopher J Porter, Miguel A Andrade, Bernard Thebaud, and Evangelos D Michelakis. A mitochondria-K+ channel axis is suppressed in cancer and its normalization promotes apoptosis and inhibits cancer growth. *Cancer cell*, 11(1):37–51, January 2007.

[15] Alexander S. Bratus', Vladimir P. Posvyanskii, and Artem S. Novozhilov. A note on the replicator equation with explicit space and global regulation. *Arxiv preprint arXiv:1006.2452*, page 23, June 2010.

[16] Ragan M Callaway, Giles C Thelen, Alex Rodriguez, and William E Holben. Soil biota and exotic plant invasion. *Nature*, 427(6976):731–3, February 2004.

[17] Peter Carmeliet. VEGF as a key mediator of angiogenesis in cancer. *Oncology*, 69 Suppl 3(3):4–10, January 2005.

[18] Pingyan Cheng, Cesar A Corzo, Noreen Luetteke, Bin Yu, Srinivas Nagaraj, Marylin M Bui, Myrna Ortiz, Wolfgang Nacken, Clemens Sorg, Thomas Vogl, Johannes Roth, and Dmitry I Gabrilovich. Inhibition of dendritic cell differentiation and accumulation of myeloid-derived suppressor cells in cancer is regulated by S100A9 protein. *The Journal of experimental medicine*, 205(10):2235–49, September 2008.

[19] N. Chikatsu, Y. Nakamura, H. Sato, T. Fujita, S. Asano, and T. Motokura. p53 mutations and tetraploids under r-and K-selection. *Oncogene*, 21(19):3043–9, 2002.

[20] James S Clark. Individuals and the variation needed for high species diversity in forest trees. *Science (New York, N.Y.)*, 327(5969):1129–32, February 2010.

[21] W.C. Clark and Simon A Levin. Toward a Science of Sustainability: Executive Summary. In *Toward a Science of Sustainability Conference Airlie Center*, pages 4–10, 2009.

[22] C. A. Corzo, T. Condamine, L. Lu, M. J. Cotter, J.-I. Youn, P. Cheng, H.-I. Cho, E. Celis, D. G. Quiceno, T. Padhya, T. V. McCaffrey, J. C. McCaffrey, and D. I. Gabrilovich. HIF-1 regulates function and differentiation of myeloid-derived suppressor cells in the tumor microenvironment. *Journal of Experimental Medicine*, 207(11):2439–2453, September 2010.

[23] J.W. Costerton, Z. Lewandowski, D.E. Caldwell, D.R. Korber, and H.M. Lappin-Scott. Microbial biofilms. *Annual Reviews in Microbiology*, 49(1):711–745, 1995.

[24] Lisa M Coussens and Zena Werb. Inflammation and cancer. *Nature*, 420(6917):860–7, January 2002.

[25] B. Crespi and K. Summers. Evolutionary biology of cancer. *Trends in ecology & evolution*, 20(10):545–552, 2005.

[26] Alysha K Croker, Jason L Townson, Alison L Allan, and Ann F Chambers. Stem Cells and Cancer. *Stem Cells*, 2009.

[27] Charles Darwin. On the origin of species by means of natural selection, or the preservation of favoured races in the struggle for life. 1878.

[28] L G de Pillis, W Gu, and A E Radunskaya. Mixed immunotherapy and chemotherapy of tumors: modeling, applications and biological interpretations. *Journal of theoretical biology*, 238(4):841–62, February 2006.

[29] Lisette G de Pillis, Ami E Radunskaya, and Charles L Wiseman. A validated mathematical model of cell-mediated immune response to tumor growth. *Cancer research*, 65(17):7950–8, September 2005.

[30] Karin E de Visser, Alexandra Eichten, and Lisa M Coussens. Paradoxical roles of the immune system during cancer development. *Nature reviews. Cancer*, 6(1):24–37, January 2006.

[31] James Degregori. Evolved Tumor Suppression: Why Are We So Good at Not Getting Cancer? *Cancer research*, May 2011.

[32] R Demicheli, M W Retsky, W J M Hrushesky, M Baum, and I D Gukas. The effects of surgery on tumor growth: a century of investigations. *Annals of oncology : official journal of the European Society for Medical Oncology / ESMO*, 19(11):1821–8, November 2008.

[33] V.J. Denef, L.H. Kalnejais, R.S. Mueller, P. Wilmes, B.J. Baker, B.C. Thomas, N.C. VerBerkmoes, R.L. Hettich, and J.F. Banfield. Proteogenomic basis for ecological divergence of closely related bacteria in natural acidophilic microbial communities. *Proceedings of the National Academy of Sciences*, 107(6):2383–2390, 2010.

[34] Raphael K Didham, Jason M Tylianakis, Neil J Gemmell, Tatyana a Rand, and Robert M Ewers. Interactive effects of habitat modification and species invasion on native species decline. *Trends in ecology & evolution (Personal edition)*, 22(9):489–96, September 2007.

[35] Theodosius Dobzhansky. The evolution in the tropics. *American Scientist*, 38:209–221, 1950.

[36] Nadiya M Druzhyna, Glenn L Wilson, and Susan P LeDoux. Mitochondrial DNA repair in aging and disease. *Mechanisms of ageing and development*, 129(7-8):383–90.

[37] F. Dumortier. Singularities of vector fields on the plane. *Journal of Differential Equations*, 23(0022-0396):53—-106, 1977.

[38] James Elser. Biological stoichiometry: a chemical bridge between ecosystem ecology and evolutionary biology. *The American naturalist*, 168 Suppl(december):S25–35, December 2006.

[39] James J Elser, Marcia M Kyle, Marilyn S Smith, and John D Nagy. Biological stoichiometry in human cancer. *PloS one*, 2(10):e1028, January 2007.

[40] James J. Elser, John D. Nagy, and Yang Kuang. Biological Stoichiometry: An Ecological Perspective on Tumor Dynamics. *BioScience*, 53(11):1112, 2003.

[41] Jennifer S Fang, Robert D Gillies, and Robert A Gatenby. Adaptation to hypoxia and acidosis in carcinogenesis and tumor progression. *Seminars in cancer biology*, 18(5):330–7, October 2008.

[42] R.A. Fisher. The fundamental theorem of natural selection. *The Genetical Theory of Natural Selection*, pages 22–47, 1930.

[43] Carl Folke, Thomas Hahn, Per Olsson, and Jon Norberg. Adaptive Governance of Social-Ecological Systems. *Annual Review of Environment and Resources*, 30(1):441–473, November 2005.

[44] K.R. Foster, A. Fortunato, J.E. Strassmann, and D.C. Queller. The costs and benefits of being a chimera. *Proceedings of the Royal Society of London. Series B: Biological Sciences*, 269(1507), 2002.

[45] Ingo Fricke, Noweeda Mirza, Jakob Dupont, Craig Lockhart, Autumn Jackson, Ji-Hyun Lee, Jeffrey A Sosman, and Dmitry I Gabrilovich. Vascular endothelial growth factor-trap overcomes defects in dendritic cell differentiation but does not improve antigen-specific immune responses. *Clinical cancer research : an official journal of the American Association for Cancer Research*, 13(16):4840–8, August 2007.

[46] Dmitry I Gabrilovich and Srinivas Nagaraj. Myeloid-derived suppressor cells as regulators of the immune system. *Nature reviews. Immunology*, 9(3):162–74, March 2009.

[47] Vadivel Ganapathy, Muthusamy Thangaraju, and Puttur D Prasad. Nutrient transporters in cancer: relevance to Warburg hypothesis and beyond. *Pharmacology & therapeutics*, 121(1):29–40, January 2009.

[48] Robert a Gatenby. A change of strategy in the war on cancer. *Nature*, 459(7246):508–9, May 2009.

[49] Robert a Gatenby and Robert J Gillies. Why do cancers have high aerobic glycolysis? *Nature reviews. Cancer*, 4(11):891–9, November 2004.

[50] Robert a Gatenby and Robert J Gillies. A microenvironmental model of carcinogenesis. *Nature reviews. Cancer*, 8(1):56–61, January 2008.

[51] Robert a Gatenby, Ariosto S Silva, Robert J Gillies, and B Roy Frieden. Adaptive therapy. *Cancer research*, 69(11):4894–903, June 2009.

[52] S.A.H. Geritz, Eva Kisdi, N.A. Meszena, and J.A.J. Metz. Evolutionarily singular strategies and the adaptive growth and branching of the evolutionary tree. *Evolutionary Ecology*, 12(1):35–57, 1997.

[53] N.B. Grimm, S.H. Faeth, N.E. Golubiewski, C.L. Redman, J. Wu, X. Bai, and J.M. Briggs. Global change and the ecology of cities. *Science*, 319(5864):756–760, 2008.

[54] Volker Grimm, Uta Berger, Donald L Deangelis, J. Gary Polhill, Jarl Giske, and Steven Railsback. The ODD protocol. A review and first update. *Ecological Modelling*, 221(23):27660–2768, 2010.

[55] M J Grimshaw and F R Balkwill. Inhibition of monocyte and macrophage chemotaxis by hypoxia and inflammation–a potential mechanism. *European journal of immunology*, 31(2):480–9, February 2001.

[56] J. Grinnell. The niche-relationships of the California Thrasher. *The Auk*, 34(4):427–433, 1917.

[57] G Hardin. The Tragedy of the Commons. *Science (New York, N.Y.)*, 162(5364):1243–8, December 1968.

[58] Alan Hastings. Timescales, dynamics, and ecological understanding. *Ecology*, 91:3471–3480, 2010.

[59] Curtis J Henry, Andriy Marusyk, Vadym Zaberezhnyy, Biniam Adane, and James Degregori. Declining lymphoid progenitor fitness promotes aging-associated leukemogenesis. *Proceedings of the National Academy of Sciences of the United States of America*, 107(50):21713–21718, November 2010.

[60] D. U. Hooper, III F. S. Chapin, J. J. Ewel, A. Hector, P. Inchausti, S. Lavorel, J. H. Lawton, D. M. Lodge, M. Loreau, S. Naeem, B. Schmid, H. Setälä, A. J. Symstad, J. Vandermeer, and D. A. Wardle. Effects of Biodiversity on Ecosystem Functioning: A Consensus of Current Knowledge. *Ecological Monographs*, 75(1):3–35, 2005.

[61] S.B. Hsu, T.W. Hwang, and Yang Kuang. Global analysis of the Michaelis-Menten-type ratio-dependent predator-prey system. *Journal of mathematical biology*, 42(6):489–506, 2001.

[62] F.B. Hu, W.C. Willett, T. Li, M.J. Stampfer, G.A. Colditz, and J.A.E. Manson. Adiposity as compared with physical activity in predicting mortality among women. *Obstetrical & gynecological survey*, 60(5), 2005.

[63] T.J. Hudson, W. Anderson, A. Aretz, A.D. Barker, C. Bell, R.R. Bernabe, M.K. Bhan, F. Calvo, I. Eerola, and D.S. Gerhard. International network of cancer genome projects. *Nature*, 464:993–998, 2010.

[64] E.T. Jaynes and G.L. Bretthorst. *Probability theory: the logic of science*. Cambridge University Press, 2003.

[65] Hua Jin, Cheng-Xiong Xu, Hwang-Tae Lim, Sung-Jin Park, Ji-Young Shin, Youn-Sun Chung, Se-Chang Park, Seung-Hee Chang, Hee-Jeong Youn, Kee-Ho Lee, Yeon-Sook Lee, Yoon-Cheol Ha, Chan-Hee Chae, George R Beck, and Myung-Haing Cho. High dietary inorganic phosphate increases lung tumorigenesis and alters Akt signaling. *American journal of respiratory and critical care medicine*, 179(1):59–68, January 2009.

[66] Magnus Johansson, David G Denardo, and Lisa M Coussens. Polarized immune responses differentially regulate cancer development. *Immunological reviews*, 222:145–54, April 2008.

[67] William G Kaelin, Jr and Craig B Thompson. Clues from cell metabolism. *Nature*, 465(June):3–5, 2010.

[68] J.N. Kapur. *Maximum-entropy models in science and engineering*. John Wiley & Sons, 1989.

[69] Georgy P Karev. On mathematical theory of selection: continuous time population dynamics. *Journal of mathematical biology*, 60(1):107–29, January 2010.

[70] Georgy P Karev. Principle of Minimum Discrimination Information and Replica Dynamics. *Entropy*, 12(7):1673–1695, 2010.

[71] Irina Kareva. What can ecology teach us about cancer? *Translational Oncology*, 4(5):266–270, 2011.

[72] Jung-whan Kim and Chi V Dang. Cancer's molecular sweet tooth and the Warburg effect. *Cancer research*, 66(18):8927–30, September 2006.

[73] Denise Kirschner and John Carl Panetta. Modeling immunotherapy of the tumor - immune interaction. *Journal of Mathematical Biology*, 37(3):235–252, September 1998.

[74] Marcin Kortylewski, Maciej Kujawski, Tianhong Wang, Sheng Wei, Shumin Zhang, Shari Pilon-Thomas, Guilian Niu, Heidi Kay, James Mulé, William G Kerr, Richard Jove, Drew Pardoll, and Hua Yu. Inhibiting Stat3 signaling in the hematopoietic system elicits multicomponent antitumor immunity. *Nature medicine*, 11(12):1314–21, December 2005.

[75] David C Krakauer, Karen M Page, and Douglas H Erwin. Diversity, dilemmas, and monopolies of niche construction. *The American naturalist*, 173(1):26–40, January 2009.

[76] Yang Kuang and E. Beretta. Global qualitative analysis of a ratio-dependent predator-prey system. *Journal of mathematical biology*, 36(4):389–406, 1998.

[77] Author G C Kujoth, A Hiona, T D Pugh, S Someya, K Panzer, S E Wohlgemuth, A Y Seo, R Sullivan, W A Jobling, J D Morrow, H Van Remmen, J M Sedivy, M Tanokura, R Weindruch, C Leeuwenburgh, and T A Prolla. Mitochondrial DNA Mutations , Oxidative Stress , and Apoptosis in Mammalian Aging. *Sciencecience*, 309(5733):481–484, 2005.

[78] Sergei Kusmartsev and Dmitry I Gabrilovich. Effect of tumor-derived cytokines and growth factors on differentiation and immune suppressive features of myeloid cells in cancer. *Cancer metastasis reviews*, 25(3):323–31, September 2006.

[79] Sergei Kusmartsev, Yulia Nefedova, Daniel Yoder, and Dmitry I. Gabrilovich. Antigen-Specific Inhibition of CD8+ T Cell Response by Immature Myeloid Cells in Cancer Is Mediated by Reactive Oxygen Species. *J. Immunol.*, 172(2):989–999, 2004.

[80] Y. Kuznetsov. *Elements of applied bifurcation theory*. Springer New York, 1998.

[81] K. Lange and F.J. Oyarzun. The attractiveness of the Droop equations. *Mathematical biosciences*, 111(0025-5564):261–278, 1992.

[82] A. Lanzavecchia. Dynamics of T Lymphocyte Responses: Intermediates, Effectors, and Memory Cells. *Science*, 290(5489):92–97, October 2000.

[83] Louis Lebel, John M Anderies, Bruce Campbell, Carl Folke, Steve Hatfield-dodds, Terry P Hughes, and James Wilson. Governance and the Capacity to Manage Resilience in Regional Social-Ecological Systems. *Ecology and Society*, 11(1), 2006.

[84] R D Leek, R J Landers, A L Harris, and C E Lewis. Necrosis correlates with high vascular density and focal macrophage infiltration in invasive carcinoma of the breast. *British journal of cancer*, 79(5-6):991–5, February 1999.

[85] Simon A Levin. Ecosystems and the Biosphere as Complex Adaptive Systems. *Ecosystems*, 1(5):431–436, 1998.

[86] Simon a. Levin. Multiple Scales and the Maintenance of Biodiversity. *Ecosystems*, 3(6):498–506, November 2000.

[87] Simon A Levin and Carlos Castillo-Chavez. Topics in evolutionary biology. *Mathematical and Statistical Developments of Evolutionary Theory, NATO ASI Series*, 299:327–358, 1988.

[88] Nancy J Linford, Samuel E Schriner, and Peter S Rabinovitch. Oxidative damage and aging: spotlight on mitochondria. *Cancer research*, 66(5):2497–9, March 2006.

[89] J. Liu, T. Dietz, S.R. Carpenter, M. Alberti, C. Folke, E. Moran, A.N. Pell, P. Deadman, T. Kratz, and J. Lubchenco. Complexity of coupled human and natural systems. *Science*, 317(5844), 2007.

[90] G López-Lluch, N Hunt, B Jones, M Zhu, H Jamieson, S Hilmer, M V Cascajo, J Allard, D K Ingram, P Navas, and R de Cabo. Calorie restriction induces mitochondrial biogenesis and bioenergetic efficiency. *Proceedings of the National Academy of Sciences of the United States of America*, 103(6):1768–73, March 2006.

[91] Huasheng Lu, Robert A Forbes, and Ajay Verma. Hypoxia-inducible factor 1 activation by aerobic glycolysis implicates the Warburg effect in carcinogenesis. *The Journal of biological chemistry*, 277(26):23111–5, June 2002.

[92] Robert H. MacArthur and Edward O. Wilson. *The theory of island biogeography*. Princeton University Press, 1967.

[93] D.W. Macdonald, C. Newman, P.M. Nouvellet, and C.D. Buesching. An analysis of Eurasian badger (Meles meles) population dynamics: Implications for regulatory mechanisms. *Journal of Mammology*, 90(6):1392–1403, 2009.

[94] Alberto Mantovani, Paola Allavena, and Antonio Sica. Tumour-associated macrophages as a prototypic type II polarised phagocyte population: role in tumour progression. *European journal of cancer (Oxford, England : 1990)*, 40(11):1660–7, July 2004.

[95] Alberto Mantovani, Paola Allavena, Antonio Sica, and Frances Balkwill. Cancer-related inflammation. *Nature*, 454(7203):436–444, July 2008.

[96] Andriy Marusyk and James DeGregori. Declining cellular fitness with age promotes cancer initiation by selecting for adaptive oncogenic mutations. *Biochimica et biophysica acta*, 1785(1):1–11, January 2008.

[97] Benedetta Mattioli, Elisabetta Straface, Maria Giovanna Quaranta, Luciana Giordani, and Marina Viora. Leptin Promotes Differentiation and Survival of Human Dendritic Cells and Licenses Them for Th1 Priming. *J. Immunol.*, 174(11):6820–6828, 2005.

[98] Karim Mekhail, Lakshman Gunaratnam, Marie-Eve Bonicalzi, and Stephen Lee. HIF activation by pH-dependent nucleolar sequestration of VHL. *Nature Cell Biology*, 6:642–647, 2004.

[99] Duncan N L Menge, Stephen W Pacala, and Lars O Hedin. Emergence and maintenance of nutrient limitation over multiple timescales in terrestrial ecosystems. *The American naturalist*, 173(2):164–75, February 2009.

[100] Lauren MF Merlo, John W Pepper, Brian J Reid, and Carlo C Maley. Cancer as an evolutionary and ecological process. *Nature Reviews Cancer*, 6:924–935, 2006.

[101] Manfred Milinski, Dirk Semmann, and Hans-Jürgen Krambeck. Reputation helps solve the 'tragedy of the commons'. *Nature*, 415(6870):424–6, January 2002.

[102] J.H. Miller and S.E. Page. *Complex adaptive systems: An introduction to computational models of social life*. Princeton University Press, 2007.

[103] Christian Mulder and James J. Elser. Soil acidity, ecological stoichiometry and allometric scaling in grassland food webs. *Global Change Biology*, 15(11):2730–2738, November 2009.

[104] Craig Murdoch, Munitta Muthana, Seth B Coffelt, and Claire E Lewis. The role of myeloid cells in the promotion of tumour angiogenesis. *Nature reviews. Cancer*, 8(8):618–31, August 2008.

[105] Kenneth Murphy, Paul Travers, and Mark Walport. *Janeway's Immunobiology*. Garland Science, 7th edition, 2007.

[106] Ville Mustonen and Michael Lässig. From fitness landscapes to seascapes: non-equilibrium dynamics of selection and adaptation. *Trends in genetics : TIG*, 25(3):111–9, March 2009.

[107] Ville Mustonen and Michael Lässig. Fitness flux and ubiquity of adaptive evolution. *Proceedings of the National Academy of Sciences of the United States of America*, 107(9):4248–53, March 2010.

[108] Srinivas Nagaraj, Kapil Gupta, Vladimir Pisarev, Leo Kinarsky, Simon Sherman, Loveleen Kang, Donna L Herber, Jonathan Schneck, and Dmitry I Gabrilovich. Altered recognition of antigen is a mechanism of CD8+ T cell tolerance in cancer. *Nature medicine*, 13(7):828–35, July 2007.

[109] John D. Nagy. The ecology and evolutionary biology of cancer: a review of mathematical models of necrosis and tumor cell diversity. *Mathematical Biosciences and Engineering*, 2(2):381, 2005.

[110] John Nash. Equilibrium points in n-person games. *Proceedings of the National Academy of Sciences*, 36(1):48–49, 1950.

[111] George N Naumov, Elise Bender, David Zurakowski, Soo-Young Kang, David Sampson, Evelyn Flynn, Randolph S Watnick, Oddbjorn Straume, Lars a Akslen, Judah Folkman, and Nava Almog. A model of human tumor dormancy: an angiogenic switch from the nonangiogenic phenotype. *Journal of the National Cancer Institute*, 98(5):316–25, March 2006.

[112] George N Naumov, Judah Folkman, and Oddbjorn Straume. Tumor dormancy due to failure of angiogenesis: role of the microenvironment. *Clinical & experimental metastasis*, 26(1):51–60, January 2009.

[113] Yulia Nefedova, Srinivas Nagaraj, Amsler Rosenbauer, Carlos Muro-Cacho, Said M Sebti, and Dmitry I Gabrilovich. Regulation of dendritic cell differentiation and antitumor immune response in cancer by pharmacologic-selective inhibition of the janus-activated kinase 2/signal transducers and activators of transcription 3 pathway. *Cancer research*, 65(20):9525–35, October 2005.

[114] Martin Nowak. *Evolutionary dynamics: exploring the equations of life*. Belknap Pres, 2006.

[115] F. John Odling-Smee. Niche construction, genetic evolution and cultural change. *Behavioural Processes*, 35:195–205, 1995.

[116] F. John Odling-Smee, Kevin N. Laland, and Marcus W. Feldman. *Niche construction: the neglected process in evolution*. Princeton University Press, 2003.

[117] Elinor Ostrom. *Governing the commons: The evolution of institutions for collective action*. Cambridge University Press, 1990.

[118] Elinor Ostrom. A general framework for analyzing sustainability of social-ecological systems. *Science (New York, N.Y.)*, 325(5939):419–22, July 2009.

[119] S.E. Page. *The Di erence: How the Power of Diversity Creates Better Groups, Firms, Schools, and Societies*. Princeton University Press, 2007.

[120] S.E. Page. *Diversity and Complexity*. Princeton University Press, 2010.

[121] John D Parker, Deron E Burkepile, and Mark E Hay. Opposing effects of native and exotic herbivores on plant invasions. *Science (New York, N.Y.)*, 311(5766):1459–61, March 2006.

[122] T.B. Parkin and E.C. Berry. Microbial nitrogen transformations in earthworm burrows. *Soil Biology and Biochemistry*, 5(8):789–801, 2002.

[123] John W Pepper. Defeating pathogen drug resistance: guidance from evolutionary theory. *Evolution; international journal of organic evolution*, 62(12):3185–91, December 2008.

[124] Eric R Pianka. Niche Overlap and Diffuse Competition. *Proceedings of the National Academy of Sciences*, 71(5):2141–2145, 1974.

[125] B. Prakash, BM Veeregowda, and G. Krishnappa. Biofilms: A survival strategy of bacteria. *Current Science*, 85(9):1299–1307, 2003.

[126] DL Preston, E. Ron, S. Tokuoka, S. Funamoto, N. Nishi, M. Soda, K. Mabuchi, and K. Kodama. Solid cancer incidence in atomic bomb survivors: 1958-1998. *Radiation research*, 168(0033-7587):1–64, 2007.

[127] Gabriel A Rabinovich, Dmitry Gabrilovich, and Eduardo M Sotomayor. Immunosuppressive strategies that are mediated by tumor cells. *Annual review of immunology*, 25:267–96, January 2007.

[128] Paul B Rainey and Katrina Rainey. Evolution of cooperation and conflict in experimental bacterial populations. *Nature*, 425(6953):72–74, 2003.

[129] D.J. Rankin and A. Lopez-Sepulcre. Can adaptation lead to extinction? *Oikos*, 111(3):616–619, 2005.

[130] M W Retsky, R Demicheli, W J M Hrushesky, J Speer, Swartzendruber D, and Wardwell R. Recent translational research: computational studies of breast cancer. *Breast Cancer Research*, 7:37–40, 2004.

[131] Ian F Robey, Brenda K Baggett, Nathaniel D Kirkpatrick, Denise J Roe, Julie Dosescu, Bonnie F Sloane, Arig Ibrahim Hashim, David L Morse, Natarajan Raghunand, Robert A Gatenby, and Robert J Gillies. Bicarbonate increases tumor pH and inhibits spontaneous metastases. *Cancer research*, 69(6):2260–8, March 2009.

[132] Martin Röcken. Early tumor dissemination , but late metastasis : insights into tumor dormancy. *The Journal of Clinical Investigation*, 120(6), 2010.

[133] Brian Ruffell, David G DeNardo, Nesrine I Affara, and Lisa M Coussens. Lymphocytes in cancer development: polarization towards pro-tumor immunity. *Cytokine & growth factor reviews*, 21(1):3–10, February 2010.

[134] T.L. Russell, D.W. Lwetoijera, B.G.J. Knols, W. Takken, G.F. Killeen, and H.M. Ferguson. Linking individual phenotype to density-dependent population growth: the influence of body size on the population dynamics of malaria vectors. *Proceedings of the Royal Society B: Biological Sciences*, 2011.

[135] Dov F Sax, John J Stachowicz, James H Brown, John F Bruno, Michael N Dawson, Steven D Gaines, Richard K Grosberg, Alan Hastings, Robert D Holt, Margaret M Mayfield, Mary I O'Connor, and William R Rice. Ecological and evolutionary insights from species invasions. *Trends in ecology & evolution (Personal edition)*, 22(9):465–71, September 2007.

[136] M. Scheffer, S. Carpenter, J.A. Foley, C. Folke, and B. Walker. Catastrophic shifts in ecosystems. *Nature*, 413(6856):591–596, 2001.

[137] Marten Scheffer, Jordi Bascompte, William a Brock, Victor Brovkin, Stephen R Carpenter, Vasilis Dakos, Hermann Held, Egbert H van Nes, Max Rietkerk, and George Sugihara. Early-warning signals for critical transitions. *Nature*, 461(7260):53–9, September 2009.

[138] Thomas Schelling. *The strategy of conflict*. Harvard University Press, 1980.

[139] S. Scheu. Microbial activity and nutrient dynamics in earthworm casts (Lumbricidae). *Biology and fertility of soils*, 5(3):230–234, 1987.

[140] Bjoern Schwer, Mark Eckersdorff, Yu Li, Jeffrey C Silva, Damian Fermin, Martin V Kurtev, Cosmas Giallourakis, Michael J Comb, Frederick W Alt, and David B Lombard. Calorie restriction alters mitochondrial protein acetylation. *Aging cell*, 8(5):604–6, September 2009.

[141] G L Semenza. Defining the role of hypoxia-inducible factor 1 in cancer biology and therapeutics. *Oncogene*, 29(5):625–34, February 2010.

[142] Gregg L Semenza. Regulation of cancer cell metabolism by hypoxia-inducible factor 1. *Seminars in cancer biology*, 19:12–16, 2009.

[143] Gregg L Semenza. A return to cancer metabolism. *Journal of molecular medicine (Berlin, Germany)*, 89(3):203–4, March 2011.

[144] M. K. Shigenaga. Oxidative Damage and Mitochondrial Decay in Aging. *Proceedings of the National Academy of Sciences*, 91(23):10771–10778, November 1994.

[145] B. Smit and J. Wandel. Adaptation, adaptive capacity and vulnerability. *Global Environmental Change*, 16(3):282–292, 2006.

[146] John Maynard Smith and G. R. Price. The logic of animal conflict. *Nature*, 246:15–17, 1973.

[147] Baojun Song, Carlos Castillo-Chavez, and Juan Pablo Aparicio. Tuberculosis models with fast and slow dynamics: the role of close and casual contacts. *Mathematical Biosciences*, 180(1-2):187–205, 2002.

[148] Debbie K Song and Russel R Lonser. Pathological satiety caused by brainstem hemangioblastoma. *Journal of Neurosurgery: Pediatrics*, 2(6):397–401, 2008.

[149] Kathleen Sprouffske, John W Pepper, and Carlo C Maley. Accurate reconstruction of the temporal order of mutations in neoplastic progression. *Cancer prevention research (Philadelphia, Pa.)*, April 2011.

[150] S C Stearns. Life history evolution: successes, limitations, and prospects. *Die Naturwissenschaften*, 87(11):476–86, November 2000.

[151] S.C. Stearns. The evolution of life history traits: a critique of the theory and a review of the data. *Annual Review of Ecology and Systematics*, 8:145–171, 1977.

[152] S.C. Stearns. *The evolution of life histories*. Oxford University Press, USA, 1992.

[153] Michael Stratton, Peter Campbell, and P. Andrew Futreal. The cancer genome. *Nature*, 458:719–724, 2009.

[154] F. Takens. Homoclinic points in conservative systems. *Inventiones Mathematicae*, 18(0020-9910):267–292, 1972.

[155] Michele W L Teng, Jeremy B Swann, Catherine M Koebel, Robert D Schreiber, and Mark J Smyth. Immune-mediated dormancy: an equilibrium with cancer. *Journal of leukocyte biology*, 84(4):988–93, October 2008.

[156] A. Tikhonov, A. Vasiljeva, and A. Savershnikov. *Differential Equations*. Nauka, Moscow, 1985.

[157] David Tilman. Niche tradeoffs, neutrality, and community structure: a stochastic theory of resource competition, invasion, and community assembly. *Proceedings of the National Academy of Sciences of the United States of America*, 101(30):10854–61, July 2004.

[158] David Tilman, David Wedin, and Johannes Knops. Productivity and sustainability influenced by biodiversity in grassland ecosystems. *Nature*, 379(6567):718–720, 1996.

[159] Jonathan W Uhr and Klaus Pantel. Controversies in clinical cancer dormancy. *Proceedings of the National Academy of Sciences of the United States of America*, pages 1–5, July 2011.

[160] Matthew G Vander Heiden, Lewis C Cantley, and Craig B Thomspon. Understanding the Warburg effect: the metabolic requirements of cell proliferation. *Science (New York, N.Y.)*, 324(5930):1029–33, May 2009.

[161] Thomas Vincent and Joel Brown. *Evolutionary game theory, natural selection, and Darwinian dynamics*. Cambridge University Press, 2005.

[162] B. Vollan and E. Ostrom. Cooperation and the Commons. *Science*, 330(6006):923–924, November 2010.

[163] Sarah B Voytek and Gerald F Joyce. Niche partitioning in the coevolution of 2 distinct RNA enzymes. *Proceedings of the National Academy of Sciences of the United States of America*, 106(19):7780–5, May 2009.

[164] Otto Warburg. On the origin of cancer cells. *Science*, 123(3191):309–314, 1956.

[165] Joergen Weibull. *Evolutionary game theory*. MIT Press, 1997.

[166] F. Weinberg and N.S. Chandel. Mitochondrial metabolism and cancer. *Annals of the New York Academy of Sciences*, 1177(1749-6632):66–73, 2009.

[167] T L Whiteside. The tumor microenvironment and its role in promoting tumor growth. *Oncogene*, 27(45):5904–12, October 2008.

[168] H.M. Wilbur, D.W. Tinkle, and J.P. Collins. Environmental Certainty , Trophic Level , and Resource Availability in Life History Evolution. *The American Naturalist*, 108(964):805–817, 1974.

[169] Patricia Wood, Kathleen Bove, Shaojin You, Ann F Chambers, and William Hrushesky. Cancer growth and spread are saltatory and phase-locked to the reproductive cycle through mediators of angiogenesis. *Molecular cancer therapeutics*, 4:1065–1075, 2005.

[170] M.E. Wright, S.C. Chang, A. Schatzkin, D. Albanes, V. Kipnis, T. Mouw, P. Hurwitz, A. Hollenbeck, and M.F. Leitzmann. Prospective study of adiposity and weight change in relation to prostate cancer incidence and mortality. *Cancer*, 109(4):675–684, 2007.

[171] Weon-Kyoo You and Donald M McDonald. The hepatocyte growth factor/c-Met signaling pathway as a therapeutic target to inhibit angiogenesis. *BMB reports*, 41(12):833–9, December 2008.

[172] Hua Yu, Marcin Kortylewski, and Drew Pardoll. Crosstalk between cancer and immune cells: role of STAT3 in the tumour microenvironment. *Nature reviews. Immunology*, 7(1):41–51, January 2007.

[173] E. Zea-Cabrera, Y. Iwasa, S. Levin, and I. Rodriguez-Iturbe. Tragedy of the commons in plant water use. *Water resources research*, 42(6), 2006.

Appendix A

SELECTION SYSTEMS AND THE REDUCTION THEOREM.

The selection system is a mathematical model of an inhomogeneous population, in which every individual is characterized by a vector-parameter $(a_1,...,a_n) = \mathbf{a}$ that takes on values from set $\mathbb{A}$. The vector-parameter $\mathbf{a}$ specifies an individual's inherited invariant properties and does not change with time; the set of all individuals with a given value of the vector-parameter a in the population is called a-clone.

Let $l(t,a)$ be the density of the population at the moment t over the parameter $\mathbf{a}$, so that the total population size $N(t) = \int_{\mathbb{A}} l(t,a)da$ and the current population distribution $P(t,a) = \frac{l(t,a)}{N(t)}$.

Denote $F(t,a)$ the per capita reproduction rate at the moment t. It is supposed that the reproduction rate of every $\mathbf{a}$-clone does not depend on other clones but can depend on $\mathbf{a}$ and on some general population characteristics of the system, "regulators".

The model account for extensive characteristics, which depend on the total size of the system (as in most population models) and intensive characteristics, which do not depend on the total size but only on the frequencies of clones within the population (as in most genetic models). The intensive characteristics have the form:

$$U(t) = \int_{\mathbb{A}} u(a)P(t,a)da = E^t[u] \tag{A.1}$$

and the extensive characteristics have the form

$$V(t) = \int_{\mathbb{A}} v(a)l(t,a)da = N(t)E^t[v] \tag{A.2}$$

where u,v are appropriate weight functions. The total population size is the most important regulator.

Overall, the model is specified by some intensive regulators $(U_1(t),\ldots U_k(t)) = \mathbf{U}(t)$ and some extensive regulators $(V_1(t),\ldots V_m(t)) = \mathbf{V}(t)$. It is assumed that the individual reproduction rate can depend on these sets of regulators at each time moment. The selection system under consideration is of the form:

$$dl(t,a)/dt = l(t,a)F(t,a), \tag{A.3}$$

where

$$F(t,\mathbf{a}) = \sum_{i=1}^{n} g_i(t,\mathbf{U},\mathbf{V})\varphi_i(a) \tag{A.4}$$

and g_i are continuous functions. The initial distribution $P(0,a)$ and the initial population size $N(0)$ are assumed to be given.

In model (A.3)-(A.4) the regulators and hence the reproduction rate $F(t,a)$ are not given explicitly but should be computed using the current (unknown) pdf $P(t,a)$ at each time moment, so in the general case, the model is a nonlinear equation of infinite dimensionality. Nevertheless, it can be reduced to a Cauchy problem for the escort system of ODE. To this end, introduce the generating functional:

$$\Phi(r,\lambda) = \int_{\mathbb{A}} r(\mathbf{a}) e^{\sum_{i=1}^{n} \lambda_i \phi_i(\mathbf{a})} P(0,\mathbf{a}) d\mathbf{a} \tag{A.5}$$

where $\lambda = (\lambda_1, \ldots \lambda_n)$ and $r(\mathbf{a})$ is a measurable function on $\mathbb{A}$.

Define auxiliary (keystone) variables as a solution to the escort system of differential equations:

$$\frac{dq_i}{dt} = g_i(t, U^*(t), V^*(t)), \tag{A.6}$$

where $q_i(0) = 0, i = 1, \ldots n$ and

$$V_s^*(t) = \Phi(v_s, q(t)), s = 1, \ldots m, \tag{A.7}$$

$$U_s^*(t) = \frac{\Phi(u_s, q(t))}{\Phi(1, q(t))}, s = 1, \ldots k. \tag{A.8}$$

The dimensionality of the escort system is equal to the number of regulators.

Denote $K_t(a) = e^{\sum_{i=1}^{n} q_i(t)\varphi_i(a)}$.

Reduction theorem.

Let $0 < T \leq \infty$ be the maximal value of t such that Cauchy problem A.6 has a unique global solution $q(t)$ at $t \in [0,T)$. Then the functions:

$$l(t,a) = l(t,0)K_t(a), \tag{A.9}$$

$$V_s(t) = V_s^*(t) = \Phi(v_s, q(t)), s = 1, \dots m, \tag{A.10}$$

$$U_s(t) = \Phi(u_s, q(t))/\Phi(1, q(t)), s = 1, \dots k \tag{A.11}$$

satisfy system (A.1)-(A.4) at $t \in [0, T)$.

The total size of the population $N(t) = N(0)\Phi(1, q(t))$; the current distribution of the system $P(t,a) = \frac{P(0,a)K_t(a)}{E^0[K_t]}$.

The general method is simplified in an important case of the reproduction rate

$$F(t,a) = \sum_{i=1}^{n} g_i(t,S)\varphi_i(a) \tag{A.12}$$

with the regulators S_i of the forms $N(t)$,$E^t[\varphi_i]$,$N(t)E^t[\varphi_i]$ only. In this case one can use the moment generating function of the joint initial distribution of the variables $\phi_i(a)$ only, $M_0(\lambda) = E^0[e^{\sum_{i=1}^{n} \lambda_i \phi_i(a))}]$ instead of generating functional.

The escort system reads $\frac{dq_i}{dt} = g_i(t, S^*(t))$, where $S_i(t)$ are defined with the help of the following formulas:

$$N(t) = N(0)M_0(q(t)), \tag{A.13}$$

$$E^t[\varphi_k] = \partial_k ln M_0(q(t)). \tag{A.14}$$

Appendix B

TRANSITIONAL REGIMES AS EARLY WARNING SIGNALS

Proof of Proposition 1.

Consider the Jacobian $J(N,z)$ at equilibrium points. At the point B it is given by

$$J(B) = \begin{vmatrix} \frac{c\gamma^2}{\delta^2} & 0 \\ -\frac{\gamma e(c-1)}{\delta} & -\frac{\gamma^2}{\delta} \end{vmatrix}$$

The eigenvalues of the point B are $\lambda_1(B) = \frac{c\gamma^2}{\delta^2}$, $\lambda_2(B) = -\frac{\gamma^2}{\delta}$; therefore, B is a saddle.

$$J(A) = \begin{vmatrix} -\frac{c(\gamma+c(e+\gamma)^2-c^2e)^2}{\delta^2(1+c)} & \frac{c^2(\gamma+c(e+\gamma)^2-c^2e)^2}{\delta^2(1+c)} \\ \frac{(c-1)e(c^2e-\gamma-c(e+\gamma))}{\delta(1+c)^2} & -\frac{(c^5e^2-2c^4e\gamma+\gamma^2+3c\gamma(e+\gamma)+c^3(\gamma^2-3e\gamma-3e^2)+c^2(2e^2+2e\gamma+3\gamma^2))}{\delta(1+c)^2} \end{vmatrix}$$

Since $Det(J(A)) = \frac{c(-c^2e+\gamma+c(e+\gamma))^4}{(1+c)^2\delta^3} > 0$, A is a topological node.

$Tr(J(A)) = \frac{(-c^2e+\gamma+c(e+\gamma))(ce(-c+c^3-2\delta+c\delta)-\gamma(c+1)^2(c+\delta))}{(1+c)^2\delta^2}$.

The trace vanishes at the boundary that consists of two branches: $Nul : \{\frac{\gamma}{e} = \frac{c(1-c)}{1+c}\}$and $H : \{\frac{\gamma}{e} = \frac{c(c-1)(c+c^2+2\delta+c\delta)}{(1+c)^2(c+\delta)}\}$

The boundary Nul corresponds to point A and O coinciding, and boundary H corresponds to the Hopf bifurcation accompanied by the change of stability of the equilibrium. Note that $Tr(J(A)) > 0$ if

Let $\delta > 0$, $c > 0$. Then $Tr(J(A)) > Nul$ for $c > 1$ and $Tr(J(A)) < Nul$ for $c < 1$.

Indeed, $\frac{c(c-1)}{c+1} < \frac{(c-1)c(c+c^2+2\delta+c\delta)}{(1+c)^2(c+\delta)}$, so $\frac{c+c^2+2\delta+c\delta}{(1+c)(c+\delta)} > 1$ for $\delta > 0$.

The Proposition is proven.

Proof of Proposition 2

System (2.4) has two integral manifolds $z = 0$ and $N = 0$. According to [12], two blowing-up transformations

$$(N,z) \to (N, u = \frac{z}{N}), N \neq 0 \tag{B.1}$$

and

$$(v,z) \to (v = \frac{z}{N}, z), z \neq 0 \tag{B.2}$$

are necessary to reveal the structure of a neighborhood of point O in the first quadrant. Applying B.1 to System 2.4 and letting $dt \to Ndt$, we obtain the system

$$\begin{cases} N' = -(1+u(c-1)-cu^2)N^2, \\ u' = u(e(1-c)+\gamma)+\gamma u)+Nu(1-\delta-(c+\delta-1)u-cu^2) \end{cases} \tag{B.3}$$

The system has equilibria along u-axis (see Figure 2.2) at the points $ou(u=0, N=0)$ and $a(u=\frac{e(c-1)-\gamma}{\gamma}, N=0)$.

It is easy to see that these equilibria are non-hyperbolic, since both have one zero eigenvalue. Therefore, formally we cannot directly apply the results that were formulated in [12] to this problem.

Taking into consideration that we are interested only in non-negative values of N, let us resolve this problem in the following way. Instead of (B.3) let us consider the system

$$\begin{cases} N' = -(1+u(c-1)-cu^2)N, \\ u' = u(e(1-c)+\gamma)+\gamma u)+Nu(1-\delta-(c+\delta-1)u-cu^2), \end{cases} \tag{B.4}$$

which is topologically equivalent to System (B.3) on a narrow stripe $\{N \geq 0\}$ adjacent to axis u [37, 154]. Equilibria of System (B.4) located on the u-axis are already hyperbolic.

Eigenvalues of ou are $\lambda_1(ou) = (1-c)e+\gamma$, $\lambda_2(ou) = -1$. Thus ou is a saddle if $\frac{\gamma}{e} > c-1$ and an attracting node if $0 < \frac{\gamma}{e} < c-1$. Eigenvalues of a are $\lambda_1(a) = \frac{(1-c)(ce+\gamma(1+c))}{\gamma^2}$, $\lambda_2(a) = -2((1-c)e+\gamma)$. Thus, positive a is a saddle if $c > 1$ and a repelling node if $c < 1$.

Applying (B.2) to System (2.4) and letting $dt \to zdt$ we obtain the system

$$\begin{cases} v' = -v(\gamma+(e(1-c)+\gamma)v)+z^2(\delta-c+(\delta-c+1)v+v^2, \\ z' = z(\gamma+(e(1-c)+\gamma)v)-\delta z^2(1+v) \end{cases} \tag{B.5}$$

All equilibria of (B.5) that are located along the axis $z=0$ are identical to those of System (B.3) except at one point $ov(z=0,v=0)$. It can be easily verified that ov is a saddle for any $\gamma \neq 0$.

The results of this analysis are summarized in Figure 2.2. Note that the portraits in domains 2 and 3 are topologically equivalent (although the orbits can have different asymptotic behavior), so we combine these two domains into one.

Proposition is proven.

Note that Proposition allowed revealing one more parameter boundary of qualitatively different behaviors of Model (2.4), defined by $K: \frac{\gamma}{e} = c-1, \gamma > 0$.

Proof of Proposition 3

Equilibrium A can change stability via Hopf bifurcation for a range of parameter values that belong to the surface H.

To understand whether the bifurcation is sub- or supercritical, we compute the first Lyapunov value [7]. We see that

$$L_1 = \frac{(c-1)^6 c^6 \delta (c+c^2+2\delta - c\delta) e^6}{(1+c)^{10}(c+\delta)^5},$$

for $\frac{\gamma}{e} = \frac{c(c-1)(c+c^2+2\delta+c\delta)}{(1+c)^2(c+\delta)}$).

Thus, $L_1 > 0$ for $c^2 + c(1-\delta) + 2\delta > 0$ and $L_1 < 0$ for $c^2 + c(1-\delta) + 2\delta < 0$. The former case corresponds to the *subcritical* Hopf bifurcation, and the latter case corresponds to the *supercritical* Hopf bifurcation at $\frac{dTr(A)}{d(\gamma/e)} \neq 0$ (see [80]).

For our System,

$$\frac{dTr(J(A))}{d(\gamma/e)} = \frac{1}{\delta^2}\left(\frac{c(c^3+c(\delta-1)-2\delta)e-(1+c)^2(c+\delta)\gamma}{1+c} - (c+\delta)(-c^2 e+\gamma+c(e+\gamma))\right)$$

vanishes for $\frac{\gamma}{e} = \frac{c(2c^3+c(\delta-2)-3\delta+c^2\delta)}{2(1+c)^2(c+\delta)}$, which does not coincide with the condition for boundary H.

The first Lyapunov value L_1 vanishes for c and δ that satisfy $c^2+c(1-\delta)+2\delta=0$. Thus, $L_1=0$ when $c^*=\frac{1}{2}(\delta-1-\sqrt{1-10\delta+\delta^2})$, which exists if $0<\delta<5-\sqrt{24}=0.1$ and $\delta>5+\sqrt{24}=9.9$. Since only the values of $c>0$ are relevant in the context of the model, only the second condition is of interest. Then, $L_1<0$ if $0<\delta<5+\sqrt{24}$ and $L_1>0$ if $\delta>5+\sqrt{24}$.

The case $L_1=0$ corresponds to the co-dimension 2 Bautin bifurcation if two conditions hold:

(i) $\frac{dL_1}{dc}(c=c^*)\neq 0$,

(ii) $L_2\neq 0$ for $L_1=0$, where L_2 is the second Lyapunov value of the equilibrium.

In our case,

$$\frac{dL_1}{dc}=\frac{(c-1)^6c^6\delta e^6\sqrt{1-10\delta+d^2}}{(1+c)^{10}(c+d)^5}.$$

Therefore, $\frac{dL_1}{dc}(c=c^*)\neq 0$ if $\sqrt{1-10\delta+\delta^2}\neq 0$.

The second Lyapunov value was calculated using the analytic formulae given in [7]. The sign of L_2 is the same as that of the following expression:

$$L_{2t}=-4+28\delta-55\delta^2+7\delta^3+(4-20\delta+7\delta^2)\sqrt{1-10\delta+\delta^2},$$

which is positive for $1-10\delta+\delta^2\geq 0$.

So, all the conditions of Bautin theorem are fulfilled.

The Proposition is proven.

Appendix C

MIXED STRATEGIES IN RESOURCE ALLOCATION.

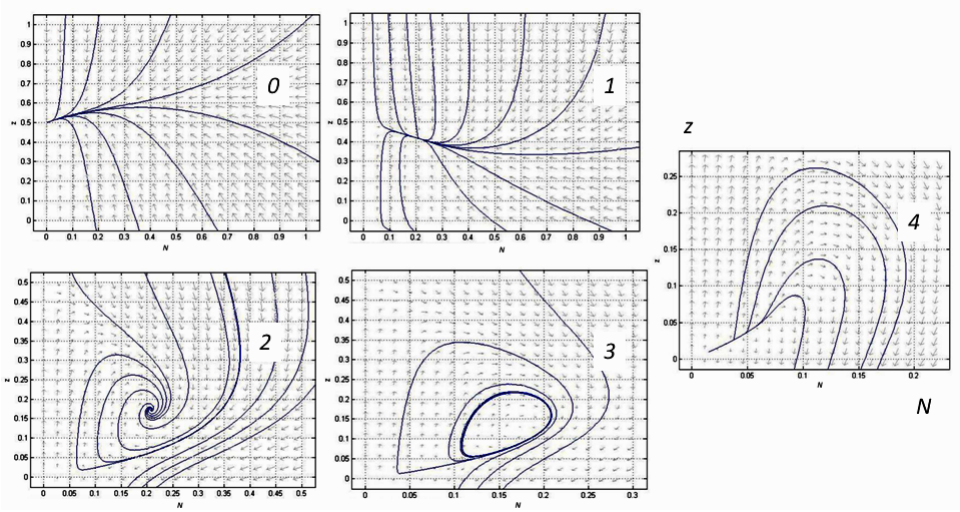

Figure C.1: Phase-parameter portraits of System (4.1) with $\alpha = 0$ under variation of parameter c_2: in Domain 0 (where $0 < c_2 < \phi$), only the trivial equilibrium B is an attractor. In Domain 1, non-trivial equilibrium point A is a global attractor. Domain 2 is a region of bistability: there are two attracting points, A and origin O, whose basins of attraction are divided by separatrix of point O. Point A is a stable focus, attracting only those trajectories that fall within its domain of attraction. In Domain 3, an unstable limit cycle is formed around stable point A, further decreasing its basin of attraction. Finally, in Domain 4, the limit cycle shrinks, "sits" on the point A, making it unstable. Starting from Domain 2 most trajectories in fact travel outside of the first quadrant, predicting negative population size and resource amount, thus rendering the model biologically irrelevant in this region of phase-parameter space.

Critical case when $\alpha = 0$

The phase-parameter portraits of System (4.1) with $\alpha = 0$ were topologically similar to those obtained at $\alpha = 1$ with the addition of Domain 0. In the original formulation of the model, as it was given in Krakauer et al. (2009) some trajectories left the first quadrant, thus causing the model to lose biological relevance. Combining the proposed model with the model that was discussed in the previous chapter eliminated that problem when rescaling the system through a change of variables $z(N+z)dt \to d\tau$ resulted in trajectories that were previously tending to the negative quadrant to tend to origin instead.

Equilibria

In order to simplify analysis, let us first make the following change of variables:

$$z(N+z)dt \to d\tau,$$

yielding a system of equations that is topologically equivalent to System (4.1) for $N \geq 0$, $z \geq 0$:

$$\begin{cases} \frac{dN}{dt} = N(\alpha(c_1 z - N)(N+z) + (1-\alpha)z(c_2 z - \phi(N+z))) \equiv F(N,z) = Nf(N,z), \\ \frac{dz}{dt} = z((\gamma - \delta z)(N+z) + e(\alpha(1-c_1) + (1-\alpha)(1-c_2))N) \equiv F(n,z) = zg(N,z). \end{cases} \tag{C.1}$$

For any α, System (C.1) has trivial equilibria $O(0,0)$ and $B(0,\frac{\gamma}{\delta})$. The system can also have one positive non-trivial equilibrium $A(\hat{N}_\alpha, \hat{z}_\alpha)$, where coordinates$(\hat{N}_\alpha, \hat{z}_\alpha)$ of non-trivial equilibrium satisfy equations

$$\begin{cases} \alpha(c_1 z - N)(N+z) + (1-\alpha)z(c_2 z - \phi(N+z)) = 0 \\ ((\gamma - \delta z)(N+z) + e(\alpha(1-c_1) + (1-\alpha)(1-c_2))N) = 0 \end{cases} \tag{C.2}$$

The first equation of 4.1 is homogeneous. Letting

$$z = K_\alpha N \tag{C.3}$$

we get equation for K_α:

$$(\alpha c_1 + (1-\alpha)(c_2 - \phi))K_\alpha^2 - ((1-\alpha)\phi + \alpha(c_1 - 1))K_\alpha - \alpha = 0, \tag{C.4}$$

which has the unique positive solution

$$K_\alpha = \frac{(1-\alpha)\phi + \alpha(c_1 - 1) + \sqrt{((1-\alpha)\phi + \alpha(c_1-1))^2 + 4\alpha(\alpha c_1 + (1-\alpha)(c_2 - \phi))}}{2(\alpha c_1 + (1-\alpha)(c_2 - \phi))} \tag{C.5}$$

if

$$A(\alpha, c_1, c_2, \phi) \equiv \alpha c_1 + (1-\alpha)(c_2 - \phi) > 0 \tag{C.6}$$

From C.2 and C.3 we get coordinates of non-trivial equilibrium expressed with K_α

$$\begin{cases} \hat{N}_\alpha = \frac{1}{\delta K_\alpha}(\gamma + \frac{e(1-\alpha c_1 - c_2(1-\alpha)}{1+K_\alpha}) \\ \hat{z}_\alpha = \frac{1}{\delta}(\gamma + \frac{e(1-\alpha c_1 - c_2(1-\alpha)}{1+K_\alpha}) \end{cases} \tag{C.7}$$

Remark 2.

$K_{\alpha=0} = \frac{\phi}{c_2-\phi}, \hat{N}_{\alpha=0} = \frac{c_2-\phi}{\delta\phi}(\gamma + \frac{(1-c_2)(c_2-\phi)}{c_2}), \hat{z}_{\alpha=0} = \frac{1}{\delta}(\gamma + \frac{(1-c_2)(c_2-\phi)}{c_2})$

and

$K_{\alpha=1} = \frac{1}{c_1}, \hat{N}_{\alpha=1} = \frac{c_1}{\delta}(\gamma + \frac{c_1(1-c_1)}{1+c_1}), \hat{z}_{\alpha=1} = \frac{1}{\delta}(\gamma + \frac{c_1(1-c_1)}{1+c_1})$

Structure

Jacobian $J_\alpha = (a_{ij}), i,j = 1,2$ of System (C.1) consists of elements

$$\begin{cases} a_{11} = \alpha(-3N^2 + 2(c_1+\phi-1)Nz + (c_1-c_2+\phi)z^2) + z(c_2 z - \phi(2N+z)), \\ a_{12} = N(2c_2 z - \phi(N+2z) + \alpha((c_1+\phi-1)N + 2(c_1+\phi-c_2)z), \\ a_{21} = z(e(1-\alpha(c_1-c_2)-c_2) + \gamma - \delta z), \\ a_{22} = eN(1-\alpha(c_1-c_2)-c_2) + \gamma(N+2z) - \delta z(2N+3z) \end{cases}$$

It is easy to verify that

$$Det(J_\alpha(B(0, \frac{\gamma}{\delta})) = -\frac{(\alpha c_1 + (1-\alpha)(c_2-\phi))\gamma^4}{\delta^3}$$

and

$$Trace(J_\alpha(B(0, \frac{\gamma}{\delta})) = \frac{(\alpha c_1 + (1-\alpha)(c_2-\phi) - \delta)\gamma^2}{\delta^2}.$$

Thus point B is a saddle if $Det(J_\alpha(B(0, \frac{\gamma}{\delta})) < 0$ and a stable node if $Det(J_\alpha(B(0, \frac{\gamma}{\delta})) > 0$. Due to condition C.6, we can state that B is a saddle if the model has positive equilibrium A, and can be a stable node if positive A does not exist. Analysis of expression C.6 shows

that it is satisfied for positive coefficients c_1, c_2 and $\alpha \in [0,1]$only if $c_2 < \phi$ (see Domain 0 in Figure C.1).

The expressions for $Det(J_\alpha(A(\hat{N}_\alpha, \hat{z}_\alpha))$ and $Trace(J_\alpha(A(\hat{N}_\alpha, \hat{z}_\alpha))$ are very complex but can be simplified using the following Lemma:

If the system of differential equations

(a) has non-zero equilibrium $A(N_0, z_0)$ *such that* $f(N_0, z_0) = 0, g(N_0, z_0) = 0$, *and*

(b) function $f(N,z)$ *is homogeneous of order* n *with respect to* N, z.

Then

$$Det(J(N_0, z_0)) \quad = \quad Nf_N(zg_z + Ng_N)|_{(N,z)=(N_0,z_0)},$$

$$Trace(J(N_0, z_0)) = Nf_N + zg_z|_{(N,z)=(N_0,z_0)} = z(g_z - f_z)|_{(N,z)=(N_0,z_0)}$$

Proof.

Jacobian of the System at point A is

$$\begin{pmatrix} f + Nf_N & Nf_z \\ zg_N & g + zg_z \end{pmatrix}_{(N,z)=(N_0,z_0)} = \begin{pmatrix} N_0 f_N(A) & N_0 f_z(A) \\ z_0 g_N(A) & z_0 g_z(A) \end{pmatrix} = \begin{pmatrix} N_0 f_N(A) & \frac{-N_0^2}{z_0} f_N(A) \\ z_0 g_N(A) & z_0 g_z(A) \end{pmatrix}$$

The first equality follows from the condition (a). The second equality follows from the Euler property for homogeneous functions, i.e. that $f(N,z) : Nf_N(N,z) + zf_z(N,z) = nf(N,z)$, and again from condition (a): since $f(N_0, z_0) = 0$, then

$N_0 f_N(N_0, z_0) = -z_0 f_z(N_0, z_0)$,

$f_z(N_0, z_0) = \frac{-N_0}{z_0} f_N(N_0, z_0)$.

Statements are proven.

Applying Lemma 1 to the expression for the Jacobian $J_\alpha(A)$, we obtain $Det(J_\alpha(A(\hat{N}_\alpha, \hat{z}_\alpha))$ and $Trace(J_\alpha(A(\hat{N}_\alpha, \hat{z}_\alpha))$. Combining the obtained results we prove the following

Theorem 2.

For any $\alpha \in [0,1]$, if condition C.4 holds, the nontrivial equilibrium $A_\alpha(\hat{N}_\alpha, \hat{z}_\alpha)$, whose coordinates are given in C.5, is a positive non-saddle point. It appears as an unstable node at the fold surfaces $\Delta_\alpha : Det(J_\alpha(A_\alpha) = 0$

$$\Delta_\alpha : \gamma/e = \frac{-(1-\alpha c_1 - c_2(1-\alpha))}{1+K_\alpha} \tag{C.8}$$

and changes stability at the Hopf surface $H_\alpha : Trace(J_\alpha(A_\alpha) = 0$

$$H_\alpha : \gamma/e = \frac{-(1-\alpha c_1 - c_2(1-\alpha))}{1+K_\alpha} \frac{A+2BK_\alpha}{A+(2B-\delta)K_\alpha} \tag{C.9}$$

where K_α is given in C.3, $A = \delta - l + \alpha(c_1 + l - 1)$, $B = A + \alpha + (1-\alpha)c_2$.

Remark 3.

For $\alpha = 1$ fold and Hopf surfaces are of the form $\Delta_{\alpha=1} = 0 : \frac{\gamma}{e} = \frac{c_1(c_1-1)}{c_1+1}$, $H_{\alpha=1} : \frac{\gamma}{e} = \frac{c_1(c_1-1)(c_1+2\delta+c_1\delta+c_1^2)}{(c_1+1)^2(c_1+\delta)}$;

For $\alpha = 0$ fold and Hopf surfaces are of the form $\Delta_{\alpha=0} = 0 : \frac{\gamma}{e} = \frac{(c_2-\phi)(c_2-1)}{c_2}$, $H_{\alpha=0} : \frac{\gamma}{e} = \frac{(c_2-\phi)(c_2-1)((\delta-\phi)\phi+c_2(\delta+\phi))}{c_2(-\phi^2+c_2(\delta+\phi)}$).

Non-hyperbolic equilibrium $O(0,0)$

For analysis of topological and asymptotical structure of the equilibrium in the first quadrant of (N,z)-plane we use methods described in [12]. Let us apply the following change of variables (also known as the "blowing-up" transformation) to System (C.1):

$$(N,z) \to (N, u = z/N), N \neq 0,$$

transforming point $(0,0)$ to the axis u, and changing the independent variable to $Ndt = d\tau$, which results in the following system of equations:

$$\begin{cases} \frac{dN}{d\tau} = N^2(\alpha(1+u)(c_1u-1)-(1-\alpha)u(\phi-(c_2-\phi)u), \\ \frac{du}{d\tau} = u((e(1-\alpha c_1-(1-\alpha)c_2+\gamma(1+u))+N(-\delta u(1+u)- \\ -\alpha(1+u)(c_1u-1)+(1-\alpha)u(\phi-(c_2-\phi)u))) \end{cases} \tag{C.10}$$

System (C.10) has two equilibrium points at axis $N=0$: $u_1=0$ with eigenvalue $\lambda_1^1 = (1-\alpha c_1-(1-\alpha)c_2)-\gamma)$ and $u_2=-e(1-\alpha c_1-(1-\alpha)c_2)-\gamma)/\gamma$ with eigenvalue $\lambda_1^2=-\lambda_1^1$. Although the second eigenvalue is zero for both points ($\lambda_2^1=\lambda_2^2=0$), their structure can be strictly defined in the positive (N,z)-quadrant using the method described in [12]. Denote

$$E = e(1-\alpha c_1-(1-\alpha)c_2)+\gamma \tag{C.11}$$

If $E>0$, then only equilibrium $(0,u_1)$ belongs to the first quadrant and has an attractive node sector; if $E<0$, then two equilibria $(0,u_1)$ and $(0,u_2)$ belong to the first quadrant; $(0,u_1)$ is a saddle and $(0,u_2)$ can be a saddle, as well as an attractive node. $E=0$ corresponds to merging $u_1=u_2=0$. The second change of variables

$$(N,z)\to(v=N/z,z), z\neq 0 \tag{C.12}$$

maps point $(0,0)$ to the axis v, and through changing time using transformation $zdt=d\tau$, System (4.2) becomes:

$$\begin{cases} \frac{dv}{d\tau} = v(-\gamma-(e(1-\alpha c_1-(1-\alpha)c_2)+\gamma)v+ \\ +((1+v)(\delta+\alpha(c_1-v)+(1-\alpha)(c_2-\phi(1+v)))z, \\ \frac{dz}{d\tau} = z(-(e(1-\alpha c_1-(1-\alpha)c_2)+\gamma)v-\delta(1+v)z) \end{cases} \tag{C.13}$$

The equilibrium $(v=0,z=0)$ is a saddle $(\lambda_1=\gamma,\lambda_2=-\gamma)$

To return to the initial variables, we prove the following statement: Proposition 1. In System (C.1) for all $\alpha\in(0,1]$ and the specified values of other parameters c_1, c_2, $\phi>0$, $\gamma\geq 0$,$0<e\leq 1$ there exist only three different phase-parameter portraits in the neighborhood

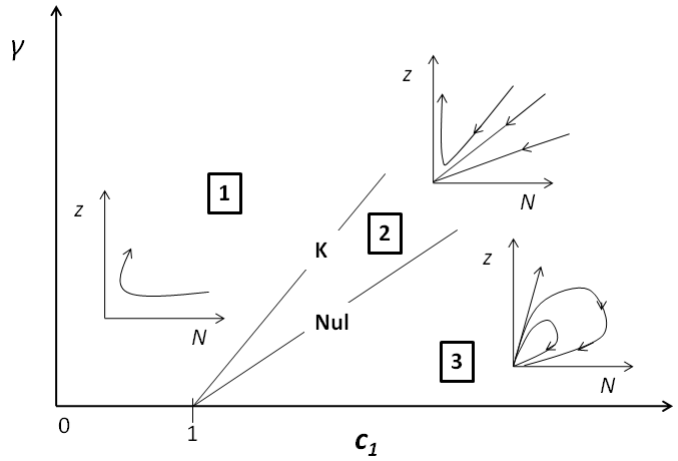

Figure C.2: A schematic bifurcation diagram of the equilibrium point O for System (C.1) in the (γ, c_1) parameter-and (N,z)- phase spaces for positive fixed values of parameters $e \leq 1, c_2 > \phi$, $c_{2>\delta}$. The parameter space is divided into three domains: Domain 1 contains hyperbolic sector only, Domain 2 contains hyperbolic and attractive parabolic sectors, in Domain 3 there exists an elliptic sector (family of homoclinic orbits). The boundary K between domains 1 and 2 corresponds to the non-local heteroclinic bifurcation; the boundary Nul between domains 2 and 3 corresponds to disappearance of hyperbolic sector and non-trivial equilibrium.

of equilibrium point O, which are topologically equivalent to the portraits that are shown in Figure C.2.

B4. Equilibria "at infinity"

The structure of equilibrium points "at infinity" will be studied using the Poincare sphere [7].

(a) Changing variables

$$(N,z) \to (u = 1/N, v = z/N), N \neq 0 \tag{C.14}$$

and

$$dt = u^2 d\tau \tag{C.15}$$

transforms System (4.2) to

$$\begin{cases} \frac{du}{d\tau} = u(v(\phi(1+v)-c_2)-\alpha((c_1+\phi-1)v-1+(c_1+\phi-c_2)v^2)), \\ \frac{du}{d\tau} = v(v(\phi(1+v)-c_2)-\alpha((c_1+\phi-1)v-1+(c_1+\phi-c_2)v^2)+ \\ +(1+v)(\gamma u-\delta v)-eu(\alpha(c_1-c_2)+c_2-1)) \end{cases} \tag{C.16}$$

Equilibrium points of Systems (C.16) for $u=0$ are $v=0$ satisfy the equation:

$$(\alpha c_1+\delta+(1-\alpha)(c_2-\phi))v^2-(\alpha(1-c_1-\phi)+\phi-\delta)v-\alpha=0 \tag{C.17}$$

Lemma 2.

Only one of the roots of Equation C.17, $v=v*(\alpha)$, can be positive for $0<\alpha\leq 1$; at $\alpha=0$, $v*(\alpha=0)=0$.

Proof.

Rewrite equation C.17 in the form: $B(\alpha)v^2-A(\alpha)v-\alpha=0$, where $A(\alpha)=\alpha(1-c_1-\phi)+\phi-\delta$, $B(\alpha)=\alpha(c_2-c_1-\phi)+\phi-\delta-c_2$. The validity of Lemma 2 is evident if $B(\alpha)>0$. If $B_\alpha=0$, then $\alpha=\frac{c_2-\phi+\delta}{c_2-\phi-c_1}$, and $\alpha\in[0,1]\Leftrightarrow c_2-\phi+\delta\leq 0$ for $c_1,c_2,\delta,\phi\geq 0$. So, Equation C.17 has no positive roots if $\alpha\neq 0$.

Statement is proven.

It can be verified that eigenvalues of $u=v=0$ are $\lambda_1=\lambda_2=\alpha$, and eigenvalues of $u=0, v=v*(\alpha)$ are

$$\lambda_1(\alpha)=\delta v*(\alpha)(1+v*(\alpha))>0,$$

$$\lambda_2(\alpha)=-v*(\alpha)(\delta-\phi+\alpha(c_1+\phi-1)+2(c_2+(\delta-\phi)+\alpha(c_1+\phi-c_2))v*(\alpha))$$

Therefore, point $u=0, v=v*(\alpha)>0$ is a saddle.

Remark 4.

For $\alpha=1$, $v*=\frac{1}{c_1+\delta}$ and the eigenvalues are $\lambda_1=\frac{\delta(c_1+\delta+1)}{(c_1+\delta)^2}$, $\lambda_2=-\frac{(c_1+\delta+1)}{(c_1+\delta)}$.

For $\alpha = 0$, $v* = \frac{\phi-\delta}{c_2-\phi+\delta}$. If $\phi > \delta$, then $v* > 0$. The corresponding eigenvalues are $\lambda_1 = \frac{\delta c_2(\phi-\delta)}{(c_2+\delta-\phi)^2}$, $\lambda_2 = \frac{-(\phi-\delta)^2}{(c_2+\delta-\phi)}$.

Note, that system

$\frac{du}{d\tau} = u((\phi(1+v) - c_2 v)$,

$\frac{dv}{d\tau} = e(1-c_2)u + (1+v)(\gamma u - \delta v) + v(\phi - (c_2 - \phi)v)$,

which was obtained from the System (C.1) through the change of variables (C.14) and (C.15), does not have an equilibrium point at $u = v = 0$ for $\phi < \delta$. For $\phi = \delta$ equilibrium $u = v = 0$ is not hyperbolic; it contains hyperbolic sector for positive u, v.

(c) Making the transformation

$$(N, z) \to (u = 1/z, w = N/z), z \neq 0 \tag{C.18}$$

and putting it together with expression (C.15), we obtain System

$$\begin{cases} \frac{du}{d\tau} = u(\delta(1+w) - u(\gamma(1+w) - ew(\alpha c_1 - 1 + c_2(1-\alpha)), \\ \frac{dw}{d\tau} = w(\delta(1+w) + c_2 - \phi - \gamma u(1+w) - \phi w - euw(1-c_2) + \\ +\alpha((\phi - w)(1+w) + (c_1 - c_2)(1+euw))) \end{cases} \tag{C.19}$$

This System has the only one new equilibrium (when compared with equation C.16): $(u = 0, w = 0)$. Eigenvalues at this point, namely $\lambda_1 = \delta$, $\lambda_2 = \alpha c_1 + (1-\alpha)(c_2 - \phi + \delta)$, are positive. Thus, it is an unstable node for all α. Combining the results, we get the following proven statement

Proposition 2.

For $\alpha \in (0, 1]$ in the first quadrant of (N, z)-plane, System (C.1)

(1) has a source at the end N-axis,

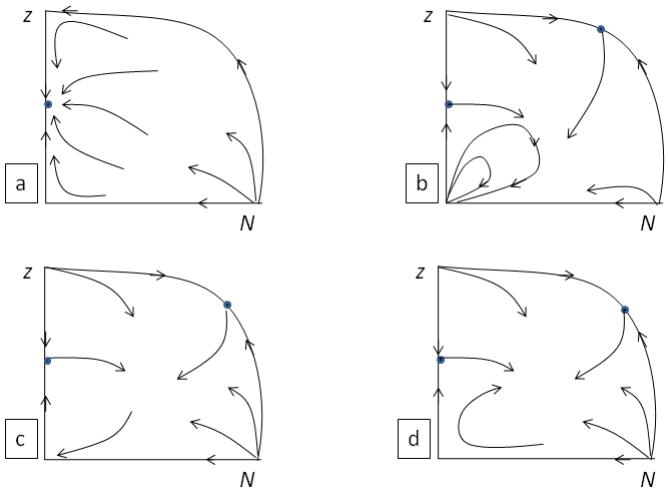

Figure C.3: (a) Only equilibrium B is attractive, (b) equilibrium O is attractive and repelling simultaneously, no more attracting equilibria, (c) equilibrium O is attractive, other attractive manifolds have to exist, (d) O is repelling (a saddle), other attractive manifolds must exist.

(2) has a source node at the end z-axis and a saddle point at the end of the axis, where $v*(\alpha)$ is a non-negative root of equation C.17 if $\alpha(c_2 - c_1 - \phi) + \phi - \delta - c_2 > 0$,

(3) has a saddle point at the end z-axis if $\alpha(c_2 - c_1 - \phi) + \phi - \delta - c_2 < 0$.

Typical structures of the "bounded" first quadrant in the (N, z)-plane are presented in Figure C.3:

Heteroclinis, homoclinics and limit cycles

Heteroclinis and homoclinics

One of the main heteroclinics of System (C.1) is the existence of a trajectory that connects point O and infinitely removed saddle point (point "at infinity"). Its appearance corresponds to the appearance an attractive parabolic sector in the positive neighborhood of point O; the boundary K in the phase-parameter portrait (see Figure C.4a) divides these phase portraits.

Another important heteroclinics connection forms when the emergent separatrix of trivial equilibrium B coincides with the incoming separatrix of equilibrium O. The unstable limit cycle is generated containing nontrivial equilibrium A (see, Figure C.4b, where parametric boundary S corresponds to this bifurcation). Elliptic sector in the neighborhood of point

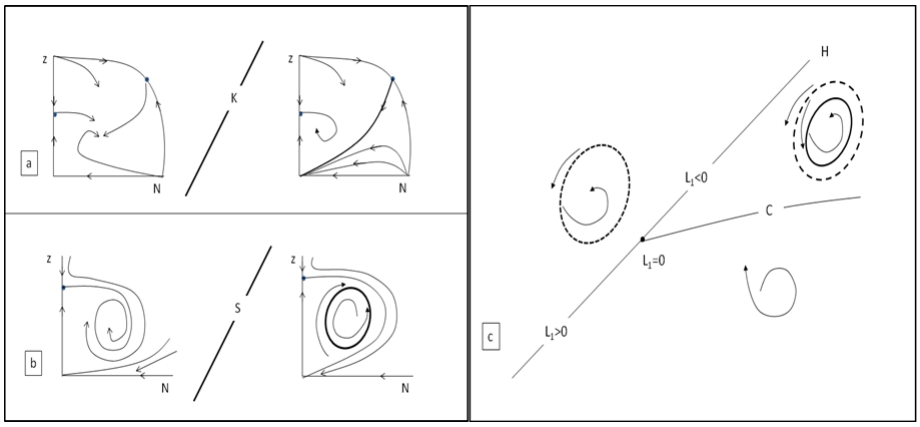

Figure C.4: Schematic bifurcation diagrams of heteroclinics- and Hopf bifurcations that are realized in the System (C.1): (a) appearance\disappearance of attractive parabolic sector in a neighborhood of the origin; (b) appearance/disappearance of unstable limit cycle containing A, and (c) generalized Hopf bifurcation $L_1(H)=0$ in a neighborhood of A.

O, shown in Figure C.2 (Domain 3) and in Figure C.3b consists of a family of homoclinics tending to O with $t \to \pm\infty$

Hopf bifurcations

Equilibrium A of System (C.1) can change stability via Hopf bifurcation for a range of parameter values that belong to the surface H_α (see equation C.9). To understand whether the bifurcation is sub- or supercritical, we compute the first Lyapunov value L_1 [7].

For $\alpha=1$, $H_{\alpha=1}: \frac{\gamma}{e}=\frac{c_1(c_1-1)(c_1+2\delta+c_1\delta+c_1^2)}{(c_1+1)^2(c_1+\delta)}$, and the corresponding first Lyapunov value is $L_1(H_{\alpha=1}) \cong \frac{(c-1)^6c^6\delta(c^2+c+2\delta-c\delta)}{(c+1)^{10}(c+\delta)^5}$. Thus, $L_1>0$ for $(c^2+c+2\delta-c\delta)>0$ and $L_1<0$ for $(c^2+c+2\delta-c\delta)<0$. The former case corresponds to the subcritical Hopf bifurcation, and the latter case corresponds to the supercritical Hopf bifurcation for $\frac{dTr(A)}{d(\gamma/e)} \neq 0$ [80].

The case $L_1(H_{\alpha=1})=0$ corresponds to Bautin (generalized Hopf) bifurcation of co-dimension 2. It is realized in the System (C.1), $\alpha=1$ for large δ; the schematic bifurcation diagram is presented in Figure AC.4-c.

Now we consider System C.1 with $\alpha=0$; to be more precise, we will analyze direction of Hopf bifurcation for System (C.1).

Proposition 3.

Equilibrium A of System (C.1) with $\alpha = 0$ changes stability only via subcritical (catastrophic) Hopf bifurcation.

Proof.

$H_{\alpha=0}: \frac{\gamma}{e} = \frac{(c_2-\phi)(c_2-1)(c_2(\delta+\phi)+\phi(\delta-\phi))}{c_2(c_2\delta+\phi(c_2-\phi))}$,

and

$N_0(\alpha=0) = \frac{(c_2-\phi)^2 e(c_2-1)}{c_2(c_2\delta+\phi(c_2-\phi))}$

The sign of the first Lyapunov quantity L_1 is calculated using the formula given in [7]. We have shown that $L_1 = l\widehat{L}$, where $l > 0$ is some constant, the exact value of which is unimportant, and $\hat{L}_1 = \delta(-(c_2-\phi)(c_2-\phi+\delta)+c_2(c_2-\phi+2\delta))((c_2-1)(c_2-\phi)^2 e - c_2\delta N_0)$.

It is easy to verify that $\hat{L}_1 = 0$ for$\delta = 0$, $\delta = -\frac{\phi(c_2-\phi)}{c_2+\phi}$ that are non-positive for positive N_0. $\hat{L}_1 = 0$ also for $\delta = -\frac{\phi(c_2-\phi)}{c_2-1}$, which is negative for the required $c_2 > \phi$ and $c_2 > 1$; if $c_2 < 1$ then $\frac{\gamma}{e} = \frac{(c_2-\phi)(1+\phi)(c_2-1)}{c_2} < 0$. Thus, at this point $L_1(H) > 0$.

The statement is proven.

To summarize, we show that for $\alpha = 1$, $L_1(H) = 0$ for some parameter values and for $\alpha = 0$, $L_1(H) \neq 0$ for all parameter values. By continuity, there must exist some $0 < \alpha* < 1$ such that for $1 \geq \alpha > \alpha*$ the model has stable limit cycle in some parameter domain and has no stable limit cycle for $0 \leq \alpha < \alpha*$.

Bifurcation diagrams of System (4.1) and interpretation of model dynamics

Based on results formulated in Propositions 1-3 we are able to present the schematic bifurcation diagram of System (C.1):

Theorem 3.

(1) For any $\alpha \in [0,1]$, positive c_1, c_2, e, δ, γ-parameter space of System (C.1), can be

divided into seven domains of topologically non-equivalent phase portraits with non-negative coordinates (N,z) (see Figure 4.1 and Figure C.1):

In Domain 0, $c_2 \in (0,\phi)$; only point $B(N=0,z=\frac{\gamma}{\delta})$ is attractive (see Figure C.3-a). In Domain 1, the only non-trivial equilibrium point $A_\alpha(\hat{N}_\alpha,\hat{z}_\alpha)$ is attractive; its coordinates are given in Equation C.7. In Domains 2 and 3, point A shares basins of attraction with equilibrium point O at the origin. The separatrix of O and the unstable limit cycle that contains point A serve correspondingly as the boundaries of the basins of attraction. In Domain 4, only equilibrium O is globally attractive; it contains attractive parabolic sector. Equilibrium A is positive and unstable. In Domain 5, only point O is globally attractive. It contains an elliptic sector in its positive neighborhood. In this region, there is no non-trivial positive equilibrium. Domain 6 exists only for $1 \geq \alpha > \alpha^* > 0$ (i.e., when α is closer to 1 than to 0). It is a domain of bistability. In it there are two attractive manifolds: a stable limit cycle, which contains an unstable equilibrium point A, and an equilibrium point O at the origin.

(2) Boundaries between Domains correspond to the following bifurcations in System (C.1): K and S correspond to heteroclinic connection between point O, an infinitely removed saddle point (see Figure C.4a,b), and point B. Boundary H corresponds to the Hopf bifurcation (H^+ and H^- correspond to sub- and supercritical bifurcations respectively). $Nul \equiv \Delta$ corresponds to the appearance of an unstable point A in the positive quadrant. Boundary C corresponds to the fold bifurcation of limit cycles.

Note that parameter portraits in Figure 4.1 are schematic slices of complete bifurcation portraits, projected to the planes (α,c_1) and (N,z). The boundary lines correspond to bifurcations of co-dimension 1, and points of intersections of the lines correspond to bifurcations of higher co-dimensions.

Appendix D

BIOLOGICAL STOICHIOMETRY IN TUMOR MICROENVIRONMENT.

The equation for the rate of change of the concentration of extracellular phosphorus.

The concentration of extracellular phosphorus that is available for the cells to consume is $P_t^{ex} = P^{ex}N(t)$, where P_t^{ex} is the absolute number of moles of phosphorus available, P^{ex} is concentration of phosphorus per cell clone. The inflow of phosphorus from the blood stream is accounted for with the term $g_2(P_0 - P^{ex})$, where P_0 is the gradient constant, and g_2 is the rate of inflow-outflow. The term is chosen based on standard models that deal with modeling chemostat [81]. Extracellular phosphorus P^{ex} is absorbed by the cells and is converted to intracellular phosphorus P^{in} at the rate $p(P^{ex} - P^{in})\frac{N(t)}{k_2 + P^{ex} - P^{in}}$, which accounts for diffusion of carbon through the cell wall based on the difference between intra- and extracellular phosphorus concentrations; the limitation $k_2 + P^{ex} - P^{in}$ is to account for the fact that there is only that much phosphorus that a cell can absorb. The difference in rates of phosphorus uptake between competitive and proliferative cells is accounted for through the term $m = m_a(1 - E^t[\alpha]) + m_g E^t[\alpha]$. There is also an inflow of phosphorus that was released from the cells that died either naturally, coming from the equation for x_α. So,

$$\frac{dP^{ex}(t)N(t)}{dt} = \frac{dP^{ex}(t)}{dt}N(t) + P^{ex}(t)\frac{dN(t)}{dt} = \tag{D.1}$$

$$= g_2(P_0 - P^{ex}(t)) - mN(t)\frac{P^{ex}(t) - P^{in}(t)}{k_2 + (P^{ex}(t) - P^{in}(t))} + N(t)P^{in}(t)d \tag{D.2}$$

Therefore, the concentration of P^{ex} is

$$\frac{dP^{ex}}{dt} = g_2(\frac{P_0 - P^{ex}(t)}{N(t)}) - m\frac{P^{ex}(t) - P^{in}(t)}{k_2 + (P^{ex}(t) - P^{in}(t))} + P^{in}(t)d - P^{ex}(t)E^t[F] \tag{D.3}$$

The expression $\frac{N(t)'}{N(t)}$ is derived from the first equation and is

$$\frac{N'(t)}{N(t)} = E^t[F] = E^t[\alpha]r_c(1 - \frac{N(t)}{z(t)}) + (1 - E^t[\alpha])r_p(\frac{z(t)}{N(t) + z(t)^2}) - d), \tag{D.4}$$

where $z(t) = \frac{C^{in}P^{in}}{C^{in} + P^{in}}$.

The equation for rate of change of concentration of intracellular phosphorus.

The total amount of intracellular phosphorus available for the cells of typeα is $P_{t,\alpha}^{in} = P^{in}x_\alpha$, where P^{in} is the concentration of phosphorus per cell. The inflow of phosphorus into each cell clone x_α is accounted for by the term $mx_\alpha\frac{P^{ex} - P^{in}}{k_2 + (P^{ex} - P^{in})}$. Intracellular phosphorus P^{in} is

conserved, i.e., it is not consumed irreversibly as fuel but is used for building DNA, RNA, ribosomes, etc. The rate of change of total amount of intracellular phosphorus in the cells of clone type x_α is

$$\frac{dP^{in}_{t,\alpha}}{dt} = m x_\alpha(t) \frac{P^{ex}(t) - P^{in}(t)}{k_2 + (P^{ex}(t) - P^{in}(t))} \tag{D.5}$$

Since

$$\frac{dP^{in}_t}{dt} = \frac{dP^{in}(t)N(t)}{dt} = \frac{dP^{in}(t)}{dt} N(t) + P^{in}(t) \frac{dN(t)}{dt}, \tag{D.6}$$

the rate of change of P^{in} is

$$\frac{dP^{in}}{dt} = m \frac{P^{ex}(t) - P^{in}(t)}{k_2 + (P^{ex}(t) - P^{in}(t))} - P^{in}(t) E^t[F]. \tag{D.7}$$

Appendix E

PRISONER'S DILEMMA IN CANCER METABOLISM.

Model Derivation

A note on notation:

For all expressions of the type $\frac{\sum_{\mathbb{A}} x_\alpha(t) f(\alpha)}{N(t)}$ we use the standard notation of the expected value $E^t[f(\alpha)]$ of the function $f(\alpha)$ over the distribution $P_\alpha(t) = \frac{x_\alpha(t)}{N(t)}$, where $N(t) = \sum_{\mathbb{A}} x_\alpha(t)$ is the total size of the population if the number of possible values of α is finite and $N(t) = \int_{\mathbb{A}} x_\alpha d\alpha$ if it is infinite.

Equation for the dynamics of cell clones.

The dynamics of clones x_α is governed by the following equation

$$\frac{dx_\alpha}{dt} = x_\alpha(r_a(1-\alpha)(\frac{\beta C^{in}}{\beta + C^{in}}) + r_g \alpha C^{in} - d - b_\alpha r_g C^{in} E^t[\alpha]) \tag{E.1}$$

where the growth rate of glycolytic clones α is limited only by availability of intracellular carbon C^{in}, and the growth rate of aerobic clones $(1-\alpha)$ is limited both by carbon C^{in} and oxygen β (for the purposes of this model oxygen inflow is constant and can thus be modeled as a parameter). Cells also die at some constant average rate d.

Incorporating effects of toxicity of lactic acid on the non-glycolytic cell clones is accounted for through the additional death term $b_\alpha = B - b_1 \alpha$, where B and b_1 are constants, and where $b_1 < \frac{B}{\alpha}$ due to restriction on $\alpha \in [0,1]$. This functional form incorporates the assumption that the more lactic acid the cell produces, the less sensitive to its toxicity it is (since the clones that produce lactic acid and then immediately die from it cannot persist in the population). Hydrogen transporters are also up-regulated in cancer cells to pump out the acid from the cell.

The total amount of lactic acid released per cell is accounted for by the term $\frac{\sum_A r_g \alpha x_\alpha C^{in}}{N(t)} = r_g C^{in} E^t[\alpha]$, and the cells of type $(1-\alpha)$ that are killed by lactic acid are accounted for with $b_\alpha x_\alpha r_g C^{in} E^t[\alpha]$.

Equation for the dynamics of extracellular carbon.

The concentration of extracellular carbon that is available for the cells to consume is $C_t^{ex} = C^{ex}N(t)$, where C_t^{ex} is the absolute number of moles of carbon available, C^{ex} is concentration of carbon per cell clone. The inflow of carbon from the blood stream is accounted for with the term $g_1(C_0 - C^{ex})$, where C_0 is the gradient constant, and g_1 is the rate of inflow-outflow. The term is chosen based on standard models that deal with modeling chemostat [81].

Extracellular carbon C^{ex} is absorbed by the cells and is converted to intracellular carbon C^{in} at the rate $p(C^{ex} - C^{in})\frac{N(t)}{k_1 + C^{ex} - C^{in}}$, which accounts for diffusion of carbon through the cell wall based on the difference between intra- and extracellular carbon concentrations; the limitation $(k_1 + C^{ex} - C^{in})$ is to account for the fact that there is only that much carbon that a cell can absorb. Parameter $p = p_a(1-\alpha) + p_g(\alpha)$, allowing to take into account the difference in glucose uptake rates between aerobic and glycolytic cells. There is also an inflow of carbon that was released from the cells that died either naturally or due to being killed by lactic acid, coming from the equation for x_α.

So,

$$\frac{d\ C_t^{ex}}{dt} = \frac{dC^{ex}}{dt}N + C^{ex}\frac{N'}{N} = g_1(C_0 - C^{ex}) - p(C^{ex} - C^{in})\frac{N(t)}{k_1 + (C^{ex} - C^{in})} + \quad \text{(E.2)}$$

$$+cC^{in}\sum_{\alpha} x_\alpha(d + b_\alpha r_g C^{in} E^t[\alpha]). \quad \text{(E.3)}$$

However, when the population of cells is small, which is the focus of the question, for which this system was proposed, the increase in the total population size N' is negligible with respect to the entire population. Therefore, in this case $C^{ex}\frac{N'}{N} \to 0$, yielding the following equation for the change in the concentration of extracellular carbon:

$$\frac{dC^{ex}}{dt} = g_1(\frac{C_0 - C^{ex}}{N}) - p\frac{C^{ex} - C^{in}}{k_1 + (C^{ex} - C^{in})} + C^{in}d + (C^{in})^2 E^t[b]E^t[\alpha]. \quad \text{(E.4)}$$

Equation for the dynamics of intracellular carbon

The total amount of intracellular carbon available for the cells of type α is $C^{in}_{t,\alpha} = C^{in}x_\alpha$, where C^{in} is the concentration of carbon per cell. The inflow of carbon into each cell clone x_α is accounted for by the term $p\frac{C^{ex}-C^{in}}{k_1+(C^{ex}-C^{in})}$.

Total amount of carbon consumed by the clone x_α is $s(r_g\alpha+(1-\alpha)r_a)C^{in}$, where s is the conversion factor for exactly how much carbon was actually used. How much of it is going to be used for aerobic or anaerobic metabolism depends on the value of the parameter α.

So, similarly to the equation for C^{ex}, the equation for C^{in} becomes

$$\frac{dC^{in}}{dt} = p\frac{C^{ex}-C^{in}}{k_1+(C^{ex}-C^{in})} - sC^{in}(r_a\xi(1-E^t[\alpha])+r_gE^t[\alpha]) \tag{E.5}$$

where $p = (p_gE^t[\alpha]+p_a(1-E^t[\alpha]))$.

Distribution of α

Consider System (6.1), where we assume that each clone is characterized by their own intrinsic value of the parameter α but where there is no detectable toxicity from lactic acid (i.e., a case when $b_\alpha = 0$)

Let us introduce keystone variables $g(t)$ and $q(t)$, such that

$$\begin{cases} \frac{dq(t)}{dt} = r_a\beta\frac{C^{in}}{\beta+C^{in}}, \\ \frac{dg(t)}{dt} = r_gC^{in}. \end{cases} \tag{E.6}$$

Then $x_\alpha(t)' = x_\alpha(t)((1-\alpha)q'(t)+\alpha g'(t)-\delta)$.

Consequently,

$$x_\alpha(t) = x_\alpha(0)e^{(1-\alpha)q(t)+\alpha g(t)-\delta t} \tag{E.7}$$

Full population size of cells x_α is then given by

$$N(t) = \int_A x_\alpha(t)d\alpha = N(0)\int_A e^{q(t)-\delta t}e^{\alpha(g(t)-q(t))}P_0(\alpha)d\alpha = N(0)e^{q(t)-\delta t}M_0[g(t)-q(t)] \tag{E.8}$$

where $P_\alpha(0) = \frac{x_\alpha(0)}{N(0)}$ and where $M_0(g(t)-q(t)) = \int_0^\infty e^{\alpha(g(t)-q(t))}P_\alpha(0)d\alpha$ is the moment generating function (mgf) of the initial distribution of clones $P_\alpha(0)$ within the population. The final distribution would then be given by

$$P_t(\alpha) = \frac{x_\alpha(t)}{N(t)} = \frac{e^{\alpha(g(t)-q(t))}}{M_0[g(t)-q(t)]} \tag{E.9}$$

System (6.1) thus becomes

$$\begin{cases} \frac{dC^{ex}}{dt} = g_1(\frac{C_0-C^{ex}}{N}) - p\frac{C^{ex}-C^{in}}{k_1+(C^{ex}-C^{in})} + C^{in}d, \\ \frac{dC^{in}}{dt} = p\frac{C^{ex}-C^{in}}{k_1+(C^{ex}-C^{in})} - sC^{in}(r_a\xi(1-E^t[\alpha])\frac{\beta}{\beta+C^{in}} - r_gE^t[\alpha]), \\ \frac{dq}{dt} = r_a\beta\frac{C^{in}}{\beta+C^{in}}, \\ \frac{dg}{dt} = r_gC^{in}. \end{cases} \tag{E.10}$$

The expected value of α at each time t is calculated through Equation (E.9):

$$E^t[\alpha] = \int \alpha P_t(\alpha)d\alpha = \int P_0(\alpha)\frac{\alpha e^{\alpha(g(t)-q(t))}}{M_0[g(t)-q(t)]}d\alpha = \frac{M_0'[g(t)-q(t)]}{M_0[g(t)-q(t)]}. \tag{E.11}$$

Let us assume that the initial distribution of the clones within the population is truncated exponential, such that $\alpha \in [0,1]$.

For initial truncated exponential distribution with parameter μ, the moment generating function $M_0[g(t)-q(t)]$ is

$$M_0[g(t)-q(t)] = \frac{\mu(e^\mu - e^{g(t)-q(t)})}{(e^\mu-1)(\mu-(g(t)-q(t)))}, \tag{E.12}$$

and expected value of α is calculated by

$$E^t[\alpha] = \frac{e^\mu - e^{g(t)-q(t)}(g(t)-q(t)-\mu-1)}{(e^{g(t)-q(t)}-e^\mu)(g(t)-q(t)-\mu)}. \tag{E.13}$$

The parameter $\mu \gg 0$ to ensure that the initial distribution of clones within the population is skewed towards $\alpha \to 0$, that is, such that the majority of the cells have aerobic phenotype, which is what is to be observed in the normal tissue.

For more details on the method see [69, 70] and the references within.

Distribution of α, when $b_\alpha \neq 0$

Now consider a case, when there is also increased cell mortality from the lactic acid that is produced by the glycolytic clones. This is accounted for through the additional death term $b_\alpha = B - b_1\alpha$, where B and b_1 are constants, and where $b_1 < \frac{B}{\alpha}$ due to restriction on $\alpha \in [0,1]$, which also incorporates the assumption that the more lactic acid the cell produces, the less sensitive to its toxicity it is (the clones that produce lactic acid and then die from it cannot persist in the population). Hydrogen transporters are also up-regulated in cancer cells to pump out the acid from the cell.

In order to study this model, we need to introduce a third keystone equation in addition to System (E.1):

$$\frac{dv}{dt} = r_g C^{in} E^t[\alpha]. \tag{E.14}$$

Then the equation for x'_α becomes

$$x'_\alpha = x_\alpha(q'(1-\alpha) + \alpha g' - d - (B - b_1\alpha)v') \tag{E.15}$$

Integrating this expression yields

$$x_\alpha(t) = x_\alpha(0)e^{q(t)-dt-Bv(t)+\alpha(g(t)-q(t)-b_1v(t))}. \tag{E.16}$$

Full population size is then given by

$$N(t) = N(0)e^{q(t)-dt-Bv(t)}M_0(g(t)-q(t)-b_1v(t)) \tag{E.17}$$

and the distribution of clones is given by

$$P_t(\alpha) = \frac{x_\alpha(t)}{N(t)} = \frac{e^{\alpha(g(t)-q(t)-b_1v(t))}}{M_0(g(t)-q(t)-b_1v(t))}. \tag{E.18}$$

The full system thus becomes

$$\begin{cases} \frac{dC^{ex}}{dt} = g_1(\frac{C_0 - C^{ex}}{N}) - p\frac{C^{ex} - C^{in}}{k_1 + (C^{ex} - C^{in})} + C^{in}d + (C^{in})^2 E^t[b]E^t[\alpha], \\ \frac{dC^{in}}{dt} = p\frac{C^{ex} - C^{in}}{k_1 + (C^{ex} - C^{in})} - sC^{in}(r_a\xi(1 - E^t[\alpha])\frac{\beta}{\beta + C^{in}} - r_g E^t[\alpha]), \\ \frac{dq}{dt} = r_a\beta\frac{C^{in}}{\beta + C^{in}}, \\ \frac{dg}{dt} = r_g C^{in}, \\ \frac{dv}{dt} = r_g C^{in} E^t[\alpha]. \end{cases} \tag{E.19}$$

The proposed system is used to address two different questions: 1) whether the changes in nutrient availability are sufficient to switch population composition towards glycolytic phenotype, and 2) whether excessive toxicity from lactic acid can cause the population to commit evolutionary suicide. For the purposes set out by the first question, parameter b_α is taken to be zero. This is done to be able to more clearly see, whether the shift can in fact occur to a significant enough extent. When $b_\alpha \neq 0$, population extinction due to acid toxicity occurs too quickly (around $E^t[\alpha] \approx 0.1$ for the considered parameter values), and the effects of excess nutrients cannot be evaluated very well.

Appendix F

MYELOID CELLS IN TUMOR-IMMUNE INTERACTIONS.

Global stability of the fast subsystem. The Dulac criterion

Here we prove that there are no periodic orbits in the fast system of (8.2) using Dulac criterion as follows:

Taking $\delta = \frac{1}{M_1}$, we have

$$\begin{aligned}
\delta\dot{M}_1 &= \frac{1}{M_1}(\Omega - \mu_1 M_1 - (\theta - g\frac{T}{p+T})M_1) \\
&= \frac{\Omega}{M_1} + g\frac{T}{p+T} - (\theta + \mu_1) \\
\frac{\partial}{\partial M_1}(\delta\dot{M}_1) &= -\frac{\Omega}{M_1^2} \\
\delta\dot{M}_2 &= \frac{1}{M_1}(-g\frac{M_1 T}{p+T} + \theta M_1 - \mu_2 M_2), \\
&= -g\frac{M_1 T}{p+T} + \theta - \frac{\mu_2 M_2}{M_1} \\
\frac{\partial}{\partial M_2}(\delta\dot{M}_2) &= -\frac{\mu_2}{M_1} \\
\frac{\partial}{\partial M_1}(\delta\dot{M}_1) - \frac{\partial}{\partial M_2}(\delta\dot{M}_2) &= -\frac{\mu_2}{M_1} - \frac{\Omega}{M_1^2}
\end{aligned}$$

The obtained expression is strictly negative in $\mathbb{R}^2_+ \setminus \{(0,0)\}$. Hence, there are no periodic orbits in the system (M_1, M_2) in $\mathbb{R}^2_+ \setminus \{(0,0)\}$.

Global stability of the fast system. Applying Poincaré-Bendixon Theorem

Now, we find a condition such that $M_1(t) + M_2(t) \leq$constant.

Solving $\dot{M}_1 + P_1 M_1 = P_2$ and $\dot{M}_2 + K_1 M_2 = K_2 M_1$,

where $P_1 = -g\frac{T}{p+T} + \theta + \mu_1$, $P_2 = \Omega$, $K_1 = \mu_2$, and $K_2 = -g\frac{T}{p+T} + \theta$ are positive, we obtain

$$\begin{aligned}
M_1 &= \frac{P_2}{P_1} + (M_1(0) - \frac{P_1}{P_2})e^{-P_1 t}, \\
M_2 &= \frac{K_2}{K_1} + r_1 e^{-K_2 t} + r_2 e^{-P_1 t},
\end{aligned}$$

where r_1 and r_2 are constants.

Then,

$$\begin{aligned}\lim_{t\to\infty} M_1(t) &= \frac{P_2}{P_1},\\ \lim_{t\to\infty} M_2(t) &= \frac{K_2}{K_1}.\end{aligned}$$

Therefore, the (M_1, M_2)-subsystem of system (8.1) is bounded. Hence, the unique equilibrium point $(M_1^*, M_2^*) = (\frac{\Omega}{\mu_1+V}, \frac{\Omega V}{\mu_2(\mu_1+V)}$ is globally asymptotically stable for any V.

Proof of the Theorem 1

Further, we consider a polynomial system, which is orbitally equivalent to (8.4) for positive x, y and $ds = \frac{d\tau}{\beta+x}$:

$$\begin{cases} \frac{dx}{ds} &= x(\beta+x) - \alpha xy(1+x), \\ \\ \frac{dy}{ds} &= -\gamma y(\beta+x) - xy^2(1+x) \end{cases} \tag{F.1}$$

For the parameters α, β, γ, where $\beta = \frac{\alpha(1+\gamma+\alpha\gamma^2)}{\alpha(1-\gamma)-1}$, the real part of eigenvalues $Re(\lambda_{1,2})$ of the Jacobian $J(x,y)$ of (F.1) around equilibrium $A(\alpha\gamma, \frac{\beta+\alpha\gamma}{\alpha(1+\alpha\gamma)})$ is equal to zero. To apply the Andronov-Hopf Theorem [?] we need to check whether non-degeneracy conditions are satisfied. Since

$$Re(\lambda_{1,2}) = \frac{Tr(A)}{2} = \frac{\gamma(\beta()1+\alpha(\gamma-1)) + \alpha(1+\gamma+\alpha\gamma^2)}{(1+\alpha\gamma)(\beta+\alpha\gamma)}$$

we have

$$\frac{dTr(J(A))}{2} = \frac{\gamma(1-\alpha(1-\gamma))}{\alpha(1+\alpha\gamma)} \neq 0$$

if $\gamma \neq 0, \alpha \neq \frac{1}{1-\gamma}$. Thus in the first condition of non-degeneracy holds.

To compute the first Lyapunov value l_1, we need to fix the parameters at the surface (8.5) and shift $A(x_0, y_0)$ to the origin:

$$x \to x - x^*, y \to y - y^*$$

The system (F.1) takes the form:

$$\begin{cases} \frac{dx}{ds} &= x\frac{\alpha(1+\gamma+\alpha\gamma^2)}{1-\alpha(1-\gamma)} - \alpha^2\gamma(1+\alpha\gamma)y + x^2\frac{1+\alpha\gamma}{1-\alpha(1-\gamma)} - \alpha(1+2\alpha\gamma)xy - \alpha x^2 y \\ \\ \frac{dy}{ds} &= x\frac{(1+\gamma)(1+\alpha\gamma)}{(1-\alpha(1-\gamma))^2} - y\frac{\alpha(1+\gamma+\alpha\gamma^2)}{1-\alpha(1-\gamma)} + x^2\frac{1+\alpha\gamma}{1-\alpha(1-\gamma)} - xy\frac{\gamma+3\alpha\gamma+\alpha\gamma^2}{1-\alpha(1-\gamma)} + \\ & \quad +\alpha\gamma(1+\alpha\gamma)y^2 + xy^2(1+\alpha\gamma) + x^2y^2 \end{cases} \tag{F.2}$$

This representation of our system of equations allows us to apply the formula given in [7] to obtain an expression for the first Lyapunov value:

$$l_1 = C\frac{1+\gamma+\alpha^2\gamma(1-\gamma)^2 - \alpha(2+\gamma-2\gamma^2)}{\alpha^2\sqrt{\gamma}(1+\alpha\gamma)^2}$$

where C is a positive constant. l_1 vanishes for $\alpha_1(\gamma) = \frac{2+\gamma-2\gamma^2+\sqrt{4-3\gamma^2}}{2\gamma(1-\gamma)^2}$ and $\alpha_2(\gamma) = \frac{2+\gamma-2\gamma^2-\sqrt{4-3\gamma^2}}{2\gamma(1-\gamma)^2}$. Both $\alpha_1(\gamma)$ and $\alpha_2(\gamma)$ are positive for $\gamma \in (0,1)$. Moreover, l_1 is positive for $\alpha_2(\gamma) < \alpha < \alpha_1(\gamma)$ and is negative for $\alpha > \alpha_1(\gamma)$, $\alpha < \alpha_2(\gamma)$. It is easily verified that α that is greater then $\alpha_2(\gamma)$ and β (defined by Equation (8.5)) are positive for $\gamma \in (0,1)$. This proves statement $2i$ of Theorem 1.

Statement $2ii$ follows from the fact that β defined by (8.5) is negative for α_2, and so only $\alpha > \alpha_1(\gamma)$, where $l_1 < 0$ is suitable.

Thus, for $\alpha, \beta > 0$ and $\gamma \in (0,1)$, Hopf bifurcation with zero Lyapunov value occurs only for:

$$\alpha = \alpha_1(\gamma) = \frac{2+\gamma-2\gamma^2+\sqrt{4-3\gamma^2}}{2\gamma(1-\gamma)^2} \tag{F.3}$$
$$\beta(\gamma) = \frac{\alpha_1(\gamma)(1+\gamma+\alpha_1(\gamma)\gamma)}{\alpha_1(\gamma)(1-\gamma)-1}$$

The fact that condition of non-degeneracy for this bifurcation holds and that the third Lyapunov quantity is non-zero for α, β defined by Equation (F.3) within $\gamma \in (0,1)$, was checked numerically using software package LOCBIF (created by Khibnik et al., 1993). Bautin theorem [80] allows us to demonstrate that the parameters of the bifurcation contain boundaries corresponding to saddle-node limit cycle bifurcation. This proves statement $2iii$ of the theorem. The bifurcation diagram of the bifurcation is shown in Figure 8.1.